

**A Thesis Submitted for the Degree of PhD at the University of Warwick**

**Permanent WRAP URL:**

<http://wrap.warwick.ac.uk/134512>

**Copyright and reuse:**

This thesis is made available online and is protected by original copyright.

Please scroll down to view the document itself.

Please refer to the repository record for this item for information to help you to cite it.

Our policy information is available from the repository home page.

For more information, please contact the WRAP Team at: [wrap@warwick.ac.uk](mailto:wrap@warwick.ac.uk)

**Studies on the peripheral light-harvesting  
chlorophyll-protein complex of photosystem I in  
*Pisum sativum* L.**

**By**

**Richard Stephen Williams**

**B.Sc. (Birmingham)**

**M.Sc. (Reading)**

**F.L.S.**

**Submitted for the degree of Doctor of Philosophy**

**Department of Biological Sciences,  
University of Warwick,  
Coventry, CV4 7AL**

**March 1987**

I've *suffered* for my science.....  
.....now it's *your* turn

*They prate of Gods believe it, fellow-creatures,  
There's no such bugbears: all was made by Nature.  
We know all came of nothing, and shall pass  
Into the same condition once it was.....*

-a Ranter Christmas carol, in *The Arraignement and  
Tryall, with a Declaration of the Ranters* (1650).



*"The little man will whip the big man every time if the  
little man's in the right and keeps comin'..."*

-Terry Southern (1970).

CONTENTS

	Page
CONTENTS .....	(i)
FIGURES AND TABLES .....	(viii)
ACKNOWLEDGEMENTS .....	(xv)
DECLARATION .....	(xvi)
SUMMARY .....	(xvii)
ABBREVIATIONS .....	(xviii)

PART I: INTRODUCTION

(1.1) The Role of the Chloroplast in Photosynthesis .....	(1)
(1.2) Essential Features of Photosynthetic Membranes .....	(6)
(1.3) Photosynthetic Prokaryotes .....	(8)
(1.3a) The blue-green bacteria .....	(10)
(1.3b) The green and purple bacteria .....	(12)
(1.4) The Chloroplast of Higher Plants .....	(22)
(1.4a) The envelope membrane .....	(22)
(1.4b) The stroma .....	(26)
(1.4c) The thylakoid membrane .....	(27)
(1.5) Photosynthetic Electron Transport and its Components .....	(30)

(1.5a)	Chlorophyll-protein complexes .....	(36)
(1.5b)	Intersystem electron carriers .....	(37)
(1)	The mobile carriers .....	(39)
(1i)	The cytochrome $b_6/f$ complex .....	(42)
(1.5c)	The ATP synthase .....	(44)
(1.5d)	The lipids .....	(45)
(1.6)	The Photosynthetic Reaction Centres .....	(49)
(1.6a)	The photosystem II (PS II) reaction centre (RC II) .....	(49)
(1.6b)	The photosystem I (PS I) reaction centre (RC I) .....	(57)
(1.7)	The Light-Harvesting Antennae .....	(66)
(1.7a)	The light-harvesting antenna of photosystem II (the LHC II) .....	(66)
(1.7b)	The light-harvesting antenna of photosystem I (the LHC I) .....	(77)
(1.8)	Aims of the Present Research .....	(84)

## PART 2: MATERIALS AND METHODS

(2.1)	Materials .....	(89)
(2.2)	Growth of Plants .....	(90)
(2.2a)	Normal growth .....	(90)
(2.2b)	The etiolation system .....	(91)
(2.2c)	Intermittent illumination .....	(92)
(2.3)	Polyacrylamide Gel Electrophoresis .....	(92)

[2.4]	Gel Staining and Destaining .....	(96)
[2.4a]	Coomassie blue .....	(96)
[2.4b]	Silver staining .....	(97)
[2.5]	Autoradiography .....	(98)
[2.6]	Densitometric Scanning of Stained Gels .....	(99)
[2.7]	Two-Dimensional Gel Electrophoresis .....	(100)
[2.8]	Proteolytic Mapping of Purified Polypeptides .....	(103)
[2.9]	<i>In vivo</i> Labelling of Thylakoid Proteins .....	(105)
[2.10]	Estimation of Protein in Thylakoid Samples .....	(107)
[2.11]	Isolation of Intact Chloroplasts .....	(110)
[2.11a]	Rapid isolation of a crude preparation .....	(110)
[2.11b]	Isolation using Percoll gradients .....	(111)
[2.12]	Isolation of Thylakoid Membranes .....	(112)
[2.13]	Isolation of Chlorophyll-Protein Complexes .....	(113)
[2.13a]	Isolation of PS I by the method of Mullet <i>et al</i> .....	(113)
[2.13b]	Isolation of PS I by the 'high salt' method.....	(116)

(2.13c)	Isolation of PS I by the Tris-HCl method .....	(116)
(2.13d)	Isolation of LHC I .....	(117)
(2.13e)	Isolation of LHC II .....	(118)
(2.14)	Electroelution of LHC I and RC I Proteins .....	(119)
(2.15)	Immunological Techniques .....	(123)
(2.15a)	Preparation of polyclonal antisera to the LHC I and PS I reaction centre apoproteins ...	(123)
(2.15b)	Preparation of a polyclonal antiserum to the 26 kDa apoprotein of the LHC II .....	(124)
(2.15c)	Preparation of monoclonal antibodies to the apoproteins of the LHC I .....	(125)
(i)	Immunisation of mice .....	(125)
(ii)	Fusion of myeloma and spleen cells .....	(127)
(iii)	Hybridoma selection .....	(130)
(iv)	Hybridoma culture .....	(131)
(2.15d)	Immunoblotting .....	(132)
(i)	Iodination of protein A .....	(132)
(ii)	Radio-immunodetection of antigens .....	(133)



(iii) Antigen detection using the biotin-streptavidin system ...	(135)
(2.15e) Immunoprecipitation .....	(137)
(2.16) Low Temperature Fluorescence Spectroscopy .....	(139)
(2.17) Chlorophyll Determination .....	(140)
(2.18) Freeze-Fracture Electron Microscopy .....	(140)
(2.19) Assay of PS I Reaction Centre Photochemical Activity .....	(141)
(2.20) Isolation of Poly(A)-Enriched RNA .....	(142)
(2.21) <i>In vitro</i> Translation of Poly(A)-Enriched RNA .....	(147)
(2.22) Measurement of Incorporation of [ <sup>35</sup> S]-Labelled Methionine into Protein.....	(148)
(2.23) Determination of Amino-Terminal Amino Acid Sequences of the LHC I Apoproteins .....	(149)
(2.24) Immunological Identification of Thylakoid Proteins Labelled <i>in vivo</i> with [ <sup>35</sup> S]-Labelled Methionine .....	(149)

### PART 3: RESULTS

(3.1) Isolation of Photosystem I .....	(153)
(3.1a) The method of Mullet <i>et al</i> .....	(155)
(3.1b) The 'high salt' method .....	(184)
(3.1c) The Tris-HCl method .....	(201)

(3.2)	Preparation of Polyclonal Antisera .....	(233)
(3.2a)	Purification of antigens .....	(233)
(3.2b)	Assay of LHC I antibody specificity .....	(243)
(3.2c)	Assay of RC I antibody specificity .....	(266)
(3.3)	Preparation of Monoclonal Antibodies .....	(270)
(3.3a)	Screening of hybridoma supernatants and assay of antibody specificity .....	(270)
(3.4)	Proteolytic Mapping of LHC I Apoproteins ....	(277)
(3.4a)	The use of staphylococcal V8 protease .....	(277)
(3.4b)	The use of cyanogen bromide .....	(280)
(3.5)	Comparison of Amino-Terminal Regions of LHC I and LHC II Apoproteins .....	(285)
(3.6)	Site of Synthesis of LHC I Apoproteins .....	(288)
(3.7)	Photocontrol of LHC I Accumulation .....	(297)
(3.7a)	LHC I accumulation under intermittent light .....	(299)
(3.7b)	LHC I accumulation in de-etiolating plants .....	(314)
(1)	Loss of chlorophyll in the dark .....	(318)
(11)	Accumulation of LHC II apoproteins .....	(320)

(iii)	Accumulation of LHC I	
	apoproteins .....	(327)
(iv)	Accumulation of RC I	
	apoproteins .....	(331)
(v)	Synthesis of LHC I	
	apoproteins in the dark .....	(337)

**PART 4: GENERAL DISCUSSION**

14.11	Isolation of PS I-Containing	
	Chlorophyll-Protein Complexes .....	(350)
14.21	Structural Relationships of	
	Chlorophyll-Protein Complexes .....	(356)
14.31	Regulation of Assembly of Photosystem I	
	and Control of the Biogenesis of the	
	Photosynthetic membrane .....	(361)

<b><u>BIBLIOGRAPHY</u></b> .....	(369)
----------------------------------	-------

**FIGURES AND TABLES**

<b>Figure</b>	<b>Page</b>
1.1 Diagram to show the gross structure of the chloroplast of eukaryotic plant cells .....	(5)
1.2 Diagram to show the organisation of a 'typical' photosynthetic unit .....	(9)
1.3 Diagram to show the organisation of the photosynthetic reaction centre of <i>Rhodospseudomonas viridis</i> .....	(16)
1.4 Diagram to show possible paths of cyclic and non-cyclic electron flow in anoxygenic photosynthetic bacteria .....	(32)
1.5 Diagram to show the non-cyclic electron transport pathway in the chloroplast .....	(34)
1.6 Schematic representation of the architecture of the thylakoid membrane .....	(87)
2.1 Diagram to show apparatus used for the electroelution of proteins from polyacrylamide gels .....	(120)
2.2 Method for screening of monoclonal supernatants by immunoblotting .....	(128)
2.3 Method for immunological identification of thylakoid proteins labelled <i>in vivo</i> with [ <sup>35</sup> S]methionine .....	(151)
3.1 Sucrose density gradient containing green bands resulting from solubilisation of unstacked thylakoids with Triton X-100 following the method of Mullet <i>et al</i> (1980a) .....	(159)

3.2	Distribution of chlorophyll on sucrose density gradient following membrane solubilisation by the method of Mullet <i>et al</i> (1980a) .....	(160)
3.3	Relative distribution of chlorophylls <i>a</i> and <i>b</i> on sucrose density gradient following membrane solubilisation by the method of Mullet <i>et al</i> (1980a) .....	(160)
3.4	Comparison of absorption spectra of pigments extracted from unfractionated thylakoids and sucrose gradient fraction 23 .....	(162)
3.5	Distribution of PS I-mediated electron transport activity in sucrose density gradient following membrane solubilisation by the method of Mullet <i>et al</i> (1980a) .....	(164)
3.6	SDS-PAGE analysis of fractions from the sucrose density gradient following membrane solubilisation by the method of Mullet <i>et al</i> (1980a) .....	(168)
3.7	SDS-PAGE analysis of fraction 23 from the sucrose density gradient following membrane solubilisation by the method of Mullet <i>et al</i> (1980a) .....	(168)
3.8	Fluorescence emission spectra (77 K) of fraction 23 from the sucrose density gradient following membrane solubilisation by the method of Mullet <i>et al</i> (1980a) .....	(172)
3.9	Freeze-fracture electron micrograph of washed, unstacked thylakoids prior to addition of detergent .....	(174)
3.10	Freeze-fracture electron micrograph of washed, unstacked thylakoids prior to addition of detergent .....	(177)
3.11	Freeze-fracture electron micrograph of material derived from fraction 23 of the sucrose density gradient .....	(179)
3.12	Freeze-fracture electron micrograph of material derived from fraction 23 of the sucrose density gradient .....	(182)

3.13	Comparison of absorption spectra of pigments extracted from thylakoid membranes and the 'high salt' pellet .....	(186)
3.14	Fluorescence emission spectrum (77 K) of 'high salt' pellet .....	(187)
3.15	SDS-PAGE analysis of the polypeptide content of the 'high salt' pellet .....	(188)
3.16	Freeze-fracture electron micrograph of washed, unstacked thylakoids prior to washing with 0.8 M NaCl .....	(190)
3.17	Freeze-fracture electron micrograph of thylakoid membranes after washing with 0.8 M NaCl .....	(193)
3.18	Freeze-fracture electron micrograph of thylakoid membranes after washing with 0.8 M NaCl .....	(195)
3.19	Freeze-fracture electron micrograph of material derived from the 'high salt' pellet following solubilisation of salt-treated thylakoid membranes with Triton X-100 .....	(197)
3.20	Comparison of absorption spectra of pigments extracted from thylakoid membranes, the Tris-HCl pellet and purified LHC II .....	(202)
3.21	SDS-polyacrylamide gel analysis of PS I material prepared by the three methods described in Section 2.13 .....	(205)
3.22	Freeze-fracture electron micrograph of material derived from the Tris-HCl pellet ....	(207)
3.23	Freeze-fracture electron micrograph of material derived from the Tris-HCl pellet ....	(210)
3.24	Fluorescence emission spectra (77 K) of material derived from the Tris-HCl pellet in the presence and absence of MgCl <sub>2</sub> .....	(215)

3.25	Fluorescence emission spectra of PS I material prepared by the method of Mullet <i>et al</i> (1980a), in the presence and absence of $MgCl_2$ .....	(216)
3.26	Fluorescence excitation spectra (77 K) of the Tris-HCl pellet taken in the absence of $MgCl_2$ .....	(220)
3.27	Fluorescence excitation spectra (77 K) of the Tris-HCl pellet taken in the presence of added $MgCl_2$ .....	(220)
3.28	Graph showing the relationship between rate of PS I-mediated electron transport and increasing light intensity for PS I particles prepared by the method of Mullet <i>et al</i> (1980a) .....	(225)
3.29	Lindweaver-Burk plot of the data displayed in Figure 3.28 .....	(225)
3.30	SDS-PAGE analysis of a PS I preparation used for the isolation and purification of the apoproteins of the LHC I .....	(235)
3.31	SDS-PAGE analysis of purified LHC I polypeptides .....	(238)
3.32	SDS-PAGE analysis of purified LHC I polypeptides (silver stain) .....	(240)
3.33	autoradiographs of immunoblot assays showing specificities of antibodies raised against the apoproteins of the LHC I and LHC II .....	(244)
3.34	Sucrose density gradient showing green bands resulting from the solubilization of PS I material with Zwittergent-16 and dodecyl- $\beta$ -D-maltoside .....	(251)
3.35	Absorption spectra of pigments extracted from component pigment-protein complexes of PS I .....	(253)
3.36	Low temperature (77 K) fluorescence emission spectra of material representing purified LHC I and undissociated PS I .....	(255)

3.37	Immunoblot analysis of the immunological similarities between LHC I and LHC II apoproteins .....	(258)
3.38	Assay of specificity of antibody raised against the PS I reaction centre (RC I) proteins .....	(267)
3.39	Autoradiograph of immunoblot of six mouse sera after immunisation with PS I material prepared by the Tris-HCl method .....	(272)
3.40	Characterisation of three hybridoma supernatants containing antibodies to the polypeptides of the LHC I .....	(273)
3.41	Comparison of staphylococcal V8 protease digestion patterns for the LHCP and the apoproteins of the LHC I .....	(279)
3.42	Comparison of CNBr digestion patterns for the LHCP and the apoproteins of the LHC I .....	(281)
3.43	Comparison of the amino-terminal amino acid sequences of the two LHC I apoproteins P2 and P3, and of the LHCP .....	(286)
3.44	Autoradiograph of immunoprecipitates resulting from the treatment of radio-labelled <i>in vitro</i> translation products with LHC I antibodies .....	(292)
3.45	Comparison of pea shoots from seedlings grown in darkness, intermittent light, and continuous light .....	(303)
3.46	Changes in chlorophyll content of third node thylakoids resulting from transfer of plants from intermittent to continuous illumination .....	(306)
3.47	SDS-PAGE analysis of the polypeptide content of third node thylakoids following transfer of plants from intermittent to continuous light .....	(308)
3.48	Autoradiograph of immunoblot showing the accumulation of the LHC I and LHC II apoproteins upon transfer of plants from intermittent to continuous light .....	(308)



3.49	Changes in chlorophyll content within third node leaves upon transfer of greening plants to darkness .....	(316)
3.50	SDS-PAGE analysis of third node thylakoid membranes after exposure of etiolated pea seedlings to 48 h light, 64 h light or 48 h light followed by 16 h darkness .....	(321)
3.51	Scanning densitometer traces of the third node thylakoid tracks shown in Figure 3.50 .....	(325)
3.52	Autoradiograph of immunoblot showing pattern of accumulation of the LHC I apoproteins when de-etiolating pea seedlings are returned to the dark .....	(329)
3.53	Immunoblot showing destruction of the RC I polypeptides resulting from the acetone treatment of thylakoid membranes .....	(333)
3.54	Immunoblot showing the pattern of accumulation of the RC I polypeptides when de-etiolating pea seedlings are returned to the dark .....	(333)
3.55	Immunodetection of LHC I polypeptides among thylakoid proteins labelled with [ <sup>35</sup> S]methionine in the light .....	(341)
3.56	Immunodetection of LHC I polypeptides among thylakoid proteins labelled with [ <sup>35</sup> S]methionine in the dark .....	(345)

TablePage

3.1	The effect of varying Triton X-100 concentration upon recovery of membranes after solubilisation .....	(156)
3.2	Comparison of PS I-mediated electron transport rates in unsolubilised and solubilised thylakoid membranes .....	(165)

3.3 Summary of properties of PS I particles prepared by the three different methods described in Section 2.13 .....	(203)
3.4 Estimates of $K_m$ and $V_{max}$ for the four PS I-mediated electron transport assays shown in Figures 3.28 and 3.29 .....	(229)
3.5 Summary of specificities of three monoclonal antibodies .....	(275)
3.6 Comparison of accumulation of the $\alpha$ and $\beta$ subunits of the ATP synthase and the LHCP .....	(326)

#### ACKNOWLEDGEMENTS

I would like to express my thanks to Professor R.J.Ellis for providing the opportunity to carry out this work, to the S.E.R.C. for providing funds, and to other members of the department of Biological Sciences with whom I have had stimulating discussions.

In addition, I would like to thank John Allen for all his help with the chlorophyll fluorescence work and Pete Thomas and Tony Brain for their help with the electron microscopy (and for the software).

I would also like to thank Janet for her unending patience, Bryn for being 'wicks', Mum and Dad for making me homozygous for the 'STUBBORN' mutation, and Linda 'just because'.

Lastly, I would like to thank Marshall Chulkev and the men and women of the Red Army for their heroic defence of Stalingrad, 1942.

DECLARATION

All of the work described in this thesis, apart from that listed below, was carried out by the author in the Plant Biochemistry Laboratory in the Department of Biological Sciences, University of Warwick.

Low temperature (77 K) fluorescence emission and excitation spectra were gathered with the aid of Dr. John F. Allen in the Department of Plant Sciences, University of Leeds.

Freeze-fracture electron microscopy and associated sample preparation was performed by Mr. Tony Brain and with the aid of Dr. Peter Thomas in the laboratory of Drs. Peter Quinn and Patrick Williams, Chelsea College, University of London.

#### SUMMARY

Two novel sub-thylakoid fractions from *Pisum sativum* L. containing the photosystem I reaction centre and peripheral light-harvesting complex were characterised. Both preparations displayed a number of spectral and biochemical properties in common with those exhibited by a standard photosystem I preparation. However, both differed markedly in their sedimentation properties when compared with the standard preparation.

In addition, one of the novel preparations was found to contain large amounts of the chlorophyll *a/b*-binding light-harvesting complex of photosystem II (LHC II). It was shown that excitation energy is transferred from the LHC II component to the photosystem I component within this preparation. Such excitation energy transfer has not previously been demonstrated in a sub-thylakoid preparation.

Monoclonal and polyclonal antibodies were raised to the apoproteins of the chlorophyll *a/b*-binding peripheral light-harvesting complex of photosystem I (LHC I). Assays of polyclonal antibody specificity showed immunological cross-reaction between individual LHC I apoproteins and between the apoproteins of the LHC I and LHC II. The immunological cross-reactivity between the polypeptides of the LHC I and LHC II were shown to be spurious. The LHC I apoproteins were found to fall into two distinct immunological groupings which were supported by assays of monoclonal antibody specificity and by a comparison of their partial peptide maps.

Immunoblot assays showed that the LHC I apoproteins failed to accumulate in the thylakoid membrane under intermittent illumination. When greening pea seedlings were placed in the dark, the LHC I apoproteins not only failed to accumulate but underwent a net loss during the dark period. *In vivo* radiolabelling experiments showed that the apoproteins of the LHC I continued to be synthesised even after 16 h darkness. The failure of these proteins to accumulate in the thylakoid in the dark is therefore due to protein turnover.

ABBREVIATIONS

ADP	adenosine 5'- diphosphate
ala	alanine
APS	ammonium persulphate
ATP	adenosine 5'-triphosphate
asp	aspartate
arg	arginine
Bchl <i>b</i>	bacteriochlorophyll <i>b</i>
BPh <i>b</i>	bacteriopheophytin <i>b</i>
BPB	bromophenol blue
BSA	bovine serum albumin
cDNA	DNA strand complimentary to a mRNA molecule
CF	coupling factor
CI	curie ( $\approx 3.7 \times 10^{10}$ disintegrations per second)
CMC	critical micelle concentration
c.p.m.	radioactive counts per minute
D1	diffuse protein 1 (32 kDa polypeptide of the PS II reaction centre complex)
D2	diffuse protein 2 (34 kDa polypeptide of the PS II reaction centre complex)
Da	dalton (1/12 of the mass of an atom of nuclide $^{12}\text{C}$ )

DABS	diazonium benzene sulphonate
DCNU	dichlorophenyldimethylurea
DCPIP	dichlorophenol-indophenol
DGDG	digalactosyldiacylglycerol
DNA	deoxyribonucleic acid
DNase I	deoxyribonuclease I
DTT	dithiothreitol
EDTA	ethylene-diamine tetraacetic acid
EF	exoplasmic fracture face
EPR	electron paramagnetic resonance
FCS	fetal calf serum
FNR	ferredoxin-NADP oxidoreductase
glu	glutamate
gly	glycine
GTP	guanosine 5'-triphosphate
HEPES	N-2-(hydroxyethyl)piperazine-N'-yl)ethane sulphonic acid
his	histidine
IEF	isoelectric focussing
ile	isoleucine
leu	leucine
LHC I	peripheral chlorophyll a/b-binding complex of PS I
LHC II	peripheral chlorophyll a/b-binding complex of PS II

(xx)

LHCF	the major 26 kDa apoprotein of the LHC II in <i>Pisum sativum</i>
lys	lysine
MGDG	monogalactosyldiacylglycerol
mRNA	messenger ribonucleic acid
MV	methyl viologen
NAD <sup>+</sup>	nicotinamide adenine dinucleotide
NADP <sup>+</sup>	nicotinamide adenine dinucleotide phosphate
NADPH	reduced NADP
NP40	Nonidet P40
oligo(dT)	oligo-deoxythymidilic acid
PAGE	polyacrylamide gel electrophoresis
PBS	phosphate-buffered saline*
PEG	polyethylene glycol
PF	protoplasmic fracture face
phe	phenylalanine
PMSF	phenylmethylsulphonyl fluoride
poly(A)	poly-adenylic acid
PS I	photosystem I
PS II	photosystem II
pro	proline
RC I	PS I reaction centre
RC II	PS II reaction centre
RNA	ribonucleic acid

\*See (xxi)



RUBISCO	ribulose biphosphate carboxylase- oxygenase
SDS	sodium dodecyl sulphate
ser	serine
TEMED	N,N,N',N'-tetramethylethylene diamine
thr	threonine
Triton X-100	octyl phenoxy polyethoxyethanol
trp	tryptophan
tyr	tyrosine
val	valine
PBS	140 mM NaCl ; 3 mM KCl, 8 mM Na <sub>2</sub> HPO <sub>4</sub> , 1.4 mM KH <sub>2</sub> PO <sub>4</sub>

**PART 1**

**INTRODUCTION**

### [1.1] The Role of the Chloroplast in Photosynthesis

All biological systems maintain themselves by consuming energy in one form or another. The ultimate source of this energy is the sun, without which the biosphere could not exist. Certain classes of organisms, including the green plants, algae and some bacteria, are able to trap incident solar energy in the form of light and convert it to chemical energy. The chemical energy produced in this way is stored in organic carbon compounds.

This process of energy transduction is termed photosynthesis, and photosynthetic organisms constitute the primary source of food for all other forms of life. In addition to energy trapping and food production, those photosynthetic organisms capable of using water as a source of reducing power also release oxygen which can be utilised in respiration. This form of photosynthesis is believed to be responsible for the present oxygen-rich atmosphere of the Earth (Schopf, 1978).

Cells which can be clearly interpreted as photosynthetic organisms are amongst the earliest fossils yet found (Schopf, 1978). Clearly, photosynthesis is an extremely ancient and important biological process, but unlike certain other important processes it is not

immediately obvious to the casual observer. The first tentative steps towards its recognition came in the 18th century with the work of Joseph Priestley. Priestley noticed that air "burned out" by a candle inside a sealed glass container was incapable of supporting a living mouse. By placing a spray of mint inside the container, the air could be restored ("dephlogisticated") such that it was capable of supporting a mouse for a short while. Priestley had observed, although he did not know it, the light-induced production of oxygen as a by-product of photosynthesis.

Throughout the following century the work of Ingenhousz, de Saussure, Mayer and others showed that plants need light, green pigment (chlorophyll) and carbon dioxide to oxygenate the air, and it was suggested that carbon dioxide was the source of all the organic matter in the plant. The basic process of photosynthesis could be represented in the following way:



Here, carbon dioxide and water are consumed, in the presence of light and chlorophyll, to produce organic matter (represented here as sugar), and molecular oxygen. Today, this comparatively simple equation is known to

summarise an extremely complex system of biophysical and biochemical interactions. Some of these interactions are driven by incident light (the light reactions), but others do not depend on light as their driving force (the dark reactions).

In the cells of eukaryotic photosynthetic organisms, all of the apparatus needed for the photosynthetic process is compartmentalised in subcellular organelles which come under the general name of plastids (Kirk and Tilney-Bassett, 1978). Plastids exist in a variety of forms, but by far the most common form is the green chlorophyll *a* and chlorophyll *b*-containing chloroplast present in all higher plants and some algae. In other algae, plastids may assume a variety of colours due to the presence of various pigment molecules such as phycoerythrin, phycocyanin and fucoxanthin.

The chloroplast is a complex organelle assuming the general shape of a rugby football. Chloroplasts range in size from 3-10  $\mu\text{m}$  in length and 1-5  $\mu\text{m}$  in diameter, but their overall dimensions may vary according to their environment. Structurally, the chloroplast can be broadly divided into three parts. The first of these is the chloroplast envelope which forms a double membrane boundary between the interior of the organelle and the rest of the plant cell. The envelope encloses the fluid matrix or stroma which contains a large number of soluble

proteins, including those involved in the dark reactions of photosynthesis, in addition to many other organic and inorganic components.

The stroma surrounds the extensive internal photosynthetic membrane system composed of flattened sac-like structures termed thylakoids. The thylakoids are structurally very complex and contain the vast majority of the components needed for the light reactions of photosynthesis. The thylakoid membrane system is the site at which incident photons are trapped and energy transduction takes place, and as such, its importance to the chloroplast, the plant cell and to life in general can hardly be overstressed. The features described above are summarised in Figure 1.1, and a more detailed account of chloroplast structure can be found in Section 1.3.

It is clear from the brief discussion above that the chloroplasts of the algae and higher plants are indispensable to the process of photosynthesis, constituting the 'factories' in which energy conversion and primary food production takes place. The possession of such plastids makes possible the autotrophic life of plants, and forms the major distinction between the animal and plant cell.

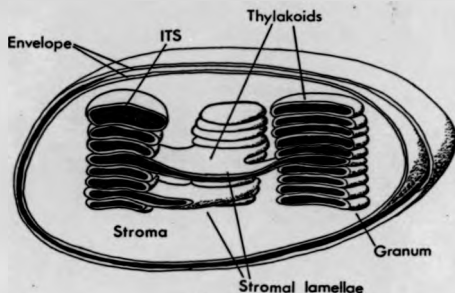


**Figure 1.1** Diagram to show the gross structure of the chloroplast of eukaryotic plant cells. The chloroplast is bounded by an envelope consisting of two closely spaced membranes. Inside the envelope is the hydrophilic phase or stroma, containing proteins, nucleic acids and other organic and inorganic molecules involved in the metabolic functions of the organelle. Within the stroma lies the green photosynthetic thylakoid membrane system. This membrane system consists of a number of flattened sac-like structures (thylakoids), which are believed to form a complex ramifying network enclosing a continuous intra-thylakoid space (labelled ITS in the Figure). The intra-thylakoid space is separated from the stroma by the thylakoid lipid bilayer. The thylakoid is divided into regions of stacked (granal) and unstacked (stromal) lamellae.

### (1.2) Essential Features of Photosynthetic Membranes

In higher plants, the thylakoid membrane is the site of the primary photosynthetic processes, that is, the trapping of light and its conversion to chemical energy which can be used in organic syntheses. The machinery which carries out these processes displays a number of features which are common to all photosynthetic organisms. These features will be briefly described here.

The trapping of light by photosynthetic membranes is achieved by absorption of incident photons by pigment molecules. In higher plants the most important of these pigments is chlorophyll. Photosynthetic pigments are not merely dissolved in the membrane bilayer but are organised into pigment-protein complexes by specific association with hydrophobic proteins embedded in the membrane (Ogawa *et al.*, 1966; Thornber *et al.*, 1967, 1979; Thornber, 1975). This association between pigment and protein creates a microenvironment suitable for the efficient trapping and transfer of excitation energy.

Pigment-protein complexes are divided into two functionally and spectrally distinct classes—the photochemical reaction centres and the light-harvesting complexes. The vast majority of the pigment in the photosynthetic membrane is bound to the light-harvesting complexes. The light-harvesting pigments act to absorb incident photons and pass the resulting excitation energy



to the reaction centre pigments. The reaction centres form the sites at which complex photochemistry takes place to produce an electric voltage across the membrane. A reaction centre and its functionally associated light-harvesting complexes form a photosynthetic unit (Clayton, 1980).

In many organisms, including all the higher green plants, the photosynthetic units occur as two distinct types which differ from each other both in their pigment and protein content, and also in their spectral properties. These different types of photosynthetic unit represent two distinct photosystems termed photosystem I and photosystem II. In the chloroplast thylakoid, the two photosystems are linked via an electron transport chain.

The absorption of a photon by a light-harvesting chlorophyll molecule results in the excitation of an electron in the molecule to an excited singlet state. This excitation then passes among the light-harvesting pigments until it encounters a reaction centre, where separation of the excited electron from a positively charged hole occurs. This charge separation acts vectorially across the membrane, and results from the presence, in the reaction centre, of primary electron acceptors which quickly stabilise the separated charge.

This vectorial movement of electrons sets up a transmembrane electric field capable of driving protons

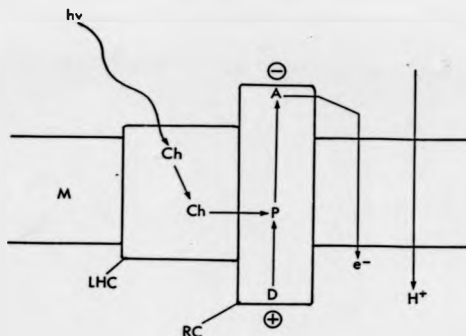
across the lipid bilayer. The resulting proton gradient is utilised as an energy source for the production of adenosine triphosphate molecules (ATP) in the photophosphorylation reaction. In addition to the formation of ATP, transmembrane charge separation also results in the reduction of electron acceptors such as nicotinamide adenosine dinucleotide phosphate ( $\text{NADP}^+$ ) on one side of the membrane, and oxidation of electron donors (such as water) on the other. NADPH provides a source of reducing power for many of the biochemical reactions occurring in the cell.

Figure 1.2 shows a schematic representation of a 'typical' photosynthetic unit, summarising the reactions briefly described above. A more detailed description of these reactions is given by Sauer (1986).

The chloroplasts found in eukaryotic cells are not the only sites of photosynthesis. Many bacteria are also capable of photosynthesis and these are briefly discussed in the next Section.

### 11.3) Photosynthetic Prokaryotes

Photosynthetic prokaryotes do not contain plastids but can themselves be considered analogous to the plastids contained within eukaryotic plant cells. The photosynthetic prokaryotes are composed of three well-defined groups: the blue-green, green and purple



**Figure 1.2** Diagram to show the organisation of a 'typical' photosynthetic unit.

Pigments are organised in the photosynthetic membrane (M) in the form of light-harvesting (LHC) and reaction centre (RC) pigment-protein complexes. When a light-harvesting chlorophyll (Ch) absorbs a photon, the excitation energy is passed around the light-harvesting pigment bed until it reaches the primary electron donor (P) in the reaction centre complex. Excitation of the primary electron donor results in electron transfer to a primary acceptor (A) on one side of the membrane. An electron donor (D) on the other side of the membrane returns the primary donor to its reduced state, resulting in charge separation across the membrane. In bacteria containing only one photosystem, electrons captured by the primary acceptor cycle back to the RC in a cyclical fashion via a proton translocating system. In chloroplasts, the electrons are transported from photosystem II via a proton-translocating electron transport chain to photosystem I in a non-cyclic system. Proton translocation across the membrane results in the production of the transmembrane electrochemical potential used to provide energy for ATP synthesis.

bacteria.

[1.3a] The blue-green bacteria

The blue-green bacteria (cyanobacteria) are a large and diverse group of organisms which possess photosynthetic machinery similar in many respects to that found in eukaryotic cells, particularly those of the red algae. Like the chloroplasts, the cyanobacteria perform oxygenic photosynthesis using water as the primary electron donor and  $\text{CO}_2$  as the photosynthetic carbon source.

The photosynthetic pigments of the cyanobacteria, like those of all other photosynthetic organisms, are associated with specific proteins in the form of pigment-protein complexes (Thorner *et al.*, 1983). These complexes are found in, or attached to the surface of, the photosynthetic membranes which are morphologically very similar to the thylakoids of the higher plant chloroplasts. Also in common with the chloroplasts, cyanobacterial thylakoids contain two distinct photosystems. Other photosynthetic bacteria possess only one photosystem (Thorner, 1986).

One of the chief characteristics which distinguishes the cyanobacteria from the other photosynthetic prokaryotic groups, and which they share in common with the red algae, is the possession of unique antenna

systems called phycobilisomes. Under the microscope these appear as 'Knobs' attached to the outer surfaces of the thylakoids, and they can be easily removed by washing the membranes with aqueous buffers.

Phycobilisomes are complex structures composed of a number of phycobiliproteins to which pigments are bound. These pigments come under the collective name of phycobilins. The phycobilins include phycoerythrin, phycocyanin, allophycocyanin and allophycocyanin B. These pigments are present in the phycobilisomes in a distinctive layered arrangement which allows efficient transfer of excitation energy from the exterior to the interior of the complex (Zuber, 1986). The phycobilins perform an antenna function and are coupled closely with the chlorophyll *a* present in the bacterial photosystem II. Most of the energy absorbed by the phycobilins is trapped by photosystem II, but a large proportion is also transferred from photosystem II to photosystem I reaction centres. Unlike chloroplasts, the cyanobacteria contain no chlorophyll *b* and all the chlorophyll *a* is bound to the two photosystem 'cores' which are embedded in the thylakoid bilayer.

With the exception of the phycobilisomes, the arrangement of the photosynthetic machinery of the cyanobacteria is very similar in pattern to that of the chloroplasts of higher plants. For this reason,

cyanobacterial photosynthesis will not be discussed in detail here, but will be referred to in later Sections of the Introduction concerning the photosynthetic machinery of the chloroplast.

[1.3b] The green and purple bacteria

Both the green and purple bacteria form very small taxonomic groups, there being about 30 recognised species of purple bacteria and only nine species of green bacteria. The members of these two groups are unlike either the cyanobacteria or the chloroplasts of higher plants in that their photosynthesis is anoxygenic. Most of the detailed information concerning the photosynthetic apparatus of these organisms is derived from work carried out on the purple bacteria, and these will form the main subject of this Section.

All purple bacteria are capable of autotrophic existence, using  $\text{CO}_2$  as the main source of carbon. None are capable, however, of oxidising water, and must use reduced inorganic compounds such as  $\text{H}_2\text{S}$  as the electron donor. Purple bacteria can also develop photoheterotrophically in the light under anaerobic conditions at the expense of organic compounds such as acetate.

In general, purple bacteria are divided into two main groups based upon their physiology—the purple sulphur and

the purple non-sulphur bacteria. The purple sulphur bacteria are anaerobic photoautotrophs and use  $H_2S$  as the electron donor, whereas the purple non-sulphur bacteria are predominantly photoheterotrophic and generally find  $H_2S$  to be toxic. The photosynthetic machinery of certain non-sulphur purple bacteria has been particularly well characterised, and work with species of the genus *Rhodopseudomonas* in recent years has pointed towards the first real understanding of the relationship between the structure and function of a photosynthetic reaction centre (Thornber, 1986).

In *Rhodopseudomonas sphaeroides*, as well as other species of photosynthetic bacteria, the cytoplasmic membrane displays invaginations which appear in bacterial sections under the microscope as round vesicles within the cell (Clayton, 1980). The membranes forming the vesicles are specialised photosynthetic structures called intracytoplasmic membranes. These membranes contain the reaction centres and their associated light-harvesting antennae.

The pigment-protein complexes of *Rhodopseudomonas* (*Rps.*) species have been extremely well studied. The first photochemical reaction centres to be successfully isolated were derived from carotenoidless mutants of *Rps. sphaeroides* and *Rps. rubrum* (Reed and Clayton, 1968; Gingras and Jolchine, 1969). The reaction centre complex

of wild-type *Rps. viridis* was isolated soon after (Thornber *et al*, 1969). *Rps. viridis* is a gram-negative non-sulphur photosynthetic bacterium which contains bacteriochlorophyll *b* (BChl *b*), bacteriopheophytin *b* (BPh *b*), and a number of different carotenoids. Most of these pigments are contained within the light-harvesting complexes, only about 1-2% being found in the reaction centres (Thornber, 1986). Each reaction centre contains four molecules of BChl *b*, two molecules of BPh *b*, two different quinones and one carotenoid molecule. In addition, there are also four haem groups and one non-haem iron (Henderson, 1985).

The reaction centre chromophores listed above are bound to reaction centre proteins consisting of four polypeptides, the L, M and H subunits and a C-type cytochrome, of molecular masses 24 kDa, 28 kDa, 35 kDa and 38 kDa respectively (Barber, 1985; Thornber, 1986). The means by which these pigment and protein components fit together to form a functional reaction centre in the bacterial membrane was not known until crystals of the reaction centre were obtained (Michel, 1982). These crystals were shown to retain reaction centre photochemical activity, indicating that the reaction centre complexes had not been denatured by the crystallisation process (Zinth *et al*, 1983).

Successful crystallisation of the *Rps. viridis*



reaction centre complex allowed detailed analysis of its molecular structure by X-ray crystallography (Daisenhofer *et al.*, 1984, 1985). A schematic drawing of the resulting model is shown in Figure 1.3.

Comparison of Figure 1.3 with the generalised reaction centre scheme shown in Figure 1.2 reveals the essential features of the *Rps. viridis* reaction centre. In this bacterium, the primary electron donor (P in Figure 1.2), is represented by a BChl *b* 'special pair' or dimer. The members of this dimer are held in their correct orientation within the membrane by attachment to the L and M protein subunits, and represent the P960 long-wavelength-absorbing species characteristic of the *Rps. viridis* reaction centres.

Both L and M protein subunits contain five membrane-spanning helices which together form a roughly cylindrical structure of length 50 Å, and which is oriented perpendicularly to the plane of the lipid bilayer. Within this cylinder are bound the BChl, BPh and quinone molecules, together with the non-haem iron. The globular cytochrome subunits lie in close proximity to the L and M subunits, and contain the four haem groups. The H subunits also form globular structures associated with the L and M subunit cylinder, but they do not seem to be directly involved in reaction centre charge separation (Barber, 1985).

**Figure 1.3**

Diagram to show the organisation of the photosynthetic reaction centre of *Rhodospseudomonas viridis*. Charge separation occurs after excitation energy is passed from a light-harvesting complex (LHC) to the primary electron donor in the reaction centre (RC). In *Rps. viridis* the primary donor takes the form of a dimer of bacteriochlorophyll *b* molecules (BChl)<sub>2</sub> which are held in close proximity to each other by attachment to the L and M protein subunits. Electrons are passed from this 'special pair' to a molecule of BChl *b* and thence to a molecule of bacteriopheophytin (BPh). Finally, electrons pass to a menaquinone (MQ)-non-haem iron (Fe) complex and then to ubiquinone (UQ). Meanwhile, the oxidised 'special pair' is reduced by donation of electrons from the haem species present in the cytochrome *c* subunit. Ultimately, electrons are derived from the oxidation of a reduced substrate represented as XM in the Figure. The reaction centre has a plane of symmetry perpendicular to the plane of the photosynthetic membrane (M). The L and M protein subunits form a cylinder in the lipid bilayer within which are bound pairs of monomeric BChl and BPh molecules. This arrangement produces two possible electron transport pathways, but evidence suggests that the pathway shown in the Figure is preferred (see text). Based on information in Deisenhofer *et al.*, 1984, 1985; Barber, 1985).

\* See p. 15

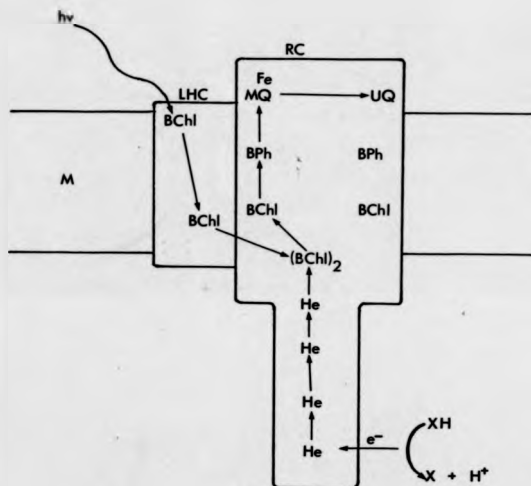


Figure 1.3

The process of charge separation begins when the BChl *b* 'special pair' absorbs excitation energy passed from the light-harvesting pigment bed. Within a few picoseconds, an electron is transferred from the dimer to one of the two monomeric BChl molecules also present in the reaction centre. The electron is then transferred via a BPh molecule to a menaquinone. This process is accomplished within 200 picoseconds of the original energy absorption by the primary donor (Thornber, 1986). This very rapid removal of the unpaired electron from the region of the reaction centre occupied by the oxidised primary donor minimises the chance of a reverse reaction resulting in the reduction of the primary donor and the consequent wastage of absorbed excitation energy. The oxidised primary donor is reduced by electrons transferred from cytochrome-bound haem groups (see Figure 1.3).

The nature of the bacterial reaction centre as a light-driven electron pump can be clearly seen from Figure 1.3. The pigment and protein subunit compositions of the reaction centre complexes of other species of purple bacteria (eg, *Rps. sphaeroides*), and one green filamentous bacterium (*Chloroflexus aurantiacus*) have also been closely studied, and have proved to be strikingly similar to that of *Rps. viridis*. Recently, crystals of the reaction centre of *Rps. sphaeroides* have been obtained, and preliminary analyses suggest that the

detailed structure of this reaction centre is very similar to that of *Rps. viridis* (Chang et al, 1986). It seems likely therefore, that the scheme worked out for *Rps. viridis* will be generally applicable to other photosynthetic bacteria.

The light-harvesting systems of the anoxygenic photosynthetic bacteria are extremely varied. In common with all antenna systems, however, the light-harvesting pigments must be arranged such that there is efficient transfer of excitation energy to the reaction centres. This is generally accomplished by organising the light-harvesting pigment-protein complexes in such a way that the pigments absorbing at longer wavelengths are situated closer to the reaction centres than are the shorter wavelength pigment forms. Such an arrangement produces a heterogeneous energy transfer system, in which excitation energy flows from the shorter to the longer wavelength absorbing pigments, and thence to the reaction centre 'traps' in a directed manner (Zuber, 1986).

As described in Section 1.3a, this kind of directed energy transfer is accomplished in the cyanobacteria by a 'layering' of the phycobilins in the phycobilisome. In the green and purple bacteria it is accomplished by organising the light-harvesting system into core and peripheral antenna species. These are arranged in a concentric fashion around the reaction centres, with

excitation energy passing from the shorter wavelength peripheral forms to the longer wavelength core complexes (Zuber, 1986).

*Rps. viridis* has only one light-harvesting complex. This complex is termed the B1015 complex, B standing for bulk (antenna) pigment, and 1015 denoting the long-wavelength absorption maximum of the BChl. associated with this complex. Other species such as *Rps. sphaeroides* possess two antenna complexes denoted B870 and B800-850. The B800-850 complexes are believed to be situated peripherally to the B870 complexes, which appear to be closely bound to the reaction centres. The reaction centres and the core antenna complexes tend to have a fixed stoichiometry, while the relative amounts of the peripheral antenna complexes can vary according to environmental conditions (Thornber, 1983).

The polypeptides of the light-harvesting complexes are of low molecular mass (less than 10 kDa) and exist as structural heterodimers composed of  $\alpha$  and  $\beta$  subunits (Zuber, 1985). Amino acid sequence analysis of the  $\alpha$  and  $\beta$  subunits from a number of bacterial species indicates that these polypeptides contain polar, charged domains at their N- and C-termini, with a central hydrophobic domain between. This structure strongly suggests a trans-membrane orientation for these proteins (Zuber, 1985, 1986).

The simple light-harvesting antenna system of *Rps. viridis* has been used to investigate the relationship between the light-harvesting complexes and the reaction centres in the membrane. Electron microscopy of the *Rps. viridis* photosynthetic membrane, coupled with Fourier analysis, has yielded some detailed information concerning the structure of the bacterial photosynthetic unit (Miller, 1982). The results suggest that the light-harvesting complexes are arranged around a central reaction centre complex in a highly ordered hexagonal system. Treatment of the photosynthetic membrane with proteases such as trypsin and pronase shows that the reaction centre polypeptides are accessible to digestion while the light-harvesting polypeptides are not (Jacob and Miller, 1983). These results indicate that the light-harvesting complexes are buried in the lipid bilayer, while the reaction centres contain regions which project above the membrane.

The photosynthetic bacteria serve as useful models for understanding the structure and function of the components of photosynthetic membranes. Rather less is known about the detailed structure of the components of the chloroplast thylakoid. The chloroplast will be discussed in the following Section.

#### [1.4] The Chloroplast of Higher Plants

Unlike the photosynthetic bacteria, chloroplasts reside within eukaryotic plant cells and are incapable of an independent existence. As briefly described in Section 1.1, they are composed of three main components, the envelope, the stroma and the thylakoid membrane system. The envelope and stroma will be briefly described here, and the thylakoid membrane and its components will then form the subject of the remainder of the Introduction.

##### [1.4a] The envelope membrane

The chloroplast is bounded by a membrane system called the chloroplast envelope which is a double system composed of an inner and an outer membrane. Electron micrographs reveal that both membranes have a thickness of 60-80 Å, and that they are separated by an intermembrane space approximately 100-200 Å in width (Heber and Heldt, 1981).

The chloroplast envelope is unusual in terms of its protein and lipid content, when judged against other cell and plastid membranes. The major lipid components of the envelope membranes are monogalactosyldiacylglycerol (MGDG), digalactosyldiacylglycerol (DGDG), phosphatidylcholine (PC) and phosphatidylglycerol (PG). These lipids are also present in large amounts in the thylakoids but in different proportions (Douce and



Joyard, 1979). The protein content of the envelope membranes is relatively low. Lipids account for approximately 58% of the total dry weight of these membranes, giving a lipid/protein ratio of 1.2. The corresponding ratio for the thylakoids is about 0.5 (Douce and Joyard, 1979). The protein found in the envelope membranes accounts for only about 0.6-0.8% of the total protein found in the chloroplast (Foyer, 1984).

The inner and outer envelope membranes differ in the amount of integral protein that they contain. Estimates from freeze-fracture studies of spinach chloroplasts indicate that the density of protein particles on the complementary fracture faces of the outer envelope is equal, at about 280 particles  $\mu\text{m}^{-2}$ . The inner envelope shows not only a greater particle density, but also an unequal distribution of particles between fracture faces. Here, the face in closest contact with the stroma shows a particle density of about 1820 particles  $\mu\text{m}^{-2}$ , while the face closest to the cytoplasm shows a density of about 980 particles  $\mu\text{m}^{-2}$  (Sprey and Laetsch, 1976).

The chloroplast envelope forms the boundary between the interior of the chloroplast and the cytoplasm. It is clear therefore that any communication between the chloroplast and the rest of the cell must occur via the envelope membranes. The envelope is not freely permeable to organic and inorganic molecules but displays a high

degree of selective permeability. This selectivity lies primarily with the inner envelope membrane, the outer envelope being freely permeable to molecules with molecular masses up to 10 kDa (Douce and Joyard, 1979; Heber and Heldt, 1981).

A number of substances, including phosphate, ATP and glucose, to which the inner membrane is impermeable, are transported across the membrane by means of specific translocators (Heber and Heldt, 1981). One of the best characterised of these translocators is the phosphate translocator. The phosphate translocator facilitates the export of products of the reductive pentose phosphate pathway (3-phosphoglycerate or triosephosphate) from the chloroplast in exchange for inorganic phosphate. This system of counterexchange across the membrane is common to a number of the envelope translocator systems and serves an important role in the regulation of chloroplast metabolism (Foyer, 1984).

The selective transport of proteins into the chloroplast is also mediated across the envelope. It has become clear that the majority of proteins found in the chloroplast are encoded in nuclear DNA and synthesised on cytoplasmic ribosomes. Such proteins include the small subunit of ribulose biphosphate carboxylase-oxygenase (RUBISCO), and the light-harvesting chlorophyll *a/b* binding protein of the thylakoid (Ellis, 1981). These

proteins are synthesised as higher molecular weight precursors and are actively transported into the chloroplast by an energy-requiring uptake and transport mechanism (Grossman *et al*, 1980). The nature of this selective protein uptake system remains unknown.

In addition to the selective translocation of metabolites and proteins, the envelope is also the site of a number of enzymic activities. These activities include a  $Mg^{2+}$ -dependent ATPase activity of uncertain function (Sabris *et al*, 1970), and the synthesis of galactolipids. The enzyme, UDP-galactose, diacylglycerol galactosyl-transferase, which catalyses the synthesis of MGDC, is known to be localised on the inner envelope (Douce, 1974). The envelope membranes also appear to play a part in the synthesis of carotenoids (Douce and Joyard, 1982).

The chloroplast envelope therefore does not act as a simple barrier between the chloroplast and the rest of the cell, but functions as a selective membrane actively involved in the two-way movement of metabolites and the import of protein from the cytoplasm. In addition to these roles, the envelope acts as the site of synthesis of a number of important organic molecules.

(1.4b) The stroma

The stroma is the name given to the bulk hydrophilic phase of the chloroplast. The stroma contains a bewildering variety of organic and inorganic molecules, and is the site of the photosynthetic dark reactions involving the incorporation of  $\text{CO}_2$  into carbohydrate. In addition, the stroma contains soluble enzyme systems involved in many other biosynthetic pathways such as fatty acid synthesis and nitrogen assimilation, and also contains many intermediary metabolites (Givan and Harwood, 1977).

Approximately 50% of the total chloroplast protein is found in the stroma, the most abundant stromal protein being ribulose biphosphate carboxylase-oxygenase (RUBISCO). This protein accounts for up to 65% of the soluble protein in aqueous leaf extracts (Foyer, 1984). RUBISCO catalyses the first step in the reductive pentose phosphate pathway (Calvin cycle), combining  $\text{CO}_2$  with the phosphorylated, sugar ribulose-1,5-bisphosphate (RuBP), to give two molecules of 3-phosphoglyceric acid (PGA). RUBISCO also displays an oxygenase activity, catalysing the incorporation of oxygen into the RuBP molecule to produce PGA and 2-phosphoglycolate. This reaction is the first step in the photorespiratory pathway (Tolbert, 1980). The same active site on the enzyme is responsible for both the oxygenase and carboxylase activities, and

therefore the presence of oxygen reduces the rate of carbon fixation.

In addition to proteins such as RUBISCO, the stroma also contains DNA, RNA and the polymerase enzymes needed for their replication (Boulter *et al.*, 1972), as well as the necessary machinery for protein synthesis including transfer RNA species and amino acid activating enzymes (Frankl *et al.*, 1965). Although the majority of chloroplast proteins are encoded in the nucleus, the chloroplast genetic system produces about 100 chloroplast polypeptides (Ellis, 1984), including some photosystem reaction centre polypeptides and the large subunit of RUBISCO. The chloroplast genetic system therefore plays a vital role in the development and growth of the plastid.

#### (1.4c) The thylakoid membrane

The thylakoid membrane and certain of its components are the subject of this thesis, and so the remainder of the Introduction will be devoted to this unique membrane system.

As described in Section 1.1, the thylakoid membrane lies within the stroma of the chloroplast, forming a structurally complex ramifying system of flattened, sac-like membranes. This membrane system is thought to be continuous, and to enclose an intrathylakoid space or thylakoid lumen, which is isolated from the stroma

(Anderson, 1981; Ort, 1986; Whittmarsh, 1986).

Perhaps the most striking structural feature of the thylakoids of the higher plants is their arrangement into appressed and non-appressed regions. In the appressed regions, adjacent membrane surfaces approach each other to within distances of 4 nm (Ryrie *et al.*, 1980), and form membrane stacks or grana (Figure 1.1). The non-appressed membrane regions are represented by the end surfaces and margins of the granal stacks which are not in close contact with other membrane surfaces, and by the regions of single membranes (stromal lamellae) which connect the appressed regions. The outer surfaces of the non-appressed membranes are in direct contact with the stroma, while the outer surfaces of the appressed membranes have only restricted access to the stroma (Anderson, 1981). The mechanisms underlying the formation of appressed membrane regions, and their significance to photosynthesis, are not well understood (Ort, 1986). This aspect of the architecture of the thylakoid will be discussed later in the Introduction.

By weight the thylakoid membrane is composed of about 50%-70% protein, 10% pigment and 20%-40% acyl lipid (Ford *et al.*, 1982; Murphy and Woodrow, 1983; Gounaris *et al.*, 1986). Analysis of the protein content of the thylakoid by SDS-polyacrylamide gel electrophoresis (SDS-PAGE) reveals about 40-50 different stainable

protein bands (Andersson and Anderson, 1985; Gounaris *et al.*, 1986), of which a large number are of unknown identity. However, nucleotide sequences have been obtained for the genes encoding fourteen thylakoid proteins (Dyer, 1985; Cramer *et al.*, 1985), and the functions of many of the protein components of the photosynthetic apparatus have been identified. A large number of these proteins have been found to be encoded in nuclear genes and post-translationally imported into the chloroplast (Grossman *et al.*, 1980; Gounaris *et al.*, 1986).

The thylakoids contain all of the chlorophyll present in the plant cell, and are the site of the light-reactions of photosynthesis which result in the production of ATP and NADPH. These products are then utilised in metabolism, including the dark reactions of photosynthesis in which  $\text{CO}_2$  is used as a source of carbon for the synthesis of carbohydrates.

The conversion of light energy to chemical energy in the form of ATP and NADPH requires the co-operation of a number of different reactions. These reactions include the capture of light, the separation of charge across the photosynthetic membrane, electron transport through a coupled series of membrane-bound electron carriers, the translocation of protons, and enzyme catalysis (Andersson and Anderson, 1985). All of these reactions are achieved in and around the thylakoid membrane.

It is clear from the above brief review that the thylakoids, stroma and chloroplast envelope do not function as autonomous entities but are mutually dependent. By their ability to trap and convert light energy, however, the thylakoid membranes provide the driving force necessary to power the numerous biochemical reactions taking place within the chloroplast, and thereby provide the plant as a whole with a source of organic carbon.

[1.5] Photosynthetic Electron Transport and its Components

Many parallels exist between the oxygenic photosynthesis practised by the chloroplast and the anoxygenic photosynthesis practised by the green and purple bacteria. In both systems the photosynthetic pigments are bound to specific proteins, and organised into light-harvesting and reaction centre complexes (Section 1.3). In addition, both systems rely upon the light-induced separation of charge in the reaction centres to produce a transmembrane proton gradient capable of driving ATP synthesis. A major difference between the oxygenic and anoxygenic systems lies in the machinery used to generate this proton gradient.

The anoxygenic photosynthetic bacteria possess only one type of reaction centre (i.e. only one photosystem).



Following the absorption of excitation energy by the reaction centre primary donor, electrons are ejected from the reaction centre on one side of the membrane (see Figure 1.2). These electrons may be used to reduce  $\text{NAD}^+$  (the bacterial equivalent of  $\text{NADP}^+$ ). Where electrons are lost in this way, they are replaced by the oxidation of an external substrate, thus producing a linear flow of electrons from a donor to an acceptor.

Alternatively, electrons may flow back to the other side of the membrane, via a system of electron carriers situated in the lipid bilayer. These electrons are then available for recycling through the reaction centre. Thus, in anoxygenic bacterial photosynthesis, electron transport can be both cyclic and non-cyclic. Coupled to the cyclic electron transport pathway is the translocation of protons from one side of the membrane to the other, producing the transmembrane electrochemical potential required as an energy source for ATP synthesis (Clayton, 1980; Nicholls, 1982). Figure 1.4 shows a generalized scheme for the pathways of photosynthetic electron transport in the anoxygenic bacteria.

Oxygenic photosynthetic systems are characterised by the possession of two distinct kinds of reaction centre representing photosystem I (PS I) and photosystem II (PS II). The two photosystems are linked via a complex electron transport chain, and act in series to produce a



non-cyclic electron flow through the thylakoid membrane. This non-cyclic electron flow is also coupled to proton translocation across the thylakoid and the consequent production of a transmembrane electrochemical potential. This two-photosystem, non-cyclic electron transport chain, and the unique ability to oxidise water, are features which characterise the oxygenic mode of photosynthesis (Ort, 1986). Figure 1.5 shows the non-cyclic electron transport pathway of the chloroplast in a simplified form.

The chloroplast photosynthetic electron transport chain shown in Figure 1.5 has often been represented in terms of an energy diagram represented by the familiar "Z" scheme (Hill and Bendall, 1960). Such diagrams represent the relationships between the components of the chain in terms of their ability to oxidise (remove electrons from) and reduce (donate electrons to) their neighbours in the chain (i.e. their redox potentials). Photosynthetic electron transport is essentially an oxidation-reduction process where each member of the electron transport chain cycles between its reduced and oxidised forms. Reduction of one component is accompanied by the oxidation of the preceding component in the chain.

The following three subsections contain brief discussions of the components of the chloroplast electron transport chain, and the final Sections of the

**Figure 1.5**

Diagrama to show the non-cyclic electron transport pathway in the chloroplast. After absorption of light by a chlorophyll (Chl) molecule in the light-harvesting complex of PS II, (LHC II), excitation energy is transferred to the primary donor (P II) in the reaction centre (RC II). Electrons donated from P II through pheophytin (Ph) to the bound quinones  $Q_A$  and  $Q_B$  are accumulated by the plastoquinone pool (PQ) in the membrane (M). Meanwhile, the primary donor P II is reduced as a result of the oxidation of water, leading to the release of oxygen and protons into the thylakoid lumen. The plastoquinone pool donates electrons to the cytochrome  $b_6/f$  complex which then reduces plastocyanin situated on the luminal side of the thylakoid, thus completing the transport of electrons across the membrane. This translocation of electrons is accompanied by the translocation of protons to the thylakoid lumen (see Section 1.5b(1)). Transfer of excitation energy from the light-harvesting complex of PS I (LHC I) causes oxidation of the the primary donor (P I) and transfer of electrons to the acceptor  $A_0$ . From here electrons are passed to  $NADP^+$  via a series of carriers including ferredoxin (Fd) and a flavoprotein (Fp). For details of the various electron carriers, see text.

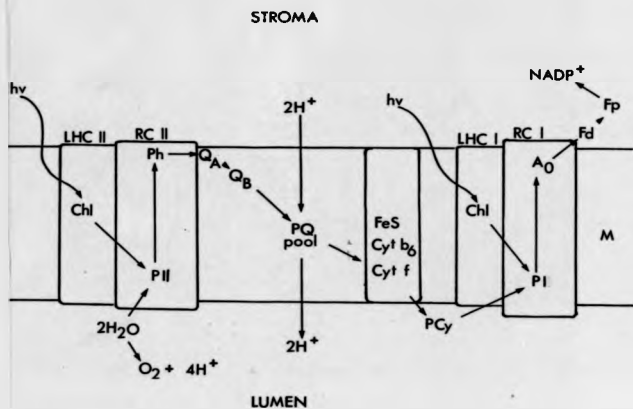


**Figure 1.5**

Introduction will concentrate only on the chlorophyll-containing components.

(1.5a) Chlorophyll-protein complexes

The proteins of the chloroplast thylakoid membrane are organised into four supramolecular complexes. Three of these complexes, the PS II complex, the cytochrome  $b_6/f$  complex and the PS I complex, are directly involved in photosynthetic electron transport. The fourth complex, the ATP synthase, makes use of the transmembrane proton gradient as an energy source for the energetically unfavourable synthesis of ATP (Andersson and Anderson, 1985).

Of the three complexes directly associated with electron transport, only two, the PS I and PS II complexes, bind pigments such as chlorophyll and are capable of photon capture. Like the bacterial photosynthetic units described in Section 1.3, both PS I and PS II complexes consist of two distinct subunits; a central core complex composed of the reaction centre and tightly associated chlorophyll  $a$ -containing complexes, and arranged around this, a peripheral light-harvesting complex which binds both chlorophyll  $a$  and chlorophyll  $b$ .

The core and antenna complexes of PS I and PS II are dealt with in detail in Sections 1.6 and 1.7.

(1.5b) Intersystem electron carriers

Figure 1.5 shows a highly simplified representation of the chloroplast photosynthetic electron transport chain. The two photosystem reaction centres RC I and RC II behave as two light-driven electron pumps acting in series. The two photosystems are connected by a number of intersystem electron carriers which include plastoquinone, the cytochrome  $b_6/f$  complex and plastocyanin.

This visualisation of the electron transport chain would be adequate if the components of the chain were homogeneously distributed throughout the membrane. Work carried out during the last ten years, however, has shown this simple assumption to be invalid. Electron microscope studies using the freeze-fracture technique have shown major differences in the size and density of the freeze-fracture particles found in appressed (stacked) and unappressed regions of the thylakoid (Staehelin, 1976; Staehelin *et al.*, 1977; Arntzen, 1978). This reflects a difference in the content of major thylakoid macromolecular complexes in the two membrane regions (Anderson, 1981).

In addition to the evidence from electron microscopy, studies involving the fractionation of the thylakoids into stacked and unstacked regions by use of detergent or mechanical methods have shown that the structural

heterogeneity of the membrane is accompanied by a functional heterogeneity (Anderson, 1981; Andersson and Anderson, 1985). The sub-thylakoid fractions representing the appressed membrane regions are enriched in PS II, while the unappressed stromal lamellae are enriched in PS I (Arntzen and Briantais, 1975; Arntzen, 1978; Boardman *et al.*, 1978). In the light of this evidence, it has been suggested that there exists in the thylakoid an extreme lateral heterogeneity in the distribution of the two photosystems, PS I being almost entirely confined to the unappressed membrane regions, and PS II being found mainly in the closely-packed membranes of the grana (Andersson and Anderson, 1980).

This heterogeneous lateral distribution of the two photosystems has important consequences for electron transport. If PS II is confined to the grana and PS I to the stromal lamellae, then mobile electron carriers are required to bridge the gap between the two types of reaction centre (Anderson, 1981; Gounaris *et al.*, 1986; Whitmarsh, 1986). The spatial separation between PS I and PS II can be of the order of 1,000 Å (see Whitmarsh, 1986). Thus, electrons need to be transferred very rapidly over long distances in order to maintain the kind of linear electron flow shown in Figure 1.5.



(i) The mobile carriers

The primary candidate for the title of mobile electron carrier is plastoquinone. Plastoquinone is a lipid-soluble molecule consisting of a six-membered carbon ring to which is attached a fifty-carbon chain composed of ten isoprenoid units. Plastoquinone is identical to the ubiquinone found in bacteria except that the plastoquinone carbon ring contains two methyl groups instead of two methoxy groups (Robertson, 1983).

In the chloroplast electron transport chain, plastoquinone performs a dual function as an electron carrier and proton translocator, linking the PS II complex with the cytochrome  $b_6/f$  complex. The electron and proton carrying functions require that two electrons are used to reduce one molecule of plastoquinone. These electrons are derived from the oxidation of  $Q_A$  which acts as a two-electron gate on the reducing side of PS II. During the reduction of plastoquinone, two protons are taken up from the aqueous phase on the stromal side of the membrane, resulting in a fully reduced and protonated plastoquinol molecule (Ort, 1986).

Plastoquinol is oxidised by the cytochrome  $b_6/f$  complex. The mechanism by which this oxidation occurs is complicated and is the subject of some debate (for a brief review see Ort, 1986). Oxidation of plastoquinol results in the regeneration of plastoquinone and the

release of the two bound protons into the aqueous phase on the luminal side of the thylakoid (see Figure 1.5). Thus, plastoquinone carries both electrons and protons from one side of the membrane to the other.

There are several reasons for regarding plastoquinone as the major mobile electron carrier responsible for the movement of electrons between appressed and unappressed membrane regions. One reason for this view is that plastoquinone exists as a delocalised pool in the membrane, each molecule being in potential contact with several electron transport chains (Witt, 1971). This, and other points are briefly reviewed by Anderson (1981).

The major objection to the idea that the mobile entity might be found buried in the lipid bilayer (as would be the case with plastoquinone), comes from the fact that the lipid molecules would impose a drag force on the electron carrier, thereby limiting rates of diffusion and electron transport. This objection has been overcome to some extent by the realisation that the thylakoid membrane is composed chiefly of the galactolipids MGDG and DGDG (Gounaris *et al.*, 1986; Gounaris and Barber, 1983). The highly unsaturated acyl chains of MGDG would produce a high degree of fluidity in the lipid matrix, particularly in the mid-plane of the bilayer where acyl chain movement is at its most fluid (Robertson, 1983). Millner and Barber (1984) have argued

that it is in this mid-plane that plastoquinone shows rapid diffusion rates. The lipids of the thylakoid membrane will be discussed in Section 1.5d.

A second candidate for the role of mobile electron carrier is plastocyanin. This redox component is a nuclear-encoded copper-containing protein with a molecular mass of about 10.5 kDa. Plastocyanin is situated on the inner surface of the thylakoid, and mediates electron transfer between the cytochrome  $b_6/f$  complex and the PS I reaction centre (Gounaris *et al.*, 1986).

The idea that a redox component situated in the thylakoid lumen could mediate long-range electron transfer is an attractive one since it overcomes the objection outlined above for plastoquinone. There is now a substantial body of evidence that the cytochrome  $b_6/f$  complex is distributed randomly between the appressed and non-appressed membrane regions (Cox and Andersson, 1981; Anderson and Malkin, 1982; Allred and Staehelin, 1985). Cytochrome  $b_6/f$  complexes situated in the appressed regions would be partitioned away from the bulk of the PS I reaction centres, and would therefore require a mobile pool of plastocyanin to mediate the reduction of the oxidised PS I primary donor.

It is most probable that both plastocyanin and plastoquinone mediate long-range electron transport in

the thylakoid. This view points towards a picture of the photosynthetic electron transport chain that is somewhat less rigid than that depicted in Figure 1.5. A modified view must incorporate the idea of a long-range lateral segregation of the photosystems accompanied by a delocalisation of electron transport chains as a direct consequence of the need for mobile pools of electron carriers.

#### (11) The cytochrome $b_6/f$ complex

The mobile electron carriers described above are linked in the oxidation/reduction chain by the third major protein complex involved in electron transport, the cytochrome  $b_6/f$  complex.

The cytochrome  $b_6/f$  complex performs the role of a plastoquinol-plastocyanin oxidoreductase and is a multisubunit complex containing cytochrome  $f$ , cytochrome  $b_6$  and the Rieske iron-sulphur protein. In addition this complex also contains a 17 kDa polypeptide of unknown function (Gounaris et al, 1986; Ort, 1986). Besides the PS I and PS II complexes, the cytochrome  $b_6/f$  complex is the only other complex directly involved in the thylakoid electron transport chain (see Figures 1.5 and 1.6).

The mechanism by which the oxidation of plastoquinol and the reduction of plastocyanin is brought about is not clear, but in recent years models involving a Q-cycle of electron flow around the complex have replaced those

involving a more linear flow. Detailed descriptions of the proposed Q-cycle models are beyond the scope of this brief Introduction, but an overview can be found in Barber (1983b) and Ort (1986).

In addition to its role as a plastoquinol-plastocyanin oxidoreductase, the cytochrome  $b_6/f$  complex also plays a role as a ferredoxin-plastocyanin oxidoreductase. Ferredoxin accepts electrons from the reducing side of the PS I reaction centre and then reduces  $NADP^+$  via ferredoxin-NADP oxidoreductase (see Section 1.6b), thus completing the non-cyclic electron transport chain. Alternatively, reduced ferredoxin can participate in cyclic electron flow around PS I by interacting with the cytochrome  $b_6/f$  complex.

The details of the interaction of ferredoxin with the cytochrome  $b_6/f$  complex have not yet been worked out. However, the cytochrome  $b_6/f$  complex isolated from EDTA-washed spinach thylakoids has been found to contain a 37 kDa polypeptide which has been identified as ferredoxin-NADP $^+$  oxidoreductase (Clark *et al.*, 1984). This protein is bound tightly to the surface of the cytochrome  $b_6/f$  complex and is believed to mediate electron transfer from ferredoxin to plastoquinone. Clark *et al.* (1984) have suggested that the location of the ferredoxin-NADP $^+$  oxidoreductase on the cytochrome  $b_6/f$  complex allows it to regulate the distribution of electrons between the

linear or cyclic electron transfer pathways by directing electrons to the stroma (to reduce  $\text{NADP}^+$ ) or to the membrane (to reduce plastoquinone).

#### [1.5c] The ATP synthase

Although not directly involved in the thylakoid electron transport chain, the ATP synthase complex is an essential component of the thylakoid membrane since it performs the vital function of coupling the transmembrane proton gradient to the synthesis of ATP. For this reason it has often been called the 'coupling factor' (McCarty and Carmeli, 1982).

The ATP synthase is composed of two multisubunit components, the  $\text{CF}_0$  and  $\text{CF}_1$  complexes. The  $\text{CF}_1$  component is water-soluble and resides on the outer surface of the thylakoid membrane, where it is associated through ionic interactions with the membrane-intrinsic  $\text{CF}_0$  component. Direct localisation of the ATP synthase complex in thin sections of spinach chloroplasts using immunocytochemical labelling has shown that this complex is restricted to the unappressed regions of the thylakoids (Allred and Staehelin, 1985).

$\text{CF}_1$  is easily seen under the electron microscope, appearing as distinct 'knobs' on the thylakoid membrane surface. It is this component of the ATP synthase which contains the active sites which mediate the synthesis of

ATP (Ort, 1986).  $CF_1$  is composed of five different protein subunits, labelled  $\alpha, \beta, \gamma, \delta$  and  $\epsilon$ , ranging in molecular mass from 14-58 kDa (Gray *et al.*, 1984). There are now thought to be three of the  $\alpha$  and  $\beta$  subunits, and one of each of the other subunits, in each  $CF_1$  complex.

The  $CF_0$  complex is embedded in the thylakoid lipid bilayer and is composed of three types of polypeptide subunit labelled I, II and III, of molecular masses 18 kDa, 16 kDa and 8 kDa respectively (McCarty and Carmeli, 1982; Gray *et al.*, 1984). It is currently believed that six of the subunit III polypeptides form a channel through the membrane, through which protons pass from the intrathylakoid space to the stroma (Gounaris *et al.*, 1986).

The movement of protons from the inside to the outside of the thylakoid via the ATP synthase complex is driven by the transmembrane proton gradient. This proton gradient is set up by the translocation of protons in the opposite direction as a result of electron transport. The means by which this movement of protons back across the membrane is coupled to the phosphorylation of ADP by the  $CF_1$  component is still unclear (Ort, 1986).

#### [1.5d] The lipids

In discussions of the thylakoid electron transport chain, the lipid component of the membrane is often

ignored, the underlying assumption being that the major role of the lipids is to provide a hydrophobic matrix into which protein components are inserted. The rather unusual lipid composition of the thylakoid membrane, however, has prompted the question as to whether thylakoid lipids play a functional as well as a structural role in the photosynthetic membrane (Gounaris *et al.*, 1986).

Up to 50% of the thylakoid lipid is accounted for by MGDG, and a further 25% by DGDG. The phospholipids which predominate in other membranes account for only about 10% of the thylakoid lipids (Gounaris and Barber, 1983; Gounaris *et al.*, 1986). Other lipids present in the thylakoid membrane are sulphoquinovosyldiacylglycerol (SQDG) accounting for about 10% of the of the membrane, and phosphatidylcholine (PC) accounting for less than 5%. In higher plants such as spinach, the fatty acyl chains of the thylakoid lipids are found to be highly unsaturated (Guinn and Williams, 1983).

Several proposals have been put forward for specific roles of the galactolipids in the structure and function of the thylakoid membrane. The first proposal is that these lipids may serve to securely anchor integral membrane proteins in the lipid bilayer (Israelachvili *et al.*, 1980). Lipid molecules such as MGDG have comparatively small head groups and therefore their



overall shape can be approximated to a cone. Such a shape might be useful in packing these lipids around globular proteins in the membrane.

A second proposal is that the unusual complement of thylakoid lipids reflects the existence of specific lipid-protein interactions needed for the correct functioning of the various thylakoid protein complexes. In support of this idea, Siefermann-Harms *et al* (1982) have shown that the addition of MGDG to Triton X-100-solubilised thylakoids brings about a reconstitution of the ability of the LHC II to transfer excitation energy to the photosystem core complexes. Similarly, Pick *et al* (1984) have provided evidence that chloroplast lipids, particularly MGDG, are required for the activation of the ATP synthase complex in reconstituted proteoliposomes.

A means of testing the possibility of specific lipid-protein interactions is presented by the fact that the various thylakoid protein complexes are not uniformly distributed throughout the membrane (see Section 1.5b(1)). Thus, any lipid classes specifically associated with PS II complexes, for example, would be expected to be enriched in granal membrane fractions where the majority of PS II complexes are found.

The search for large differences in the lateral distribution of thylakoid lipids has not yielded

startling results. However, Gounaris *et al* (1983) have reported that MGDG is more prominent in the appressed membrane regions than in the non-appressed regions, although the difference is small compared to differences in protein distribution.

A second approach to the same problem is to subfractionate the thylakoid membrane into its constituent protein complexes and examine any lipids which may co-purify with the proteins. This approach is severely hampered by the necessary use of detergents in the fractionation process. Here, it is difficult to distinguish between specific functional association of lipid and protein and association due to interactions between lipid, protein and detergent. This problem has hindered the interpretation of experimental results. A short review of the results obtained by this approach is given in Quinn and Williams (1983).

A third possible role of the thylakoid lipids is in the maintenance of the very unusual stacked morphology of the thylakoid membrane. The end regions of the granal membranes are subject to extreme curvatures which must inevitably place steric constraints upon the lipids and proteins in the lipid bilayer in these regions. The cone-like shape of the MGDG molecule may be valuable in accommodating and stabilising these structures (a review of this aspect of membrane architecture can be found in

Murphy, 1982).

Figure 1.6 represents a summary of current understanding of the architecture of the thylakoid membrane.

#### [1.6] The Photosynthetic Reaction Centres

##### [1.6a] The photosystem II (PS II) reaction centre (RCII)

As detailed in earlier Sections of this Introduction, photosynthetic reaction centre complexes are those entities which are capable of transducing absorbed light energy to a transmembrane asymmetry in electrical charge. For the purposes of this discussion, the PS II reaction centre, RC II, will be regarded as the pigment-protein unit capable of oxidising water to protons and oxygen, and of reducing plastoquinone to plastoquinol. For convenience, the term RC II will also include those light-harvesting antenna species which are closely bound to the photochemically-active reaction centre. In this sense, RC II corresponds to a PS II core complex. The peripheral chlorophyll *a/b* light-harvesting antenna complex (LHC II) will be dealt with separately in Section 1.7a.

Of the chlorophyll-protein complexes present in the thylakoid, RC II has proved to be the most difficult to

isolate. Early attempts at fractionating the thylakoid into component pigment-protein complexes involved the use of detergents to solubilise the membranes followed by the analysis of the solubilised material by polyacrylamide gel electrophoresis (PAGE). Thornber *et al* (1966, 1967) used sodium dodecyl benzenesulphonate to extract all the thylakoid pigment and protein into aqueous solution. This extract was then subjected to PAGE, resulting in the resolution of three chlorophyll-containing bands termed components I, II and III.

Components I and II were found to contain protein, while component III contained only chlorophyll and carotene, and was therefore regarded as free pigment which had been dissociated from protein during the detergent extraction. Component I was found to have a chlorophyll *a/b* ratio greater than 7, while component II contained chlorophylls *a* and *b* in the ratio 1.1-1.8. Subsequent work resulted in the identification of component I as the PS I reaction centre protein (CP I meaning chlorophyll-protein I), and the identification of component II as a chlorophyll *a/b* light-harvesting complex associated with PS II (CP II) (Thornber, 1975).

Improvements in the procedures used for the detergent extraction of thylakoids resulted in a rather confusing increase in the number of resolvable chlorophyll-containing bands during PAGE, with a corresponding

decrease in the amount of free pigment liberated during extraction. It was not until 1976, however, that the first report of pigmented bands representing the PS II reaction centre appeared (Hayden and Hopkins, 1976).

Delapalme and Chua (1981), working with *Chlamydomonas reinhardtii* and using lithium dodecyl sulphate in conjunction with low temperature (4°C) PAGE, resolved three minor chlorophyll-containing bands in addition to CP I and CP II which they termed CP III, CP IV and CP V. The CP III and CP IV bands were each found to contain one apoprotein of molecular mass 43-48 kDa. The absence of these chlorophyll-containing bands in mutants lacking PS II photochemical activity suggested that they represented the chlorophyll-proteins of the PS II reaction centre. Similar chlorophyll-containing bands were observed by other workers employing different detergents and gel systems (Anderson *et al.*, 1978; Cann and Green, 1980). Two chlorophyll-containing bands analogous to CP III and CP IV have been designated CP 47 and CP 43 or CPa-1 and CPa-2 respectively (Cann and Green, 1980; Green and Cann, 1984).

Evidence has been presented that the photochemically active chlorophyll of the PS II reaction centre (P-680) which acts as the primary electron donor, is associated with the apoprotein of the chlorophyll *a*-containing band CPa-1 (CP 47) (Green and Cann, 1984; Nakatani *et al.*, 1984;

Yamagishi and Katoh, 1984). This apoprotein has an apparent molecular mass of 47 kDa. The 43 kDa apoprotein of CPa-2 has been assigned a role as a chlorophyll *a*-binding light-harvesting polypeptide situated in the PS II core (Green and Cann, 1984).

An additional chlorophyll-containing band often appears in some membrane extraction protocols. This band is called CP29 (29 representing the apparent molecular mass of the single apoprotein of this complex in kDa) (Cann and Green, 1980). This band contains both chlorophyll *a* and chlorophyll *b* and appears to represent a light-harvesting chlorophyll *a/b*-binding complex which is closely associated with the PS II core complex (RC II). CP29 is immunologically unrelated to the major chlorophyll *a/b*-binding complex LHC II.

A second approach to the characterisation of the components of the PS II reaction centre is to prepare a sub-thylakoid fraction containing a minimum number of protein and pigment components, but which is capable of carrying out PS II-mediated photochemistry. Significant progress in this area has come about only within the last several years. A number of preparations are now characterised (Satch and Butler, 1978; Satch *et al*, 1983; Sprague *et al*, 1985), and it has become clear that five different polypeptides are associated with the PS II core complex. These polypeptides range in size from 10 kDa to

47 kDa (Ort, 1986).

The protein with the highest apparent molecular mass is the 47 kDa polypeptide mentioned briefly above. This polypeptide is known to bind chlorophyll *a* (see above), and has been identified as the protein which binds the PS II reaction centre chlorophyll P-680 (Green and Cann, 1984; Nakatani *et al*, 1984). In addition, spectroscopic measurements suggest that this polypeptide, in the CPa-1 form, also binds the PS II primary electron acceptor pheophytin (Nakatani, 1983; Nakatani *et al*, 1984). This polypeptide, therefore, is currently the best candidate for the title of PS II reaction centre protein. Morris and Hermann (1984) have isolated and sequenced the gene encoding this protein from spinach chloroplast DNA. The derived amino acid sequence indicates that the true molecular mass is 56.2 kDa, and that this protein contains seven membrane-spanning regions.

The apoprotein of the CPa-2 complex, the 43 kDa polypeptide, is thought not to be involved in RC II primary photochemistry since it can be removed from the PS II complex without incurring significant loss in photoactivity (Yamagashi and Katoh, 1984).

Two polypeptides in the 30 kDa-34 kDa molecular mass range are found associated with PS II preparations. These polypeptides stain poorly with Coomassie blue in polyacrylamide gels and have been designated D1 and D2.

where D refers to 'diffuse band', but are often assigned molecular masses of 32 kDa and 34 kDa respectively (Arntzen and Pakrasi, 1986). The 32 kDa protein has been designated the  $Q_D$  protein since it can be labelled with photoaffinity probes which interfere with the activity of the redox component  $Q_D$  on the reducing side of the PS II reaction centre. This protein also appears to be involved in the binding of a number of herbicides (Steinback *et al*, 1981). Another feature of the D1 protein is that is very rapidly synthesised and is subject to high rates of turnover in the light (Edelman and Reisfield, 1978; Steinback *et al*, 1981).

The function of the D2 polypeptide at about 34 kDa is not clear. However, the *psbD* gene encoding the D2 polypeptide has recently been sequenced in several different species (Rochaix *et al*, 1984; Alt *et al*, 1984), and shows some sequence homology with the *psbA* gene encoding the D1 ( $Q_D$ ) protein. This homology has prompted the suggestion that the D2 polypeptide may have a quinone-binding function (Rochaix *et al*, 1984).

The smallest protein constituent of the RC II complex is the 10 kDa polypeptide. This has been identified as the apoprotein of cytochrome b-559. Information gained from the examination of cloned DNA encoding cytochrome b-559 from spinach, however, indicates that this protein may be a heterodimer composed of a 9.4 kDa and a 4.4 kDa



protein (Arntzen and Pakrasi, 1986). The precise function of cytochrome b-559 in the RC II complex is still a matter of debate.

In addition to the complement of polypeptides described above, three more proteins, situated peripherally to the core complex, are directly involved in the oxidation of water and the donation of electrons to the PS II reaction centre. These three polypeptides are water-soluble, have apparent molecular masses of 33 kDa, 23 kDa and 16 kDa, and are situated on the inner surface of the thylakoid membrane. All three polypeptides can be released from everted membrane vesicles by washing with alkaline Tris (Yasamoto and Nishimura, 1983; Akerlund, 1983). The release of the 33 kDa polypeptide is correlated with the loss of manganese. This correlation does not apply to either the 23 kDa or the 16 kDa polypeptide (Andersson, 1986). It is beyond the scope of this Introduction to examine the mechanism of water oxidation, but a useful review of current ideas may be found in Yocum (1986).

All the RC II polypeptides described above, with the exception of the three polypeptides directly involved in water oxidation, are now known to be encoded by genes located in the chloroplast genome.

Recent advances in the isolation and cloning of many of the RC II genes, and a comparison of their sequences

with known sequences of genes encoding bacterial reaction centre proteins, have led to a re-appraisal of the role of some of the polypeptide components of the PS II reaction centre. It has been pointed out that the sequence of electron acceptors in the RC II complex has some similarities to that of purple bacteria (Mathis, 1987). These similarities include the fact that there are two quinones ( $Q_A$  and  $Q_B$ ) present in the PS II reaction centre (compare Figure 1.3). Also, pheophytin is believed to be the primary acceptor in PS II, and this reduces  $Q_A$ . Thirdly, a non-haem iron interacts with both  $Q_A$  and  $Q_B$  in a similar manner to that found in bacterial reaction centres (Rutherford and Zimmerman, 1984).

It might be expected that similarities in the organisation of reaction centre redox components might be reflected in primary sequence homologies of some of the reaction centre polypeptides. Such homologies have been reported between the L and M subunits of the reaction centres of the purple bacteria and the D1 and D2 polypeptides of the RC II (Barber, 1986; Mathis, 1987). Like the L and M subunits of the purple bacteria, the D1 and D2 polypeptides may both contain five membrane-spanning helices. In addition, the localisation of four histidine residues on the D1 and D2 proteins is similar to those believed to be involved in the binding of the non-haem iron in the L and M subunits. This similarity

suggests that the non-haem iron present in the RC II complex may be bound in a similar way.

If the D1 and D2 polypeptides represent the reaction centre proteins, then the 47 kDa and 43 kDa proteins must be considered as chlorophyll *a*-binding light-harvesting proteins. Furthermore, the possible involvement of D1 in the binding of the reaction centre redox components leaves open the question of the rapid turnover of this protein, and its functional significance.

Although significant progress has been made in the identification and characterisation of the RC II components, little is known of the overall molecular organisation of this complex, especially the precise nature, location and orientation of some of the redox components on the oxidising side of the reaction centre. Such detailed information will have to await X-ray studies on crystals of the purified complex.

Figure 1.6 includes a schematic representation of current understanding of the RC II complex.

[1.6b] The photosystem I (PS I) reaction centre (RC I)

For the purposes of this discussion, the RC I complex will be considered to be that entity which is capable of carrying out the light-induced oxidation of plastocyanin and reduction of ferredoxin, coupled with the generation of a transmembrane asymmetry of electrical charge.

Although intrinsically easier to isolate, the RC I complex is currently less well characterized than the RC II complex. As briefly described above, early work involving the analysis of detergent-solubilised thylakoids by PAGE produced a chlorophyll-containing band in polyacrylamide gels which was designated CP I. This green band was later characterized as a PS I chlorophyll-protein complex, and was found to contain a photochemically active chlorophyll P-700, the primary donor of PS I. Typically, there were found to be about 40 chlorophyll *a* molecules for every P-700 molecule in these preparations (Thornber, 1986).

The CP I complex was found to contain a polypeptide with an apparent molecular mass of about 68 kDa, and this was identified as the P-700-chlorophyll-apoprotein (Chua *et al.*, 1975). There remains some doubt as to the number of protein subunits in the CP I complex. It is often the case that two closely-migrating protein bands, or one very broad band in the 60kDa-70 kDa molecular mass range, are observed when the CP I complex is subjected to denaturing SDS-PAGE (Chua *et al.*, 1975; Vierling and Alberte, 1983). The presence of two protein bands with similar apparent molecular masses has been explained by invoking proteolytic breakdown of a single component (Chua *et al.*, 1975).

Vierling and Alberte (1983), have shown that the two

protein bands of 58 kDa and 62 kDa derived from the CP I of *Hordeum vulgare* L. yield very similar proteolytic breakdown patterns upon treatment with either *S. aureus* V8 protease or cyanogen bromide. In addition, Vierling and Alberte (1983) found that the use of the protease inhibitor PMSF in the preparation procedure did not prevent the appearance of two CP I protein bands, indicating that proteolysis may not be responsible for the presence of two polypeptides in this complex. These authors suggested that the PS I reaction centre complex CP I contains two very similar polypeptides which may be no more than conformational variants of a single polypeptide species. The idea that these two polypeptides are different is supported by the fact that it has been shown that the two CP I polypeptides are coded for by two genes with slightly different sequences in maize (Fish et al, 1985).

It is now clear that in addition to P-700, there are about 40-60 chlorophyll *a* molecules present in the CP I complex (Wollman, 1986). Since these chlorophyll molecules must be bound to the two CP I polypeptides which presumably bind the P-700 molecule, there would seem to be no prospect of isolating a native PS I reaction centre which is further enriched with P-700. This is in contrast to the reaction centre of PS II where, in principle, it might be possible to isolate a

reaction centre complex which is stripped of all internal light-harvesting pigments, and yet is able to carry out the primary photoact. This complication will create difficulties for the study of the detailed structure of the PS I reaction centre.

The primary donor P-700 was first characterised by Kok in the 1950's, and it was believed until recently that P-700 represented a chlorophyll a 'special pair' (cf the purple bacteria) (Malkin, 1982). This view of P-700 as a chlorophyll a dimer is now being challenged by evidence that the unpaired electron of the oxidised form of P-700, (P-700<sup>+</sup>), is held on only one chlorophyll a molecule (Setif and Mathis, 1986).

Since the discovery of the iron-sulphur centre A by low temperature EPR (Malkin and Bearden, 1971), the PS I reaction centre has been extensively studied in terms of the kinetics of electron transfer from P-700 to primary electron acceptors.

The PS I reaction centre is currently known to possess five redox components in addition to the primary donor P-700. These components have been labelled A<sub>0</sub>, A<sub>1</sub>, F<sub>x</sub>, F<sub>A</sub> and F<sub>B</sub> (Mathis, 1987), and operate as electron acceptors between P-700 and ferredoxin. The precise nature of some of these components, and the detailed pathway of electron flow through the reaction centre have not yet been worked out.

The first two electron acceptors in the pathway from P-700 to ferredoxin are  $A_0$  and  $A_1$ . The chemical nature of these two redox components is uncertain. It has been suggested that  $A_0$  is a chlorophyll *a* species, but the available evidence on this point is not strong (Setif and Mathis, 1986). Component  $A_1$  is not chlorophyll *a*, but its real identity is unknown.

Two of the remaining three redox components ( $F_A$  and  $F_B$ ) have been shown to be iron-sulphur centres (Malkin, 1982; Setif and Mathis, 1986). The identity of the  $F_X$  component is not clear, but it may be a third iron-sulphur centre (Setif and Mathis, 1986). There is some confusion as to the precise role of these three components in the transfer of electrons from P-700 to ferredoxin. It has been proposed that  $F_A$  and  $F_B$  act in parallel in the transfer of electrons to ferredoxin (Golbeck and Warden, 1982). Malkin (1984), however, has shown that treatment of spinach chloroplast membranes with diazonium benzene sulphonate (DABS) causes modification of the  $F_B$  component resulting in the loss of the ability of  $F_A$  to be reduced at low temperatures. This result implies that  $F_B$  reduces  $F_A$  as part of a linear electron transfer pathway.

The confusion concerning the electron transport pathway on the reducing side of P-700 is further compounded by the fact that there exists an alternative

cyclic electron transport pathway around PS I. It has been suggested that the iron sulphur centre  $F_A$  acts primarily to pass electrons to soluble ferredoxin and  $NADP^+$  in the non-cyclic electron transport pathway, while  $F_B$  is involved in the cyclic pathway. In this scheme, the redox component  $F_X$  acts as a common source of electrons for both  $F_A$  and  $F_B$  (Malkin, 1982). It is clear that more experimental evidence is needed on this point.

Electrophoretic methods of preparing the CP I complex indicate that up to 30% of the total chlorophyll in the thylakoid is present in the PS I reaction centre (Malkin, 1982). However, the 60 kDa-70 kDa polypeptides present in such preparations are now known not to be the only chlorophyll-proteins associated with PS I. A number of studies using non-electrophoretic methods for the preparation of PS I-containing sub-thylakoid fractions have shown that at least five other proteins are associated with the PS I reaction centre.

Bengis and Nelson (1975) produced a purified PS I preparation from Swiss chard which contains six polypeptides designated Subunits I, II, III, IV, V and VI. These polypeptides show apparent molecular masses of 70 kDa, 25 kDa, 20 kDa, 18 kDa, 16 kDa and 8 kDa respectively. Subunit I represents the CP I P-700-binding apoprotein. This Subunit was further purified by treatment of the PS I preparation with SDS. The resulting



preparation was found to be capable of supporting the light-induced reversible bleaching of P-700, but incapable of mediating the photoreduction of  $\text{NADP}^+$  (Bengis and Nelson, 1975; 1977). These results indicate that the 70 kDa polypeptide contains a primary electron acceptor ( $A_{0.7}$ ) in addition to the P-700 primary donor, but lacks other redox components situated between P-700 and ferredoxin.

The functions of the other lower molecular weight polypeptides were investigated by treatment of the PS I preparation with SDS and Triton X-100 in order to selectively deplete the preparation of specific polypeptides (Bengis and Nelson, 1977). The resulting evidence suggested that Subunit III (20 kDa) mediates electron transfer from plastocyanin to P-700. In addition, subunits IV, V and VI are positioned on the reducing side of the reaction centre between ferredoxin and P-700.

Evidence that an 8 kDa polypeptide from a spinach PS I preparation contains one of the iron-sulphur centres has been put forward by Lagoutte *et al* (1984), while Bonnerjee *et al* (1985) have identified a 19 kDa polypeptide as a possible iron-sulphur centre protein.

Mullet *et al* (1980a) have produced a PS I preparation by solubilising EDTA-washed pea thylakoids with low concentrations of Triton X-100. This procedure results in

a PS I preparation which contains about 110 chlorophyll molecules per P-700 (designated PS I-110), and at least eleven different polypeptides. These include two reaction centre polypeptides at 68 kDa and 66 kDa, and a number of lower molecular weight polypeptides ranging in apparent molecular mass from 10.5 kDa to 21 kDa. In addition to these protein components, this preparation also contains three or four polypeptides between 22 and 24 kDa which can be easily removed by further Triton detergent treatment. These polypeptides have been assigned to a peripheral PS I light-harvesting complex (LHC I) (Mullet *et al.*, 1980a; Haworth *et al.*, 1983). This light-harvesting complex will be discussed in detail in Section 1.7b.

The LHC I-depleted PS I preparation contains about 65 chlorophyll molecules per P-700, and has been designated PS I-65 (Mullet *et al.*, 1980a). PS I-65 is enriched with chlorophyll *a* forms absorbing at 697 nm and shows a 77 K fluorescence emission maximum at 722 nm. This preparation can be further fractionated by additional detergent treatment to produce a PS I reaction centre complex containing about 40 chlorophyll molecules per P-700. This fraction, designated PS I-40, contains chlorophyll *a* absorbing at 680 nm and 690 nm, and showing a 77 K fluorescence maximum at 694 nm. PS I-40 seems to be equivalent to CP I.

The sequential removal of chlorophylls from PS I-110,

and the existence of the PS I-65 form, indicates that in addition to the LHC I and the 40 chlorophyll *a* molecules associated with PS I-40, there seems to be at least one tightly-bound internal light-harvesting system in the PS I reaction centre (Mullet *et al*, 1980a). Which of the lower molecular weight PS I polypeptides binds these internal light-harvesting chlorophylls is at present unknown.

At the present time the available data indicate that the PS I reaction centre (RC I) is composed of two polypeptides of between 60 kDa and 70 kDa which bind the primary donor P-700, at least one primary electron acceptor and approximately 40 chlorophyll *a* molecules. Also included in the reaction centre are at least five other lower molecular weight polypeptides. Some of these polypeptides are responsible for binding the iron-sulphur centres which mediate electron transport from the primary acceptors to ferredoxin, while others may be the apoproteins of at least one internal chlorophyll *a*-containing light-harvesting complex.

The 60-70 kDa RC I polypeptides are known to be encoded in the chloroplast genome and synthesised on chloroplast ribosomes (Gray *et al*, 1984; Wollman, 1986). The site of synthesis of the lower molecular weight polypeptides is not clear, although several reports from different species suggest that some of these proteins may

be encoded in the nuclear genome and synthesised on cytoplasmic ribosomes (Nechushtai and Nelson, 1981; Nechushtai *et al.*, 1981; Westhoff *et al.*, 1983). The RC I complex is therefore composed of the products of both plastid and cytoplasmic protein synthesis.

Figure 1.6 includes a model which summarises the current understanding of the structure of the RC I complex.

#### 1.7] The Light-Harvesting Antennae

It will be evident from the discussions in Section 1.6 that the light-harvesting antennae of the two photosystems are not simple structures, but are composed of a number of complexes bound to a greater or lesser degree to the photochemically active reaction centre complexes. This Section will consider only the peripheral chlorophyll *a/b*-containing light-harvesting complexes.

##### 1.7a] The light-harvesting antenna of PS II (the LHC II)

The LHC II is by far the most abundant of the thylakoid protein complexes, comprising about 30% of the total thylakoid protein and up to 50% of the chlorophyll (Bennett, 1983). It is also the most intensively studied. The literature dealing with this chlorophyll-protein complex is very extensive, and it is only possible here to describe some of its salient features.

The LHC II was first discovered in the form of the chlorophyll-containing band CP II when detergent-solubilised thylakoids were subjected to PAGE (see Section 1.6a). CP II was found to contain almost equal amounts of chlorophylls *a* and *b*, and was attributed to PS II. The discovery that the chlorophyll *b*-less *chlorina* f2 mutant of barley contained no CP II, and yet displayed PS II activity, prompted the conclusion that CP II was not a reaction centre but represented a PS II light-harvesting complex (Thorner and Highkin, 1974).

Unlike the photosynthetic reaction centres, a light-harvesting complex has no characteristic photochemical activity by which it can be defined. Any definition of such complexes must be in terms of the procedures used to purify them. Thorner (1975) proposed that CP II should be termed the light-harvesting chlorophyll *a/b* protein. Since the discovery of at least two other chlorophyll *a/b*-binding complexes in the thylakoid (CP29 and the LHC I), this term has become rather ambiguous. Throughout this thesis I shall refer to the CP II complex as the LHC II (light-harvesting complex II), and the major 26 kDa apoprotein of the LHC II as the LHCP (light-harvesting chlorophyll protein).

The LHC II can easily be prepared in large quantities by the method described by Burke *et al* (1978). This method involves the solubilisation of unstacked thylakoid

membranes with Triton X-100. The solubilised membrane material is then subjected to sucrose density gradient centrifugation to achieve partial separation of the LHC II from other thylakoid complexes. The most highly fluorescent sucrose gradient fractions are then treated with  $MgCl_2$  which specifically precipitates the LHC II by a poorly understood mechanism (see Section 2.13e). Such LHC II preparations contain chlorophylls *a* and *b* in a ratio of approximately 1.2, as well as the xanthophylls, neoxanthin and lutein.

The polypeptide content of LHC II preparations varies significantly between species (Bennett, 1983). In pea there is a major stainable LHC II polypeptide with an apparent molecular mass of 26 kDa, and two or three minor polypeptides between 24 kDa and 27 kDa. Studies employing inside-out and right-side-out thylakoid vesicles have shown that the apoproteins of the LHC II span the thylakoid membrane, although they are only vulnerable to protease attack at the outer surface of the thylakoid (Andersson *et al.*, 1982). Furthermore, the LHC II is thought to exist in oligomeric form in the thylakoid. This idea is based on a number of observations, including the behaviour of this complex in certain mildly denaturing gel electrophoresis systems (eg Markwell *et al.*, 1978).

The LHC II plays both a structural and functional

role in the operation of the thylakoid membrane. In addition to its light-harvesting role, it appears to play an important part in the mechanism of membrane stacking. When thylakoids are washed in media of low ionic strength they unstack and the thylakoid protein complexes become randomly distributed throughout the bilayer (Staehelin, 1976). Subsequent addition of monovalent or divalent cations to these unstacked membranes causes the formation of stacked membrane regions, accompanied by a lateral segregation of the RC II and LHC II complexes into the appressed membranes (Staehelin, 1976).

The cation-mediated grana formation described above can be strongly inhibited if thylakoids are pre-treated with trypsin. This protease selectively cleaves a 2 kDa surface-exposed fragment of the LHCP while having no apparent effect upon other components of the membrane (Steinback *et al.*, 1978). It has also been shown that cations induce aggregation of proteoliposomes into which purified LHC II has been incorporated. This cation-induced aggregation is also largely abolished by prior trypsin treatment (Ryrie *et al.*, 1980). It therefore appears that the surface-exposed fragment of the LHCP plays an important role in the formation of grana.

The mechanism underlying cation-induced grana formation is not clearly understood, but models involving the electrostatic screening of negative membrane surface

charge have gained some acceptance (for a full explanation of this idea see Barber, 1980).

The phenomenon of thylakoid membrane stacking is closely associated with a second important function of the LHC II, its role in State 1-State 2 transitions. It has been known for some time that oxygen-evolving photosynthetic organisms can regulate the rate at which the two photosystems function in order to maintain non-cyclic electron transport at its most efficient under given lighting conditions (Bonaventura and Myers, 1969). Such regulation is necessary because the two photosystems do not absorb light maximally at the same wavelengths.

When plants are exposed to light which preferentially excites PS II (light 2), PS II reaction centres become overexcited with respect to PS I reaction centres. This causes a net reduction of the intersystem electron transport chain. To overcome this, an adaptive change takes place which results in a redistribution of some of the PS II excitation energy to the PS I pigment bed, thus balancing the rate of electron flow through the reaction centres. This situation is called State 2 (Barber, 1983a; Bennett, 1983). Conversely, when PS I reaction centres are overexcited with respect to PS II (light 1), excitation energy becomes redistributed in favour of the PS II pigment bed (State 1).

The first clue to the mechanism of these State 1-



State 2 transitions came with the discovery of the light-induced phosphorylation of the LHCP, together with a number of other PS II-located polypeptides, by a membrane-bound kinase(s) (Bennett, 1977; 1979). The kinetics of phosphorylation of the LHCP correlates with the kinetics of State 1-State 2 transitions.

Dephosphorylation of the LHCP was shown to occur in the dark and is mediated by a membrane-bound phosphatase (Bennett, 1980). It was later shown that the protein kinase activity was sensitive to the redox state of the thylakoid plastoquinone pool (Allen *et al.*, 1981; Horton *et al.*, 1981). Light 2 produces a net reduction of the plastoquinone pool which activates the membrane-bound kinase resulting in phosphorylation of the LHCP. Similarly, light 1 causes a net oxidation of the plastoquinone pool resulting in inactivation of the kinase and dephosphorylation of the LHCP (Allen *et al.*, 1981; Bennett, 1983).

The scheme discussed above explains how the thylakoid detects an imbalance in the rate of excitation of the two photosystems, but does not explain how LHCP phosphorylation rectifies this imbalance. A number of lines of evidence have shown that the phosphorylation of the LHCP leads directly to a transfer of excitation energy to PS I at the expense of PS II. This evidence usually takes the form of ATP-induced fluorescence

changes in isolated thylakoids measured at either room temperature or at 77 K. Under conditions conducive to protein phosphorylation, ATP induces a slow decrease in chlorophyll fluorescence at 20°C and an increase in the fluorescence emanating from the PS I pigment bed relative to that from the PS II pigment bed at 77 K (Bennett *et al.*, 1980; Horton and Black, 1981; Allen *et al.*, 1981). These observations are consistent with an ATP-induced redistribution of excitation energy from PS II in favour of PS I, implying that phosphorylation of the LHCP causes the LHC II to donate excitation energy to PS I instead of PS II.

Currently available evidence suggests that phosphorylation of the LHCP component of the LHC II causes this complex to migrate laterally through the lipid bilayer from the appressed to the non-appressed membranes, where it has a greater chance of donating absorbed excitation energy to the PS I pigment bed (Kyle *et al.*, 1983). Dephosphorylation of the LHCP causes the LHC II to re-associate with the PS II reaction centres in the appressed membranes. It has been shown that the phosphorylation sites of the LHCP reside on the surface-exposed, trypsin-sensitive N-terminal fragment (Bennett, 1980). This observation has prompted the idea that the proposed lateral migration of the LHC II is a consequence of changes in electrostatic surface charge screening

brought about by the addition of charged phosphate groups to the surface-exposed part of the protein (Barber, 1983a).

A subtle complication of this model, based upon the analysis of room-temperature fluorescence induction transients, suggests that it is not only phosphorylated LHC II complexes which move laterally in the membrane, but phosphorylated LHC II attached to RC II complexes. This idea implies that there are two populations of PS II reaction centres, a mobile population ( $\beta$  centres) which specifically associate with phosphorylated LHC II complexes, and a static population ( $\alpha$  centres), which are essentially confined to the appressed membranes and are associated with non-phosphorylated antenna complexes (see Kyle *et al.* 1982). The alternative view suggests that only the phosphorylated LHC II complexes are mobile. These may form a specific mobile sub-group of the total LHC II population in the thylakoid (see Barber, 1983a). This problem has not yet been resolved.

The biosynthesis of the protein component of the LHC II has been studied in detail at the levels of transcription, translation and post-translational assembly into the holocomplex (Bennett *et al.* 1984). The LHCP is encoded in nuclear DNA in the form of a multigene family (Dunsavir *et al.* 1983; Tinko and Cashmore, 1983). These genes have been designated *Cab* genes. The LHCP

polypeptides are synthesised on cytoplasmic ribosomes (Apel and Kloppstech, 1978; Cusing and Bennett, 1981). The product of synthesis is a 32 kDa precursor polypeptide which is then post-translationally imported into the chloroplast, processed to its mature (26 kDa) size, ligated with its pigment components and inserted into the thylakoid membrane. The precise sequence in which the uptake, processing and assembly events occur is not known.

In addition to the 32 kDa LHCP precursor, there exists a second polypeptide of 30 kDa which is strongly immunologically related to the 32 kDa protein, and which is often observed as a product of the *in vitro* translation of poly(A)-enriched mRNA. It has been suggested that this polypeptide may be the precursor to the minor 24 kDa polypeptide component of the LHC II (Cusing and Bennett, 1981), but no clear proof of this contention has been presented. Recently, however, Stayton *et al.* (1986) have isolated a *Cab* gene in petunia which encodes a polypeptide showing the same apparent molecular mass as the 30 kDa component on SDS-PAGE. This new *Cab* gene differs from other petunia *Cab* genes in that the functionally important N-terminus of the mature polypeptide which it encodes is significantly diverged from the N-terminal of other petunia LHCP polypeptides.

The short polypeptide fragment which is removed when

the precursor is cleaved to the mature form is not related to any of the equivalent fragments of other petunia LHCP proteins. Evidence concerning the relationship between the precursor polypeptide which this new petunia *Cab* gene encodes, and specific LHC II polypeptides in the thylakoid, has not yet been published.

The role of light in the control of synthesis of the LHCP has come under close scrutiny since the appearance of cloned nucleic acid probes for the genes encoding this protein, and it has become clear that photocontrol can act at several stages in the synthesis of the LHCP.

It has been shown by cDNA/RNA hybridisation experiments that LHCP mRNA is detectable in etiolated pea seedlings, although no LHCP is immunologically detectable (Bennett *et al*, 1984). A proportion of this mRNA is translatable in the wheat germ system (Cumling and Bennett, 1981). This result contrasts with that found in etiolated barley leaves, where no LHCP mRNA was found (Apel and Kleppstech, 1978). Upon continuous illumination of etiolated pea seedlings, the amount of LHCP mRNA increases. This increase in mRNA is accompanied by the appearance of immunologically detectable LHCP in the greening buds.

Although LHCP mRNA is detectable in etiolated pea seedlings, the levels of LHCP mRNA in the plant seems to

be under at least partial phytochrome control (Jenkins *et al.*, 1983; Bennett *et al.* 1984; Gollmer and Apel, 1983). The amount of LHCP message does not necessarily correlate with the amount of LHCP in the plant. This is not only evident in etiolated plants but also in plants which have been grown under intermittent illumination (2 min light, 118 min dark). No LHCP is detectable in etiolated pea seedlings which have undergone 48 h intermittent illumination, but levels of translatable LHCP mRNA are 50% of those in plants treated to 48 h continuous illumination (Cuming and Bennett, 1981).

The fact that LHCP mRNA is detectable in polysomes isolated from intermittently-illuminated peas, and that such polysomes can be successfully 'run off' *in vitro*, indicates that the failure of accumulation of the LHCP under intermittent light is due to some form of post-translational control (Cuming and Bennett, 1981). Synthesis of the LHCP in greening plants continues when the plants are placed in darkness. Under these conditions, however, the LHCP fails to accumulate in the thylakoid membrane due to polypeptide turnover in the dark (Bennett, 1981; Cuming and Bennett, 1981). It has been argued that turnover of the LHCP in the absence of light is a direct result of the lack of chlorophyll synthesis in the dark (Bennett, 1983).

The synthesis of both chlorophyll *a* and chlorophyll *b*

is necessary for the accumulation of the LHCP in the thylakoid, but not sufficient for its stabilisation, since some pre-existing LHCP is degraded when greening peas are returned to darkness (Bennett, 1981). It is possible that complete stabilisation of the LHC II in the developing thylakoid requires not only chlorophyll synthesis, but also some additional factor such as incorporation of the complex into appressed membranes (see Bennett, 1983).

[1.7b] The light-harvesting antenna of photosystem I  
(the LHC I)

Compared to the LHC II, the LHC I is poorly characterised both in terms of its protein components and its synthesis. The first identification of polypeptides which might be involved in a peripheral light-harvesting antenna complex specifically associated with PS I was made in 1980 (Mullet *et al.*, 1980a). This work involved the isolation of a PS I complex from unstacked pea thylakoids which had been treated with Triton X-100. The PS I-110 complex prepared in this way contains approximately 110 chlorophyll molecules per P-700, and also contains three or four polypeptides in the molecular mass range 22.5-24.5 kDa which are not usually present in PS I particles prepared by other methods (see Section 1.6b).

It was found that further treatment of PS I-110 with Triton X-100 resulted in the selective removal of the 22.5-24.5 kDa proteins. The loss of these proteins was accompanied by the loss of approximately 45 chlorophyll molecules per P-700 and a shift in the 77 K fluorescence emission maximum of the complex from 730 nm to 722 nm. It was concluded that the 22.5-24.5 kDa polypeptides represent the apoproteins of a peripheral light-harvesting complex associated with the PS I core complex. It was further concluded that this peripheral complex contains the chlorophyll species responsible for the 77 K fluorescence emission maximum characteristic of the PS I pigment bed.

The correlated loss of protein and chlorophyll from a PS I preparation, however, does not constitute proof of the existence of a PS I peripheral light-harvesting complex. Efforts were therefore made in several laboratories to isolate such a complex intact. By treating a PS I-110 preparation with the detergents dodecyl  $\beta$ -D-saltoside and Zwittergent 16, Haworth *et al* (1983) were able to isolate a chlorophyll-protein complex which contains the three or four polypeptides in the molecular mass range 21-23.5 kDa, plus a much less prominent polypeptide with an apparent molecular mass of 10 kDa. This complex, designated LHC I, also contains chlorophyll *b*, displaying a chlorophyll *a/b* ratio of



about 3.7.

In addition to its polypeptide and chlorophyll content, the LHC I isolated by Haworth *et al* displayed a 77 K fluorescence maximum at 730 nm. This was interpreted as strong evidence that the LHC I isolated by this method was in a native state.

A spinach LHC I isolated by the method of Haworth *et al* was fractionated further by treatment with Triton X-100 (Lam *et al*, 1984a). This fractionation procedure results in the isolation of two chlorophyll-containing complexes designated LHCPIa and LHCPIb. LHCPIa was found to contain two polypeptide components with apparent molecular masses of 22 kDa and 23 kDa. LHCPIb was found to be heavily enriched with a 20 kDa protein. Both fractions display chlorophyll a/b ratios of between 3.0 and 4.0.

The 77 K fluorescence spectrum of the LHCPIa preparation gave one maximum at 680 nm, while that of the LHCPIb preparation gave a single maximum at 730 nm. This difference was interpreted as indicating that the chlorophyll species in each of these two complexes were held in slightly different environments. Thus it is the LHCPIb pigments that are responsible for the long wavelength 77 K fluorescence maximum typical of PS I in the thylakoid (Lam *et al*, 1984a). This idea is supported by the work of Kuang *et al* (1984), who have demonstrated

that the long-wavelength (730 nm-735 nm) 77 K fluorescence emission maxima observed in several different LHC I preparations is clearly associated with the pigment species bound to a 21 kDa LHC I apoprotein.

A second method for preparing LHC I involves the solubilisation of a PS I-110 sample with a mixture of Triton X-100 and lithium dodecyl sulphate (Lam *et al.*, 1984b). The solubilised material can then be analysed by either SDS-PAGE or by column chromatography. The LHC I preparation resulting from these procedures contains only one polypeptide with an apparent molecular mass of 20 kDa, and displays a chlorophyll *a/b* ratio of between 3.0 and 4.0. The 77 K fluorescence spectrum of this LHC I complex shows an emission maxima at 681 nm, and only a broad shoulder at longer wavelengths. The status of this complex is uncertain, but it is probable that the loss of the long wavelength fluorescence emission maxima at 730 nm is indicative of a perturbation of the structure of the complex during the isolation procedure.

A PS I complex containing both CP I and the LHC I can be isolated by treating thylakoids with SDS and then subjecting the solubilised material to either SDS-sucrose density gradient centrifugation or mildly denaturing SDS-PAGE (Anderson *et al.*, 1978; Argyroudi-Akoyunoglou, 1984). Because of its spectral similarity to the CP I complex isolated by mildly denaturing SDS-PAGE, this

complex has been designated CP Ia (Anderson *et al.*, 1978).

CP Ia can be further resolved into its two chlorophyll-containing components CP I and LHC I (Argyroudi-Akoyunoglou, 1984). Once again, the LHC I complex isolated by this method is found to contain only one polypeptide with an apparent molecular mass of 21 kDa. The 77 K fluorescence emission spectrum of this LHC I preparation shows emission maxima at 691 nm and 717 nm, the exact position of the short-wavelength maxima varying between preparations. It is highly probable that the existence of only one polypeptide in this LHC I preparation, and the absence of a 77 K fluorescence maximum at or above 730 nm is the result of partial denaturation of the complex during the isolation procedure.

From the above brief survey of current LHC I isolation methods it is clear that this complex exists as a chlorophyll *b*-containing entity which is closely bound to the periphery of the RC I complex. Any analogy with the LHC II must be limited however, since there is currently no evidence of the existence of any mobile sub-population of LHC I complexes. In addition, unlike the LHC II, the LHC I may be composed of two distinct sub-complexes, one containing a 20 kDa-21 kDa polypeptide (LHCPIb), and another less stable complex containing two polypeptides of 22 kDa-24 kDa (LHCPIa).

In *Chlamydomonas reinhardtii* an LHC I complex has been reported which contains at least five protein subunits ranging in apparent molecular mass from 18 kDa to 27.5 kDa (Wollman and Bennoun, 1982). This complex also contains chlorophyll *b* but exhibits a 77 K fluorescence maximum at 707 nm (Wollman and Bennoun, 1982). It would thus appear that this green alga contains a LHC I which is spectrally and structurally different from that found in higher plants.

The antenna function of the LHC I has been demonstrated in an experimental system involving the reconstitution of the LHC I with an antenna-depleted PS I core complex (Ortiz et al, 1984). Here, the relative size of the PS I light-harvesting antenna was determined indirectly by measuring the rate constant of P-700 photooxidation ( $K_{P-700}$ ). It was found that the rate constant for the antenna-depleted PS I preparation was about half that for the preparation containing the LHC I. Reconstitution of the LHC I with the antenna-depleted PS I core complex was found to substantially restore the P-700 photooxidation rate.

At the commencement of the current work, little was known concerning the synthesis and assembly of the LHC I. The currently available evidence suggests that the LHC I polypeptides are encoded in the nucleus, are synthesised on cytoplasmic ribosomes and are imported into the

chloroplast, exactly as for the LMCP. The chief source of evidence for this conclusion are the results obtained from *in vitro* protein uptake experiments involving isolated intact chloroplasts (Mullet *et al*, 1981). These experiments involved the translation of poly(A)-enriched RNA in a wheat-germ *in vitro* system. The radiolabelled translation products were then incubated with isolated intact chloroplasts in the light. Thylakoid polypeptides which had been imported into the chloroplasts and assembled in the thylakoids were analysed by fractionation of the thylakoids into their constituent protein complexes by the method of Mullet *et al* (1980a). The results indicated that the polypeptides involved in the peripheral light-harvesting complex of PS I were imported (but see Section 3.6).

Mullet *et al* (1980b) have reported that the apoproteins of the LHC I are absent from cucumber plants that have been subjected to intermittent illumination. These authors also reported that in common with the polypeptides of the LHC II, the LHC I apoproteins were absent from the thylakoids of a chlorophyll *b*-less barley mutant. Both these results indicate that at least some of the controls acting on the assembly of the LHC I may be similar to those acting on the LHC II (Mullet *et al*, 1980b; Lee *et al*, 1984a).

It must be stressed, however, that these studies did

not involve the use of specific antibodies to identify the LHC I apoproteins. Although a lack of antibodies does not constitute a problem where the protein of interest is abundant and easily identified by SDS-PAGE, immunological identification becomes necessary where the protein does not constitute a major component of the sample under study. This case is often true in developing systems, where controls acting on the accumulation of a given polypeptide may result in the polypeptide being present at very low levels.

At the present time no information is available concerning the possible regulation of synthesis of the LHC I apoproteins at the levels of transcription and/or translation.

#### (1.8) Aims of the Present Research

At the time when the present study was commenced two major aspects of the molecular biology of the peripheral light-harvesting system of PS I were in need of study. Firstly, the individual polypeptides of the LHC I had been characterised only in terms of their apparent molecular masses, and no information was available regarding their structural relationships, either with one another, or with the apoproteins of other thylakoid chlorophyll-binding complexes. Secondly, very little work had been carried out on the synthesis and assembly of the

## LHC I.

The work reported in this thesis was designed to investigate aspects of both of the problems listed above. In addition, it was intended to characterise two novel methods for preparing sub-thylakoid fractions containing the PS I reaction centre and its associated LHC I. The PS I material prepared by these methods would be compared with a 'standard' PS I preparation in the form of the PS I-110 particle of Mullet *et al* (1980a). Comparisons would be carried out in terms of polypeptide and chlorophyll content, the ability to carry out PS I-mediated photochemical activity, and also by electron microscopy.

The structural relationships of the LHC I proteins would be investigated using two approaches. Firstly, polyclonal and monoclonal antibodies would be raised against the LHC I apoproteins, and these would be used to probe possible immunological similarities between the individual LHC I polypeptides. At the same time the possibility of immunological relationships with other chlorophyll proteins, especially the LHCP, would be investigated. The LHCP is of particular interest here since it binds a similar complement of pigments, performs a similar peripheral light-harvesting function, and displays some aspects of its synthesis in common with the LHC I apoproteins (see Sections 1.7a and 1.7b).

The second means of exploring the structural relationships of the LHC I apoproteins would be by the use of specific proteolytic agents to generate partial peptide maps whose patterns could be directly compared.

The synthesis of the LHC I apoproteins and their assembly in the thylakoid would be investigated as far as possible by immunological techniques. Once again, special emphasis would be placed upon a comparison with the LHCP of PS II.



Figure 1.6

Schematic representation of the architecture of the thylakoid membrane. In this model the membrane is divided into appressed and non-appressed regions with a corresponding lateral asymmetry in the distribution of the components of the electron transport chain. PS II reaction centre complexes are largely confined to the appressed membrane regions, while PS I and ATP synthase complexes are located chiefly in the unappressed stromal lamellae and granal end regions. The cytochrome  $b_6/f$  complex is believed to be evenly distributed throughout the thylakoid membrane.

The oxidation of the primary donor of PS II (P-680) results in the production of a strong oxidant (Z) which removes electrons from water. This process involves the three polypeptides of the water-splitting complex and manganese in a way which is not yet understood. Pheophytin removes electrons from P-680 and passes them to  $Q_A$  and  $Q_B$ . In this model, the D1 and D2 polypeptides are shown as the reaction centre proteins, with the 43 kDa and 47 kDa polypeptides acting as core light-harvesting proteins. These roles could be reversed. Bound to the PS II core complex are bound and mobile forms of the LHC II. The mobile form is in the unphosphorylated state.

$Q_A$  acts as a two-electron gate reducing plastoquinone to plastoquinol. Plastoquinol is oxidised by the cytochrome  $b_6/f$  complex, liberating protons into the thylakoid lumen. Electrons are then passed to plastocyanin (PCy) which reduces oxidised P-700. The pathway of electron transport between P-700 and ferredoxin (Fd) is not well characterised but involves at least five redox components, some of which are protein-bound iron-sulphur centres. The non-cyclic electron transport pathway is completed with the reduction of NADP<sup>+</sup> via ferredoxin-NADP oxidoreductase (FNR). The cyclic pathway (dotted line) involves the oxidation of Fd by FNR bound to the cytochrome  $b_6/f$  complex. Phosphorylated mobile LHC II can be seen in close proximity to the LHC I of PS I. The ATP synthase complex can be seen at the edge of the picture. The small number associated with each polypeptide represents the approximate molecular mass of the protein in kDa.

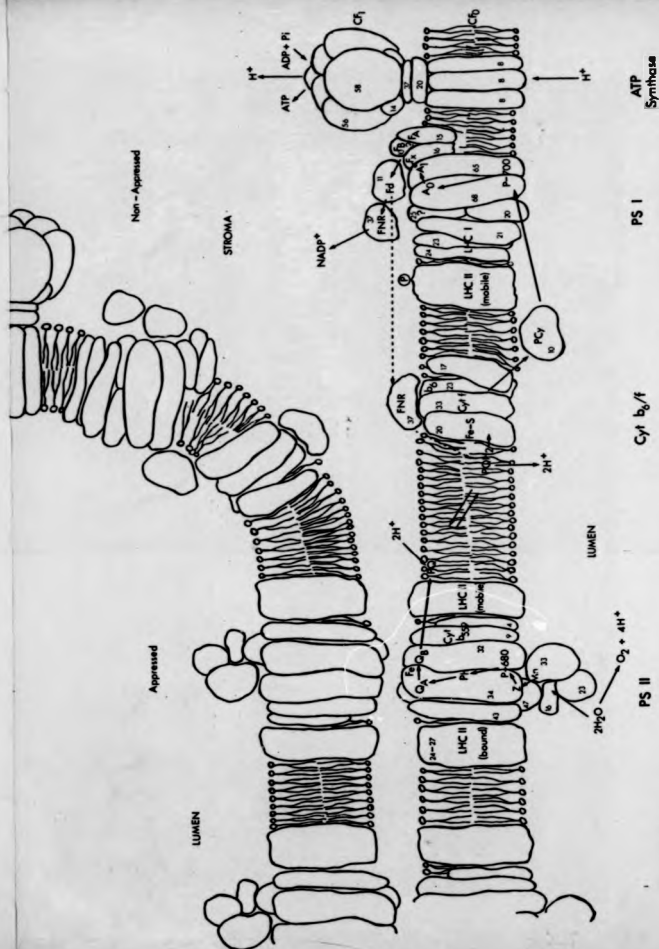


Figure 1.6

**PART 2**

**MATERIALS AND METHODS**

(2.1) Materials

All chemicals and biochemicals used were of the highest analytical grade available. All materials were obtained from the Sigma Chemical Company, Poole, Dorset, except those listed below.

BDH Chemicals, Poole, Dorset: Acrylamide, bromophenol blue, Nonidet-P40, ammonium persulphate, sodium lauryl sulphate (sodium dodecyl sulphate, SDS), N-2-(hydroxyethyl)piperazine-N'-yl)ethane sulphonate acid (HEPES), citric acid, potassium dihydrogen orthophosphate, di-potassium hydrogen orthophosphate.

Fisons plc, Loughborough: Ethylene-diamine tetraacetic acid (EDTA), sucrose, magnesium chloride, sodium chloride, glycerol, sorbitol, liquified phenol (89% w/w in water), acetic acid, butan-1-ol.

Worthington Diagnostic Systems Inc., New Jersey, U.S.A.: staphylococcal V8 protease.

ICN Biochemicals, High Wycombe, Bucks.: Rabbit anti-mouse IgG (RAM).

Eastman Kodak, Rochester, New York, U.S.A.: N-N'-methylene bisacrylamide, N,N,N,N'-tetramethylethylene diamine (TEMED).

Uniscience, Cambridge: Oligo(dT)-cellulose.

Calbiochem-Behring Corp., La Jolla, California, U.S.A.: Zwittergent 3-16, Dodecyl- $\beta$ -D-maltoside, Miracloth.

Amersham International, Little Chalfont, Bucks.: L-[ $^3$ H]-methionine (not less than 1,000 Ci/mole), [ $^3$ H] (350-600 mCi/ml).

## (2.2) Growth of Plants

### (2.2a) Normal growth

Seeds of *Pisum sativum* L. var Feltham First (Charles Sharpe and Co., Sleaford) were sown in 3 cm of 'Levingtons' potting compost (Fisons plc, Ipswich) in seed trays, the compost thoroughly soaked, and the trays placed under 'warm white' 80 W fluorescent tubes (Philips), emitting photosynthetically active radiation (400-700 nm) with a quantum flux density of 50  $\mu\text{mol}/\text{m}^2/\text{s}$  at the level of the tray. The seeds were allowed to germinate and grow under a 12 h photoperiod at a temperature ranging between 17°C and 24°C. Seed trays

were lightly watered every second day.

Under these growth conditions, pea seedlings were found to germinate after 24 h and to emerge from the soil after 3-4 days. After eight days growth the third node leaves and stipules were folded but expanding, and after ten days were fully expanded. For PS I preparations plants were harvested at 11-12 days from sowing.

(2.2b) The etiolation system

Pea seeds were sown in exactly the same way as described in Section 2.2a, except that less water was applied to the compost in order to reduce the risk of fungal growth. The seed trays were then placed in sealed cupboards inside a light-tight dark growth room and left to germinate and grow for 7 days at a constant temperature of 22°C. After 7 days, the plants were placed under a light box containing two 'warm white' 20 W fluorescent tubes, delivering a quantum flux density of  $33 \mu\text{m}^2/\text{s}$  at the level of the seed tray. Greening of the etiolated plants was continued under these conditions for 48 h, after which time plants were either subjected to further illumination or returned to the dark for later harvesting.

### (2.2c) Intermittent Illumination

Pea seeds were sown in compost and left for 7 days in the dark as described in Section 2.2b. After this time, the plants were transferred to a sealed, light-tight cupboard containing a single, 40 W domestic electric light bulb. The bulb was connected to a timer which caused the bulb to light for 2 min in every 2 h period. Plants were subjected to this light regime for 48 h, after which time they were placed under continuous illumination as described in Section 2.2b.

### (2.3) Polyacrylamide Gel Electrophoresis

Analysis of protein mixtures by SDS-polyacrylamide gel electrophoresis, (SDS-PAGE), was carried out using a variety of gel compositions to suit different purposes. All buffer systems used were based on those described by Laemmli (1970). Gels were cast between glass plates measuring 20 cm x 20 cm, separated by spacers of thickness 1.5 mm. Where good resolution of the apoproteins of the LHC I was required, larger glass plates measuring 40 cm x 20 cm were used giving a gel twice the standard length. Gels incorporating gradients of acrylamide were poured with the aid of a two-chambered gradient maker, where the solution of lowest acrylamide concentration was pumped into and mixed with the solution of highest acrylamide concentration, at half the rate

that the latter was pumped between the glass plates. In all cases, glycerol was used to stabilise the acrylamide gradient prior to polymerisation. Immediately before pouring, solutions were degassed under vacuum and an appropriate volume of fresh 10% (w/v) ammonium persulphate (APS) was added. Polymerisation was initiated by the addition of N,N,N',N'-tetramethylethylenediamine (TEMED). After pouring, gels were overlaid with 1 ml of iso-butanol. Routinely, gels were left to polymerise overnight. Following this, a stacking gel was cast above the resolving gel and a Teflon comb was employed to make slots in the stacking gel into which samples could be loaded.

The compositions of the different acrylamide solutions used to make polyacrylamide gels are given below. Volumes quoted are designed for standard gels of 40 ml total volume.

For a 10%-30% linear acrylamide gradient:

The 10% acrylamide solution:

Acrylamide	7.3 ml of a stock containing 30% (w/v) acrylamide and 0.8% (w/v) bisacrylamide.
Water	11.7 ml
3 M Tris-HCl (pH 8.8)	2.75 ml
10% (w/v) SDS	0.22 ml



TEMED	10 $\mu$ l
10% (w/v) APS	50 $\mu$ l
The 30% acrylamide solution:	
Acrylamide	11 ml of a stock containing 60% (w/v) acrylamide and 0.3% (w/v) bisacrylamide.
Glycerol	8 ml of a 75% (w/v) stock solution.
3 M Tris-HCl (pH 8.8)	2.75 ml
10% (w/v) SDS	0.22 ml
TEMED	10 $\mu$ l
10% (w/v) APS	20 $\mu$ l

For a 10%-16% linear acrylamide gradient:

The 10% acrylamide solution is made as above.

The 16% acrylamide solution:

Acrylamide	11.73 ml of a stock containing 30% (w/v) acrylamide and 0.8% (w/v) bisacrylamide.
Glycerol	7.3 ml of a 75% (w/v) stock solution.
3 M Tris-HCl (pH 8.8)	2.75 ml
10% (w/v) SDS	0.22 ml
TEMED	10 $\mu$ l
10% (w/v) APS	100 $\mu$ l

For a 20% single concentration gel:

Acrylamide	26.66 ml of a stock containing 30% (w/v) acrylamide and 0.8% (w/v) bisacrylamide.
3 M Tris-HCl (pH 8.8)	5.0 ml
10% (w/v) SDS	0.4 ml
Water	7.94 ml
TEMED	15 $\mu$ l
10% (w/v) APS	150 $\mu$ l

For 10ml of stacking gel solution:

Acrylamide	5.0 ml of a stock containing 10% (w/v) acrylamide and 0.5% (w/v) bisacrylamide.
Water	2.4 ml
62 mM Tris-HCl (pH 6.8)	2.4 ml
10% (w/v) SDS	0.1 ml
TEMED	5 $\mu$ l
10% (w/v) APS	100 $\mu$ l

Protein samples were prepared for SDS-PAGE by solubilisation in SDS sample buffer. This was done in two stages. Firstly, the protein sample was resuspended in a solution containing 0.1 M sodium carbonate and 0.1 M

dithiothreitol (DTT). Once thoroughly resuspended in this solution, an equal volume of a solution containing 4% (w/v) SDS, 15% (w/v) glycerol and 0.01% bromophenol blue was added, and the resulting solution mixed. The material was then routinely boiled for 2 min prior to loading on the gel, unless otherwise stated. Electrophoresis buffer consisted of 25 mM Tris, 192 mM glycine (pH 8.3), 0.1% (w/v) SDS. Electrophoresis was carried out at 18 mA for 16 h in the case of 10%-30% gradient gels, or at 10 mA for 16 h in the case of 10%-15% gradient gels. Gels were run at room temperature.

#### [2.4] Gel Staining and Destaining

##### [2.4a] Coomassie blue

For Coomassie blue staining, the composition of the stain was as follows:

50% (v/v) methanol

7% (v/v) acetic acid

0.025% (w/v) Coomassie blue

Once made, the stain was filtered and used no more than three times. Gels were routinely stained for 1.5 h at room temperature with constant shaking, then destained. For identification of protein bands for amino acid sequencing, gels were stained for no more than 15 min.

Destain was made up as follows:

40% (v/v) methanol

7% (v/v) acetic acid

Gels were destained at room temperature with constant shaking until no background stain remained in the gel matrix. Destained gels were then photographed and dried down under vacuum at 70°C for 1.5 h.

#### [2.4b] Silver staining

The method used to silver stain polyacrylamide gels is based on that of Wray et al (1981). Gels were soaked in at least three changes of reagent grade methanol for 24 h to ensure removal of Tris and glycine from the acrylamide matrix. The following solutions were then made up:

Solution A: 20% (w/v) silver nitrate in distilled water.

Solution B: 21 ml 0.36% NaOH was mixed with 1.4 ml 14.8 M ammonium hydroxide.

Solution C: Solution A was added dropwise to Solution B then increased to 100 ml with water.

The gel was soaked for 15 min in solution C, (the staining solution), with constant agitation, then washed in deionised water for a further 5 min. Following this, the developing solution was made up as follows:

Solution D: 2.5 ml 1% (w/v) citric acid was mixed with 0.25 ml 38% formaldehyde. This was increased to 500 ml with water.

The gel was soaked in solution D to develop the silver stain for at least 5 min, and then washed in deionised water. Development of the stain was arrested by soaking the gel in 45% (v/v) methanol, 10% (v/v) acetic acid. Where the stain was overdeveloped and an objectionable dark background appeared, the gel was destained with Kodak Rapid Fix until the background was reduced. Destaining was arrested by soaking the gel in 50% (v/v) methanol. The gel was then photographed and dried down as described in Section 2.4a.

#### [2.5] Autoradiography

Polyacrylamide gels containing [<sup>35</sup>S]-methionine-labelled polypeptides were stained and dried as described in Section 2.4a. The dried gels were exposed to X-Omat S X-ray film (Kodak) inside light-tight cassettes (Harzer) at room temperature. Where radioactivity was low (below 25,000 c.p.m per track), the stained wet gel was soaked for 30 min in Amplify (Amersham) at room temperature prior to being dried down. Gels thus treated were subject to autoradiography at -80°C in the presence of an intensifying screen (Dupont Cronex Lightning-Plus). Where polyacrylamide gels contained [<sup>32</sup>P]-labelled

polypeptides, autoradiography was carried out at room temperature with no intensifier present.

Autoradiography of nitrocellulose filters bearing [ $^{125}$ I]-labelled proteins was carried out at  $-80^{\circ}\text{C}$  in the presence of an intensifying screen. In all cases, the exposure time was determined empirically by short-term test exposures. After exposure, X-ray film was developed for 5 min in fresh Kodak DX-80 or LX-24 (diluted 5-fold), then fixed for 10 min in fresh Kodak FX-40 (diluted 5-fold). Film was then washed in running tap water, rinsed in distilled water and dried in air.

#### (2.6) Densitometric Scanning of Stained Gels

The stained wet polyacrylamide gel to be scanned was carefully laid on a glass plate and overlaid with a second glass plate such that no air bubbles were trapped between the glass and gel surfaces. Small volumes of water were periodically introduced between the glass plates to prevent the drying of the gel. The glass plates containing the gel were then laid on the mobile carriage of the scanning densitometer (Joyce-Loebl, Tyneside). Stained gel tracks were scanned for 80 s using wedge 1050. Data were automatically collected and printed using a BBC model B microcomputer. Data were analysed using dedicated software (Warwick Control Systems, UK).

## [2.7] Two-Dimensional Gel Electrophoresis

The method used for two-dimensional gel electrophoresis of thylakoid polypeptides followed closely that described by Roscoe and Ellis (1982), using isoelectric focussing (IEF) in the first dimension and SDS-PAGE in the second.

Thylakoid membranes were washed in 10 mM Tris-HCl (pH 8.0) containing 5 mM 2-mercaptoethanol, and sedimented at 30,000xg for 10 min. The pellet was then resuspended in the same buffer and the final volume measured. Four volumes of acetone were added, the sample thoroughly mixed, and proteins left to precipitate on ice for 30 min in the dark. The protein precipitate was then pelleted by centrifugation at 4,000xg for 10 min and the supernatant retained for the determination of extracted chlorophyll (Section 2.17). The acetone wash was repeated and the resulting pellet dried under a stream of nitrogen. The dry pellet was resuspended in 100  $\mu$ l of water to give as fine a suspension as possible, and to this was added an equal volume of 10% (w/v) SDS. The suspension was solubilized as far as possible by passing the liquid up and down a micropipette tip, and the solution was then transferred to an Eppendorf microcentrifuge tube and boiled for 2 min. The boiled solution was cooled under flowing water and to this solution was added four volumes of 'lysis buffer' (LB - 9.5 M (w/v) urea, 1.6% (v/v)

ampholines of pH range 5.0-7.0, 0.4% (v/v) ampholines of pH range 3.5-10.0, 5% (v/v) 2-mercaptoethanol, and 2% (v/v) Nonidet P40). The resulting solution was subjected to centrifugation at 12,000xg for 5 min to remove any unsolubilised material, and the supernatant loaded onto IEF tube gels.

The acrylamide solution used to form the IEF gels was made up as follows:

Urea (Ultrapure grade)	5.5 g
Nonidet P40	2 ml of a 10% (w/v) stock solution.
Acrylamide	1.33 ml of a stock solution containing 28.3% (w/v) acrylamide and 1.6% (w/v) bisacrylamide.
Water	1.97 ml
Ampholines	0.4 ml pH range 5.0-7.0 0.1 ml pH range 3.5-10.0

The urea was dissolved by warming the solution at 37°C in a constant temperature water bath. The solution was thoroughly mixed and 10 µl of 10% (w/v) APS were added. The solution was then degassed under vacuum and 10 µl TEMED added. Gels were formed in glass tubes measuring 120 x 7 mm. Once poured, each gel was overlaid with 50 µl of 8 M urea. Once polymerised, the 8 M urea was removed and replaced with 50 µl LB followed by 50 µl



'sample overlay buffer' (SOB - 9.0 M urea, 0.8% (v/v) ampholines of pH range 5.0-7.0, and 0.2% (v/v) ampholines of pH range 3.5-10.0). The gels were then placed in a tube gel apparatus, the lower reservoir filled with 0.01M  $H_2PO_4$  and the upper reservoir filled with degassed 0.02 M NaOH. Gels were pre-run at 200 V for 15 min, 300 V for 30 min, and 350 V for a further 30 min. After this time the upper reservoir was drained and the samples loaded onto the gels. Routinely, thylakoid protein representing 20-30  $\mu$ g chlorophyll was loaded per gel. Loaded protein samples were overlaid with 50  $\mu$ l SOB and the upper reservoir refilled with buffer. Gels were run for 16 h at a constant 350 V.

After focussing, gels were carefully removed from their glass tubes by injection of water between glass and gel from a syringe, and the gels were either used for second dimension electrophoresis, or wrapped in silver foil and stored at  $-80^\circ C$  for future use.

Second dimension SDS-PAGE was carried out as described in Section 2.3. Polyacrylamide gels incorporating a 10%-16% acrylamide gradient were poured between standard glass plates and left to polymerise. A stacking gel was poured above the resolving gel to within 2 mm of the edge of the notched glass plate. The stacking gel was overlaid with distilled water and allowed to polymerise. IEF gels were equilibrated in 3x10 ml of 'SDS

sample buffer' (SSB - 62 mM Tris-HCl (pH 6.8), 10% (w/v) glycerol, 2% SDS, and 0.5% (v/v) 2-mercaptoethanol). They were then carefully laid on the stacking gel surface and all air bubbles between the two gels removed. The IEF gels were sealed in place with melted 1% (w/v) agarose containing SSB and 5% (v/v) 2-mercaptoethanol. The gels were run for 16 h as described in Section 2.3.

#### (2.8) Proteolytic Mapping of Purified Polypeptides

Partial proteolysis of polypeptides provides a useful means by which their structural relationships may be compared. Similarities in the patterns of peptide fragments produced by partial proteolysis of different proteins imply similarities in structure. In this study, partial proteolysis of the light-harvesting polypeptides of PS I and PS II was used, in conjunction with antibody work, to investigate possible structural relationships between proteins performing very similar functions.

Samples of purified P1, P2, P3, and the LHCP were subjected to digestion using either staphylococcal V8 protease or cyanogen bromide. For digestion by V8 protease, the method described by Cleveland *et al.* (1976) was used. Apoproteins of the LHC I were purified by gel electrophoresis and electroelution as described in Section 2.14. LHC II was purified as described in Section 2.13a. The three purified LHC I polypeptides, and a

sample of purified LHC II containing 20  $\mu$ g of chlorophyll, were subjected to SDS-PAGE on a single concentration (20%) gel for 16 h at 18 mA. The gel was stained and destained, and the bands representing the LHC I apoproteins and the 26 kDa polypeptide of the LHC II were excised using a razor blade. These excised gel strips were equilibrated in 10 ml of equilibration buffer (62.5 mM Tris-HCl (pH 6.8), 0.1% (w/v) SDS, and 1 mM EDTA) for 30 min at 22°C with occasional shaking. Each strip was then carefully placed in a slot cast in a 5 cm deep stacking gel overlaying a 10%-30% linear gradient SDS-polyacrylamide gel. The stacking gel contained 1 mM EDTA. The gel strips were pushed to the bottom of each slot with a spatula, and each strip was then overlaid with 20  $\mu$ l of equilibration buffer containing 20% (w/v) glycerol and 1% (w/v) BPE. This solution was then overlaid with 20  $\mu$ l of equilibration buffer containing 10% (w/v) glycerol and *Staphylococcus aureus* V8 protease. For each protein, three treatments were carried out, one with no protease added, a second with 0.2  $\mu$ g of protease added, and a third with 1  $\mu$ g of protease added. The upper and lower reservoirs were carefully filled with SDS running buffer and electrophoresis was continued for 2-3 h at a constant 40 mA until the bromophenol blue had migrated to the bottom of the stacking gel. The current was switched off and the gel left for 30 min while

proteolytic digestion of the samples took place in the stacking gel. Electrophoresis was recommenced and continued for a further 16 h at 14 mA. The gel was then prepared for silver staining as in Section 2.4b.

For cyanogen bromide digestion, proteins were purified by SDS-PAGE as described above and freeze-dried. The samples were each resuspended in 200  $\mu$ l of distilled water (made possible by the presence of residual SDS in the freeze-dried samples), and to each was added 700  $\mu$ l of formic acid. Cyanogen bromide was then added to the samples to a final concentration of 2 mg/ml, and the samples were incubated at 4°C for 4 h and 16 h. After incubation, cyanogen bromide and formic acid were removed from the samples by lyophilisation, and the dried samples were prepared for SDS-PAGE as in Section 2.3. The resulting gels were stained with silver.

#### (2.9) In Vivo Labelling of Thylakoid Proteins

Protein synthesis can<sup>be</sup> monitored *in vivo* by allowing plants to take up [<sup>35</sup>S]-methionine via their vascular system. This radiolabelled amino acid is then incorporated into newly-synthesised proteins, which may then be analysed by a variety of techniques including SDS-PAGE. Labelling of proteins in this way provides a means of investigating protein synthesis under a variety of environmental conditions. In this study this technique

was used to compare protein synthesis in the presence and absence of light.

Ten 1.5 ml Eppendorf microcentrifuge tubes were taken and their conical ends cut off with a razor blade. The cut ends were then placed in the wells in a plastic Eppendorf tube rack. Into each of these tube ends was placed 100  $\mu$ l of sterile distilled water containing 50  $\mu$ Ci [ $^{35}$ S]-methionine. The plants to be labelled were taken and their stems cut under water in order to avoid disruption of the transpiration stream. Unless otherwise stated, the third node leaf pair was then dissected from the seedling under water, and the cut end of the petiole placed in one of the tube ends containing the isotope. This procedure was repeated until all the tube ends were filled. Typically, 20 leaf pairs were used when labelling was carried out in the dark, and 10 leaf pairs were used when labelling in the light. Labelling in the light was carried out under the lighting conditions described in Section 2.2a. For plants labelled in the dark, all manipulations were carried out in complete darkness inside a light-tight room, with no safe-light present.

Plants were left to take up isotope for 5-6 h, with occasional addition of water to the tubes where necessary. Often, transpiration in the dark was assisted by blowing air gently across the leaves with an electric fan. Following this incubation, the labelled leaf pairs

were harvested and used to make thylakoid membrane preparations as described in Section 2.12.

#### (2.10) Estimation of Protein in Thylakoid Samples

Estimation of the amount of protein in samples of thylakoid membranes was carried out using the method described by Brashall *et al* (1969). This method uses the ability of Coomassie brilliant blue to stain proteins. The degree of staining is directly related (within limits) to the amount of protein present in the sample, and the unknown protein is estimated against a known protein standard.

Whatman No. 42 filter paper was marked off into 1 cm x 2 cm rectangles with a pencil. Bovine serum albumin was made up in serial dilution to cover a range of concentrations from 0 mg/ml to 8 mg/ml. An aliquot (5  $\mu$ l) of each dilution was spotted into a rectangle on the filter paper, giving protein loadings ranging from 0  $\mu$ g to 40  $\mu$ g. Samples of thylakoids were taken and each was diluted such that each sample was represented by three dilutions containing 2  $\mu$ g, 10  $\mu$ g and 20  $\mu$ g chlorophyll respectively. These were spotted into rectangles as described above. The filter was then dried and completely immersed in 7.5% (w/v) TCA. The filter was incubated for 30 min at 80°C, then washed once in ether/ethanol (1:1), then in ether. The filter was then

carefully dried under a stream of warm air.

The dried filter was immersed in a solution of 1% (w/v) Coomassie blue (G250) containing 7% acetic acid, and incubated for 15 min at 50°C. The background stain on the filter was removed by soaking the filter in 7% acetic acid at 50°C-60°C. The background was usually found to be virtually clear after about 1 h with 2-3 changes of destain.

Stoppered glass tubes were taken and into each was placed 5 ml of protein destain solution, consisting of 66 ml methanol, 34 ml water and 1 ml concentrated ammonium hydroxide. Filter rectangles into which protein had been spotted were cut out and each was placed into a tube containing the protein destain solution. Protein spots were destained for 45-60 min with gentle whirlmixing, following which the destain solution was drawn off and its absorbance read at 610 nm against a destain solution blank.

Absorbance readings for the BSA standard samples were plotted against protein concentration to obtain a standard protein curve. For BSA loadings below 40 µg, the standard protein curve is linear. Linearity was found to be well maintained for thylakoid samples up to a loading of 25 µg protein.

The advantage of this protein estimation method lies in the fact that thylakoid samples do not need to be

delipidated prior to the estimation. Chlorophyll and detergents such as SDS and Triton X-100, known to affect results obtained with other protein estimation procedures, do not interfere with this method. Furthermore, the protein is immobilized on filter paper and therefore no problems of protein solubility, particularly acute in membrane preparations, are encountered with this method.

A second, more indirect method of determining the amount of protein in a given thylakoid sample involves the estimation of chlorophyll. The amount of chlorophyll in the membrane is directly related to the amount of protein present since chlorophyll is bound to protein in the thylakoid.

A number of leaves (10-20) were harvested and thoroughly ground in 90% v/v aqueous acetone in a cold mortar. The homogenate was then poured into stoppered centrifuge tubes and left at 4°C for 10 min., after which time insoluble material was pelleted by centrifugation at 2,000g for 10 min. The chlorophyll content of the resulting supernatant was determined as described in Section 2.17.

A second batch of leaves were harvested and thylakoids were isolated as described in Section 2.12. The thylakoids were resuspended in a small volume of 10mM Tris-HCl (pH 8.0) and four volumes of acetone were added.



The solution was then left at 4°C for 10 min., and the insoluble material removed by centrifugation as described above. The chlorophyll content of the resulting supernatant was determined as described in Section 2.17.

A comparison of the amount of chlorophyll recovered in the isolated thylakoids with that present in the unfractionated leaves allowed the protein present in the isolated thylakoids to be expressed in terms of whole leaves. Thus, an amount of thylakoid protein equivalent to a stated fraction of a whole leaf could be loaded onto each track for SDS-PAGE. The advantages of this method of protein estimation are discussed in detail in Section 3.7b(111).

#### (2.11) Isolation of Intact Chloroplasts

##### (2.11a) Rapid isolation of a crude preparation

The procedure employed for the rapid isolation of intact chloroplasts was based on that described by Blair and Ellis (1973). Muslin was cut into squares (20 cm x 20 cm), and two sets of 8 layers were washed once in distilled water, then once in ice-cold sterile sucrose isolation medium (SIM), composed of 25 mM HEPES-NaOH (pH 7.6), 350 mM sucrose, and 2 mM EDTA. Pea leaves were harvested with gloved hands, weighed and placed in a frozen perspex container. The tissue was then covered with

a semi-frozen slurry of SIM to which had been added D-isoscorbate to a final concentration of 2 mM. Typically, 100 ml of SIM was used for every 15 g of tissue harvested. The material was quickly homogenised using a Polytron homogeniser, (Kinematica GmbH, Switzerland), two 4-second bursts with the Polytron set at position 7 usually being sufficient to produce a uniform homogenate. The homogenate was squeezed through one set of 8 layers of cold muslin into a glass beaker kept on ice. The filtrate was then poured through the second set of 8 layers into a second ice-cold beaker and the resulting filtrate quickly centrifuged at 2,800xg at 5°C. for 1 min. The supernatant was poured away and the inner surface of the centrifuge tube wiped with absorbant tissue to remove froth. The chloroplast pellet was then resuspended in an appropriate buffer for further work.

#### (2.11b) Isolation using Percoll gradients

In order to produce an intact chloroplast preparation of high purity, a chloroplast preparation such as that described in Section 2.11a was further purified by centrifugation on a Percoll density gradient. This method was used for some small-scale chloroplast preparations for use in the isolation of PS I material.

A crude chloroplast pellet was prepared as in Section 2.11a and this was gently resuspended by swirling in

ice-cold resuspension medium composed of 50 mM HEPES-KOH (pH 8.0), and 330 mM sorbitol. The resulting chloroplast suspension was loaded over a 10%-80% gradient of Percoll preformed in a centrifuge tube. The gradient contained the resuspension medium described above. Typically, a volume of the chloroplast suspension containing 2 mg of chlorophyll was loaded over a 20 ml gradient. The gradient was centrifuged at 2,000g for 20 min in a swing-out rotor at 4°C, resulting in a gradient containing two distinct green bands. The upper band represented broken chloroplasts, while the lower band represented intact chloroplasts. The lower green band was carefully removed by long-form Pasteur pipette and placed in a centrifuge tube kept on ice. The suspension was diluted three-fold with the resuspension medium and the chloroplasts pelleted at 4,000g for 1 min. The resulting pellet was then resuspended in an appropriate medium and chloroplasts checked for intactness by phase contrast microscopy.

#### (2.12) Isolation of Thylakoid Membranes

Thylakoid membranes were routinely prepared by bursting isolated chloroplasts by hypotonic shock, and sedimenting the thylakoid membranes by centrifugation. Isolated chloroplasts made by either of the methods described in Section 2.11 were pelleted and resuspended

in lysis buffer composed of 10 mM Tris-HCl (pH 8.0) and 5 mM 2-mercaptoethanol. The suspension was left on ice for 5 min, following which it was subjected to centrifugation at 10,000xg for 10 min at 4°C. This centrifugation resulted in a green pellet and a pale, straw-coloured supernatant. The pellet represented a thylakoid membrane fraction, while the supernatant contained soluble stromal proteins. The pellet was washed twice in the same lysis buffer and then used either for further fractionation or for analysis by SDS-PAGE.

## (2.13) Isolation of Chlorophyll-Protein Complexes

### (2.13a) Isolation of PS I by the method of Mullett et al.

The method used to isolate photosystem I particles for the purpose of raising antibodies to the polypeptides of the LHC I was based upon that described by Mullett et al (1980a). Two alternative methods for producing particles of similar composition are described in detail below. In all preparations, to reduce the risk of proteolytic degradation, phenylmethylsulphonyl fluoride (PMSF) was added to all buffers to a final concentration of 200  $\mu$ M. For large scale preparations, 250-300 g (fresh weight) mature pea leaves were harvested from plants grown for 10-12 days under a 12 h photoperiod. This material was then homogenised in 1.2 l sucrose isolation

medium consisting of 0.33 M sucrose, 25 mM Hepes, 2 mM EDTA, made to pH 7.6 with NaOH. Homogenisation was carried out using an Atomix blender pre-cooled to 0°C. The sucrose isolation medium was itself cooled until it attained the consistency of an icy slurry. The tissue was ground in two bursts, each of 6 seconds duration. The homogenate was filtered twice through 8 layers of muslin into cold 300 ml centrifuge bottles and crude intact chloroplast pellets recovered by centrifugation at 3000xg for 5 min. The pellets were pooled in a resuspension buffer consisting of 6.2 mM Tris, 48 mM glycine (pH 8.3). This buffer lysed any intact chloroplasts in the preparation. Thylakoid membranes were removed from suspension by centrifugation at 10,000xg for 10 min, following which they were resuspended in a large volume (usually 50 ml) of resuspension buffer. At this stage any DNA sedimenting with the thylakoid membranes was removed by the addition of DNaseI and  $MgCl_2$ , to a final concentration of 100 µg/ml and 2.5 mM respectively. Incubation with DNase was carried out for 30 min at 0°C following which the thylakoid membranes were pelleted by centrifugation at 10,000xg for 10 min. The pellets were washed once in 50 mM sorbitol, 5 mM EDTA, made to pH 7.8 with NaOH, in order to unstack the thylakoids, then washed twice in resuspension buffer. The washed membranes were resuspended in a minimum of resuspension buffer and

a small volume removed for chlorophyll determination. Resuspension buffer was then added, followed by 5% (w/v) Triton X-100 such that the final concentrations of chlorophyll and detergent were 500 µg/ml and 0.5% respectively. Detergent solubilisation was carried out for 30 min at 22°C with constant gentle stirring. The material was then centrifuged at 30,000xg for 30 min to pellet any unsolubilised membrane material, and the resulting green supernatant loaded onto 0.1 M-0.7 M linear sucrose density gradients with a 2 M sucrose cushion. The gradients contained resuspension buffer and Triton X-100 to a final concentration of 0.02% (w/v). For large scale preparations, 50 ml gradients were used, with a sample volume of 10 ml per gradient. For small scale preparations, these volumes were halved. The sucrose gradients were centrifuged at 100,000xg for 16 h using a swing-out rotor. This centrifugation resulted in gradients containing two major green bands (see Figure 3.1 ). The band sedimenting in the upper third of the gradient is highly fluorescent when back-illuminated, due to enrichment with the LHC II. The thin green band sedimenting at the 0.7 M/2.0 M sucrose interface represents the released 'native' PS I particle. This material was carefully removed from the gradients by long-form Pasteur pipette, dialysed against two changes of resuspension buffer at 4°C and stored at -20°C.

(2.13b) Isolation of PS I by the 'high salt' method.

This method dispenses with the need for both the DNAase and sucrose gradient steps, and produces a PS I particle identical in terms of polypeptide content to that isolated as described in Section 2.13a. Plant material was homogenised and crude chloroplast pellets obtained exactly as described in Section 2.13a. The pellets were pooled and washed once in 50 mM sorbitol, 5 mM EDTA (pH 7.8), and the membranes recovered by centrifugation at 10,000xg for 10 min. The resulting pellet was gently dispersed in resuspension buffer containing 0.8 M NaCl by sucking up and down in a pipette, and membranes were re-pelleted at 10,000xg, following which they were washed twice in resuspension buffer and solubilised by detergent under the conditions described in Section 2.13a. The solubilised material was then centrifuged at 30,000xg for 30 min and the resulting pellet resuspended in a small volume of resuspension buffer. This suspension was then stored at -20°C.

(2.13c) Isolation of PS I by the Tris-HCl method.

This method differs from those described above in that it produces a particle containing the polypeptides of the LHC II in addition to those recognized as components of PS I. All steps in this preparation were as

described in Section 2.13a, except that the solubilisation of the membrane by Triton X-100 was carried out in 25 mM Tris-HCl (pH 8.3), rather than in the Tris-glycine buffer. Following the solubilisation step, the material was centrifuged at 30,000xg for 30 min. This step results in a large dark-green pellet and a pale-green supernatant. The pellet was resuspended in a minimum volume of resuspension buffer and stored at -20°C.

(2.13d) Isolation of LHC I

The method used to isolate LHC I particles was that described by Haworth et al (1983). The starting material consisted of an isolated PS I preparation made by either of the methods described in Sections 2.13a and 2.13b. The PS I preparation was first dialysed against 50 mM sorbitol at 4°C for 24 h to remove sucrose and excess Triton X-100. The dialysed material was then recovered by pelleting at 30,000xg for 10 min, then resuspended in a small volume of 20 mM Tricine-NaOH (pH 7.8). An aliquot, (50 µl), was removed for chlorophyll determination and the material was diluted with the same buffer to a chlorophyll concentration of 0.5 µg/ml. At the same time, the zwitterionic detergent Zwittergent-16 and the neutral detergent dodecyl- $\beta$ -D-maltonide were added to final concentrations of 2 µg/ml and 1.5 µg/ml respectively.



Thus treated, the solution was left at 4°C with constant gentle stirring for 1 h. Following incubation, the solution (4-5 ml) was layered over a linear 0.1 M-1.0 M sucrose density gradient (20 ml) formed over a 2 M sucrose cushion, and centrifuged at 100,000g for 16 h in a swing-out rotor. This procedure resulted in a sucrose gradient containing three green bands (Figure 3.33). The uppermost band consisted of purified, intact LHC I. This was carefully removed from the gradient by pasteur pipette and frozen away at -20°C.

#### (2.13e) Isolation of LHC II

The light-harvesting complex of photosystem II was isolated as a by-product of the photosystem I isolation procedure, following the method of Burke et al (1978). As described in Section 2.13a, solubilisation of unstacked thylakoids with Triton X-100, followed by separation of released complexes by sucrose density gradient centrifugation, results in two resolvable green bands. The green band occupying the upper third of the gradient, and exhibiting marked red fluorescence when back-illuminated with white light, was removed by Pasteur pipette and made 5 mM with respect to  $MgCl_2$ . This suspension was then incubated at room temperature with gentle stirring for 5 min, and carefully layered over a sucrose pad of equal volume, consisting of 0.4 M sucrose,

6.2 mM Tris, 48 mM glycine, and 5 mM  $MgCl_2$ . The material was then centrifuged at 15,000g for 10 min in a fixed-angle rotor, resulting in the formation of a large green pellet at the bottom of the sucrose pad. The supernatant was poured away and the pellet resuspended in 6.2 mM Tris, 48 mM glycine (pH 8.2), prior to being stored at  $-20^{\circ}C$ .

(2.14) Electroelution of LHC I and PS I Reaction  
Centre Proteins

Following SDS-PAGE on 40 cm gels, staining with Coomassie brilliant blue and destaining, the LHC I and PS I reaction centre apoproteins were recovered by electroelution from the gel matrix. Glass tubes of length 10 cm and internal diameter of 7 mm were slightly constricted at one end by flaming for 2-3 min. This end was then sealed with Nescofilm to allow the casting of a stacking gel plug of depth 1 cm. This plug was quickly overlaid with 100  $\mu$ l water. Once the acrylamide plugs had set, the tubes were placed in a tube gel apparatus as shown in Figure 2.1, and the Nescofilm removed. Short lengths of boiled Visking tubing were sealed at one end with plastic clips and filled with 1-1.5 ml of Laemmli buffer. These pieces of dialysis tubing were then carefully slipped over the plugged ends of the tubes such that the lower faces of the stacking gel plugs were

Figure 2.1

Diagram to show apparatus used for the electroelution of proteins from polyacrylamide gels (for explanation see Section 2.14).

- UR      Upper reservoir containing Laemmli electrophoresis buffer.
- RG      Rubber grommet.
- GT      Glass tube
- GF      Gel fragments excised from a stained polyacrylamide gel.
- SG      Stacking gel forming a plug at the lower end of the glass tube.
- DT      Dialysis tubing containing 0.1 M Laemmli reservoir buffer.
- C      plastic clip to seal the dialysis tubing.
- LR      Lower reservoir containing Laemmli buffer.

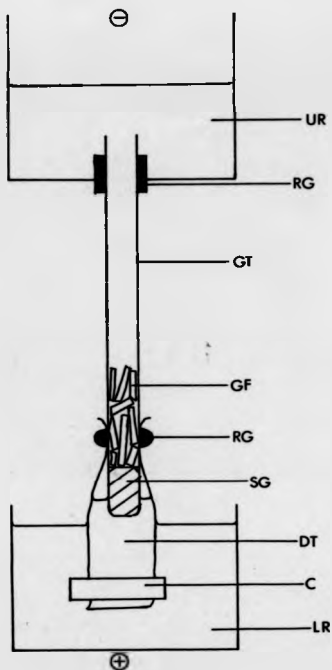


Figure 2.1

immersed in the buffer. The tubing was then sealed to the glass with rubber grommets and the apparatus set up such that the buffer within the Visking tubing was continuous with that in the lower reservoir of the elution apparatus.

Stained wet gels were placed upon a light box and the protein bands of interest were identified. These bands were then excised from the gel by razor blade, care being taken to keep the excised gel strip as narrow as possible to avoid contamination with proteins in neighbouring stained bands. The excised strips were then soaked for a total of 30 min in three changes of Laemmli buffer in order to remove methanol and acetic acid. Individual strips were cut into short lengths and these were placed in the glass tubes on the elution apparatus. The tubes and upper reservoir were filled with Laemmli buffer and the excised proteins eluted into the Visking tubing for 16 h at a constant 90 volts. After electroelution, the current was reversed for 30 seconds in order to free any protein bound to the Visking tubing, and the tubing was carefully removed from the apparatus. The free ends of the tubing were sealed with a second plastic clip and the proteins dialysed over night against two changes of Laemmli buffer lacking SDS. The dialysed protein preparations were either stored at  $-20^{\circ}\text{C}$  or prepared for SDS-PAGE to check for purity.

(2.15) Immunological Techniques(2.15a) Preparation of polyclonal antisera to the  
LHC I and PS I reaction centre apoproteins

Polyclonal antisera to PS I polypeptides were prepared from samples electroeluted as described in Section 2.14. Samples representing approximately 50-100  $\mu$ g protein were emulsified with an equal volume of Freund's complete adjuvant until the emulsion achieved a stiff consistency. The samples (no more than 1.5 ml) were then administered to rabbits subcutaneously. All subsequent injections were carried out in the same manner except that the antigen was emulsified with Freund's incomplete adjuvant. Injections were administered at intervals of 14 days. The first bleeds were taken at 7-10 days after the third injections, subsequent bleeds being taken at 10 days following each booster injection. Rabbits were bled from the ear veins, approximately 20-40 ml blood being removed on each occasion. Blood was left for 6 h at 4°C to allow clot formation. The serum was then removed by Pasteur pipette and centrifuged at 4,000xg for 10 min in order to remove any free erythrocytes. Saturated ammonium sulphate in PBS was added dropwise to the sera on ice to a final concentration of 40% saturation. The resulting

precipitates were pelleted by centrifugation at 30,000xg for 10 min, and resuspended in PBS to a volume representing half that of the original serum. Sera were then divided into 100  $\mu$ l aliquots and stored at  $-20^{\circ}\text{C}$ .

(2.15b) Preparation of a polyclonal antiserum to the 26 kDa apoprotein of the LHC II

The method employed to raise antiserum to the 26 kDa apoprotein of the LHC II has been described in some detail by Bennett (1980). The purification of the antigen did not rely upon the purification of a 'native' LHC II chlorophyll-protein complex. Instead, it utilised two features of the apoprotein: phosphorylation and solubility in chloroform/methanol, which in combination allow it to be distinguished from the majority of other thylakoid membrane components.

Firstly, isolated intact chloroplasts were incubated in the light with [ $^{32}\text{P}$ ]-orthophosphate in order to bring about light-driven phosphorylation of the apoproteins of the LHC II. After incubation, the chloroplasts were lysed and the thylakoid membranes recovered by centrifugation. The membranes were resuspended in a small volume of buffer containing 50 mM  $\text{NaHCO}_3$ , 10 mM DTT, and 20 volumes chloroform/methanol (2:1, v/v) added. After thorough mixing this material was stored at  $-20^{\circ}\text{C}$  for 16 h, after which the liquid was filtered to remove precipitated

proteins, and an equal volume of ether added. This mixture was again stored, after thorough mixing, at  $-20^{\circ}\text{C}$  for 16 h, following which the precipitated material was recovered by centrifugation. The pelleted material was dried and prepared for SDS-PAGE by resuspension in SDS sample buffer. The sample was subjected to SDS-PAGE for 16 h on a 20% (w/v) polyacrylamide gel, and subjected to wet autoradiography for 2-4 h in order to visualise the phosphorylated protein bands. The 26 kDa phosphoprotein was then excised from the gel and protein eluted from the gel matrix by diffusion into solution containing 1% (w/v) SDS and 1% (v/v) 2-mercaptoethanol. The eluted protein was concentrated by acetone precipitation and resuspended in PBS. This preparation was then used as antigen after checking for purity by SDS-PAGE.

[2.15c] Preparation of monoclonal antibodies to the  
apoproteins of the LHC I

(1) Immunisation of mice

Mice (female Balb/c, 6-weeks old) were injected peritoneally with photosystem I material prepared by the Tris-HCl method described in Section 2.13c. This preparation contained up to 16 different stainable polypeptides, including those representative of the PS I reaction centre and its associated LHC I, plus the light-harvesting chlorophyll a/b-binding complex of PS II



(LHC II). The pelleted PS I material was resuspended in a small volume of sterile, distilled water and SDS added to a final concentration of 1% (w/v). This suspension was then boiled for 5 min. Approximately 50  $\mu$ g protein was injected into each mouse, after emulsification with an equal volume of Freund's complete adjuvant.

Between two and four weeks after the first injection, a similar injection was carried out using Freund's incomplete adjuvant. This was followed 7 days later with a tail vein injection with no adjuvant. Tail vein bleeds were taken 2 days later (100  $\mu$ l per mouse), and the sera were used in an immunoblot to screen for the production of antibody by each mouse.

In order to screen mouse sera for antibody production, a 20% polyacrylamide gel was cast with a continuous stacking gel containing no slots. An amount of the PS I preparation containing 200  $\mu$ g chlorophyll, was diluted with sample buffer and heated to 70°C for 5 min prior to loading across the full width of the gel. Electrophoresis was carried out for 20 h at 18 mA following which the gel was subjected to electrophoretic transfer to nitrocellulose as described in Section 2.15d. The resulting filter was then soaked in phosphate buffer containing 8% BSA for 1 h, and dried under a flow of warm air. The filter was cut into longitudinal strips, each 5 mm wide. Strips were then placed inside stoppered glass

tubes containing 2 ml of phosphate buffer, and a few  $\mu$ l of serum from an individual mouse was added to each. The tubes were laid on their sides and securely fixed to a shaker, with the filter strips fully immersed in the buffer. The strips were then put through the remainder of the immunoblot procedure as described in Section 2.15d, [ $^{125}$ I]-rabbit anti-mouse IgG (RAM) being used to visualise the antigenic polypeptides.

This method was also used to screen hybridoma supernatants (see Section 2.15c(iv)) and is summarised in Figure 2.2.

(ii) Fusion of myeloma cells and lymphocytes

Lymphocytes capable of secreting antibodies are difficult to culture, and therefore, in order to set up monoclonal cell lines, it is necessary to fuse them with cells which readily grow *in vitro*. Mouse myeloma cells grow easily and rapidly in culture and represent a convenient source material for fusion.

After screening of mouse sera as described above, the mouse showing the best immune response to the widest range of polypeptides was killed and its spleen removed. This organ was washed quickly in ethanol in a Petri dish and placed in 10 ml bicarbonate-buffered serum-free medium (SPM). The spleen was cut at one end with sharp scissors and the spleen cells gently teased out into the medium with sterile tweezers, a pipette being used to

**Figure 2.2** Method for screening of monoclonal supernatants by immunoblotting.

(1) Immunise mouse (Section 2.15c(i)) with PS I prepared by the Tris-HCl method (Section 2.13c).

(2) Remove mouse spleen and fuse spleen cells with myeloma cells (Section 2.15c(ii)). Select hybridoma lines by culture in selective HAT medium (Section 2.15c(iii)). Generate monoclonal hybridoma lines by dilution and subsequent culture in non-selective medium (Section 2.15c(iv)).

(3) Load antigen across the width of a polyacrylamide slab gel, and subject to SDS-PAGE to resolve protein constituents.

(4) Blot the resolved proteins electrophoretically onto a nitrocellulose sheet. Block the sheet with bovine serum albumin, dry and cut into identical strips.

(5) Incubate nitrocellulose strips with supernatants derived from individual hybridoma cultures. Wash away unbound antibody and incubate strips with [<sup>125</sup>I]-labelled rabbit anti-mouse IgG (RAM). Wash away any unbound radioactivity.

(6) Dry filter strips and subject to autoradiography.

For full details of this method see Sections 2.15c(i) and 2.15c(iv).

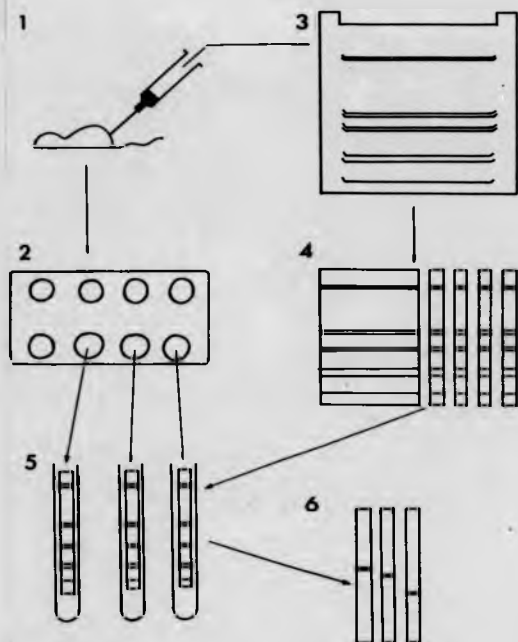


**Figure 2.2**

disperse any clumped cells. The cells were then transferred to a sterile plastic 25 ml bottle and to this was added  $10^6$  myeloma cells (strain NS 1). The cells were then recovered by centrifugation at  $1200 \times g$  for 5 min and the supernatant poured away. The pellet was resuspended in the residual liquid by gentle agitation and left at  $37^\circ C$  for 1 min. Sterile polyethyleneglycol (PEG 1000, 100% w/v in SFM) was added to the resuspended cells over a period of 1 min., with constant agitation to ensure adequate mixing. This mixture was then left at  $37^\circ C$  for a further 1 min after which time the suspension was slowly diluted with a further 20 ml SFM, again with gentle agitation. The suspension was then spun at  $1200 \times g$  for 15 min to pellet the cells. The supernatant was discarded. The pelleted cells were resuspended in a final volume of 40 ml medium containing 10% (v/v) fetal calf serum (FCS), glutamine, penicillin and streptomycin. This suspension was then distributed between four 96-well microtitre plates, with 0.1 ml of the cell suspension per well. The plates were incubated for 24 h at  $37^\circ C$  and 5%  $CO_2$ .

#### (iii) Hybridoma selection

Selection for cell lines resulting from the successful fusion of myeloma cells and lymphocytes (hybridomas) was necessary since cell lines surviving in culture are a mixed population of hybridomas and unfused

myeloma cells, the unfused lymphocytes having died. This selection is achieved by utilising myeloma lines defective in the enzyme hypoxanthinephosphoribosyl-transferase (HGPRT). Such lines die in culture medium containing hypoxanthine, aminopterin and thymidine (HAT). Death results because aminopterin blocks the main pathway of DNA synthesis. The alternative pathway, which uses the exogenous hypoxanthine, relies on the presence of HGPRT. Thus only hybridoma cells can survive in medium containing HAT, since the myeloma confers the ability to grow in culture and the lymphocyte provides the HGPRT needed to overcome the aminopterin block. (Similar selection procedures involving the use of myeloma lines defective in the enzyme thymidine kinase can also be used. Here, the thymidine kinase donated by the lymphocyte utilises the exogenous thymidine to overcome the aminopterin block). After the cell culture had been incubated for 24 h, a further 0.1 ml of medium containing HAT was added to each well. The plates were then incubated for 14 days at 37°C and 5% CO<sub>2</sub>, after which time they were examined for growing colonies.

(iv) Hybridoma culture

The contents of wells containing growing hybridoma colonies were transferred to 24-well plates to continue growth. This transfer was done by carefully dispersing each colony with a Pasteur pipette and transferring the

cells to a well already containing 2 ml of fresh HAT medium. After a few days growth at this stage, 1 ml of the medium from each culture was removed and screened for antibody exactly as described in Section 2.15c(1), except that in this case, each filter strip was immersed in 1 ml phosphate buffer to which had been added 1 ml of the appropriate hybridoma supernatant (see Figure 2.2). All positive cultures were then cloned by dilution and re-screened. Some of the more highly positive clonal cultures were then re-cloned and screened, cultured in bulk and the cells stored at  $-80^{\circ}\text{C}$ .

#### (2.15d) Immunoblotting

##### (1) Iodination of protein A

Solutions:

(A) 0.5 M  $\text{KH}_2\text{PO}_4$

(B) 0.5 M  $\text{K}_2\text{HPO}_4$

(C) 0.5 M phosphate buffer. This is made by adding solution A to solution B dropwise until a pH of 7.5 is achieved.

For iodination of protein A, 500  $\mu\text{Ci}$  [ $^{125}\text{I}$ ]-Na was placed in a small Eppendorf tube in a high efficiency fume hood. To this tube was added 25  $\mu\text{g}$  protein A in 25  $\mu\text{l}$  water, followed by 10  $\mu\text{l}$  chloramine-T (2 mg/ml in solution C). This solution was mixed well and left to stand at room temperature for 2 min, after which time 25  $\mu\text{l}$  saturated

tyrosine in solution C, 50  $\mu$ l 10% (w/v) BSA, and 200  $\mu$ l PBS were added to the Eppendorf and the resulting solution thoroughly mixed by gentle agitation. The solution was passed down a 5 ml Sephadex G50 (medium) column and twelve 0.5 ml fractions collected. A small volume was taken from each fraction and counted for gamma radiation. Fractions containing the first peak of radioactivity to emerge from the column contained iodinated protein A. These fractions were stored at 4°C.

(ii) Radio-immunodetection of antigens

The method used for the immunodetection of antigens follows closely the method of Vaessen, Kreike and Groot (1981), but with some modifications. Following electrophoresis, gels were removed from the running apparatus and laid upon a clean glass plate. They were then covered with a layer of cling-film, and a sheet of nitrocellulose was cut to exactly fit the shape of the gel. Where the gel was composed of an acrylamide concentration gradient, it was first soaked for 15 minutes in transfer buffer consisting of 25 mM Tris, 192 mM glycine (pH 8.3), and 20% (v/v) methanol. This was done in order to allow for differential swelling of the gel matrix. If this precaution was not observed, swelling took place during the transfer process often leading to poor and uneven transfer of proteins to the nitrocellulose filter. The filter was then soaked in transfer buffer and



carefully layered over the gel such that no air was trapped between the two. This assembly was then sandwiched between two sheets of foam and placed inside a Bio-Rad electrophoretic transfer cell, with the nitrocellulose filter oriented towards the anode. The cell was then filled with transfer buffer and proteins transferred from the gel to the nitrocellulose filter at a constant 50 V (250 mA) for 3 h. Where good transfer of higher molecular weight proteins was essential, such as with the 68 kDa PS I reaction centre polypeptide, a higher voltage of 60 V was used in conjunction with a longer transfer time of 4 h.

Following transfer, the filter was soaked in 10-30 ml PBS containing 4% BSA for 30 min in order to block free protein binding sites on the nitrocellulose. The appropriate antiserum was thawed and sufficient added to the buffer containing the filter to achieve a 1:3000 dilution of antibody. The filter was then incubated overnight at 22°C with constant shaking to ensure full immersion of the filter in the antibody-containing buffer. After this incubation, the filter was washed five times in PBS to remove any unbound antibody, and then soaked again in PBS containing 4% BSA. In a high efficiency fume hood, sufficient [<sup>125</sup>I]-labelled protein A was added to the filter to give a total of 1x10<sup>6</sup> c.p.m. The filter was left to incubate for 2 h with constant shaking, after which

time the filter was repeatedly washed with PBS containing 1% (w/v) Triton X-100, until background radioactivity from the filter had been reduced to less than 15 c.p.m. The filter was then carefully dried under a stream of warm air, and put down to autoradiograph as described in Section 2.5.

Where whole mouse antisera or mouse-derived monoclonal antibodies were used to probe the nitrocellulose filter, the position of the bound antibody was determined using [<sup>125</sup>I]-labelled rabbit anti-mouse antibody (RAM). In this system, the iodinated rabbit antibody binds mouse-derived immunoglobulins with high specificity. Iodinated RAM is used since protein A does not bind mouse immunoglobulins with high efficiency. Iodination of the RAM was carried out exactly as described for protein A in Section 2.15d(i), and incubation conditions during immunoblotting were exactly as described for the protein A system above.

(iii) Antigen detection using the biotin-streptavidin system

Several alternative methods for the detection of antigens immobilised on nitrocellulose are available which do not involve the use of radioisotopes. Instead these methods rely on specific enzyme-substrate interactions to produce a colour change which can be used to visually mark the position of a given antibody on the nitrocellulose filter. One such system utilises biotin,

streptavidin and horseradish peroxidase in a four-step detection protocol devised by Amersham (UK). Here, immobilised immunoglobulin molecules bind molecules of protein A which have been conjugated to biotin, a small, water-soluble vitamin. In a subsequent step, the immobilised biotin binds the bacterial protein streptavidin which has been conjugated to horseradish peroxidase. Lastly, incubation with hydrogen peroxide and diaminobenzidine brings about the colour change marking the position of the bound antibody.

After transfer of proteins to the nitrocellulose filter, the filter was washed three times in PBS containing 0.1% (v/v) Tween and 0.1% (w/v) BSA. Each wash was of 10 minutes duration. Following this, the filter was incubated with an appropriate volume of antibody in PBS containing 1% Tween for 4 h, then washed five times in PBS containing 0.1% Tween to remove unbound antibody. At this stage, a stock solution of biotinylated protein A was diluted 300-fold in PBS containing 0.1% Tween and 0.1% BSA. A small volume of this diluted stock, sufficient to cover the nitrocellulose filter, was sealed, together with the filter, inside a polythene bag and incubated at room temperature for 1 h. The filter was washed five times in PBS, 0.1% Tween, then sealed inside a polythene bag with streptavidin-peroxidase in PBS, 1% Tween. This bag was left to incubate for 30 min at room temperature, after

which the filter was washed twice in PBS, 0.1 % Tween, twice in PBS alone and then once in 50 mM Tris, 0.9% NaCl (pH 7.4).

The filter was then developed by the addition of diaminobenzidine (600 mg/l), and hydrogen peroxide (0.03% v/v), the colour taking not more than 10 minutes to appear. Thus stained, the filter was dried under a stream of warm air and stored away from the light to prevent fading.

#### (2.15e) Immunoprecipitation

Immunoprecipitation is a commonly used means of retrieving a given antigen from a complex mixture of polypeptides, and relies, in exactly the same way as immunoblotting, upon the specific recognition of the antigen by the immunoglobulin. The major difference between immunoblotting and immunoprecipitation is that in the former, the antigen is immobilised on an inert support, while in the latter it is part of a mixture in free solution.

The method used for the immunoprecipitation of proteins during this study is based upon that described by Cuning et al (1986). Protein samples were made 1% with respect to SDS and heated to 70°C for 4 minutes. Each sample was then diluted ten-fold with PBS containing BSA (10 mg/ml), in order to bring the detergent concentration

down to 0.1%. Following this, 5-10  $\mu$ l of antibody was added to each tube, the samples thoroughly mixed and left to incubate at 37°C for 2 h with constant agitation. Protein A-Sepharose was weighed out and then swelled in PBS containing 1% (v/v) NP-40 and 1% (w/v) BSA. Sufficient volume of the swelled matrix was then added to the antibody-antigen mixtures to give 10 mg Protein A-Sepharose per tube. The resulting slurries were incubated at 0°C for 1 h with constant mixing, then transferred to columns made from 1 ml disposable syringes plugged with glass wool. Each column was allowed to drain and the column beds were washed thoroughly with 5-10 ml PBS containing 1% (v/v) NP-40. The bound immunoprecipitates were eluted by washing each column three times with 0.4 ml 1 M acetic acid. The eluates were collected in 1.5 ml Eppendorf tubes and proteins precipitated by the addition of 100% (w/v) trichloroacetic acid (TCA) to give a final concentration of 10%. Precipitates were left to form at 0°C for 30 min and recovered by centrifugation at 12,000xg for 2 min. The precipitates were then washed twice with 80% (v/v) aqueous acetone and desiccated under vacuum, following which they were resuspended in SDS sample buffer, heated at 80°C for 5 min and small aliquots removed for TCA-insoluble radioactive count determination. The samples were then analysed by SDS-PAGE and autoradiography as described in Sections 2.3 and 2.5

respectively.

#### [2.16] Low Temperature Fluorescence Spectroscopy

Chlorophyll fluorescence was measured at 77 K using a Perkin-Elmer LS-5 luminescence spectrometer fitted with a liquid nitrogen attachment. Prior to freezing, small aliquots of each sample were taken and their chlorophyll content determined as described in Section 2.17. Samples were then diluted to give a final chlorophyll concentration of 5  $\mu\text{g}/\text{ml}$ . This relatively low concentration was used in order to avoid the risk of generating spurious signals due to re-absorption by the pigments present in the samples. An aliquot (50  $\mu\text{l}$ ) of each sample was then applied to a narrow capillary tube sealed at one end, and the tubes were quickly immersed in liquid nitrogen. Samples were stored at 77 K until used.

For fluorescence emission spectra, samples were subject to excitation at a wavelength of 440 nm, and the spectrum of fluorescence emission was read between 650 nm and 780 nm. For fluorescence excitation spectra, samples were subjected to excitation at wavelengths between 400 nm and 550 nm, fluorescence emission being read at 683 nm or 735 nm. The data were collected and plotted automatically. In all cases, fluorescence peak heights were automatically normalised to the highest recorded peak.

(2.17) Chlorophyll Determination

All samples to be analysed were diluted with 80% (v/v) aqueous acetone and placed in the dark at 4°C for 10 min. Samples were then centrifuged at 2,000g for 10 min to pellet any insoluble material, and the supernatants removed for spectrophotometry. Spectra were read using a Shimadzu UV-240 spectrophotometer with OP1-2 attachment. Data were recorded automatically. Absorbances were read at both 663 nm and 645 nm using 80% (v/v) aqueous acetone as the blank. Chlorophyll concentrations are given by the equations described by Arnon (1949):

$$[\text{Chlorophyll}]_{\text{mg/l}} = (8.02 \times A_{663}) + (20.2 \times A_{645})$$

$$[\text{Chlorophyll } a]_{\text{mg/l}} = (12.7 \times A_{663}) - (2.7 \times A_{645})$$

$$[\text{Chlorophyll } b]_{\text{mg/l}} = (22.9 \times A_{645}) - (4.7 \times A_{663})$$

(2.18) Freeze-Fracture Electron Microscopy

Freeze-fracture electron microscopy was carried out at Chelsea College, London, in collaboration with Dr. Peter Thomas. The method used was that described by Sen *et al* (1982). Small volumes of prepared chlorophyll-protein complexes were subjected to centrifugation at 12,000g for 2 min to produce small, sloppy pellets. These pellets were

resuspended in small volumes of water containing 10% (v/v) glycerol and thermally quenched from room temperature in a slurry of nitrogen. The frozen samples were then fractured at  $-115^{\circ}\text{C}$  in a Polaron freeze-fracture device. Platinum-carbon replicas were prepared, washed with solvent, and examined in a Philips EM 301 electron microscope.

#### [2.19] Assay of PS I Reaction Centre Photochemical Activity

Photosystem I reaction centre photochemical activity was measured using an oxygen electrode (Hansatech (UK)). White light was passed through a Volpi red filter (transmitting above 600 nm), and the resulting transmitted light was passed down a flexible light pipe, through a second filter transmitting at 695 nm, and into the oxygen electrode chamber. External light was eliminated by enclosing the oxygen electrode in a purpose-built box. PS I-mediated electron transport was measured by recording oxygen uptake associated with the flow of electrons from ascorbate, via reduced dichlorophenol-indophenol (DCPIP) to methyl viologen (MV). Photochemical assays were carried out using the following buffer system:

100 mM Tris (pH 7.8), 10 mM  $\text{MgCl}_2$ , 10 mM NaCl (435  $\mu\text{l}$ )

Water (435  $\mu\text{l}$ )

Chlorophyll-containing sample (50  $\mu\text{g}$  chlorophyll) (100 $\mu\text{l}$ )

200 mM ascorbate (10  $\mu\text{l}$ )



10 mM DCPIP (dissolved in ethanol) (10  $\mu$ l)

1 M sodium azide (5  $\mu$ l)

10 mM methyl viologen (5  $\mu$ l)

Data were automatically recorded and each assay was continued until a recorder trace long enough to give a good rate estimate was obtained. For assays involving the preferential excitation of either chlorophyll *a* or chlorophyll *b*, light was passed into the electrode chamber via filters transmitting at either 695 nm (for chlorophyll *a*) or at 645 nm (for chlorophyll *b*). In order to measure differences in light saturation rates between PS I preparations, a series of neutral density filters was employed to decrease the intensity of light reaching the chlorophyll in the electrode chamber.

#### (2.20) Isolation of Poly(A)-Enriched mRNA

In order to isolate a RNA fraction enriched with poly(A)-containing species, it was first necessary to isolate total leaf RNA and then further fractionate this by affinity chromatography. Total leaf RNA was isolated by the method described by Haffner *et al* (1978). Plants were germinated and grown for 7 days in darkness, then transferred to continuous light for a further 48 h. After this time expanding leaf tissue was harvested directly into liquid nitrogen. The frozen tissue was then removed from the liquid nitrogen by filtration through two layers

of muslin, and quickly weighed while still frozen. The material was transferred to a cold mortar and rapidly ground to small fragments, then placed in a large plastic centrifuge bottle. To the bottle was added liquified phenol (80% (w/v)) and an equal volume of SDS extraction buffer containing 0.5% (w/v) SDS, 100 mM Tris-HCl (pH 7.5), 35 ml of each being added for every 10 g of tissue present. This mixture was homogenised using a Polytron homogeniser, (three grinds each of six seconds duration at setting 7). The homogenate was then centrifuged at 2,000xg for 15 min. This step resulted in the generation of two distinct phases, an aqueous phase and a phenol-containing phase, separated by a narrow, opaque interface. The aqueous phase was carefully removed by pipette and the remaining phenol phase was re-extracted as described above by the addition of a second volume of SDS extraction buffer. The aqueous phase resulting from this second extraction was pooled with the aqueous phase from the first extraction, and then extracted once more with a half volume of liquified phenol. Solid NaCl was added to the resulting aqueous phase to a final concentration of 250 mM, and 2.5 volumes of absolute ethanol were added in order to precipitate total nucleic acids. The solution was left at -20°C overnight.

The precipitated nucleic acids were pelleted by centrifugation at 4,000xg, and then washed twice in 70%

(v/v) ethanol. The resulting pellet was resuspended in a small volume of sterile distilled water and 1.5 g solid NaCl added for every 10 ml volume. The salt was dissolved by rapid swirling and the solution was then stored at 4°C overnight to allow RNA to precipitate. Following this, the RNA was recovered by centrifugation at 4,000g for 10 min and the pelleted material washed twice in 2.5 M NaCl, followed by three washes in 70% (v/v) ethanol. The pellet was dried under nitrogen and dissolved in a small volume of sterile distilled water. The salt precipitation described above was then repeated three times, the final dried RNA pellet being weighed and dissolved in sterile distilled water to give a final RNA concentration of 10 mg/ml. The solution was then stored at -20°C.

Poly(A)-enriched RNA was prepared from the total RNA described above by oligo(dT)-cellulose affinity chromatography (Aviv and Leder, 1972 - modified by Highfield, 1978). The total RNA solution was thawed and concentrated stock solutions of KCl and Tris-HCl (pH 7.5) were added to give final concentrations of 0.5 M and 10 mM respectively. A small aliquot (2-5  $\mu$ l) of the total RNA solution was removed and diluted to 1 ml with water. The absorbance of this dilute sample was measured at 260 nm in a 1.5 ml cuvette, and the concentrated total RNA solution was then diluted with high salt buffer (HSB - 10 mM Tris-HCl (pH 7.5), 0.5 M KCl) such that it would give an

absorbance reading of 50 if measured in the same cuvette. The diluted RNA solution was then mixed with 2-3 g oligo(dT)-cellulose for 30 min at 4°C with constant stirring in order to allow binding of the poly(A)-containing RNA. The resulting slurry was poured into a column (Pharmacia 3x10 cm), and allowed to drain under gravity. The column thus formed was washed twice with 10 ml HSB and the pooled effluent containing unbound RNA was kept on ice. The column was then washed a further five times with 10 ml HSB and the resulting effluent discarded.

Bound RNA was eluted from the column by washing with 40 ml low salt buffer (LSB - 10 mM Tris-HCl (pH 7.5)). The LSB was maintained at 37°C in a constant temperature water bath, and the column effluent was passed through a LKB Uvicord which monitored absorbance at 254 nm. As absorbance increased, the column effluent was collected in a sterile glass tube on ice. Following this the column was equilibrated with 20 ml HSB and the original unbound RNA fraction was passed through it. The procedure described above was then repeated twice more and the bound RNA fractions were pooled, made 200 mM with respect to LiCl, and the RNA precipitated at -20°C by the addition of 2.5 volumes of ethanol.

The poly(A)-enriched RNA was recovered by centrifugation at 4,000g for 10 min, washed twice in 70% (v/v) ethanol, then once in absolute ethanol. The

resulting pellet was dried under a stream of nitrogen and dissolved in a small volume of sterile distilled water. The absorbance of this solution at 260 nm was then determined and the solution kept on ice. An oligo(dT)-cellulose column was prepared as described above and equilibrated with second high salt buffer (HSBS - 10 mM Tris-HCl (pH 7.5), 0.25% (w/v) SDS, 1 mM EDTA, 400 mM LiCl). A one-tenth volume of 0.1 M Tris-HCl (pH 7.5), 50 mM EDTA and 5% SDS was added to the RNA solution and this was then heated at 70°C for 3 min and then rapidly chilled by placing in ice. An equal volume of 10 mM Tris-HCl (pH 7.5), 5 mM EDTA, 0.5% (w/v) SDS and 0.66 M NaCl was added to the cooled solution and this was then carefully pipetted onto the oligo(dT)-cellulose column. Unbound RNA was washed through the column with HSBS and the effluent monitored by a Uvicord. Bound RNA was then eluted with second low salt buffer (LSBS - 10 mM Tris-HCl (pH 7.5), 0.25% (w/v) SDS). This buffer was maintained at 37°C in a constant temperature water bath. The bound RNA fraction was collected in a sterile glass tube on ice. The RNA was precipitated by the addition of a one-tenth volume of 2 M LiCl and 2.5 volumes of ethanol at -20°C. Following precipitation, the RNA was recovered by centrifugation at 4,000g for 10 min, washed twice in 70% (v/v) ethanol, once in absolute ethanol, then dried under a stream of nitrogen. The dried pellet was dissolved in sterile

distilled water to give a RNA concentration of 1 mg/ml. The solution was then stored at -20°C.

**(2.21) In Vitro Translation of Poly(A)-Enriched RNA**

Poly(A)-enriched RNA was translated in a wheat-germ cell-free translation system in order to produce a mixture of radio-labelled proteins containing possible precursors to the mature apoproteins of the LMC I.

All mRNA translations were carried out in sterile Eppendorf microcentrifuge tubes. The translation mixture contained the following components:

- 100 mM K acetate
- 2 mM Mg acetate
- 250  $\mu$ M spermidine
- 50  $\mu$ M spermine
- 22.5 mM HEPES-KOH, pH 7.6
- 3.5 mM dithiothreitol
- 1 mM Tris-ATP
- 10 mM phosphocreatine
- 40  $\mu$ g/ml creatine phosphokinase
- 100  $\mu$ M GTP (Type III - Sigma)
- 50  $\mu$ M each amino acid except methionine
- 800  $\mu$ Ci/ml [<sup>35</sup>S]-methionine
- 50  $\mu$ g/ml poly(A)-enriched RNA
- 25% (v/v) wheat-germ extract (S-30 fraction)

Translations were routinely carried out in 20  $\mu$ l

volumes. Where larger translation mixtures were used, these are indicated in the text. The wheat-germ extract (S-30) was the last component to be added to the mixture. Prior to this addition, 2  $\mu$ l of the mixture were removed to determine TCA-insoluble radioactive counts at zero time (Section 2.22). After addition of the wheat-germ extract, the mixture was incubated at 27°C for 60 min, at which time a further 2  $\mu$ l were removed to determine TCA-insoluble radioactive counts at the end of the incubation.

(2.22) Measurement of Incorporation of [<sup>35</sup>S]-Labelled Methionine into Protein

In order to measure incorporation of [<sup>35</sup>S]-methionine into protein, 2  $\mu$ l of the sample were removed and spotted onto a strip of Whatman No.1 paper measuring 1 cm x 2 cm. This was left to dry in air, then placed in 10% (w/v) TCA (approximately 5 ml per strip). The solution containing the strip was brought to boiling point, then left to cool for 20 min, after which the strip was transferred to an equal volume of fresh 10% (w/v) TCA and left at room temperature for 10 min. The TCA solution was then discarded and the strip washed twice with ethanol and once with diethyl ether. The washed strip was dried under a stream of nitrogen in a fume hood and then placed in a 50°C oven for 10 min. The strip was then counted for 1 min in 4 ml of Ready-Solve EP scintillant (Beckman), using a 1212 Minibeta

liquid scintillation counter (LKB).

[2.23] Determination of Amino-Terminal Amino Acid Sequences of the LHC I Apoproteins

PS I particles were prepared by the method of Mullet *et al.*, (1980a) as described in Section 2.13a. Aliquots of these were subjected to SDS-PAGE on 40 cm gels as described in Section 2.3. The gels were stained with Coomassie blue for not more than 15 min, after which they were rapidly destained, and the apoproteins of the LHC I excised and electroeluted as described in Section 2.14. The eluted polypeptides were then freeze-dried and sent to Dr. J.B.C. Findlay at the Department of Biochemistry, University of Leeds, for amino-terminal sequencing by solid-phase Edman degradation (Walker *et al.*, 1982).

[2.24] Immunological Identification of Thylakoid Proteins Labelled *in vivo* with [<sup>35</sup>S]-Labelled Methionine

Plant tissue was labelled *in vivo* with [<sup>35</sup>S]methionine as described in Section 2.9. The labelled tissue was then homogenised in ice-cold sucrose isolation medium in a cold mortar, and thylakoids were isolated as described in Section 2.12. Thylakoid proteins were then extracted and subjected to two-dimensional gel electrophoresis as described in Section 2.7, with IEF in the first dimension and SDS-PAGE in the second dimension. A marker track



containing PS I material prepared by the method of Mullet et al (1980a) was also run in the second dimension.

The proteins in the second dimension polyacrylamide gel were transferred to a nitrocellulose filter as described in Section 2.15d. This filter was dried and ink containing [<sup>35</sup>S]methionine was used to make radiolabelled marker spots on the filter. The filter was then autoradiographed to visualise the labelled thylakoid polypeptides.

The filter was then incubated overnight with 10  $\mu$ l of antiserum raised against the LHC I apoprotein P2, and then with [<sup>125</sup>I]-labelled protein A (see Section 2.15d(i)). After washing to remove excess iodinated protein A, the filter was dried and put down for autoradiography at -80°C with an enhancing screen. Two sheets of silver foil were placed between the nitrocellulose filter and the film in order to ensure that only the radio-iodine was detected by the film. Care was taken not to cover the labelled ink marker spots with the foil.

Following this second autoradiographic step, the two X-ray films were lined up using the marker ink spots and by this means [<sup>35</sup>S]-labelled LHC I apoproteins were identified.

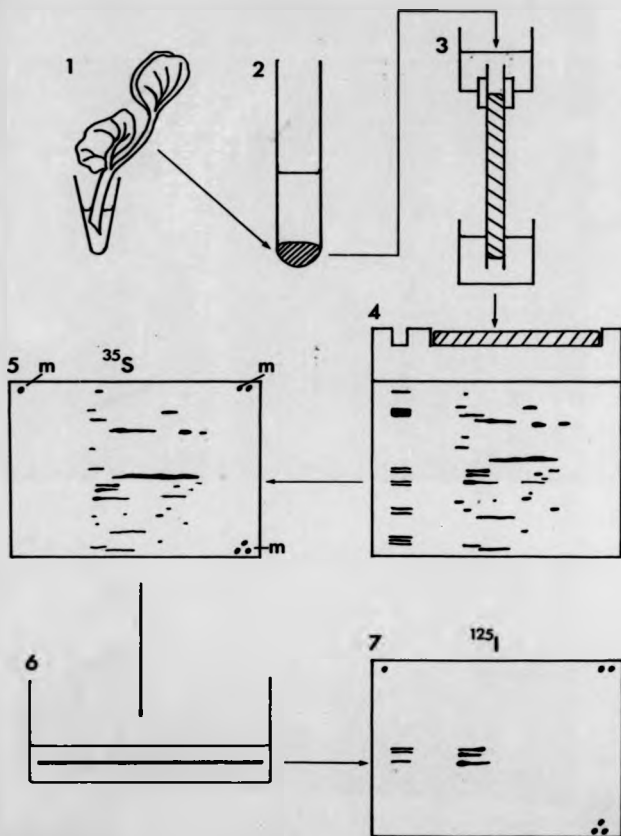
This method is summarised in Figure 2.3.

**Figure 2.3**

Method for immunological identification of thylakoid proteins labelled *in vitro* with [ $^{35}$ S]methionine.

- (1) Dissect third nodes from pea seedlings and place cut ends in microcentrifuge tubes containing [ $^{35}$ S]-labelled methionine. Allow uptake of isotope to proceed for 5-6 h.
- (2) Harvest labelled nodes and isolate thylakoid membranes (Section 2.12).
- (3) Subject thylakoids to separation in the first dimension by isoelectric focussing (IEF) as described in Section 2.7.
- (4) Lay the first dimension IEF gel horizontally on the stacker of the second dimension SDS-polyacrylamide vertical slab gel, and commence SDS-PAGE as described in Section 2.7. A sample of purified PS I is also run in a slot to the side in order to provide markers for the LHC I polypeptides.
- (5) After electrophoresis, electrophoretically blot the resolved protein spots onto a nitrocellulose filter. Dry the filter and mark with [ $^{35}$ S]-labelled ink (ink spots are marked 'm' in the Figure). Autoradiograph the filter to visualise the [ $^{35}$ S]-labelled thylakoid polypeptides.
- (6) Incubate the filter with P2 antiserum followed by [ $^{125}$ I]-labelled protein A.
- (7) Dry the filter and autoradiograph to visualise the immunologically detected LHC I apoproteins. Two sheets of silver foil are placed between the filter and the film to allow through only the signal due to iodine. Care must be taken not to cover the marker ink spots with the foil.

LHC I apoproteins are identified on the original autoradiograph by lining up the marker ink spots on the two X-ray films.

**Figure 2.3**

**PART 3**  
**RESULTS**

### [3.1] Isolation of Photosystem I

The aim of all thylakoid membrane fractionation techniques which employ detergents, is to disrupt the hydrophobic interactions between membrane protein and lipid, without perturbing the protein-protein and pigment-protein interactions responsible for maintaining the conformation of the chlorophyll-protein complexes within the membrane. Ideally, this disruption would result in the dissolution of the lipid bilayer and the simultaneous release of pigment-protein complexes displaying properties similar to those observed in the undisrupted membrane.

This ideal situation is unlikely to be achieved. Detergents vary in their ability to bind to proteins, this ability being greatly influenced by the critical micelle concentration (CMC) and charge of the detergent in question, and the hydrophilic/hydrophobic nature of the proteins being solubilised. In general, at low detergent concentrations, hydrophobic binding of detergent to protein takes place at a relatively small number of 'high affinity' sites on the protein surface (Helenius and Simons, 1975). As the CMC is approached, secondary binding takes place at non-specific 'low affinity' sites. This secondary binding usually results

in some disruption of the native conformation of the protein, and consequent loss of biological activity. In the case of a non-ionic detergent such as Triton X-100, micelle formation occurs before secondary binding can have such effect. However, in the case of charged detergents such as SDS, secondary binding can occur before the CMC is reached. Moreover, addition of charge to the surface of a protein may result in the further unfolding of the protein, allowing access of more detergent molecules to previously protected hydrophobic regions of the polypeptide chain. Hence, the degree to which different membrane proteins can retain their native conformation will depend largely upon the detergent used to disrupt the membrane. Detergents are chosen depending upon the protein complex of interest.

The methods used in this study to produce native PS I particles rely upon the use of the minimum concentration of an uncharged detergent (Triton X-100) necessary to solubilise unstacked thylakoid membranes. Unstacking of the membrane is important since the presence of appressed membranes would result in the need for higher detergent concentrations, and the uneven solubilisation of the appressed and unappressed membrane domains.

(3.1a) The method of Mullet et al (1980a)

The method for producing native PS I particles described by Mullet et al (1980a) failed in this study to reliably resolve chlorophyll-protein complexes by sucrose density gradient centrifugation. The reason for this failure remains unclear since adherence to the published method has resulted in the successful generation of PS I particles in other laboratories. In an attempt to overcome this problem, the preparation protocol was modified to include the Tris-glycine buffer system described in Section 2.13a. This resulted in the reliable recovery of PS I particles with characteristics similar or identical to those reported by Mullet et al (1980a).

An important prerequisite for the successful recovery of PS I particles was found to be the determination of the detergent concentration producing the greatest yield of PS I in the sucrose density gradient. This was done by solubilising a membrane preparation, at a chlorophyll concentration of 500 µg/ml, with increasing concentrations of Triton X-100. The solubilised material was then centrifuged for 30 min at 30,000g, and the amount of chlorophyll recovered in the resulting pellet measured. The pellet represented unsolubilised membrane material. Table 3.1 shows the relationship between the amount of chlorophyll recovered in the pellet and the concentration of detergent used. As expected, as the

**Table 3.1** The effect of varying Triton X-100 concentration upon recovery of membranes after solubilisation.  
For details of the experimental procedure, see Section 3.1a.

% (w/v) Triton X-100	% Total chlorophyll recovered in unsolubilised pellet
0.2	11.7
0.4	8.4
0.6	5.2
0.8	1.3
1.0	not measurable
2.0	not measurable



detergent concentration increases, the amount of recoverable chlorophyll decreases. When the supernatants resulting from these solubilisations were subjected to sucrose density gradient centrifugation as described in Section 2.13a, it was found that only those samples solubilised with 0.4% (w/v) or 0.6% (w/v) Triton X-100 yielded a distinct green band in the lower part of the sucrose gradient. Where higher concentrations of detergent had been used, the chlorophyll formed a smear in the upper two-thirds of the gradient. At the highest detergent concentrations, most of the chlorophyll failed to enter the gradient, suggesting that the pigment-protein complexes had been severely disrupted by the detergent treatment.

On the basis of these results, a Triton X-100 concentration of 0.5% (w/v) was routinely used to solubilise the thylakoid membranes. It should be pointed out that this procedure needed to be repeated for different batches of detergent, since the optimum concentration for membrane solubilisation differed from batch to batch. Furthermore, prolonged storage of the detergent at room temperature did not affect the concentration optimum. It is therefore strongly recommended that where this solubilisation procedure is to be used routinely, the same batch of Triton X-100 be used for all experiments, to ensure reproducible results.

Figure 3.1 shows a typical sucrose density gradient after centrifugation had been carried out at 100,000g for 16 h. Two distinct chlorophyll-containing bands can be seen, a relatively wide band occupying the upper one-third of the gradient, and a narrow band at the interface with the 2 M sucrose cushion.

Figure 3.2 shows the content of chlorophyll in fractions taken from the sucrose gradient, and Figure 3.3 shows the relative distribution of chlorophyll *a* and chlorophyll *b* in the gradient, expressed as the ratio of these two pigments in each gradient fraction. A comparison of these two graphs clearly shows that the distribution of these two chlorophyll species is not equivalent between the two chlorophyll-containing bands. The upper chlorophyll-containing region of the gradient, represented by fractions 1 to 10, displays a chlorophyll *a/b* ratio of between 1.0 and 2.0. Since the thylakoid preparation from which this material was derived displayed a chlorophyll *a/b* ratio of 3.0, these fractions are enriched with chlorophyll *b*. The lower green band, represented by fraction 23, displays a chlorophyll *a/b* ratio of 6.0, indicating that this band contains very little chlorophyll *b*. This conclusion is supported by Figure 3.4 which compares absorption spectra of acetone-extracted pigments derived from intact thylakoids and the lower green band from the sucrose density

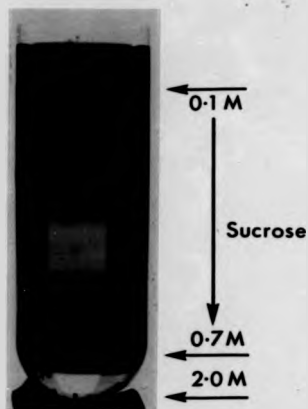


**Figure 3.1** Sucrose density gradient containing green bands resulting from solubilisation of unstacked thylakoids with Triton X-100 following the method of Mullet *et al* (1980a). Solubilised membrane material (4-5 mg chl.) was layered over a 0.1 M-0.7 M linear sucrose gradient (50 ml), containing 0.02% (w/v) Triton X-100. The sucrose gradient was formed over a 2 M sucrose cushion (5 ml). Centrifugation was carried out as described in Section 2.13a.

**Figure 3.2** Distribution of chlorophyll on sucrose density gradient following membrane solubilisation by the method of Mullet *et al* (1980a). The sucrose density gradient was divided into 25 fractions (each 2.6 ml), fractions 24 and 25 being derived from the 2 M sucrose cushion. Chlorophyll was extracted from each fraction by the addition of 4 volumes of acetone. Chlorophyll concentrations were determined as described in Section 2.17.

**Figure 3.3** Relative distribution of chlorophylls *a* and *b* on sucrose density gradient following membrane solubilisation by the method of Mullet *et al* (1980a). The sucrose gradient was divided into 25 fractions (each 2.6 ml), and chlorophyll extracted from each fraction by the addition of 4 volumes of acetone. Chlorophyll *a/b* ratios were determined using the equations described in Section 2.17.

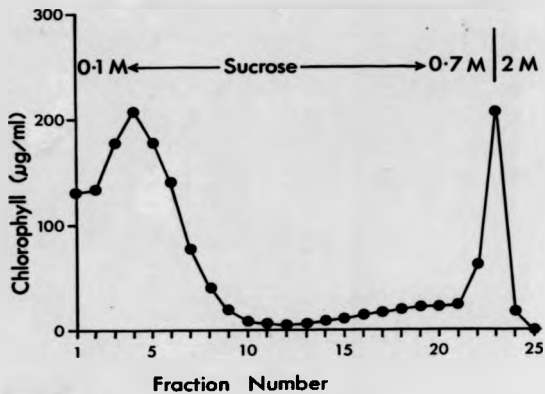


Figure 3.2

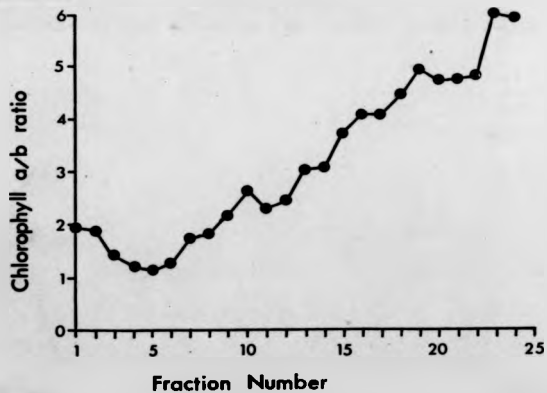
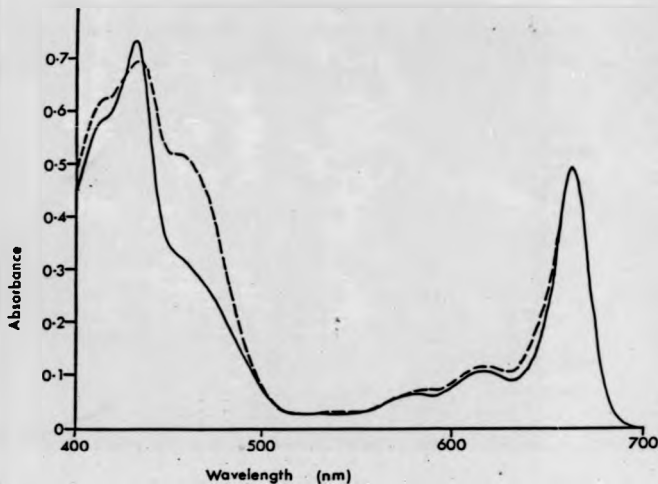


Figure 3.3



**Figure 3.4**

Comparison of absorption spectra of pigments extracted from unfractionated thylakoids and sucrose gradient fraction 23. Sucrose gradient fraction 23 was produced by the method of Mullet *et al* (1980a). Pigments were extracted from resuspended thylakoids and from fraction 23 by the addition of 4 volumes of acetone. Extraction details are given in Section 2.17.

----- Thylakoid membranes  
 ————— Sucrose gradient fraction 23

gradient. It is clear that the absorption components contributed by chlorophyll *b* in the red region (around 645 nm) and in the blue region (around 450 nm), are reduced in the sucrose gradient material compared to those in the intact membranes. Typically, the chlorophyll recovered in the lower green band represented 10%-15% of the total chlorophyll loaded onto the gradient.

Figure 3.5 shows the distribution of PS I-mediated electron transport activity in the sucrose gradient. In the upper regions of the gradient, where most of the chlorophyll *b* is concentrated, the rates of PS I-mediated electron transport never exceed 200  $\mu\text{mol}$  oxygen consumed/mg chlorophyll/h. This rate steadily increases with increasing fraction number, a maximum rate of 600  $\mu\text{mol}$ /mg chlorophyll/h being found in fraction 23.

Table 3.2 compares PS I-mediated electron transport rates in unisolubilised membranes, membranes solubilised with 0.5% (w/v) Triton X-100, and in fraction 23 from the sucrose gradient. The PS I electron transport rates for whole membranes were measured in the presence of 6  $\mu\text{M}$  dichlorophenyl dimethylurea (DCMU) to block PS II activity. It can be seen that solubilisation of the thylakoid with 0.5% (w/v) Triton X-100 reduces the rate of PS I-mediated electron transport by 50%. This decrease in rate could be due to decreased accessibility of the solubilised PS I reaction centres to the electron donor

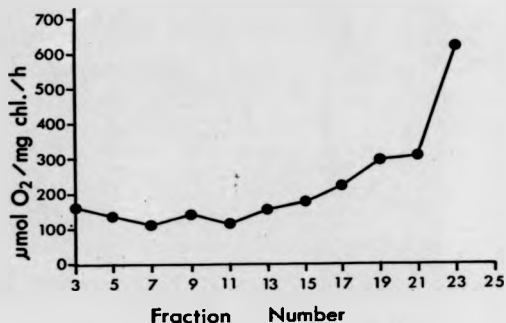


**Figure 3.5** Distribution of PS I-mediated electron transport activity in sucrose density gradient following membrane solubilisation by the method of Mullet *et al* (1980a). Sucrose gradient fractions 1-25 were assayed for PS I-mediated electron transport activity by measuring the rate of uptake of oxygen associated with light-induced electron flow from reduced DCPIP to MV, as described in Section 2.19.



**Table 3.2** Comparison of PS I-mediated electron transport rates in unsolubilized and solubilized thylakoid membranes, and in fraction 23 from sucrose gradients. All measurements were carried out as described in Section 2.19. Assays were carried out with a chlorophyll concentration of 50  $\mu\text{g/ml}$  in the oxygen electrode chamber.

Fraction	Rate of PS I-mediated electron transport (ascorbate to methylviologen; $\mu\text{mol O}_2$ consumed/ $\mu\text{g chl/h}$ )
Intact membranes + DCPIP	189
- DCPIP	15
Solubilised membranes + DCPIP	93
- DCPIP	45
Fraction 23	660
Reaction mixture with no added chlorophyll	12

(in this case reduced DCPIP), or to a detergent-induced conformational change in one or more components of the PS I complex. In the absence of DCPIP, electrons may be donated to the PS I reaction centre directly from ascorbate (Trebst, 1980). The PS I-mediated electron transport rate for intact membranes measured in the absence of DCPIP was only 8% of that measured in the presence of DCPIP. Thus, the presence of reduced DCPIP in this system is necessary for the establishment of electron flow through PS I. Where the membranes had been solubilised, the electron flow rate through PS I was reduced by only 50% in the absence of DCPIP, suggesting that the reaction centres were now more accessible to the ascorbate. These results indicate that some detergent-induced perturbation of the PS I complexes had taken place, since it is unlikely that the reduction in the rate of electron transport after solubilisation of the membrane was due to reduced accessibility to electron donors.

The rate of PS I-mediated electron transport measured in fraction 23 of the sucrose density gradient was typically three to four times that measured using intact membranes. These high rates, taken together with the lack of chlorophyll *b* in this fraction, indicate that the lower green band on the gradient is enriched with PS I reaction centres.

Figure 3.6 shows an SDS-PAGE analysis of the polypeptide content of fractions derived from the sucrose density gradient. A track showing a typical whole thylakoid polypeptide pattern is included for comparison. The major thylakoid polypeptide, the 26 kDa component of the LHC II (LHCP), is confined to the first eight fractions, being concentrated mainly in fractions 3 to 6. Since the LHC II binds chlorophyll *a* and chlorophyll *b* in approximately equimolar ratios, the majority of the thylakoid chlorophyll *b* should be concentrated in these fractions, assuming that the LHC II has not lost pigment due to the action of the detergent. This conclusion is supported strongly by Figure 3.3, in which fractions 3 to 6 display chlorophyll *a/b* ratios well below that encountered in unisolubilised thylakoids.

Fractions derived from the central region of the gradient, where little chlorophyll is found, contain the  $\alpha$  and  $\beta$  subunits of the thylakoid ATP synthase  $CF_1$  complex as the major stainable proteins. Williams and Bennett (1983) have shown that these two proteins sediment together with the other protein subunits of the  $CF_1$  complex, as a multisubunit complex in this gradient system.

Little protein is found in fractions derived from the lower regions of the gradient, until fraction 23 is reached. This fraction contains high levels of

**Figure 3.6** SDS-polyacrylamide gel analysis of fractions from the sucrose density gradient following membrane solubilisation by the method of Mullet *et al* (1980a). Track (M) Untreated thylakoid membranes, tracks (3)-(23) sucrose gradient fractions. An aliquot (50  $\mu$ l) of each gradient fraction was mixed with an equal volume of SDS sample buffer, boiled for 2 min and then subjected to SDS-PAGE. The gel consisted of a 10%-30% acrylamide gradient and was stained with Coomassie brilliant blue.

**Figure 3.7** SDS-polyacrylamide gel analysis of fraction 23 from the sucrose density gradient following membrane solubilisation by the method of Mullet *et al* (1980a). Track (1) Relative mobility markers, track (2) fraction 23. An aliquot (50  $\mu$ l) of fraction 23 was mixed with an equal volume of SDS sample buffer, boiled for 2 min and then subjected to SDS-PAGE. The gel consisted of a 10%-16% polyacrylamide gradient and was stained with Coomassie brilliant blue.

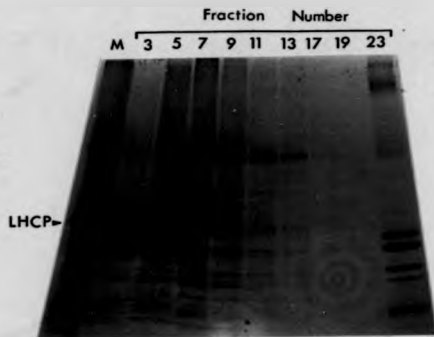


Figure 3.6

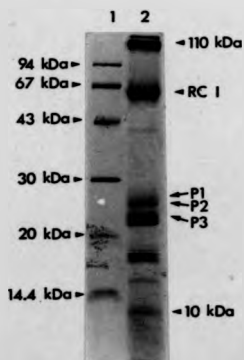


Figure 3.7

chlorophyll *a*, little chlorophyll *b* and displays high rates of PS I-mediated electron transport. Figure 3.6 shows that this fraction contains a number of polypeptides, ranging in apparent molecular mass from about 9 kDa to 110 kDa.

Figure 3.7 shows a higher resolution analysis of the polypeptide constituents of fraction 23. The 110 kDa polypeptide appears as a green chlorophyll-containing band on unstained gels. This band can be removed completely by prolonged boiling of this gradient fraction in SDS sample buffer containing 5 mM 2-mercaptoethanol, prior to electrophoresis. The disappearance of this band is accompanied by an increase in the stainable amount of protein in the 65-68 kDa region. Polypeptides in this region usually appear as a smear on polyacrylamide gels, but sometimes can be resolved into one or two distinct, closely migrating proteins. These proteins represent the P700-binding proteins of the reaction centre of PS I, and in this study will be referred to as RC I proteins (see section 1.6b).

Three polypeptides at 24 kDa, 23 kDa, and 21 kDa, labelled P1, P2, and P3 respectively, represent the apoproteins of the peripheral light-harvesting complex of PS I (LHC I) (Haworth *et al*, 1983). In some preparations, each of these three stained bands appeared as closely migrating doublets. This phenomenon has also been

observed by other workers (Haworth *et al*, 1983). The remaining polypeptide constituents of fraction 23 form a group of 6-7 proteins ranging in molecular weight from 20 kDa to 9 kDa. The identity and function of these polypeptides is largely unknown (see Section 1.6a).

The 12 polypeptides shown in figure 3.7 were consistently found in all such preparations. It is clear that this fraction represents a multisubunit PS I complex composed of the reaction centre and associated peripheral light-harvesting components. The properties of this complex described above closely resemble those reported by Mullet *et al* (1980a).

Figure 3.8 shows the 77 K fluorescence spectrum of fraction 23 obtained in collaboration with Dr. J.F. Allen of the Department of Plant Sciences, Leeds University. This spectrum is composed of two peaks, a minor peak occurring at 682 nm and a major peak at 735 nm. The fluorescence maximum at 735 nm is characteristic of PS I. The minor peak at 682 nm is characteristic of PS II fluorescence at low temperature. More precisely, this peak is a product of fluorescence from the PS II peripheral light-harvesting pigment bed (LHC II). The presence of this minor fluorescence peak indicates the presence of PS II-associated pigments in this preparation. It was found that the size of this peak varied in different preparations, and in some

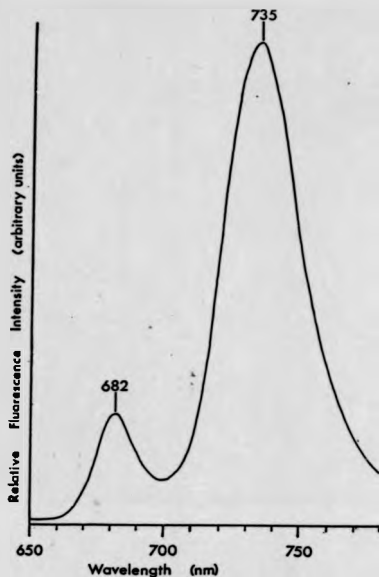


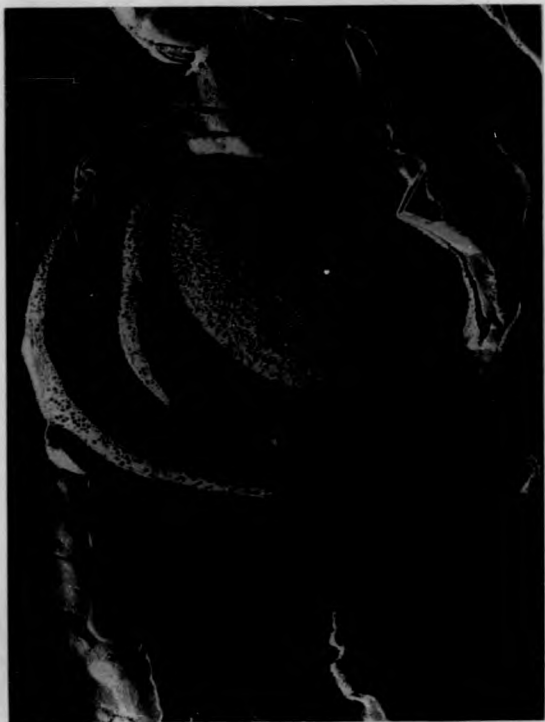
**Figure 3.8** Fluorescence emission spectrum (77 K) of fraction 23 from the sucrose density gradient following membrane solubilisation by the method of Mullet *et al* (1980a). Fluorescence was excited at 440 nm (2.5 nm slit). Fluorescence emission was collected between 650 nm and 780 nm using a 5 nm slit as described in section 2.16. The spectrum was normalised to the maximum prior to plotting.



preparations this peak was completely absent. Furthermore, the presence of this peak correlated with the presence of small, stainable amounts of the 26 kDa LHCP of the LHC II. It is clear therefore that fraction 23 can contain small amounts of LHC II polypeptides. The fact that the quantity of LHCP associated with this fraction is variable indicates that it is a contaminant and not a component of the PS I complex.

Further characterisation of this PS I preparation was carried out by freeze-fracture electron microscopy. Figure 3.9 shows an electron micrograph of a freeze-fracture replica of washed, unstacked thylakoids immediately prior to solubilisation with Triton X-100. The membranes take the form of vesicles varying in diameter between 0.3  $\mu\text{m}$  and 3.0  $\mu\text{m}$ . The vesicle depicted in Figure 3.9 is a compound structure consisting of at least three concentric vesicles. This type of structure was found to be common in these preparations, and undoubtedly results from shearing of the thylakoid bilayer during the washing procedure. Closer examination of this micrograph reveals that the membrane surface of the innermost observable vesicle is divided into two distinct regions in terms of the size and density of embedded particles. These two regions are divided by a clear boundary. Following the nomenclature of Branton et

**Figure 3.9** Freeze-fracture electron micrograph of washed, unstacked thylakoids, prior to addition of detergent. Unstacked thylakoids were prepared by lysing isolated chloroplasts in the presence of EDTA as described in Section 2.13a. Freeze-fracture replicas were prepared as described in Section 2.18. (EF) Exoplasmic fracture face, (PF) protoplasmic fracture face. Magnification x 47,880



al (1975), these two regions are very similar to the EF (exoplasmic or inner) and PF (protoplasmic or outer) fracture faces described by Stachelin (1976). The EF fracture face represents the inner leaflet of the thylakoid membrane while the PF face represents the outer leaflet. The PF face is characterized by the high density of small (80 Å) particles embedded in its surface. The EF face characteristically contains a relatively small number of large (140 Å) particles. These may represent PS I and PS II protein complexes respectively (Stachelin, 1976). The distribution of large EF particles in Figure 3.9 is homogeneous throughout the fracture face indicating that the membranes in this sample are in the unstacked condition typical of thylakoids washed in low salt buffers (Steinback *et al.*, 1978). Figure 3.10 represents a compound vesicle from the same sample as that shown in Figure 3.9, and shows the division between fracture faces more clearly.

Figure 3.11 is an electron micrograph of a freeze-fracture replica from a typical PS I preparation. The material in these preparations consisted mainly of small vesicles, varying in diameter from 100 nm to 500 nm, interspersed with interconnected, non-vesicular sheet-like domains. The most striking feature of these preparations is the presence of regular arrays of particles, of uniform size, throughout the fracture

**Figure 3.10** Freeze-fracture electron micrograph of washed, unstacked thylakoids, prior to addition of detergent. (EF) Exoplasmic fracture face, (PF) protoplasmic fracture face. Freeze-fracture replicas were prepared as described in Section 2.18. Magnification  $\times 95,760$

(178)

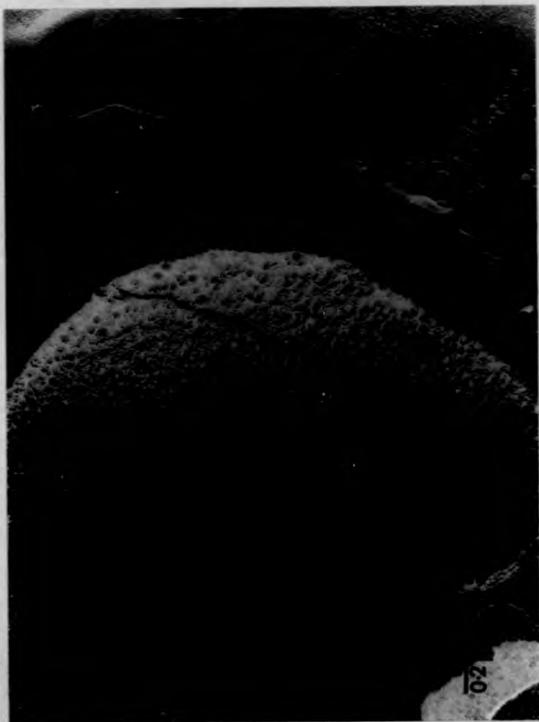


**Figure 3.11** Freeze-fracture electron micrograph of material derived from fraction 23 of the sucrose density gradient, following membrane solubilisation by the method of Mullet *et al* (1980a). Freeze-fracture replicas were prepared as described in Section 2.18.  
Magnification x 58,520





surfaces. This contrasts sharply with the picture presented in Figures 3.9 and 3.10, where particle size and distribution is non-uniform. The diameter of individual particles was measured as approximately 100 Å. Mullet *et al* (1980a), reported particle sizes of 100 Å to 130 Å in similar PS I preparations. However, although these authors observed some aggregation of individual particles, they did not report the presence of regular particle arrays such as those apparent in Figure 3.11.

Closer inspection of this preparation (Figure 3.12) shows clearly that the majority of particles are arranged in pairs, the diameter of each pair being approximately 250 Å. Furthermore, the arrays formed by the particle doublets are two-dimensional, since in no preparation were overlapping sheets of arrayed particles observed. The reasons for the differences between these preparations and those described by Mullet *et al* (1980a) are not clear. Since the only difference between the preparation procedure reported by those authors and that reported here is the inclusion of the Tris-glycine buffer, it is possible that the buffer in which solubilisation is carried out affects the aggregation properties of membrane protein complexes such as PS I. This idea will be discussed more fully in Section 4.1.

The ability of the PS I particles to sediment to the 2 M sucrose interface upon sucrose density gradient

**Figure 3.12** Freeze-fracture electron micrograph of material derived from fraction 23 of the sucrose density gradient, following membrane solubilisation by the method of Mullet *et al* (1980a). Freeze-fracture replicas were prepared as described in Section 2.18.  
Magnification x 156,940



centrifugation is not clearly understood. Mullet *et al* (1980a) have suggested that the solubilised particles lose associated detergent while sedimenting through the sucrose gradient. This loss of detergent promotes hydrophobic interactions between the PS I particles, leading to aggregation. This conclusion is supported by the observation that the inclusion of 0.5% (w/v) Triton X-100 within the gradient results in the complete abolition of a resolvable PS I band (result not shown). The aggregation of PS I particles in the preparations reported here is clearly of a very regular nature. The formation of two-dimensional arrays of paired particles may reflect some important structural feature of the PS I complex. However, the fact that no such PS I arrays have been observed in preparations derived from intact membranes suggests that this feature is a consequence of the PS I preparation procedure, and does not reflect any structure to be found *in vivo*.

### [3.1b] The 'high salt' method

The 'high salt' method for isolating PS I particles differs from the method of Mullet *et al* (1980a) in that it produces a PS I preparation which sediments at relatively low speed (30,000xg), rendering the sucrose gradient step no longer necessary. As described in Section 2.13b, the PS I preparation is recovered as a

green pellet. The properties of this preparation were studied by several different techniques.

Figure 3.13 shows absorption spectra of acetone-extracted pigments derived from intact thylakoids and from the 'high salt' PS I pellet. Comparison of Figure 3.13 with Figure 3.4 shows that the absorption spectrum of this PS I preparation is very similar to that of the PS I material produced by the method of Mullet *et al* (1980a). However, the chlorophyll *b* content of this preparation was consistently found to be higher, with chlorophyll *a/b* ratios of 3.8-4.3 (see Table 3.3). The variability in the chlorophyll *b* content of this preparation was found to be greater than that found in the preparation of Mullet *et al* (1980a).

Figure 3.14 shows the 77 K fluorescence emission spectrum of the 'high salt' PS I particle. Once again, this was found to contain two peaks of fluorescence emission, a small peak at 682 nm and a second, major peak at 735 nm. The relative size of the peak at 682 nm varies greatly between different preparations. This observation, together with the variability in the chlorophyll *b* content, suggests strongly that this method produces a variable degree of contamination of the PS I preparation with LHC II particles.

Figure 3.15 shows an analysis of the polypeptide constituents of this PS I preparation by SDS-PAGE. Also

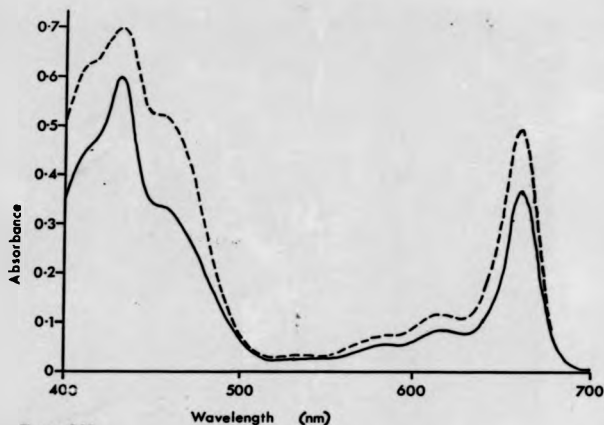
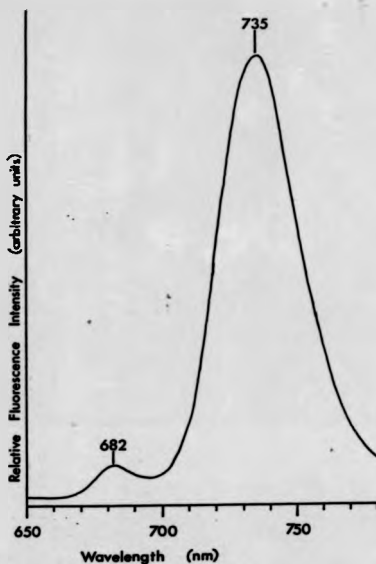


Figure 3.13

Comparison of absorption spectra of pigments extracted from thylakoid membranes and the 'high salt' PS I pellet. Pigment extractions were carried out in 80% (v/v) aqueous acetone. Extraction details are given in Section 2.17. The PS I 'high salt' pellet was prepared as described in Section 2.13(b). Thylakoid membranes were prepared as described in Section 2.12.

----- Thylakoid membranes  
 ————— 'High salt' pellet



**Figure 3.14**

Fluorescence emission spectrum (77 K) of 'high salt' pellet. Fluorescence was excited at 440 nm (2.5 nm slit). Fluorescence emission was collected between 650 nm and 780 nm using a 5 nm slit, as described in Section 2.16. The spectrum was normalized to the maximum prior to plotting. The PS I 'high salt' pellet was prepared as described in Section 2.13b.

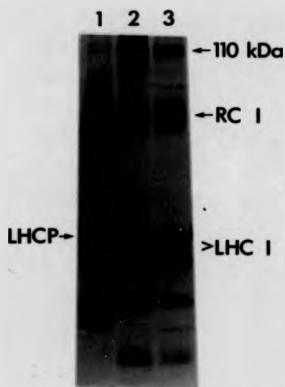


**Figure 3.15**

SDS-polyacrylamide gel analysis of the polypeptide content of the 'high salt' pellet.

Track (1) thylakoid membranes, track (2) 'high salt' pellet, track (3) PS I prepared by the method of Mullet *et al* (1980a).

RC I and LHC I refer to the polypeptides of the PS I reaction centre and peripheral light-harvesting system respectively. LHCP denotes the 26 kDa apoprotein of the LHC II.

All samples were heated in an equal volume of SDS sample buffer for 2 min prior to electrophoresis. A volume of sample containing 10 µg chlorophyll was loaded in each track. The gel consisted of a 10%-16% polyacrylamide gradient and was stained with Coomassie brilliant blue.



shown for comparison are the polypeptide profiles of intact membranes and of a PS I sample produced by the method of Mullet *et al* (1980a). It is clear from this Figure that although the PS I particles produced by this method display the same polypeptide pattern as the Mullet preparation, they also contain significant amounts of the LHC II polypeptides (see also Figure 3.21). The data Table 3.3 show that the preparation produced by this method can also carry out PS I-mediated electron transport at rates comparable to those of the Mullet preparation, indicating that the material contains active PS I reaction centres.

In view of the fact that the inclusion of the 0.8 M NaCl wash in the preparation procedure dramatically alters the sedimentation properties of the PS I particle, freeze-fracture electron microscopy was used to investigate the physical effect of the salt wash on the intact thylakoids. Prior to the salt wash, the thylakoids are washed with 50 mM sorbitol, 5 mM EDTA (pH 7.8) in order to unstack the membranes (see Section 2.13b). After unstacking, the thylakoids take on the appearance of large, often concentric vesicles, as shown in Figure 3.16. This picture is similar to those shown in Figures 3.9 and 3.10, indicating that there is no difference between the starting material for the 'high salt' preparation and that for the method of Mullet *et al*

**Figure 3.16.** Freeze-fracture electron micrograph of washed, unstacked thylakoids prior to washing with 0.8 M NaCl. Freeze-fracture replicas were prepared as described in Section 2.18. Magnification x 47,880



(1980a). When, after the Sorbitol-EDTA wash, thylakoids are recovered by centrifugation at 10,000xg, they form a large, loose green pellet which is easily dispersed in the resuspension buffer. The pellet resulting from the subsequent salt wash is smaller in area and very difficult to resuspend, forming tight clumps of membranous material. Subsequent washes with the Tris-glycine buffer result in the restoration of the large, easily resuspended pellet.

Figure 3.17 shows a freeze-fracture electron micrograph of material derived from the pellet resulting from the salt wash. Comparison of this Figure with Figure 3.16 shows a dramatic change in the morphology of the membranes. The large vesicles have been replaced by membranous sheets, reminiscent of stacked thylakoids. Figure 3.18 represents the same material at higher magnification. In this picture the differentiation between EF and PF fracture faces is very clear, indicating that although the gross morphology of the membrane is altered by the salt wash, the internal structure of the lipid bilayer remains essentially the same.

Figure 3.19 shows a freeze-fracture electron micrograph of the low speed (30,000xg) PS I pellet resulting from the solubilisation of the salt-washed membranes with Triton X-100. The material consists

**Figure 3.12.** Freeze-fracture electron micrograph of thylakoid membranes after washing with 0.8 M NaCl. Freeze-fracture replicas were prepared as described in Section 2.18. Magnification  $\times 74,480$ .



Figure 3.18 Freeze-fracture electron micrograph of thylakoid membranes after washing with 0.8 M NaCl. (EF) Exoplasmic fracture face, (PF) protoplasmic fracture face. Freeze-fracture replicas were prepared as described in Section 2.18. Magnification  $\times 156,940$ .





**Figure 3.12** Freeze-fracture electron micrograph of material derived from the 'high salt' pellet following solubilisation of salt-treated thylakoid membranes with Triton X-100. Details of the solubilisation conditions are given in Section 2.13b. Freeze-fracture replicas were prepared as described in Section 2.18. Magnification x 114,380.



largely of membrane-like sheets containing particles of a single size-class, 100-130 Å in diameter. The arrangement of these particles on the fracture faces does not resemble that of the PS I particles prepared by the method of Mullet *et al* (1980a), as shown in Figures 3.11 and 3.12. No extensive arrays of PS I particles can be seen in the 'high salt' preparation, particles being mostly solitary and not arranged in pairs as in Figure 3.12. This arrangement of particles resembles that described by Mullet *et al* (1980a).

It is concluded from these observations that the 'high salt' method produces a preparation which is similar in most respects to that described by Mullet *et al* (1980a). However, inclusion of the salt wash step prior to membrane solubilisation brings about changes in the membrane which result in the release of a PS I particle with very different sedimentation properties to those of the Mullet preparation, dispensing with the need for the sucrose density gradient step altogether. The mechanism of this change is not clear. Figures 3.16 and 3.17 demonstrate that the salt wash induces a major gross morphological change in the membrane. This change results in the formation of parallel sheets of membranes in which the internal distribution of particles within the lipid bilayer retains a pattern indicative of unstacked membranes. Subsequent solubilisation of this membrane

material with Triton X-100 releases a PS I preparation whose sedimentation characteristics resemble those of whole membranes, in that this preparation may be recovered by centrifugation at relatively low speed (30,000xg). If the supernatant resulting from this centrifugation is then subjected to sucrose gradient centrifugation as described by Mullet *et al* (1980a), no PS I-containing band is formed.

It is tempting to speculate that the salt wash induces a change in the distribution of the PS I particles within the membrane which results in their protection from full solubilisation by the detergent. In this event, the PS I material would be expected to sediment at low speed, as observed. However, no evidence for this can be found by examining the freeze-fracture electron micrographs, and the exact mechanism underlying this phenomenon remains unknown. If protection from solubilisation by the detergent were responsible, then it would be expected that this PS I preparation should contain a high concentration of thylakoid lipids relative to that found in the Mullet preparation. This lipid analysis has not yet been done, and the nature of the matrix containing the PS I particles remains unknown.

(3.1c) The Tris-HCl method

The Tris-HCl method for producing a PS I preparation differs from the method of Mullet *et al* (1980a), in that the membrane solubilisation step is carried out in the presence of 25 mM Tris-HCl (pH 8.3) instead of Tris-glycine. This solubilisation is followed by a 30 min centrifugation step at 30,000g, resulting in the formation of a large green pellet and pale green supernatant (Section 2.13c).

Figure 3.20 shows the absorption spectra of acetone-extracted pigments derived from whole thylakoids, isolated LHC II and the pellet resulting from the Tris-HCl solubilisation described above. The Tris-HCl pellet differs from the other two PS I preparations already discussed in that it displays a pronounced absorption peak around 480 nm and increased absorption at 645 nm. This indicates that this preparation has undergone some enrichment in chlorophyll *b* compared to the intact membrane. Comparison of the absorption spectrum of the Tris-HCl pellet with that derived from purified LHC II supports this conclusion. The purified LHC II typically displays a chlorophyll *a/b* ratio of 1.1 (see Table 3.3), and also shows enhanced absorption at 480 nm and 645 nm due to chlorophyll *b*. The Tris-HCl pellet displayed a chlorophyll *a/b* ratio of about 2.8 (see Table 3.3).

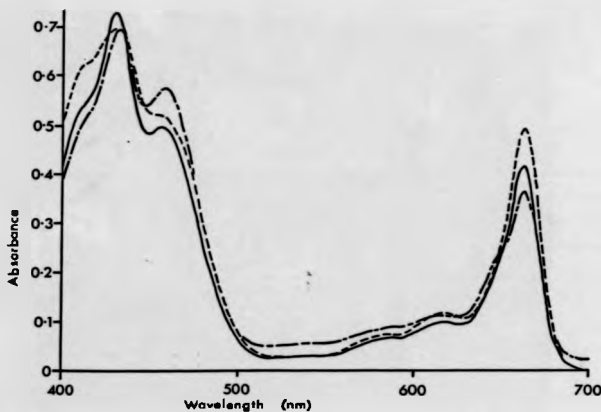


**Figure 3.20**

Comparison of absorption spectra of pigments extracted from thylakoid membranes, the Tris-HCl pellet and purified LHC II. Pigments were extracted in 80% (v/v) acetone. Extraction details are given in Section 2.17. The Tris-HCl pellet was prepared as described in Section 2.13c. The LHC II was purified as described in Section 2.13e.

— Tris-HCl pellet  
 ---- Thylakoid membranes  
 -.- Purified LHC II

**Table 3.3** Summary of properties of PS I particles prepared by the three different methods described in Section 2.13. Data for the purified LHC II are also shown for comparison

Property	Fraction			
	PS I (Mullet)	PS I (high salt)	PS I (Tria-HCl)	LHC II
Chlorophyll a/b ratio	>6.0	3.8-4.5	2.7-2.9	1.1
Rate of PS I-mediated electron transport "	>600	>500	150-170 "	-

" PS I-mediated electron transport rates are expressed as  $\mu\text{mol O}_2$  consumed/mg chlorophyll/h.

" PS I-mediated electron transport rates are expressed as rates per unit chlorophyll. Since the Tria-HCl preparation contains large quantities of LHC II-associated chlorophylls which may not contribute to PS I-mediated electron transport, the figures quoted are likely to be underestimates of the actual rates. See text for further discussion of this point.

PS I-mediated electron transport was also measured using the Tris-HCl preparation, and it was found that this preparation was capable of electron transport rates similar to, although a little lower than, those measured for the two other PS I preparations (Table 3.3). Figure 3.21 shows an analysis of the polypeptide content of the Tris-HCl pellet by SDS-PAGE. Also shown are the polypeptide profiles of PS I particles prepared by the method of Mullet *et al* (1980a) and by the 'high salt' method. It is clear from this Figure that the Tris-HCl pellet contains the same complement of polypeptides found in the other two preparations, together with a large amount of the polypeptides of the LHC II. When the supernatant corresponding to the Tris-HCl pellet was subjected to sucrose density gradient centrifugation as described by Mullet *et al* (1980a), no PS I-containing band was formed, and recovery of the LHC II from the upper fluorescent band by magnesium precipitation was greatly reduced (results not shown).

It was found that the polypeptide composition and chlorophyll *a/b* ratio of this pellet did not vary significantly between preparations, indicating that the ratio of PS I to LHC II in these preparations remained constant. This reproducibility could be attributed to two possible causes. Firstly, solubilisation of the membrane in the presence of Tris-HCl may affect the LHC II and



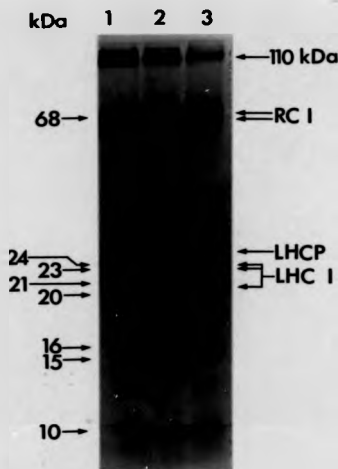


**Figure 3.21**

SDS-polyacrylamide gel analysis of PS I material prepared by the three methods described in Section 2.13. Track (1) PS I prepared by the method of Mullet *et al* (1980a), track (2) the 'high salt' pellet, track (3) the Tris-HCl pellet. The numbers to the left of track (1) represent estimates of molecular mass. For tracks (1) and (2), material containing 10  $\mu$ g chlorophyll was heated with an equal volume of SDS sample buffer for 2 min prior to electrophoresis. For track (3), material containing 20  $\mu$ g chlorophyll was subjected to the same treatment. The gel consisted of a 10%-16% polyacrylamide gradient and was stained with Coomassie brilliant blue.

PS I complexes independently and predictably, causing them both to sediment at 30,000xg, while the remainder of the thylakoid membrane protein complexes remain in the supernatant. Alternatively, the Tris-HCl solubilisation could result in the formation of a 'super complex' consisting of the PS I and LHC II complexes in some form of physical association.

In order to distinguish between these two possibilities, freeze-fracture electron microscopy was used to examine the structure of the Tris-HCl pellet. Figure 3.22 shows a freeze-fracture electron micrograph of material derived from a typical preparation. Several features of this preparation are immediately apparent. Firstly, the material consists entirely of extensive, membrane-like sheets. Secondly, two clearly distinct size-classes of particle can be seen. The larger particles range in diameter from 130 Å to 170 Å while the smaller particles display a more uniform diameter of 80 Å. Comparison of Figure 3.22 with freeze-fracture electron micrographs published by other authors (Staehelin, 1976; Ryrie *et al.*, 1980) indicates that the small particles represent LHC II complexes, while the larger particles represent PS I complexes. A third striking feature of this preparation are the very ordered, regular arrays formed by the LHC II complexes. These can be more clearly seen at higher magnification in

**FIGURE 3.22.** Freeze-fracture electron micrograph of material derived from the pellet resulting from the solubilization of unstacked thylakoids with Triton X-100 in the presence of 25 mM Tris-HCl pH 8.3 (Section 2.13c). The two component chlorophyll-protein complexes of this material, LHC II and PS I, are labelled on the micrograph. Freeze-fracture replicas were prepared as described in Section 2.18. Magnification x 74,480.

(208)



Figure 3.23. Such regular arrays are strikingly similar in appearance to the crystalline sheets of purified LHC II described by Kuhlbrandt *et al* (1983). However, unlike the arrays described by these authors, the LHC II particle arrays shown in Figures 3.22 and 3.23 are not confined to two dimensions, but form a series of planes or layers which are closely appressed (L1, L2 and L3 in Figure 3.23).

Lastly, it is clear from examination of Figures 3.22 and 3.23 that the PS I and LHC II particles occupy the same freeze-fracture faces, although both particles usually form separate domains within the same fracture surface. Examination of Figure 3.23 shows, however, that separation into distinct domains is far from complete, and individual PS I particles can often be seen embedded within LHC II particle arrays. This observation would not be expected if the Tris-HCl solubilisation had affected the two complexes independently. In this case, a more likely result would be that the two complexes would occupy distinct fracture surfaces.

The alternative view that the two complexes might be physically associated in this preparation is difficult to test directly. One approach to this problem is to attempt to discern an energetic connection resulting from any physical association between the PS I and LHC II components of this preparation. A means of doing this is

**Figure 3.23** Freeze-fracture electron micrograph of material derived from the pellet resulting from the solubilisation of unstacked thylakoids with Triton X-100 in the presence of 25 mM Tris-HCl pH 8.3. L1, L2 and L3 represent successive layers of closely appressed membrane-like sheets composed chiefly of regular arrays of the LHC II. Freeze-fracture replicas were prepared as described in Section 2.18. Magnification x 114,380.



provided by the fact that most of the chlorophyll *b* in this preparation resides in the LHC II component. Thus, by exciting the pigment bed in this preparation with wavelengths preferentially absorbed by chlorophyll *b*, excitation energy will enter the system chiefly via the LHC II. It is then a question of determining how much (if any) of this energy is transferred to the PS I pigment bed by measuring some characteristic of PS I (such as fluorescence at 735 nm or PS I-mediated electron transport) which is dependent upon energy input to the system.

Measurement of fluorescence emission at 77 K provides a very sensitive and well-characterised means of probing the energetic states of thylakoid pigment-protein complexes. At 77 K, the fluorescence emission spectrum derived from whole thylakoids contains two major peaks, one at 685 nm and another at 735 nm. Fluorescence at 685 nm arises from the PS II pigment bed, while that at 735 nm arises from PS I (Papageorgiou, 1975; Barber, 1976). However, a single fluorescence emission spectrum would only indicate the source of the fluorescence, and give little information concerning the flow of energy between the two complexes in the Tris-MCl preparation. Fluorescence measurements can be used to probe energy flow between complexes, <sup>only</sup> where the degree of flow can be modified, resulting in changes in the fluorescence



emission spectrum. Addition of divalent cations such as  $Mg^{2+}$  to unstacked thylakoids has been shown to modify the room temperature fluorescence characteristics of the membrane by inducing an increase in fluorescence emission from PS II, while at 77 K, fluorescence emission from the PS II pigment bed is increased relative to that from the PS I pigment bed (Chow *et al.*, 1981). Such fluorescence changes have been interpreted in terms of a cation-induced decrease in spillover of excitation energy from PS II to PS I due to a lateral segregation of these two complexes in the plane of the lipid bilayer.

Addition of cations to preparations of isolated LHC II has been shown to induce avid aggregation of this complex (Ryrie *et al.*, 1980; McDonnell and Staehelin, 1980). This forms the basis of the LHC II isolation procedure described in Section 2.13a (Burke *et al.*, 1978). In view of these facts, it was considered that addition of  $MgCl_2$  to the Tris-HCl pellet might bring about an increase in the aggregation of the LHC II component, resulting in a change in its connectivity to the PS I component. If such a change were accompanied by energetic changes, these could be detected by monitoring changes in the 77 K fluorescence emission spectrum of the sample.

For these reasons 77 K fluorescence emission spectra were gathered for the Tris-HCl preparation in the presence and absence of 5 mM  $MgCl_2$ . Fluorescence was

excited by light at 472 nm in order to preferentially excite chlorophyll *b* (and thus the LHC II component of the sample). Figure 3.24 shows the resulting spectra. In the absence of added cations, the fluorescence emission spectrum is very similar to those gathered for the PS I particles produced by the two methods described above (see Figures 3.8 and 3.14), with a small emission peak at 682 nm and a large peak at 735 nm. Addition of 5 mM  $MgCl_2$  increases the fluorescence intensity at 682 nm relative to that at 735 nm, paralleling the situation observed with whole thylakoids.

Since the wavelength used to excite the chlorophyll in these samples was 472 nm, which will preferentially be absorbed by chlorophyll *b*, the small size of the fluorescence peak at 682 nm in the absence of added cations is unexpected. One possible explanation of this observation is that the emission peak at 682 nm emanates from a species of chlorophyll in the PS I component of the preparation, and not from the LHC II component. If this were the case, the increase in fluorescence emission at this wavelength due to the addition of cations would be reproduced in a PS I preparation not containing the LHC II. Figure 3.25 shows 77 K fluorescence emission spectra taken from PS I particles, prepared by the method of Mullet *et al* (1980a), in the presence and absence of added cations. It is clear that the effect of the cations

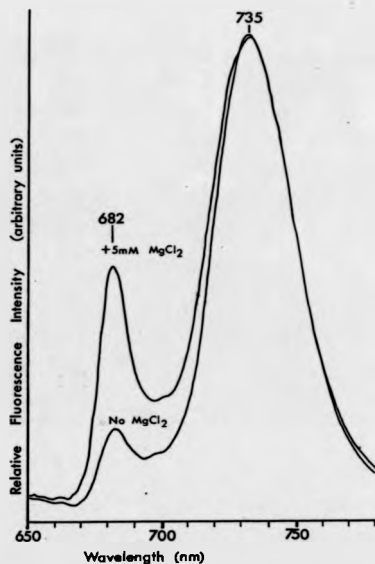


**Figure 3.24**

Fluorescence emission spectra (77 K) of material derived from the Tris-HCl pellet, both in the presence and absence of 5mM MgCl<sub>2</sub>. The Tris-HCl pellet was prepared as described in Section 2.13c. Fluorescence was excited at 472 nm using a 2.5 nm slit. Fluorescence emission was collected between 650 nm and 780 nm using a 5 nm slit as described in Section 2.16. The spectrum was normalised to the maximum prior to plotting.

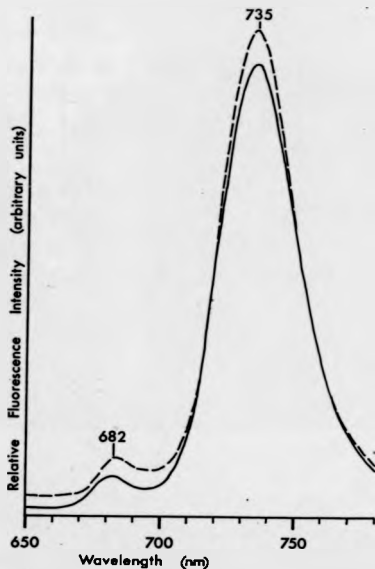


**Figure 3.25** Fluorescence emission spectra (77 K) of PS I material prepared by the method of Mullet *et al* (1980a), in the presence (broken line), and absence (solid line) of added  $MgCl_2$ . Fluorescence was excited at 472 nm using a 2.5 nm slit. Fluorescence emission was collected between 650 nm and 780 nm using a 5 nm slit, as described in Section 2.16. Spectra were normalised to the maximum prior to plotting.

on the fluorescence emission peak at 682 nm is not reproduced in PS I alone.

An alternative explanation for the low relative fluorescence emission at 682 nm, in the absence of cations, is that a proportion of the energy absorbed by the LHC II pigment bed is transferred to the PS I component, and some of this is subsequently lost as PS I fluorescence, thus contributing to the fluorescence peak at 735 nm and decreasing the relative contribution of the peak at 682 nm. Addition of  $MgCl_2$  to the preparation then causes a decrease in the transfer of excitation energy between the LHC II and PS I components, and more of the absorbed energy is lost as LHC II fluorescence at 682 nm. Since the fluorescence emission spectra are normalised to the highest peak, it is impossible to determine whether the change in fluorescence is due to an increase at 682 nm, a decrease at 735 nm or both. This has important consequences for the interpretation of the observed fluorescence changes in terms of possible energy flow within this preparation.

A more elegant means of testing the above hypothesis is provided by the use of fluorescence excitation spectra. Fluorescence emission spectra enable fluorescence emission to be monitored across a range of wavelengths, using a single wavelength to excite the pigment bed. Conversely, fluorescence excitation spectra

allow excitation to take place across a range of wavelengths, fluorescence being monitored at a fixed wavelength. In effect this allows the identification of those wavelengths most efficient at exciting fluorescence emission of a given wavelength. A fluorescence excitation spectrum of the Tris-HCl material, taken between 400 nm and 500 nm, should produce two resolvable peaks in the resulting fluorescence emission, one at around 440 nm due mainly to absorption of 440 nm light by chlorophyll *a*, and one at around 470 nm due primarily to absorption of 470 nm light by chlorophyll *b*. This should be true of fluorescence emission monitored at either 735 nm (PS I), or at 683 nm (LHC II). If excitation energy transfer from the LHC II to PS I is occurring in the Tris-HCl preparation, then in the presence of added cations, a clear decrease in the peak due to excitation by 470 nm light relative to the peak due to excitation with 440 nm light should be observed when measuring fluorescence emission at 735 nm. This is because the addition of cations should decrease the contribution to fluorescence emission at 735 nm due specifically to excitation of the extensive LHC II chlorophyll *b* component. A change in the relative sizes of the two excitation peaks should also be seen when measuring fluorescence emission at 683 nm (ie fluorescence emission primarily from the LHC II), since in the presence of cations, emission from chlorophyll *b*

should increase relative to that from chlorophyll *a*.

Figure 3.26 shows the fluorescence excitation spectra for the Tris-HCl preparation in the absence of added cations, with fluorescence emission measured at 683 nm (broken line), or at 735 nm (solid line). The two excitation maxima at around 440 nm and 470 nm can be clearly seen. Once again the spectra are normalised to the largest peaks. The most striking feature of Figure 3.26 is the similarity of the two spectra. If the two component complexes of this preparation were energetically independent, it would be expected that the emission resulting from light absorption by chlorophyll *b* (the peak at 470 nm) should be higher when emission is monitored at 683 nm than when emission is monitored at 735 nm. This is clearly not the case. This observation supports the idea that excitation energy is transferred from the LHC II to PS I in this preparation.

Figure 3.27 shows the same excitation spectra taken from the same material in the presence of 5 mM MgCl<sub>2</sub>. It is clear that where fluorescence emission is measured at 735 nm (emission from PS I), the relative size of the peak at 470 nm is significantly decreased. Similarly, where emission is measured at 683 nm (emission from LHC II), the relative size of the peak at 470 nm is slightly increased.

These results strongly support the idea that the

**Figure 3.26** Fluorescence excitation spectra (77 K) of the Tris-HCl pellet taken in the absence of added  $MgCl_2$ . Fluorescence was excited at all wavelengths between 400 nm and 550 nm using a 2.5 nm slit. Fluorescence emission was collected at either 683 nm or 735 nm using a 5 nm slit, as described in Section 2.16. All data were normalised to the maximum prior to plotting.

----- Fluorescence emission at 683 nm  
 \_\_\_\_\_ Fluorescence emission at 735 nm

**Figure 3.27** Fluorescence excitation spectra (77 K) of the Tris-HCl pellet taken in the presence of added  $MgCl_2$ . Fluorescence was excited at all wavelengths between 400 nm and 550 nm using a 2.5 nm slit. Fluorescence emission was collected at either 683 nm or 735 nm using a 5 nm slit, as described in Section 2.16. All data were normalised to the maximum prior to plotting.

----- Fluorescence emission at 683 nm  
 \_\_\_\_\_ Fluorescence emission at 735 nm



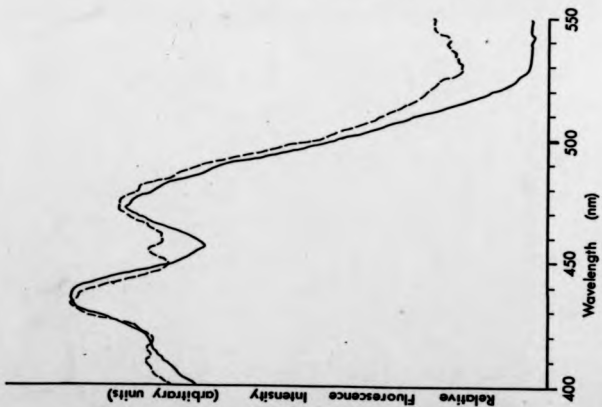


Figure 3.26

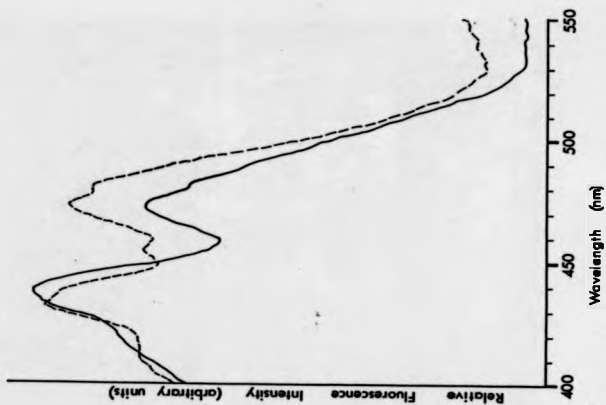


Figure 3.27

component complexes of the Tris-HCl pellet are in energetic association. However, the significance of any energy transfer in this system would lie in the ability of the transferred excitation energy to drive PS I-mediated electron transport. The fluorescence measurements described above give no indication of the way in which any energy transfer from LHC II to PS I enhances the energy trapping of the PS I reaction centres in this preparation.

An attempt was made to investigate this point by measuring PS I-mediated electron transport rates using the oxygen electrode. If there were no energetic connection between the two components of the Tris-HCl preparation, then the LHC II should make no contribution to the rate of PS I-mediated electron transport. Conversely, if the energy transfer indicated by the fluorescence data was occurring, and the transferred excitation energy was being trapped by the PS I reaction centres, then the rate of PS I-mediated electron transport would be enhanced.

The use of cations to bring about a change in the connectivity of the two component complexes was inappropriate in the oxygen electrode, since the assay medium already contained 5 mM  $MgCl_2$ , (Section 2.19). Instead, PS I-mediated electron transport was measured using PS I material prepared by both the Mullet and

Tris-HCl methods. This allowed a comparison of electron transport rates between PS I preparations where the LHC II was both present and absent.

Since such a comparison is <sup>only</sup> valid <sub>if</sub> approximately the same number of PS I reaction centres are present in all assays, it was necessary to estimate the relative proportions of each of the two component complexes in the Tris-HCl preparation, in order that direct comparisons with the Mullet-type preparations could be made.

This was done by assuming a chlorophyll *a/b* ratio of 3.0 for the Tris-HCl material. If three chlorophyll *a* molecules are present for every one chlorophyll *b* molecule, and assuming all the chlorophyll *b* resides in the LHC II, then since the LHC II binds chlorophylls *a* and *b* in equimolar quantities, two chlorophyll *a* molecules must be associated with the PS I complex for every chlorophyll *b* molecule associated with the LHC II. It follows that 50% of the total measurable chlorophyll in this preparation must be associated with the LHC II component. On this basis, the amount of chlorophyll used in each assay involving the Tris-HCl material was twice that used in assays involving PS I alone. Since unequal amounts of chlorophyll were used in the two assays, electron transport rates were measured simply as  $\mu\text{mol}$  of oxygen consumed per hour.

PS I-mediated electron transport rates were measured using light preferentially exciting chlorophyll *a* (695 nm), or chlorophyll *b* (645 nm). If LHC II excitation energy is being transferred to PS I reaction centres in the Tris-HCl preparation, then the light intensity at which PS I-mediated electron transport is saturated will be lower than would be the case for PS I in the absence of the LHC II. This difference in saturation light intensities should be much more marked where excitation is at 645 nm than at 695 nm, since the majority of chlorophyll *b* resides in the LHC II.

Figure 3.28 shows PS I-mediated electron transport rates plotted against % transmittance (100 % transmittance representing the degree of illumination in the absence of any neutral density filters). It is clear that at all light intensities, illumination of a given sample with light at 695 nm produces a greater rate of electron transport than illumination with light at 645 nm. This is undoubtedly due to the fact that since the 695 nm light preferentially excites chlorophyll *a*, the pigment bed associated with PS I will be more efficiently excited than will be the case where excitation is with 645 nm light. A point which may be related to this observation is that the samples excited by 695 nm light appear to approach saturation rates of PS I-mediated electron transport well within the light

**Figure 3.28** Graph showing the relationship between rate of PS I-mediated electron transport and increasing light intensity for PS I particles prepared by the method of Mullet et al (1980a), and for the Tris-HCl pellet. For details of the methods of preparation of these particles, see Sections 2.13a and 2.13c respectively. Samples were illuminated with light passed through filters transmitting at either 645 nm or 695 nm. PS I-mediated electron transport was measured as the amount of oxygen consumed within the oxygen electrode chamber per unit time. Details of the assay procedure are given in Section 2.19, and in the accompanying text.

- ▲ PS I illuminated at 695 nm
- PS I illuminated at 645 nm
- △ Tris-HCl pellet illuminated at 695 nm
- Tris-HCl pellet illuminated at 645 nm

**Figure 3.29** Lineweaver-Burk plot of the data displayed in Figure 3.28. The curves shown are 'best fit' lines calculated by applying linear regression analysis to the original data.

- ▲ PS I illuminated at 695 nm
- PS I illuminated at 645 nm
- △ Tris-HCl pellet illuminated at 695 nm
- Tris-HCl pellet illuminated at 645 nm

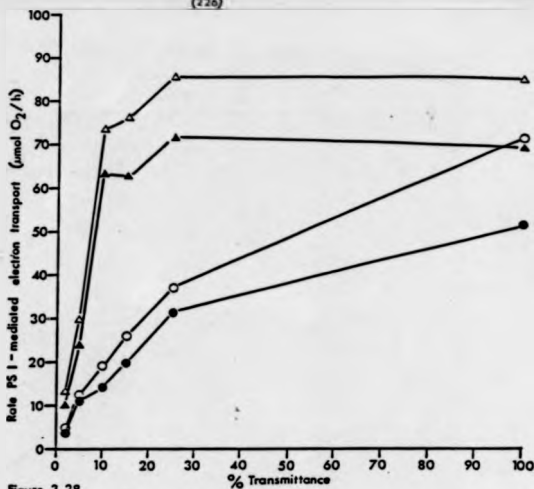


Figure 3.28

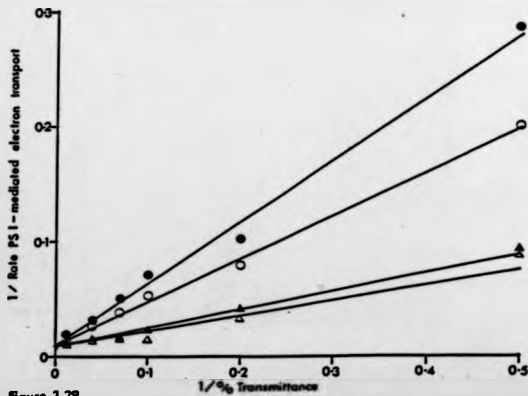


Figure 3.29

intensity range used in this experiment, whereas those samples illuminated with 645 nm light do not, electron transport rates continuing to increase even up to 100 % transmittance.

A third point to note from Figure 3.28 is that at any given light intensity, electron transport rates are higher in the presence of the LHC II than in its absence, irrespective of the wavelength used to illuminate the samples. These differences are more marked at higher light intensities. This result indicates either that the LHC II is contributing to PS I electron transport in these samples, or that more PS I reaction centres are present in the Tris-HCl sample assays than in the assays involving PS I alone.

The fact that the samples illuminated with 645 nm light did not reach saturation rendered interpretation of this result difficult, since it was impossible to determine directly from these data whether electron transport was saturated at different light intensities in the presence and absence of the LHC II. Indeed, it is not clear from the data presented in Figure 3.28 whether samples illuminated at 695 nm had reached saturation. For this reason, Lineweaver-Burk plots were employed to determine the light intensities at which electron transport rates were half-maximal (ie the  $K_m$ ) for each sample, since these are directly related to the

saturation light intensities.

Figure 3.29 represents a double reciprocal plot of PS I-mediated electron transport rates against light intensity, and Table 3.4 summarises the main features of this plot. It is important here to understand the meaning of the two axes in Figure 3.29. Double reciprocal plots usually deal with the kinetics of enzyme-substrate interactions. This experiment, however, does not deal with a conventional enzymic reaction, but with light-driven electron transport. Thus, the substrate involved in this reaction is light, and substrate concentration is measured as light intensity ( $\frac{1}{\text{transmittance}}$ ). The reaction rate is measured as the rate of consumption of oxygen in the oxygen electrode chamber, resulting, via a Mehler reaction, from the reduction of methyl viologen.

The first point to note about this plot is that the estimated values for  $V_{\text{max}}$  for each of the samples assayed are the same, being about 100  $\mu\text{mol}$  oxygen consumed per hour (Table 3.4).  $V_{\text{max}}$  is estimated as the reciprocal of the value of the intercept of each curve with the ordinate. In the context of this work, this value represents the rate of PS I-mediated electron transport at saturating light intensity, or, the theoretical maximum possible rate given the sample under assay. The fact that the maximum rates measured in this way were the same,



**Table 3.4** Estimates of  $K_m$  and  $V_{max}$  for the four PS I-mediated electron transport assays shown in Figures 3.28 and 3.29. See text for detailed discussion.

Treatment		$K_m$	$V_{max}$ %
PS I (Mullet) illuminated at :	695 nm	18	100
	645 nm	54	100
Tris-HCl pellet illuminated at :	695 nm	14	100
	645 nm	37	100

\* Rates are expressed as  $\mu\text{mol O}_2$  consumed/h.

indicates that the samples in each assay contained approximately the same number of active PS I reaction centres.

A second point to note about this plot is that since the estimate of  $V_{max}$  is the same for all four curves, then the slope of each curve is directly related to the  $K_m$ . Thus, it is clear that illumination with 645 nm light produces a relatively large difference in  $K_m$  between samples with and without the LHC II, whereas illumination with 695 nm light produces a relatively small difference. This indicates that the light intensity at which PS I-mediated electron transport is half-maximal, is influenced by the presence of the LHC II in the Tris-HCl samples. The intensity required to half saturate the PS I reaction centres is lower in the presence of the LHC II than in its absence, as would be expected if some of the energy absorbed by the LHC II pigment bed was being used to drive PS I reaction centres.

A problem arises, however, when the parameters estimated in Table 3.4 are applied directly to the original data shown in Figure 3.28. Assuming the estimates of  $V_{max}$  to be reasonable, then the half-maximal rates for each assay should be 50  $\mu\text{mol O}_2$  consumed per hour. It should then be possible to confirm each  $K_m$  shown in Table 3.4 by reading off from each curve the values of % transmittance at which the electron

transport rate is half maximal. When this is done, it is found that the data do not support the estimated parameters. The  $K_m$  for each of the assays illuminated with 695 nm light is overestimated in Table 3.4. Conversely, the  $K_m$  for each of the assays illuminated with 645 nm light is underestimated in Table 3.4.

The cause of these discrepancies is not clear, and may have several sources. A likely source of inaccuracy is that the reaction under study may not follow the simple model of enzyme-substrate interactions embodied in the Michaelis-Menten equation, and consequently this kind of analysis is naive. This possibility is difficult to test experimentally, and such work was considered to be beyond the scope of the present study.

Whatever the case, the data presented in Figure 3.28 alone indicate that a difference in the ability of the PS I reaction centres to utilise the incident light in the presence and absence of the LHC II does exist, and that this difference is greater where chlorophyll *b* is preferentially excited.

The above results are consistent with the hypothesis that the pellet resulting from the solubilisation of thylakoids with Triton X-100, in the presence of 25 mM Tris-HCl, is composed of large, quasi-membranous sheets containing PS I and LHC II chlorophyll-protein complexes. The LHC II complexes are arranged in regular, two- and

three-dimensional arrays, interspersed with the larger PS I complexes. Furthermore, the fluorescence and electron transport studies reported in this Section, together with the freeze-fracture electron microscopy, indicate that this preparation represents a two-complex aggregate in which excitation energy exchange between the two component complexes is possible.

It is clear from examination of the electron micrographs in Figures 3.22 and 3.23 that only a small proportion of the LHC II component of the Tris-HCl preparation is in physical contact with the PS I component. It could be argued that this observation represents a major objection to the idea that energy transfer from the LHC II to the PS I component accounts for the fluorescence and photochemical activity data discussed above. It need not be necessary, however, for a large proportion of the LHC II particles to be in direct contact with the PS I particles, since the PS I pigment bed, absorbing at long wavelengths, would be expected to act as an energy sink in this system.

On the basis of the evidence presented here it is not possible to say whether the Tris-HCl pellet represents a structure of any significance *in vivo*. The Tris-HCl preparation does demonstrate, however, that direct energy exchange between the LHC II and PS I pigment systems is possible. This problem will be discussed in Section 4.1.

### (3.2) Preparation of Polyclonal Antisera

A polyclonal antiserum consists of a population of immunoglobulin molecules, all of which recognise specific sites or epitopes on an antigenic molecule. Since such antisera recognise more than one epitope, it is necessary to purify the antigen to a high degree of homogeneity, in order to avoid the possibility of spurious cross-reactivity with contaminating molecules. Therefore, in order to raise monospecific polyclonal antibodies to the three apoproteins of the LHC I, and to the RC I polypeptides, it was first necessary to carry out a number of purification steps.

The strategy adopted was to purify first a PS I particle by fractionating the thylakoid into component chlorophyll-protein complexes. The polypeptide constituents of this PS I preparation were then resolved by SDS-PAGE, the proteins of interest identified and recovered from the gel matrix by electroelution.

#### (3.2a) Purification of antigens

A PS I preparation was made according to the modified method of Mullet et al (1980a) described in Section 2.13a. This method was used in preference to the 'high salt' (Section 2.13b) and Tris-HCl (Section 2.13c) methods chiefly because of the relatively low levels of

LHCP contamination encountered in PS I material prepared in this way (see Figure 3.21). This PS I material was then subjected to SDS-PAGE on a long, 40 cm polyacrylamide gel containing a 10%-16% polyacrylamide gradient (see Section 2.3).

Figure 3.30 shows a typical profile of PS I polypeptides resulting from electrophoresis on this long gel system. It can be seen from this Figure that there is a stainable band with an apparent molecular mass of 26 kDa, indicating that the preparation shown in this Figure contained stainable quantities of the LHCP. The amount of LHCP found in other such preparations varied, as described in Section 3.1a. The polypeptides with molecular masses ranging between 20 kDa and 26 kDa are well resolved. In addition, the RC I polypeptides are resolved into two distinct bands.

This long gel system was found to produce higher resolution of the three LHC I apoproteins than any other gel system employed. Resolution on this system was sufficient to allow excision of the stained LHC I bands P1, P2 and P3, without risk of contamination with stained material derived from surrounding bands. Resolution of the RC I proteins was not found to be sufficient to allow excision of individual stained bands, since a degree of smearing of the bands in this region of the gel was encountered in most preparations. For this reason, these

**Figure 3.30** SDS-PAGE analysis of a PS I preparation used for the isolation and purification of the apoproteins of the LHC I. A PS I preparation was made by the method of Mullet *et al* (1980), as described in Section 2.13a. An amount of this preparation containing 250  $\mu$ g chlorophyll was boiled for two min in SDS sample buffer and loaded across the entire width of a polyacrylamide gel of width 20 cm and length 40 cm. The gel consisted of a 10%-16% polyacrylamide gradient. Following electrophoresis, the gel was stained with Coomassie brilliant blue. Details of the electrophoretic procedure are given in Sections 2.3, 2.4 and 2.14.

RC I    Photosystem I reaction centre proteins.

LHCP    26 kDa apoprotein of the LHC II.

P1, P2 and P3 are the protein constituents of the LHC I.

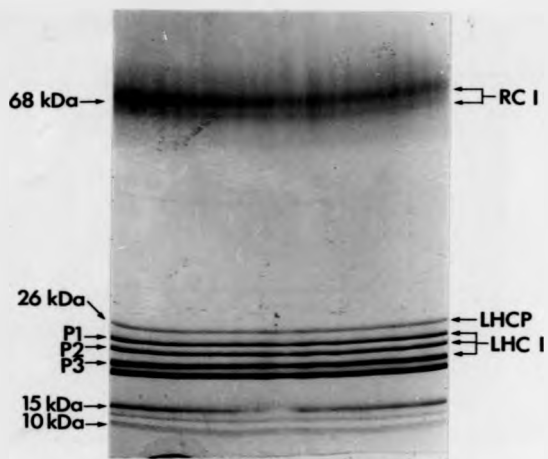


**Figure 3.30**



bands were excised together and electroeluted as a single protein sample.

After excision and electroelution, aliquots (50  $\mu$ l) of the LHC I polypeptides were subjected to SDS-PAGE in order to check for purity. Figure 3.31 shows a polyacrylamide gel stained with Coomassie blue, containing the three purified LHC I polypeptides, together with the PS I preparation from which they were derived, and a purified LHC II preparation for comparison. Each of the three tracks containing the purified LHC I polypeptides contains only one stainable band. No contamination with other LHC I polypeptides, or with the polypeptides of the LHC II can be seen.

Since the protein loadings on tracks 2, 3 and 4 of Figure 3.31 are low (each track representing approximately one tenth of the material used for each injection), it is possible that the amount of any contaminating protein may have been below that required for detection by Coomassie blue. For this reason, similar gels were subjected to the more sensitive silver staining method (see Section 2.4b) in an attempt to visualise low levels of contaminants. Figure 3.32 shows such a gel after staining with silver. Two clear differences between this Figure and Figure 3.31 can be seen. Firstly, the silver stain shows a faint polypeptide band of approximately 70 kDa not observed when gels were stained

**Figure 3.31.** SDS-PAGE analysis of purified LHC I polypeptides. Track (1) complete PS I preparation, track (2) purified P1, track (3) purified P2, track (4) purified P3, track (5) purified LHC II, track (6) complete PS I preparation. PS I was prepared by the method of Mullet et al (1980a), as described in Section 2.13a. P1, P2 and P3 were purified by SDS-PAGE and electroelution as described in Section 2.14. Samples containing 10 µg chlorophyll were loaded in tracks (1), (3) and (5). For tracks (2), (3) and (4) approximately one tenth of the material resulting from one electroelution was loaded per track. The remaining material was used to immunise rabbits. The gel consisted of a 10%-30% polyacrylamide gradient and was stained with Coomassie brilliant blue.

RC I Reaction centre proteins of PS I.  
 LHCP The 26 kDa apoprotein of the LHC II.  
 LHC I The PS I light-harvesting complex containing P1, P2 and P3.

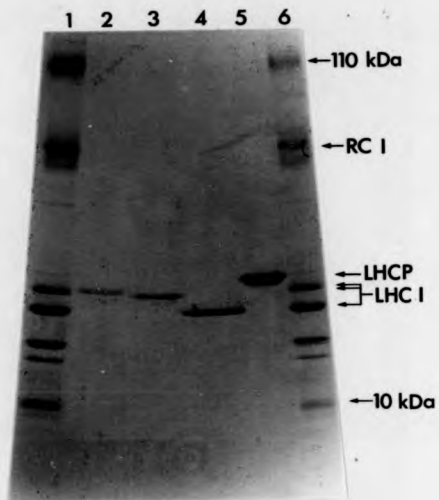


**Figure 3.31**

**Figure 3.32** SDS-PAGE analysis of purified LHC I polypeptides. Track (1) complete PS I preparation, track (2) purified P1, track (3) purified P2, track (4) purified P3, track (5) purified LHC II. PS I was prepared by the method of Mullet *et al* (1980a), as described in Section 2.13a. P1, P2 and P3 were purified by SDS-PAGE and electroelution as described in Section 2.14. Samples containing 1 µg chlorophyll were loaded in tracks (1) and (5). For tracks (2), (3) and (4), approximately one thirtieth of the material resulting from one electroelution was loaded per track. The gel consisted of a 10%-16% polyacrylamide gradient and was stained with silver as described in Section 2.4b.

RC I Reaction centre proteins of PS I.  
 LHCP The 26 kDa apoprotein of the LHC II.  
 LHC I The PS I light-harvesting complex containing P1, P2 and P3.

Polypeptides labelled a and b are dimeric forms of P1 and P2 respectively. The stained polypeptide at 70 kDa is an unknown contaminant common to all tracks.

(241)

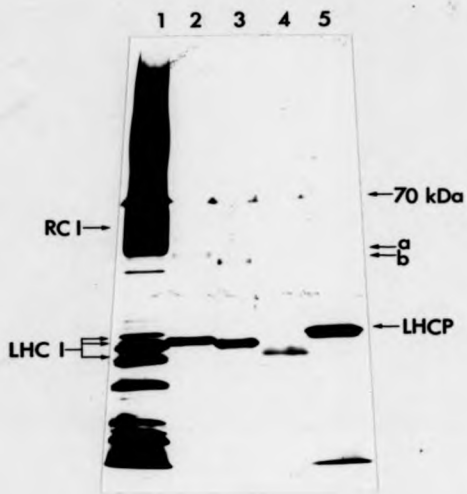


**Figure 3.32**

with Coomassie blue. This band was present in all tracks, even those in which no sample had been loaded, and was observed in almost every gel stained with silver, regardless of the nature of the samples loaded. This fact suggests that this 70 kDa polypeptide is a contaminant introduced during the electrophoresis procedure itself.

The second difference between Figures 3.31 and 3.32 is that in the latter, stained bands can be seen in tracks 2, (P1), and 3, (P2), with apparent molecular masses of about 45-50 kDa (marked a and b in Figure 3.32). Similar bands were also sometimes observed in tracks containing purified P3 and LHCP. The pattern of migration of these bands on the gel, their apparent molecular masses, and the fact that they can be largely removed by prolonged heating of the samples prior to electrophoresis, indicates that they represent dimeric forms of the polypeptides in question, and as such can not be regarded as contaminants.

No dimeric form of P3 (track 4) can be seen in Figure 3.32. This may be due to the fact that P3 did not stain well with silver. The reason for this differential staining of proteins with silver is poorly understood, although clearly, silver staining must rely upon the reduction of silver cations by exposed groups on the protein. The number and character of these groups will vary between proteins. In the model proposed by Guevara

*et al* (1982), ammoniacal silver ions bind to negatively charged groups on the protein, while Chuba and Palchaudhury (1986) suggest that cysteine residues play an important role. If this latter suggestion is valid then P3 should be found to contain relatively little cysteine.

Since silver staining of proteins has been found to be up to one hundred-fold more sensitive than Coomassie blue (Switzer *et al*, 1979), the absence of detectable cross-contamination between the purified polypeptides seen in Figure 3.31 indicated that a high degree of purity had been attained. These preparations were therefore used as antigens for polyclonal antibody production.

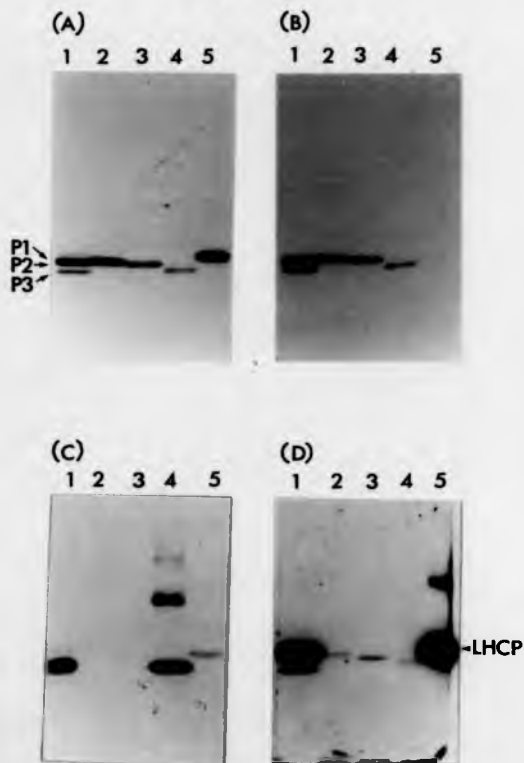
### (3.2b) Assay of LHC I antibody specificity

The specificities of antisera raised against the LHC I apoproteins P1, P2, and P3 were tested by immunoblotting, and the results are shown in Figure 3.33. Also shown is a blot probed with antibody raised against the LHCP for comparison. It is clear that a complex set of cross-reactions exist. Three main points are clear from examination of this Figure. Firstly, antisera raised against purified P1 and P3 both show some cross-reaction with the polypeptides of the LHC II. The antiserum raised against purified P2, however, shows no such cross-

**Figure 3.32** Autoradiographs of immunoblot assays showing specificities of antibodies raised against the apoproteins of the LHC I and LHC II. Identical nitrocellulose filters were probed with: (A) anti-P1 serum, (B) anti-P2 serum, (C) anti-P3 serum and (D) anti-LHCP serum. The tracks on each blot contain: (1) complete PS I particle, (2) purified P1, (3) purified P2, (4) purified P3 and (5) purified LHC II.

PS I was prepared by the method of Mullet *et al* (1980a), as described in Section 2.13a. LHC II was purified as described in Section 2.13a. A quantity of material containing 10  $\mu$ g chlorophyll was boiled in SDS sample buffer and loaded onto tracks 1 and 5. Loadings of purified LHC I polypeptides were exactly as described in the legend to Figure 3.31. Immunodetection of bound antibody was by use of  $^{125}$ I-labelled protein A, as described in Section 2.15d(11).



**Figure 3.33**

reactivity. Similarly, antiserum raised against the LHCP shows cross-reactivity with all three polypeptides of the LHC I.

Secondly, both antisera raised against the LHC I polypeptides P1 and P2 react strongly with both these proteins, but relatively poorly with P3, while the P3 antiserum reacts strongly with its own antigen but no detectable reaction is found against P1 and P2.

Finally, none of the antisera react with any other PS I polypeptides, supporting the observation made by Lam *et al* (1984b), that the apoproteins of the LHC I are immunologically distinct from the other chlorophyll-binding proteins present in this PS I preparation.

The extent to which a given antibody reacts with a polypeptide in the immunoblot system relies to some extent upon the history of the protein sample blotted. Figure 3.33 demonstrates this point clearly. In Figure 3.33(B), the P2 antiserum recognises all three LHC I polypeptides. Reaction of this antibody with the purified P3 (track 4) is weak compared to the reactions with P1 and P2. The reaction of this antibody with the P3 present in the complete PS I sample (track 1), however, is much stronger in comparison with its reaction with P1 and P2 in this sample. The difference in the strength of the reaction of the P2 antibody with P3 in tracks 1 and 4 is not due to differences in the amount of P3 present since

stainable amounts of this polypeptide in these two tracks were approximately the same (see Figure 3.31).

It is possible that these observed differences in immunological reactivity are due to the way in which the protein sample is treated prior to preparation for electrophoresis and immunoblotting. The PS I sample in tracks 1 of Figure 3.33 was derived directly from a PS I preparation removed from a sucrose density gradient. Such preparations are dialysed before use in order to remove excess Triton X-100. However, dialysis does not efficiently remove Triton X-100 bound to protein, due partly to its low CMC (Holloway, 1973), and consequently some Triton X-100 remains in the PS I preparation. The purified LHC I polypeptides had undergone SDS-PAGE, staining, destaining and electroelution prior to electrophoresis for immunoblotting, and it is likely that much of the residual detergent had been removed from the protein or had undergone exchange with SDS during these processes. These differences in treatment may affect the accessibility of antigenic sites on the protein bound to the nitrocellulose filter, leading to differential binding of antibody molecules.

The complex pattern of immunological similarities between different polypeptides shown in Figure 3.33 can be broadly divided into two components; the similarities between component polypeptides of the LHC I

and LHC II, and the similarities between the individual apoproteins of the LHC I. The apparent immunological similarities between the polypeptides of the LHC I and LHC II are of considerable interest since such similarities imply a degree of structural identity between proteins serving very similar light-harvesting pigment-binding functions, albeit in different pigment-protein complexes. Since the antibodies used in this study were raised against SDS-denatured proteins, immunological cross-reactivity may reflect similarities in the amino acid sequences of these proteins. This in turn implies that the genes encoding these polypeptides may display regions of nucleotide sequence homology. Such homology could be due either to convergent evolution, or to divergent evolution from a common ancestral sequence.

For this reason it was important to determine whether the observed immunological cross-reactivities between the polypeptides of the two light-harvesting complexes were due to structural similarities as discussed above, or to simple cross-contamination of the original antigens.

It is clear from examination of Figures 3.31 and 3.32, that the ability of the antibodies raised against P1 and P3 to recognise the polypeptides of the LHC II can not be due to contamination of these antigens with the mature 24-26 kDa LHC II proteins. However, the possibility remains that proteolytic breakdown products

of the LHC II polypeptides, created during the PS I purification procedure, could have co-purified with the LHC I antigens. This would be possible if the molecular masses of the contaminants closely matched those of the LHC I polypeptides, rendering them irresolvable by SDS-PAGE. If this were the case, then antibodies raised against the LHC I antigens would also react with the apoproteins of the LHC II. At the same time, the anti-LHCP antibody, while apparently cross-reacting with the purified LHC I apoproteins, would in reality only be reacting with the co-migrating contaminants. This situation would adequately explain the apparent immunological similarities between the polypeptides of the two light-harvesting complexes observed in Figure 3.33.

One approach to testing this hypothesis is to prepare LHC I polypeptides completely free of any possible contaminants resulting from the proteolysis of the polypeptides of the LHC II. These preparations could then be probed with the anti-LHCP antibody in order to determine whether the cross-reactivity was retained. This approach has the disadvantage that information can only be gained by a negative result. If, following further purification of the LHC I apoproteins, the cross-reactivity between the anti-LHCP serum and the LHC I proteins is abolished, then the original cross-reaction

could only have been due to contamination. If, however, the cross-reactivity is retained, then this could be due either to the continued presence of contaminants, or to real immunological similarity.

In an attempt to remove possible LHC II contaminants from the LHC I polypeptides, the LHC I was purified from a PS I preparation by the method of Haworth *et al* (1983), as described in Section 2.13d. This method involves solubilising the PS I material with a neutral detergent and a zwitterionic detergent simultaneously. The detergent-treated material is then subjected to sucrose density gradient centrifugation. Figure 3.34 shows a typical sucrose gradient resulting from this procedure. Three major chlorophyll-containing regions can be seen, one close to the top of the gradient, but sedimenting below the sample volume (band I), a relatively wide band in the central region of the gradient (band II), and a narrow band at the 0.7 M/2.0 M sucrose interface (band III).

Figure 3.35 shows the absorption spectra of acetone-extracted pigments derived from the three green bands in the sucrose gradient shown in Figure 3.34. The chlorophyll-containing band uppermost in the gradient (band I), represents a purified LHC I fraction (Haworth *et al*, 1983), and displays pronounced absorption shoulders at 480 nm and 645 nm indicating the presence of

- Figure 3.34** Sucrose density gradient showing green bands resulting from the solubilisation of PS I material with Zwittergent-16 and dodecyl- $\beta$ -D-maltoside. PS I material was prepared by the method of Mullet et al (1980a), as described in Section 2.13a. This PS I preparation was then solubilised with Zwittergent-16 and dodecyl- $\beta$ -D-maltoside, and the resulting material (4-5 ml) layered over a 0.1M-0.7M sucrose gradient (20 ml), containing 20 mM Tricine-NaOH (pH 7.8), and 1% (w/v) dodecyl- $\beta$ -D-maltoside. The sucrose gradient was formed over a 2M sucrose cushion (5ml). Full details of the solubilisation and centrifugation procedures can be found in Section 2.13d.
- I Band I representing LHC I
  - II Band II representing the PS I core complex
  - III Band III representing undissociated PS I

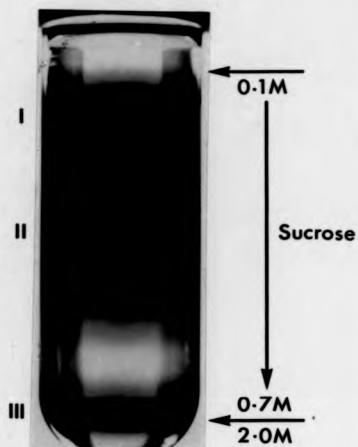


**Figure 3.34**



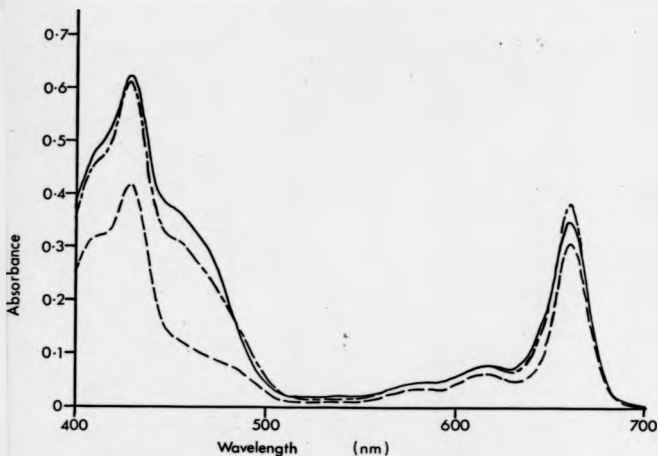


**Figure 3.35** Absorption spectra of pigments extracted from component pigment-protein complexes of PS I. PS I material prepared by the method of Mullet *et al* (1980a) was further solubilised as described in Section 2.13d, and the resulting released constituent pigment-protein complexes were resolved by sucrose density gradient centrifugation as shown in Figure 3.34. Green bands were removed from the sucrose density gradient by Pasteur pipette, and small volumes (200  $\mu$ l) were removed from each band for chlorophyll determination. Pigments were extracted by the addition of four volumes of acetone and chlorophyll concentrations were determined as described in Section 2.17.

————— Band I (LHC I)  
 - - - - - Band II (PS I core complex)  
 - · - · - Band III (Undissociated PS I)

chlorophyll *b*. This band characteristically displays a chlorophyll *a/b* ratio of about 3.5, in close agreement with the results reported by other authors (Haworth *et al*, 1983; Lam, Ortiz and Malkin, 1984).

Figure 3.36 shows the low temperature (77 K) fluorescence emission spectrum of the material derived from band I. This spectrum clearly shows the presence of two distinct fluorescence emission peaks, one at 681 nm and a second, smaller peak at 731 nm. This result does not agree with that reported by Haworth *et al* (1983). The 77 K fluorescence emission spectrum for a similar fraction reported by these authors contained a major peak at 730 nm and a very small peak at 680 nm. Since these authors were also working with pea this discrepancy is difficult to explain. However, Lam, Ortiz and Malkin (1984), working with spinach, and using a fractionation technique slightly modified from that of Haworth *et al* (1983), produced a purified LHC I fraction displaying a low-temperature fluorescence emission spectrum very similar to that shown in Figure 3.36. This difference in fluorescence emission spectra for these preparations was attributed either to differential stability of the LHC I in the two species concerned, or to differences in the antenna pigment organisation (Lam, Ortiz and Malkin, 1984). Since the present results, like those of Haworth *et al* (1983), were also obtained using

**Figure 3.36** Low temperature (77 K) fluorescence emission spectra of material representing purified LHC I and undissociated PS I. PS I material was prepared by the method of Mullet *et al* (1980a), further solubilised as described in Section 2.13d and the resulting released complexes resolved by sucrose density gradient centrifugation, as shown in Figure 3.34. Band I (LHC I) and Band III (complete PS I) were removed from the gradient and small volumes of each (100  $\mu$ l) diluted to give a chlorophyll concentration of 5  $\mu$ g/ml. Fluorescence was excited at 440 nm using a 2.5 nm slit. Fluorescence emission was collected between 650 nm and 780 nm using a 5 nm slit, as described in Section 2.16.

———— Band I (LHC I)  
 ----- Band III (complete PS I)

(255a)

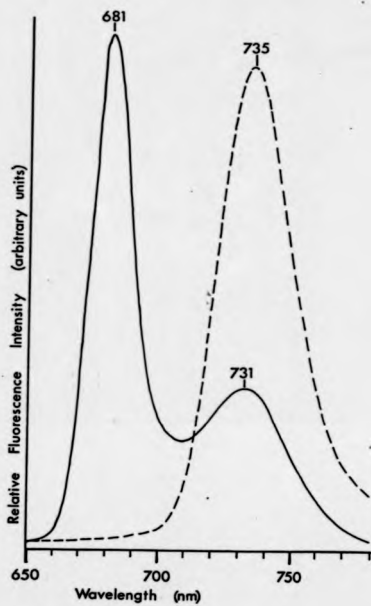


Figure 3.36

PS I material derived from pea, this explanation is clearly insufficient and requires further investigation.

The green band derived from the central region of the sucrose gradient (band II), represents the original PS I preparation from which the LHC I has been removed by the detergent treatment (Haworth *et al*, 1983). This fraction displays chlorophyll *a/b* ratios of 15.0 and higher, indicating that chlorophyll *b* in this material is below the level required for detection.

The third and lowest green band in the sucrose gradient (band III), has not been characterised by previous authors using this fractionation technique. Ortiz *et al* (1984), using a slightly modified version of the technique described by Haworth *et al* (1983), reported the presence of a third green band which they described as undissociated PS I material. No further description of this band has been published. The absorption spectrum of this band, shown in Figure 3.35, is very similar to the absorption spectrum for the complete PS I particle shown in Figure 3.4, and, in common with the PS I particle, also displays a chlorophyll *a/b* ratio of 6.0. These observations suggest that this new gradient fraction represents a portion of the original PS I preparation not affected by the detergent treatment, and which in consequence retains its peripheral light-harvesting system.

Figure 3.37(A) shows the polypeptide constituents of the three sucrose gradient bands analysed by SDS-PAGE. Band I, (the LHC I fraction), contains all three LHC I polypeptides (P1, P2 and P3). In addition, this fraction also contains a 26 kDa polypeptide representing the LHCP contamination in the original PS I material.

Band II from the sucrose gradient contains the RC I proteins, and the PS I polypeptides in the molecular mass range 9-20 kDa. There are no stainable LHC I polypeptides in this fraction, indicating that this fraction represents a PS I core complex devoid of the peripheral light-harvesting antenna.

Band III from the sucrose gradient contains P1, P2 and P3 in addition to the polypeptides found in the core complex, and thus represents a complete PS I preparation, confirming the conclusion drawn above from the acetone-extracted pigment spectra shown in Figure 3.35. This fraction, however, contains no stainable LHCP. The absence of stainable LHCP from this material may be interpreted in two ways. Firstly, the PS I particles contained in this band may represent a population of PS I particles which were originally free of any LHC II contamination. Alternatively, LHC II may have been removed from this material by the two detergents used to solubilise the original PS I material. In either case, it is clear that this solubilisation step results in the

**Figure 3.37** Immunoblot analysis of the immunological similarities between LHC I and LHC II apoproteins.

(A) SDS-PAGE analysis of the polypeptide constituents of the three green bands derived from the solubilisation of PS I and separated by sucrose density gradient centrifugation as shown in Figure 3.34: Track (1) band I-purified LHC I, track (2) band II-PS I core complex, track (3) band III-undissociated PS I. The gel consisted of a 10%-16% polyacrylamide gradient, and was stained with Coomassie brilliant blue.

(B) Autoradiograph of immunoblot using anti-LHCP serum as the antibody probe: Track (1) complete unsolubilised PS I particle, track (2) band I-purified LHC I, track (3) band II-PS I core complex, track (4) band III-undissociated PS I.

(C) Autoradiograph of immunoblot using anti-P2 serum as the antibody probe: Tracks 1-4 exactly as in (B).

For (B) and (C), the same nitrocellulose filter was probed sequentially with anti-LHCP serum followed by anti-P2 serum. In both cases, antibody was detected by use of  $^{125}\text{I}$ -labelled protein A.

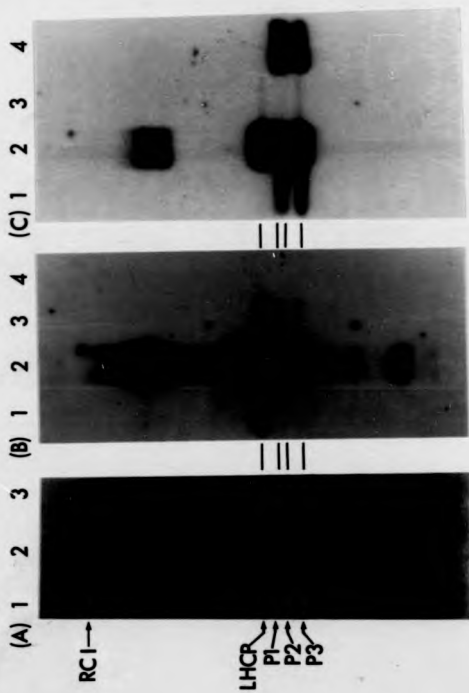


Figure 3.37



production of a PS I preparation containing little, if any, of the mature 26 kDa LHCP.

In order to test for the presence of contaminants deriving from the LHC II, each of the three sucrose gradient fractions described above were subjected to immunoblotting using the anti-LHCP serum as the antibody probe. Figure 3.37(B) shows an autoradiograph of the resulting nitrocellulose filter after probing with [<sup>32</sup>P]-labelled protein A. Track 1 represents an unfractionated PS I preparation, and the LHCP contamination at 26 kDa has been clearly recognised by the antibody. In some preparations, several polypeptides in the molecular mass range occupied by the LHC I proteins were also recognised by the LHCP antibody.

Track 2 of Figure 3.37(B) represents the LHC I material from band I of the sucrose density gradient, and is equivalent to track 1 of Figure 3.37(A). Here the LHCP antibody recognises not only the mature 26 kDa LHCP and its oligomeric form, but also a range of smaller polypeptides, notably those within the LHC I molecular mass range. These smaller polypeptides are probably proteolytic breakdown products of the LHCP. In view of this result, the LHC I fraction from the sucrose density gradient can not be used to test the observed antibody cross-reactivity since this fraction clearly contains large amounts of LHCP contamination.

A striking feature of track 2 of Figure 3.37(B) is the apparent avidity with which the LHCP antibody recognises the antigens. The size of the bands on the autoradiograph are disproportionate to the amount of corresponding stainable protein, indicating an apparent increase in the avidity of the antibody for its antigen. This phenomenon has already been discussed above in relation to the purified LHC I antigens, and seems to be a consequence of the prior detergent treatment of the proteins in question.

Track 3 of Figure 3.37(B) represents the PS I core complex and is equivalent to track 2 of Figure 3.37(A). Here again the 26 kDa LHCP is strongly recognised by the antibody, showing that although no stainable LHCP is detectable in this material, LHCP contamination still persists. The antibody also recognises a lower molecular weight polypeptide of the same apparent molecular mass as P3 of the LHC I.

Track 4 of Figure 3.37(B) represents band III from the sucrose gradient and is equivalent to track 3 of Figure 3.37(A). It can be seen that there is no immunologically detectable 26 kDa LHCP in this material, or indeed any other immunologically related polypeptides. This observation confirms the conclusion drawn above that this material represents a PS I preparation free of LHC II contamination. Furthermore, the absence of any

radioactive bands in this track indicates that the ability of the LHCP antibody to recognise the polypeptides of the LHC I has been abolished in this material, since track 3 of Figure 3.37(A) shows all three LHC I polypeptides to be present in this material in significant stainable quantities.

In order to check the identity of the LHC I polypeptides, the same nitrocellulose filter was probed with antiserum raised against P2. This is the only LHC I antibody showing no cross-reaction with the polypeptides of the LHC II, (see Figure 3.33(B)). Figure 3.37(C) shows the resulting autoradiograph.

Track 1 of Figure 3.37(C), representing the undissociated PS I control, shows three radioactive bands corresponding to the three LHC I polypeptides P1, P2 and P3, thus confirming the specificity of the anti-P2 antiserum. Track 2, the LHC I fraction, shows the three LHC I polypeptides as expected. In addition, this track also shows the radioactive signal remaining from the previous probing with the LHCP antiserum. Only the most heavily labelled LHCP bands (the 26 kDa and oligomeric bands) can still be detected. A clear feature of this track is the absence of any detectable breakdown products of the LHC I polypeptides. This contrasts very strongly with the LHCP which clearly undergoes extensive proteolysis during the PS I fractionation procedure (see

track 2, Figure 3.37(B)).

Track 3 of Figure 3.37(C), representing the PS I core complex, shows no immunologically detectable LHC I polypeptides. This result implies that the faint radioactive bands detected in track 3 of Figure 3.37(B) do not correspond to polypeptides of the LHC I, but represent proteolytic breakdown products of the LHCP.

Track 4 of Figure 3.37(C) clearly contains prominent LHC I polypeptide bands. Since these bands were not detected by the LHCP antiserum (track 4, Figure 3.37(B)), then the apparent cross-reactivity observed between the LHCP antiserum and the polypeptides of the LHC I in Figure 3.33(D) has been abolished in this PS I fraction. This evidence indicates that the cross-reactivity of the LHCP antibody with the LHC I polypeptides is spurious. The results shown in Figure 3.33(D) can most easily be explained by assuming that the radioactive bands seen in tracks 2, 3 and 4 of this Figure do not represent purified LHC I polypeptides, but breakdown products of the LHCP which cosigrate closely with the LHC I polypeptides in the polyacrylamide gel system used.

Further to this conclusion, it follows that the cross-reactions observed between the antibodies raised against P1 and P3, and the polypeptides of the LHC II (tracks 5 of Figures 3.33(A) and 3.33(C)) can also be explained by assuming that the original antigens used to

raise these two antisera were contaminated with LHCP breakdown products. These conclusions are supported by the observation that the ability of the LHCP antisera to recognise the LHC I polypeptides proved to be variable, (compare track 1, Figure 3.37(B) and track 1, Figure 3.33(D)), while the ability of the LHC I antisera to recognise the polypeptides of the LHC II was constant (results not shown). This result would be expected if the contamination of the LHC I polypeptides with breakdown products of the LHC II was subject to variation between PS I preparations.

It is likely, in view of the above discussion, that the antigen used to raise antibody against P2 of the LHC I was free of any contamination with LHC II breakdown products, although it is clear that a polypeptide capable of recognition by the anti-LHCP serum co-purifies with P2 (see track 3, Figure 3.33(D)). The lack of contamination of the P2 antigen may have been due to the improved resolution provided by the long gels used to purify the LHC I polypeptides.

On the basis of the results shown in Figure 3.37, it is not possible to support the hypothesis that the apoproteins of the LHC I are immunologically related to those of the LHC II. There is therefore no basis, on this evidence, for the idea that the amino acid sequences (and by implication the gene nucleotide sequences) of these

proteins share regions of similarity.

The apparent immunological cross-reactivities observed between the polypeptides of the LHC I could be due to contamination with either other LHC I polypeptides, or with breakdown products of the LHC II. Examination of Figure 3.33(B) shows that the P2 antibody recognises all three LHC I polypeptides, but not the polypeptides of the LHC II. It follows that these observed cross-reactions are not related to the presence of LHC II breakdown products in these samples.

It is possible that the ability of the P2 antiserum to recognise all three LHC I polypeptides could be due to cross-contamination of the three original LHC I antigens, either with other mature LHC I polypeptides, or with their breakdown products. This explanation is rendered unlikely by examination of Figure 3.33(C). Here, the antibody raised against P3 fails to recognise either P1 or P2. Since the purified protein samples used in this blot were the same as those used in the other three blots shown in Figure 3.33, it is unlikely that the ability of the P2 antiserum to recognise P3 (track 4, Figure 3.33(B)) could be due to the presence of a P1 or P2 breakdown product in the P3 antigen. As noted above, the polypeptides of the LHC I seem less prone to proteolytic degradation than those of the LHC II (compare tracks 2, Figures 3.37(B) and 3.37(C)).

The evidence presented here strongly suggests that the polypeptide components of the LHC I are immunologically distinct from those of the LHC II. It is likely, however, that the individual protein components of the LHC I share immunological similarities.

### [3.2c] Assay of RC I antibody specificity

The photosystem I reaction centre (RC I) polypeptides were purified in exactly the same way as the polypeptides of the LHC I. Figure 3.38(A) shows a stained SDS polyacrylamide gel containing tracks representing a complete Mullet PS I preparation, and two samples of purified RC I proteins. It can be seen from this gel that the RC I proteins tend to run as a smeared single band. On some occasions this smear could be resolved into two bands, but this degree of resolution was found to be unpredictable. For this reason the two RC I polypeptides were purified as a single band and this mixture was used as an antigen for raising a polyclonal antiserum.

The specificity of the antiserum raised against the RC I proteins was tested by immunoblotting. PS I material produced by the method of Mullet et al (1980a) was loaded across the entire width of a polyacrylamide gel and then subjected to SDS-PAGE. This gel was then blotted electrophoretically onto a nitrocellulose filter, and the filter cut into strips exactly as shown in Figure 2.2.

**Figure 3.38** Assay of specificity of antibody raised against the PS I reaction centre (RC I) proteins.

(A) SDS-PAGE analysis of the purified RC I proteins. PS I material was prepared by the method of Mullet *et al* (1980a), as described in Section 2.13a, and RC I proteins were purified from this PS I material by SDS-PAGE and electroelution as described in Section 2.14.

Track (1) Complete PS I, tracks (2) and (3) purified RC I proteins, track (4) molecular mass markers. PS I material containing 10  $\mu$ g chlorophyll was boiled in SDS sample buffer and loaded onto track 1. For tracks (2) and (3), material representing one tenth of the material resulting from one electroelution was loaded, the remaining material being used to immunise a rabbit. The gel consisted of a 10%-16% polyacrylamide gradient and was stained with Coomassie brilliant blue.

(B) Autoradiograph of immunoblot using anti-RC I serum as the antibody probe. PS I material was prepared by the method of Mullet *et al* (1980), as described in Section 2.13a. This material was then subjected to SDS-PAGE (10%-16% polyacrylamide gradient) and subsequently electrophoretically blotted onto a nitrocellulose sheet. The sheet was cut into a series of identical strips (Section 2.15c(1)), one of which was probed with the anti-RC I serum. Bound antibody was detected using [ $^{125}$ I]-labelled protein A.



(268)

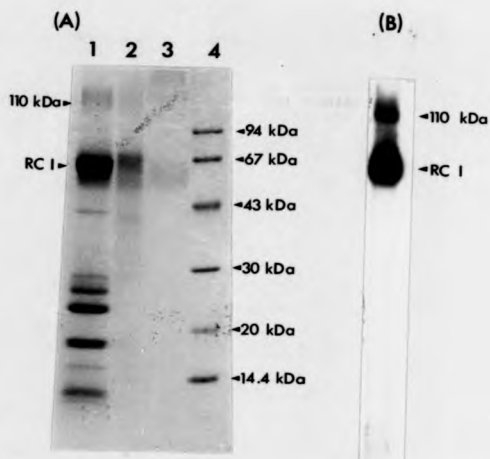


Figure 3.38

One of the filter strips was then probed with the antiserum raised against the RC I proteins. Figure 3.38(B) shows the resulting autoradiograph. The immunoblot shows that the antibody is specific for the RC I proteins, and recognises no other PS I polypeptides.

### (3.3) Preparation of Monoclonal Antibodies

In contrast to polyclonal antisera, a monoclonal antiserum consist of a homogeneous population of immunoglobulin molecules, all of which recognise the same single epitope on the molecule used as antigen. Such antibodies are derived from clonal lines of immunoglobulin-secreting cells recovered from mice immunised with the antigen. In addition to their specificity, one of the advantages of raising monoclonal rather than polyclonal antibodies is the fact that the antigen to which the antibodies are to be raised need not be highly purified when injected. If monospecific antibodies to a number of antigens are required, it is possible to inject the antigens into the mouse simultaneously, and separate antibodies of different specificity at the screening stage.

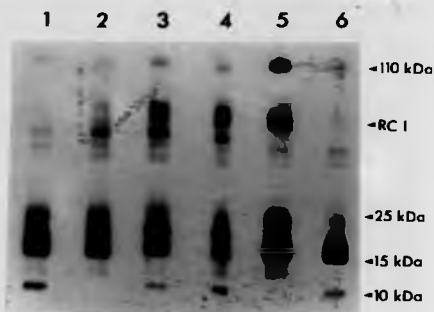
#### (3.3a) Screening of hybridoma supernatants and assay of antibody specificity

Figure 2.2 shows the procedure used for the production and screening of hybridoma supernatants. PS I material was prepared by the Tris-HCl method described in Section 2.13c. Since this material contains large amounts of the LHC II polypeptides, it was used as the antigen in order to provide the possibility of raising antibodies to the LHCP in addition to the polypeptides of PS I.

Following immunisation, blood was removed from individual mice and screened in order to estimate the range and titre of antibodies produced. Screening was carried out by immunoblot as described in Section 2.15c(1).

Figure 3.39 shows the result of such a screen carried out on six mice. This Figure demonstrates the heterogeneity of the immune response of different mice to the same antigen. This heterogeneity can be seen particularly clearly with reference to the RC I polypeptides in Figure 3.39. Such variability in the immune response of different mice underlines the need to screen sera derived from several immunised individuals prior to monoclonal antibody production.

The mouse showing the best immune response was used to obtain hybridoma cultures as described in Sections 2.15c(11) and 2.15c(111). The quality of response was judged by the number of proteins recognised by the serum and the strength of the signals obtained on autoradiography. After cloning of hybridoma lines by dilution and subsequent growth in culture, hybridoma supernatants were screened for the presence of secreted antibodies by immunoblotting as described in Section 2.15c(1). Figure 3.40 represents a composite picture showing the results of screening three hybridoma supernatants containing antibodies which recognise apoproteins of the LHC I. These results are also



**Figure 3.39**

Autoradiograph of immunoblot of six mouse sera after immunisation with PS I material prepared by the Tris-HCl method. Six mice (female, strain Balb/c) were immunised with PS I material prepared by the Tris-HCl method described in Section 2.13c. Blood was extracted from each mouse, and each serum incubated with a nitrocellulose strip onto which had been blotted the resolved polypeptides of the Tris-HCl preparation. Filter strips were washed to remove unbound antibody, and the bound antibodies were detected by incubating the strips with [ $^{125}$ I]-labelled rabbit anti-mouse IgG (RAM). Full details of this procedure are given in Section 2.15c(1). Tracks (1)-(6) each represent the autoradiograph of a single nitrocellulose strip.

RC I Reaction centre proteins of PS I.

**Figure 3.40** Characterisation of three hybridoma supernatants containing antibodies to the polypeptides of the LHC I. Mice were immunised with PS I material prepared by the Tris-HCl method described in Section 2.13. After initial screening of total mouse serum (see Figure 3.39), the spleen of a selected mouse was removed and spleen cells fused with myeloma cells as described in Section 2.15c(11). Hybridoma lines were screened for production of antibody as shown in Figure 2.2. Positive hybridoma lines were cloned by dilution, cultured and screened once again. Hybridoma lines remaining positive were cultured in bulk, the cells removed from solution by centrifugation, resuspended and stored in liquid nitrogen. The supernatants were stored at -80°C.

The three positive supernatants shown in this Figure were each incubated with nitrocellulose filters onto which had been blotted the three purified polypeptides of the LHC I, and the purified LHC II, in separate tracks (as in Figures 3.33(A-D)). Only those tracks from each filter showing a positive response are shown in this composite Figure. The interactions of the three hybridoma supernatants with each of the tracks on the filters are summarised in Table 3.5.

Track (1) SDS-PAGE analysis of the PS I antigen used to immunise the mice.

Track (2) autoradiograph of immunoblot using supernatant 2A1, showing interaction with purified P2.

Track (3) autoradiograph of immunoblot using supernatant 3C2, showing interaction with purified P3.

Tracks (4) and (5) autoradiograph of immunoblot using supernatant 1C4, showing interaction with purified P1 and P2 respectively.

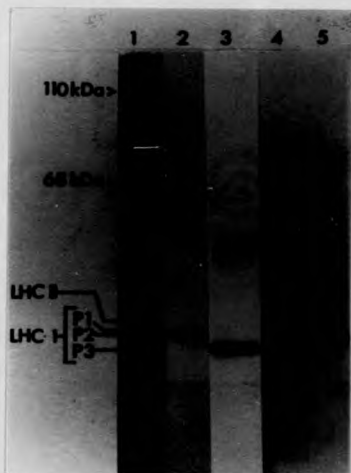


Figure 3.40

**Table 3.5** Summary of the specificities of the three monoclonal antibodies found to recognise polypeptide constituents of the LHC I. (See Figure 3.40 for accompanying autoradiographs).

Monoclonal Antibody	P1	P2	P3	LHC II
2A1	-	++	-	-
1C4	+	++	-	-
3C2	-	-	++	-

**Key**

(++) Strong reaction, (+) limited reaction, (-) no detectable reaction.

Details of the method used to culture and screen the hybridoma supernatants are given in Section 2.15c.



summarised in Table 3.5. For comparison, Figure 3.40 also includes a track showing the stained SDS-PAGE profile of the Tris-HCl pellet used as the antigen to immunise the mice.

Of the three monoclonal supernatants screened, two recognise P2, and one is specific for P3. Of the two supernatants recognising P2, one (the supernatant from culture 1C4) also shows some cross-reactivity with P1 (see Table 3.5). The reaction of this antibody with P1 appears weak compared to the reaction with P2. This result suggests that P1 and P2 share at least one common epitope. Furthermore, the difference in the relative strengths of the signals obtained with P1 and P2 may indicate that the epitope in question is present in greater amounts in P2 than in P1. This suggestion could be verified by probing blots of partial proteolytic digests of these two polypeptides with the 1C4 supernatant. This should provide information on the localisation of the antigenic determinant common to these two proteins. This work has not yet been carried out.

The pattern of cross-reactivities shown in Figure 3.40 and Table 3.5 suggests that none of the LHC I polypeptides are similar to the polypeptides of the LHC II. In addition, P1 and P2 appear to be more similar in structure to each other than either are to P3. This dichotomy is also reflected in the results obtained with

the polyclonal antisera (Figure 3.33). However, since monoclonal antibodies are specific for a single epitope, lack of cross-reactivity between proteins cannot be taken as clear evidence for lack of immunological (structural) similarity. It is possible that the antigenic determinant recognised by a given monoclonal antibody may not be common to all the polypeptides in question, and that other common determinants are not recognised by any of the monoclonal antibodies tested. It is necessary to screen a large number of monoclonal antibodies before valid conclusions concerning structural relationships between proteins can be reached. This work is in progress.

#### [3.4] Proteolytic Mapping of the LHC I Apoproteins

##### [3.4a] The use of Staphylococcal V8 protease

*Staphylococcus aureus* V8 protease is a serine protease with a molecular mass of 27 kDa. This protease acts by specifically cleaving peptide bonds on the carboxyl side of either glutamate or aspartate (Drapeau et al, 1972). In this study, the protease was used to generate partial proteolytic digests of the three LHC I polypeptides P1, P2 and P3, and the 26 kDa apoprotein of the LHC II (LHCP). The results are shown in Figure 3.41. Purified polypeptides were treated with increasing

concentrations of the protease as described in Section 2.8. Examination of Figure 3.41 demonstrates clear differences between the digestion products of the polypeptides of the LHC I. P1 gives only one stainable digestion product, even when treated with 1  $\mu$ g of protease. This digestion product shows an apparent molecular mass of approximately 15 kDa. Digestion of P2 produces a close-running doublet whose components display approximate apparent molecular masses of 14 kDa and 15 kDa. This simple digestion pattern resembles closely that of P1.

The pattern of proteolytic cleavage products generated by the treatment of P3 with Staphylococcal V8 protease is in marked contrast to those generated for either of the other two LHC I polypeptides. Cleavage of P3 results in at least two major products, one with an apparent molecular mass of 17 kDa, and a second with an apparent molecular mass of 12 kDa. In addition to these two major products, a number of minor bands can also be seen.

The cleavage pattern generated for P3 also shows some similarity to that generated for the purified LHCP. The untreated LHCP has an apparent molecular mass approximately 5 kDa larger than that of untreated P3. The first step in the cleavage of the LHCP is the production of a 20 kDa fragment. This is then further cleaved to a

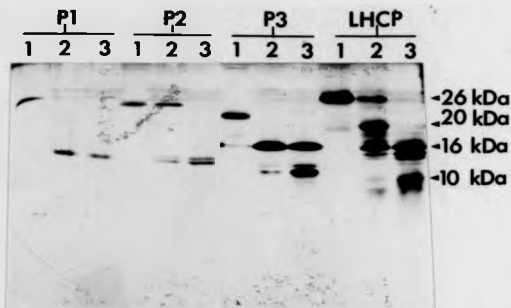


**Figure 3.41** Comparison of staphylococcal V8 protease digestion patterns for the LHCP and the apoproteins of the LHC I. P1, P2, and P3 were purified by SDS-PAGE and electroelution as described in Section 2.14. The LHCP was purified by subjecting purified LHC II to SDS-PAGE, staining the gel and excising the 26 kDa LHCP. Proteolysis was carried out exactly as described in Section 2.8. The gel was stained with silver. Each of the four proteins were subjected to three treatments: Track (1) untreated protein, track (2) protein treated with 0.2  $\mu$ g V8 protease, track (3) protein treated with 1.0  $\mu$ g V8 protease. The numbers to the right of the gel represent an approximate scale of apparent molecular mass.

fragment with an apparent molecular mass of 16-17 kDa, then to a third 15 kDa fragment. The final stainable cleavage fragment has an apparent molecular mass of approximately 10 kDa.

Although the pattern generated for P3 of the LHC I is less complex than that generated for the LHCP, these two patterns are more similar to each other than either are to the patterns generated for P1 and P2. This result suggests that a clear structural heterogeneity exists between the polypeptides of the LHC I, with the two polypeptides P1 and P2 forming a group distinct from P3.

#### 13.4b) The use of cyanogen bromide

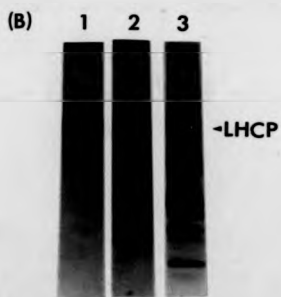
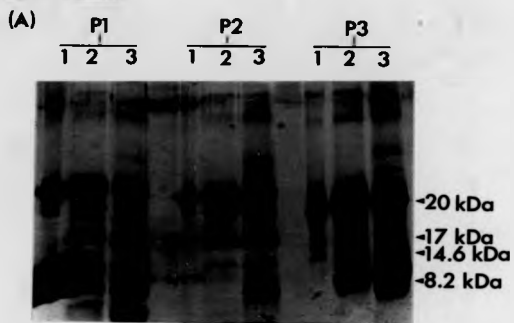
Cyanogen bromide (CNBr) cleaves polypeptide chains at the carboxyl side of methionine residues. Thus, a polypeptide containing three methionine residues will yield four cleavage products upon complete digestion. Figure 3.42(A) shows the result of treating purified P1, P2 and P3 with cyanogen bromide for 4 hr and 16 hr. For comparison, Figure 3.42(B) shows the cleavage patterns resulting when the same treatment is applied to the LHCP.

It is clear from Figure 3.42(A) that the cleavage patterns generated for P1 and P2 are extremely similar, while the pattern generated for P3 differs markedly from these. In contrast to the patterns resulting from the digestion of P1 and P2 with V8 protease, both P1 and P2

**Figure 3.42** Comparison of cyanogen bromide (CNBr) digestion patterns for the LHCP and the apoproteins of the LHC I.

(A) CNBr digestion patterns for the LHC I apoproteins. Proteins were isolated by SDS-PAGE and electroelution as described in Section 2.14. Proteins were then freeze-dried and treated with formic acid and CNBr as described in Section 2.8. Each protein was subjected to three treatments: Track (1) untreated protein, track (2) protein treated with CNBr for 4 h, track (3) protein treated with CNBr for 16 h. The numbers to the right of the gel represent an approximate scale of apparent molecular mass. The gel was stained with silver.

(B) CNBr digestion pattern for the LHCP. The LHCP was purified by subjecting purified LHC II to SDS-PAGE. The gel was stained and the 26 kDa LHCP excised and electroeluted from the gel matrix. The protein was then treated as described in (A). Tracks (1), (2) and (3) exactly as in (A). The gel was stained with silver.

**Figure 3.42**

yield a number of major cleavage products when treated with CNBr. The first of these products has an apparent molecular mass of 18 kDa, while a second major product appears at about 7 kDa. In the case of P1, a third major product can be seen with an apparent molecular mass of less than 2 kDa. This product is absent from the cleavage pattern for P2.

Assuming that these cleavage products result from the complete cleavage of these two polypeptides, then summing their molecular masses should provide good estimates of the molecular masses of the untreated proteins. For P1, the apparent molecular mass of the uncleaved protein is 24 kDa, as judged by relative migration distance on a variety of polyacrylamide gel systems. The sum of the molecular masses of the major CNBr cleavage products of this protein gives a value of 27 kDa. Similarly, the molecular mass of the uncleaved P2 is estimated as 23 kDa while summing of the cleavage fragments gives an estimate of 25 kDa.

The estimates based upon the cleavage fragments are inflated by 2-3 kDa compared to those based upon the uncleaved proteins. One important source of error in these estimates is the fact that electrophoresis was cut short in order to prevent any low molecular weight cleavage products from running into the lower electrophoresis buffer reservoir. The molecular mass



estimates, which are based upon distance migrated relative to standard molecular mass markers, are therefore likely to be too high.

Cleavage of P3 with CNBr results in the production of only one major product, with an apparent molecular mass of 11 kDa. No further digestion of this polypeptide was observed.

Figure 3.42(B) shows the pattern of cleavage products generated by treatment of the LHCP with CNBr. Three major cleavage products can be seen, and the pattern of protein breakdown does not resemble that of any of the three LHC I polypeptides shown in Figure 3.42(A).

On the basis of the evidence presented here from digestion of LHC I and LHC II apoproteins with V8 protease and CNBr, it is possible to draw only general conclusions concerning the relationships of the polypeptides of the LHC I and LHC II. However, both techniques show that the LHC I contains two polypeptides, P1 and P2, which display very similar digestion patterns, while P3 is completely different. Furthermore, none of the LHC I polypeptides shows any convincing similarity to the LHCP, indicating that the primary structures of the apoproteins of the two light-harvesting complexes LHC I and LHC II are dissimilar. These results support the conclusions derived from the monoclonal and polyclonal antibody work reported in Sections 3.2 and 3.3.

[3.5] Comparison of Amino-Terminal Regions of LHC I and LHC II Apoproteins

Figure 3.43 shows a comparison of the amino-terminal amino acid sequences of the LHC I apoproteins P2 and P3. For comparison, a corresponding amino acid sequence for the LHCP is also shown. The LHCP amino-terminal amino acid sequence is inferred from the nucleotide sequence determined for the pea cDNA clone pAB96, as described by Coruzzi *et al* (1983). This clone consists of a sequence of 833 nucleotides encoding 228 amino acid residues. The inferred sequence begins at the third amino acid from the amino-terminus of the mature protein. The first two residues of the protein were determined by amino acid sequencing of a tryptic peptide fragment cleaved from the amino-terminus of the mature protein. This fragment contains six residues in the following sequence: SER-ALA-THR-THR-LYS-LYS (Mullet *et al*, 1981). The threonyl residues in this sequence have been shown to be involved in the phosphorylation of the LHCP (Bennett, 1980).

It was not possible to determine the amino-terminal sequence of P1 since this appeared to be blocked. The sequence of P2 could be determined only as far as the eighteenth residue where a series of adjacent proline residues caused a reduction in cleavage yields. The

Cycle: 1 2 3 4 5 6 7 8 9 10 11 12  
 P2 UNK VAL ALA GLU UNK ASP ARG PRO LEU TRP PHE PRO  
 P3 ALA THR GLU ASP LYS THR ASP ALA ALA THR ASP VAL  
 LHCP SER ALA THR THR LYS LYS VAL ALA SER SER SER SER

Cycle: 13 14 15 16 17 18 19 20 21 22 23 24  
 P2 GLY SER THR PRO PRO PRO?  
 P3 ALA THR LYS GLU ALA PRO VAL GLY PHE THR PRO PRO  
 LHCP PRO TRP HIS GLY PRO ASP ARG VAL LYS TYR LEU GLY

Cycle: 25 26 27 28 29 30 31 32 33 34  
 P3 GLU LEU ASP PRO ASN THR PRO/THR GLY/SER GLU ILE  
 LHCP PRO PHE SER GLY GLU SER PRO SER TYR LEU

Cycle: 35 36  
 P3 PHE/PRO GLY?  
 LHCP THR GLY

**Figure 3.43**

Comparison of amino-terminal amino acid sequences of the two LHC I apoproteins P2 and P3, and the amino-terminal amino acid sequence for the LHCP. The polypeptides of the LHC I were purified by SDS-PAGE and electroelution as described in Section 2.14. Following electroelution, the proteins were freeze-dried and sent to Dr. Findlay at the Department of Biochemistry, Leeds University, for sequence analysis by solid-phase Edman degradation as described in Section 2.23. The amino acid sequence shown for the LHCP is deduced from the nucleotide sequence derived from the pea cDNA clone pAB96 described by Coruzzi *et al* (1983). See text for further details.

UNK Residue not identified.

? Residue identification tentative.

sequence beyond this point was difficult to interpret. The sequence of P3 was determined as far as the thirty-sixth residue.

Direct comparison of the three amino acid sequences shown in Figure 3.43 indicates that there are no regions of identity within the amino-terminal regions of these proteins. On a more general level, the sequences of all three proteins tend to be rather polar in nature, suggesting that the amino-terminal regions of these proteins may project from the lipid bilayer. In isolated thylakoids, the amino-terminus of the LHCP is accessible to attack by the soluble enzyme trypsin. Since no such attack takes place when inside-out thylakoid vesicles containing the LHC II are exposed to trypsin (Andersson *et al*, 1982), it is clear that this portion of the LHCP is exposed on the outer (stromal) surface of the thylakoid membrane. There is currently no evidence to suggest that the same is true of any of the polypeptides of the LHC I.

Although no amino acid sequence similarity between the amino-terminal of the polypeptides of the LHC I and LHC II is evident in Figure 3.43, the amino-terminal sequences shown account for only a small portion of the proteins in question. It is possible that the major parts of the LHC I polypeptides, which at present remain unsequenced, may show regions of similarity to the LHCP.

This possibility can only be explored when the full amino acid sequences of the LHC I polypeptides are known.

A second point to consider is that the LHC I polypeptides may represent versions of the LHCP which have lost lengths of the polypeptide chain from the amino-terminal region. This loss could be due to some form of post-transcriptional processing, or to deletions at the level of the genes encoding the light-harvesting proteins. If this were the case, then comparison of the amino-termini of the LHC I polypeptides with that of the LHCP would be inappropriate since unrelated regions of the proteins would be compared.

This possibility is rendered unlikely by the immunological evidence presented above. If such were the case, then large regions of similarity in primary structure of the LHC I and LHC II polypeptides would be expected. This similarity in turn, would greatly increase the likelihood of detecting immunological relatedness between these proteins. As a further check on this point, the amino-terminal sequences for P2 and P3 were used to search for homologies along the entire length of the amino acid sequence inferred from the pea LHCP cDNA clone pAB96 (Coruzzi *et al*, 1983). No homologies were detected.

### (3.6) Site of Synthesis of LHC I Apoproteins

Mullet *et al* (1981) provided evidence that the

apoproteins of the LHC I are encoded in nuclear genes. This conclusion was largely based upon the results of *in vitro* protein uptake experiments, using isolated intact chloroplasts. In these experiments, poly(A)-enriched RNA was translated *in vitro* in the presence of [<sup>35</sup>S]methionine. The radiolabelled translation products were then incubated with isolated intact chloroplasts to allow uptake, processing and assembly of labelled thylakoid proteins into their respective membrane protein complexes. The thylakoid membranes were then isolated and subfractionated by solubilisation with Triton X-100, as described in Section 2.13a. The solubilised thylakoids were analysed by sucrose density gradient centrifugation and autoradiography.

The results suggested that the polypeptides of the peripheral light-harvesting complex of PS I were imported into the chloroplast and assembled into a PS I complex. This conclusion was based on the fact that radiolabel was present in polypeptides showing the same apparent molecular mass as those of the LHC I. In addition, these labelled polypeptides sedimented on the sucrose density gradient to a position characteristically occupied by released PS I particles (Mullet *et al.*, 1980a).

These observations can be criticised in several ways. Firstly, the pea tissue used in these experiments was young and still expanding. In the hands of the present

author, such tissue does not yield a resolvable PS I particle by the method of Mullet *et al* (1980a) (result not shown). It may not be valid, therefore, to use the sedimentation properties of radiolabelled proteins on this sucrose density gradient system as a criterion for their identification.

Secondly, the radiolabelled polypeptides assigned to the LHC I were also identified on the basis of their mobility in the SDS polyacrylamide gel system used. Since there are a number of imported radiolabelled thylakoid proteins displaying apparent molecular masses which are similar to those of the polypeptides of the LHC I, (Grossman *et al*, 1980), it is important to use monospecific antibodies to confirm immunologically the identity of radiolabelled polypeptides.

For these reasons an attempt was made to determine the site of synthesis of the LHC I polypeptides using the polyclonal antibody prepared against the LHC I polypeptide P2. This antibody was chosen since it is specific for the LHC I polypeptides only (see Figure 3.33(B)). A direct means of determining whether the LHC I polypeptides are synthesised on cytoplasmic ribosomes, and therefore likely to be encoded on nuclear genes, is to identify the LHC I polypeptides, or their possible higher molecular weight precursors, among the products of translation of poly(A)-enriched RNA.

In order to do this, poly(A)-enriched RNA was prepared, as described in Section 2.20, from greening pea tissue known to be actively synthesising the polypeptides of the thylakoid pigment-protein complexes. This RNA was then translated *in vitro* using the wheat germ translation system, in the presence of [<sup>35</sup>S]methionine (Section 2.21). The resulting radiolabelled translation products were then incubated with LMCP antiserum, followed by the P2 antiserum. The incubation with LMCP antiserum was included in order to reduce non-specific binding of labelled proteins to the P2 antibody.

Immunoprecipitates were subjected to SDS-PAGE, the gels dried and autoradiographed. Figure 3.44 shows an autoradiograph resulting from a typical experiment. Track 1 shows the [<sup>35</sup>S]-labelled protein products resulting from the translation of pea poly(A)-enriched RNA in the wheat germ system. Three relatively heavily labelled bands can be seen in this track, two comprising a doublet at 30 kDa-32 kDa, and a third at 20 kDa. The major translation product at 32 kDa, (labelled P32 in Figure 3.44), has been shown to be the precursor to the major stainable protein component of the LHC II, the LMCP (Broglie *et al.*, 1981). Immunological evidence suggests that the lower member of the doublet represents the precursor to the minor 25 kDa polypeptide member of the LHC II (Cumling and Bennett, 1981). However, a clear



- Figure 3.44** Autoradiograph of immunoprecipitates resulting from the treatment of radiolabelled *in vitro* translation products with antibodies raised against the apoproteins of the LHC I. [ $^{35}$ S]-methionine was incorporated into protein products resulting from the cell-free translation of pea poly(A)-enriched RNA (Section 2.21). These radiolabelled products were then treated with LHCP antiserum, followed by antisera raised against the apoproteins of the LHC I. Immunoprecipitates were then recovered using protein A Sepharose as described in Section 2.15e, and analysed by SDS-PAGE followed by autoradiography. The gel contained a 10%-30% gradient of polyacrylamide. Incorporation of radiolabel into protein was measured as described in Section 2.22. In a typical translation,  $2.5 \times 10^6$  c.p.m. were incorporated per  $\mu$ l translation mix. Protein containing  $1 \times 10^6$  c.p.m. was loaded onto track (1). All material immunoprecipitated from 20  $\mu$ l translation mixes was used for each of the other tracks. Track (1) products of *in vitro* translation of poly(A)-enriched RNA in the wheat germ system. Track (2) immunoprecipitate resulting from the treatment of the translation products shown in track (1) with LHCP antiserum. Tracks (3)-(5) successive immunoprecipitations resulting from the treatment of translation products with P2 antiserum. Tracks (6) and (7) immunoprecipitations from translation products using P1 and P3 antisera respectively, following treatment with LHCP antiserum. Tracks (8) and (9) immunoprecipitations from translation products using P2 and P3 pre-immune sera.
- P32** The major translation product corresponding to the 32 kDa precursor to the LHCP.
- P20** The major translation product corresponding to the 20 kDa precursor to the small subunit of RUBISCO.

(292a)



Figure 3.44

precursor-product relationship has never been demonstrated for this polypeptide. This problem is discussed more fully in Section 1.7a of the Introduction. The major translation product labelled P20 in Figure 3.44 represents the precursor polypeptide to the small subunit of RUBISCO.

Track 2 of Figure 3.44 contains the immunoprecipitate resulting from the incubation of the radiolabelled translation products, shown in track 1, with the LHCP antiserum. It can be seen that the LHCP antiserum efficiently precipitates P32 together with the minor member of the doublet. In addition, a large number of labelled polypeptides of lower molecular weight can be seen, including a product with the same apparent molecular weight as P20, and a prominent product of very low molecular weight. The presence of these products in the immunoprecipitate may be the result of non-specific binding to the antibody, or to recognition by the antibody of short LHCP polypeptides resulting from premature termination of translation in the *in vitro* system.

Following incubation of the translation mixture with the LHCP antiserum and protein A sepharose, and removal of the immunoprecipitate by centrifugation, the resulting supernatant was incubated with the P2 antiserum. In this way the LHCP antiserum was used as a 'null serum' in an

attempt to reduce any non-specific binding of the LHCP precursor polypeptides in subsequent antibody incubations.

Tracks 3-5 represent the products of successive immunoprecipitations from the same translation mixture with the P2 antiserum. It can be seen that these treatments result in the precipitation of a doublet with the same apparent molecular weight as the P32 doublet shown in track 1. It can also be seen that the amount of precipitable material is steadily reduced with each subsequent antibody treatment.

Tracks 6 and 7 represent immunoprecipitates obtained by use of the LHC I antisera raised against P1 and P3 respectively. Here, the translation mixtures were first treated with LHCP antiserum (as the null serum), followed by the appropriate LHC I antiserum, as in track 2. Thus tracks 6 and 7 are exactly equivalent to track 3. In both cases, the P32 doublet is again the major precipitable material. The precipitate resulting from the use of the P1 antiserum is weaker than that from the P3 antiserum.

Tracks 8 and 9 represent immunoprecipitates resulting from the treatment of the translation mix with pre-immune sera for P2 and P3 respectively. Once again, each translation mix was pre-treated with LHCP antiserum prior to treatment with the appropriate pre-immune serum. Both these tracks show traces of the P32 doublet observed in

the other tracks, but at very low levels. The presence of these labelled bands in these tracks must be due to non-specific binding since the pre-immune sera to P2 and P3 do not recognise any thylakoid polypeptides (results not shown).

Comparison of tracks 3-5 with track 1 shows that the immunoprecipitates resulting from the incubation of the translation mix with the P2 antiserum are unlikely to be the result of non-specific binding, since the pattern of radioactive bands in these tracks does not resemble that in tracks 1 or 2. Furthermore, the steady reduction in the amount of precipitable material in tracks 3-5, and the fact that the pattern of immunoprecipitable products remains the same in these tracks, suggests strongly that the precipitable products are not present in excess over the antibody and are therefore unlikely to be the result of non-specific binding.

These considerations lead to the conclusion that the sera raised against the polypeptides of the LHC I specifically precipitate translation products of 30 kDa and 32 kDa respectively. These have the same apparent molecular weights as the precursors to the polypeptides of the LHC II. In the case of the sera raised against P1 and P3, it is possible that the precipitated bands could be the LHC II precursor proteins, since both these antisera recognise the mature LHCP. Since the P2

antisera does not recognise the mature LHCP, the apparent specificity of the immunoprecipitations involving this antiserum is more difficult to interpret.

One means by which the P2 antibody could recognise the LHCP precursor is if the antibody specifically recognised the amino-terminal extension sequence which is removed when the LHCP is processed to its mature size. This argument requires that the P2 polypeptide contains an internal amino acid sequence very similar or identical to the LHCP extension sequence. In the absence of an antibody specific for the LHCP extension sequence, this argument is not open to rigorous test.

In view of the arguments set out above, it is most likely that the radiolabelled doublet precipitated by the LHC I antibodies represents the LHCP precursors, and not LHC I polypeptide precursors which coigrate with the LHCP precursors on the gel system used. This conclusion is underlined by the fact that the two component bands of the doublet show the same relative intensities in all of the immunoprecipitations shown in Figure 3.44. These relative intensities are identical to those in the original sample of translation products from which the immunoprecipitates are derived (Figure 3.44, track 1). If the precipitated doublet represented LHC I protein precursors, this result would be extremely unlikely, in view of the differing affinities of the three anti-LHC I

sera for the three LHC I apoproteins.

The problem of the apparent specificity of the immunoprecipitations shown in Figure 3.44 remains to be resolved. Furthermore, if the LHC I antibodies are precipitating the LHC II precursor polypeptides, then these antibodies fail to detect radiolabelled precursors to the LHC I apoproteins amongst the products of translation of pea poly(A)-enriched RNA. This failure could be due to a number of causes. It is possible that the message encoding the LHC I polypeptides is not efficiently translated *in vitro*, or that it is of extremely low abundance. This latter explanation is unlikely to be the case in the rapidly greening tissue from which the RNA was extracted.

A second possibility is that the antibodies, although quite capable of detecting the mature LHC I polypeptides on an immunoblot, do not show the same efficiency in immunoprecipitations. A final possibility is that the LHC I polypeptides are encoded on chloroplast, not nuclear, DNA. This subject is discussed in Section 1.7b of the Introduction.

### [3.7] Photocontrol of LHC I Accumulation

The work reported in this Section deals with aspects of the photocontrol of the accumulation of the LHC I in the developing thylakoid membrane.

Much information is currently available concerning the photocontrols acting at the transcriptional, translational and post-translational stages of the synthesis and assembly of the LHC II (see Section 1.7a). Comparatively little is known, however, of the corresponding controls acting upon the peripheral light-harvesting system of PS I (see Section 1.7b). This lack of information has several causes. The LHC I and its component proteins are of comparatively recent discovery. The protein components of the LHC I are much less abundant in the thylakoid than those of the LHC II. Thus, direct estimations of the LHC I proteins in whole thylakoid extracts, such as can be obtained from densitometric scanning of thylakoid proteins resolved by SDS-PAGE, are rendered difficult and ambiguous. Hitherto, the lack of monospecific antibodies to the LHC I apoproteins has exacerbated this problem. Furthermore, nothing is known concerning the possible regulation of the synthesis of the LHC I apoproteins at the levels of transcription and translation, since no cloned DNA probes are currently available for use in hybridisation experiments.

The current work utilises the polyclonal antibodies characterised in Section 3.2b to study possible post-translational controls acting on the accumulation of the LHC I apoproteins in the developing thylakoid. Since the



antibodies could not be used to identify the LHC I polypeptides or their precursor forms among the products of *in vitro* translation (Section 3.6). It was not possible to assay the relative amounts of translatable LHC I message in the various tissues examined.

Two developmental systems have proved to be very useful in previous studies for investigating the control of the biogenesis of the thylakoid membrane. The first of these involves the use of intermittent (flash) illumination coupled with subsequent continuous illumination. The second system involves the controlled de-etiolation of plants by exposure of etiolated seedlings to extended periods of illumination and subsequent darkness. The work reported in the remainder of this Section is concerned with the application of these systems to the investigation of LHC I assembly in the developing thylakoid membrane.

### (3.7a) LHC I accumulation under intermittent light

Pea seedlings grown under intermittent illumination have been shown to be photosynthetically competent, indicating that their plastids contain functional PS I and PS II reaction centres (Armond *et al.*, 1976; Davis *et al.*, 1976). However, such plastids were found to lack the regions of appressed thylakoid membranes (grana) characteristic of plants grown under light regimes

incorporating more extended photoperiods. Such incompletely-developed plastids were later shown to have a reduced photosynthetic unit size, and in particular, were shown to be deficient in the light-harvesting chlorophyll *a/b* complex of PS II (Armond *et al*, 1977). Subsequent exposure of these plants to continuous illumination resulted in the rapid accumulation of the LHC II polypeptides in the thylakoids, the development of appressed membrane regions and an increase in the photosynthetic unit size.

Bennett (1981), and Cuning and Bennett (1981), demonstrated that under conditions of intermittent illumination, failure of the LHC II polypeptides to accumulate in the thylakoid was not due to synthetic blocks at the levels of transcription or translation. Instead, the failure was due to post-translational turnover of these polypeptides during the dark periods.

Mullet *et al* (1980b), working with cucumber, have shown that plants subjected to cycles of intermittent illumination (18 min dark, 2 min light), lack the long wavelength 77 K fluorescence emission maximum at 735 nm characteristic of PS I in fully greened plants. In addition, this lack of the 735 nm fluorescence maximum is directly correlated to a deficiency in stainable polypeptides in the 21 kDa-24 kDa molecular mass range. These observations were interpreted as

evidence for a failure of LHC I assembly under intermittent illumination. On subsequent continuous illumination of these plants, the appearance of polypeptides in the 21 kDa-24 kDa molecular mass range paralleled the induction of the 735 nm 77 K fluorescence maximum.

These observations suggest that intermittent illumination induces an unusual developmental situation involving the specific inhibition of assembly of the PS I and PS II peripheral light-harvesting systems. This inhibition is overcome upon exposure of intermittently illuminated plants to continuous illumination. In the case of the LHC II, failure to accumulate is due to polypeptide turnover in the dark. Intermittent illumination coupled with subsequent continuous illumination therefore offers a unique system for studying the post-translational control of assembly of the light-harvesting systems.

The evidence concerning the behaviour of the LHC I under intermittent illumination, however, is fragmentary (Mullet *et al*, 1980b). Polypeptide identification in the absence of monospecific antibodies is problematical for the reasons discussed above. In order to rectify this shortcoming, the polyclonal antibody raised against the LHC I polypeptide P2 was used to investigate the accumulation of the LHC I polypeptides in the thylakoid

membrane under intermittent illumination, and after subsequent transfer to continuous illumination.

Figure 3.45 compares three shoots removed from pea seedlings grown under different conditions of illumination. Each of the three buds has the same absolute age of nine days from seed planting, and each represents the plant body currently developed at and above the third node. The second node tissue can be seen lower down on the shoot and is included for comparison. In the present study, third node leaf tissue, comprising both the true leaves and the leaf-like stipules, proved to be ideal for monitoring changes in light-harvesting protein content for several reasons. Firstly, the third node leaf primordia are already present after seven days of etiolation, and these represent the first leaf tissue convenient to harvest in bulk. Secondly, it is clear from examination of Figure 3.45, that the third node represents the earliest tissue to undergo clear and well-defined developmental changes upon de-etiolation. Thus any comparison of changes monitored in the third node leaf tissue during a given developmental sequence will be valid, since equivalent tissue at all points in the sequence will be sampled.

For these reasons, all work described in this Section was carried out using third node leaf tissue, unless otherwise stated. The term 'third node' used here will



**Figure 3.45** Comparison of pea shoots from seedlings grown under three different light conditions. (1) Etiolated pea grown for 9 days in darkness. (2) Pea grown for 7 days in darkness followed by 2 days intermittent illumination (2 min light, 118 min dark). (3) Pea grown for 9 days under a 12 h photoperiod.  
N2 Second node  
N3 Third node leaves  
N4 Fourth node leaves  
S Stipule  
L Leaf  
All experiments on photoregulation used third node leaf material consisting of both leaves and stipules.

refer to the true leaves, petiole and leaf-like stipules making up the photosynthetic tissue of this part of the plant.

Examination of Figure 3.45 shows that light has a dramatic influence upon the development of the plant. The third node of the etiolated seedling consists of nothing more than a hook terminating in small, unexpanded leaf primordia. The internodes are elongated and there is no detectable chlorophyll present in the plant. By contrast, the plant grown for nine days under a 12 h photoperiod shows a partially expanded third node with fourth node leaf material well developed prior to internode expansion. Plants treated in this way contain high levels of chlorophyll and show a chlorophyll a/b ratio of about 3.0-3.5.

The plants subjected to seven days etiolation followed by two days intermittent illumination (2 min light, 118 min dark), assume a gross morphology intermediate between the morphologies of the etiolated and fully-greened plants. Intermittent illumination is thus sufficient to initiate leaf development and expansion. However, in these plants the level of chlorophyll in the leaves is low and the measured chlorophyll a/b ratio is often in excess of 6.0, indicating that chlorophyll b is not detectable in this tissue.

The absence of chlorophyll *b* in the intermittently-illuminated plants is consistent with the absence of the LHC II in the thylakoid membranes. Figure 3.46 shows changes in overall chlorophyll content, and in the chlorophyll *a/b* ratio, of the thylakoids derived from third node tissue when plants are removed from intermittent illumination and placed under continuous illumination. After 48 h of intermittent illumination, the chlorophyll content of the third node thylakoids remains low. Upon transfer to continuous light, the chlorophyll content quickly rises. During the first 4 h of continuous illumination, the chlorophyll *a/b* ratio declines rapidly. This decline indicates that during this period, chlorophyll *b* is accumulating in the thylakoid at a greater rate than chlorophyll *a*, suggesting that the peripheral chlorophyll *a/b*-binding light-harvesting complexes are undergoing rapid accumulation compared to the reaction centre complexes.

Over the whole 24 h illumination period, the rate of increase of chlorophyll in the third node tissue is approximately constant. However, after 4 h of continuous illumination the rate of depression of the chlorophyll *a/b* ratio decreases dramatically, tending towards a constant chlorophyll *a/b* ratio of around 3.0. This result suggests that the relative rates of accumulation of the light-harvesting complexes have decreased at this time,

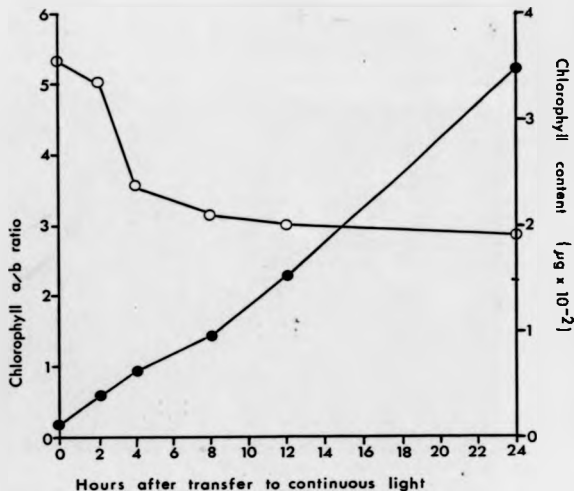


**Figure 3.46**

Changes in chlorophyll content of third node thylakoids resulting from transfer of plants from intermittent to continuous illumination. Pea seedlings were grown for 7 days in the dark followed by 48 h in intermittent light. The plants were then transferred to continuous illumination (Section 2.2). At appropriate intervals third nodes were harvested and thylakoid membranes isolated. Chlorophyll determinations were carried out as described in section 2.17. Chlorophyll content refers to the estimated chlorophyll content of thylakoids derived from a single third node. All estimates represent the mean of two replicates. Each replicate is based on the chlorophyll extracted from ten third nodes.

- Chlorophyll content per third node
- Chlorophyll a/b ratio



and that non-chlorophyll *b*-binding complexes, such as the photosystem reaction centres, are accumulating more rapidly than in the first 4 h of continuous illumination.

Since the majority of the chlorophyll *b* in the thylakoid membrane is found in the LHC II, Figure 3.46 yields little direct information on the accumulation of the LHC I in the thylakoid under these experimental conditions. In order to trace the accumulation of the LHC I during this greening period it is necessary to probe thylakoid membrane extracts with antibodies specific for the LHC I apoproteins.

Figure 3.47 shows a stained SDS-PAGE analysis of the polypeptide content of the third node tissue thylakoid membranes, isolated at different time points during greening under continuous light, following 48 h of intermittent illumination. For the purposes of comparison, a sample of PS I prepared by the method of Mullet *et al* (1980a) is also shown.

In order to directly compare the different tracks in the greening sequence, it is necessary to load equivalent amounts of thylakoid material onto each track. This was done by loading approximately equal amounts of protein from each sample taken. Thylakoid protein estimations were carried out as described in Section 2.10.

Track 2 in Figure 3.47 represents thylakoid membranes isolated from plants which have been harvested directly

**Figure 3.47** SDS-PAGE analysis of the polypeptide content of third node thylakoids following transfer of plants from intermittent to continuous illumination.

Plants were grown for 7 days in the dark and 48 h in intermittent light (Section 2.2c). Plants were then transferred to continuous illumination and, at appropriate time intervals, third nodes were harvested and thylakoids isolated. Thylakoids were washed once in 80% (v/v) aqueous acetone and the precipitated protein estimated by the method described in Section 2.10. Thylakoid samples were then resuspended in SDS sample buffer, boiled for 2 min, and a volume containing approximately 30  $\mu$ g protein was loaded onto each track. The gel contained a 10%-16% polyacrylamide gradient and was stained with Coomassie brilliant blue. Track (1) PS I prepared by the method of Mullet *et al* (1980a). Tracks (2)-(7) third node thylakoids extracted from intermittently illuminated plants subjected to 0, 2, 4, 8, 12 and 24 h continuous light respectively.  $\alpha$  and  $\beta$  refer to the  $\alpha$  and  $\beta$  subunits of the ATP synthase complex.

LHCP the 26 kDa light-harvesting chlorophyll *a/b* binding protein of PS II.

LHC I the three apoproteins of the peripheral light-harvesting complex of PS I.

Polypeptide bands labelled a, b and c represent contaminants which can be removed by treating isolated thylakoids with DNAase.

**Figure 3.48** Autoradiograph of immunoblot showing the accumulation of the apoproteins of the LHC I and LHC II upon transfer of plants from intermittent to continuous illumination. Plants were illuminated and third node thylakoid proteins extracted exactly in the manner described in the legend to Figure 3.47. Proteins were resolved by SDS-PAGE and transferred electrophoretically to a nitrocellulose filter. The filter was probed sequentially with P2 antiserum followed by LHCP antiserum, and bound antibody was detected with  $^{125}$ I-labelled protein A. The individual tracks were as labelled in the Figure. The track labelled 'Membranes' contained thylakoid proteins extracted from third node leaves of peas grown for 11 days under a 12 h photoperiod.

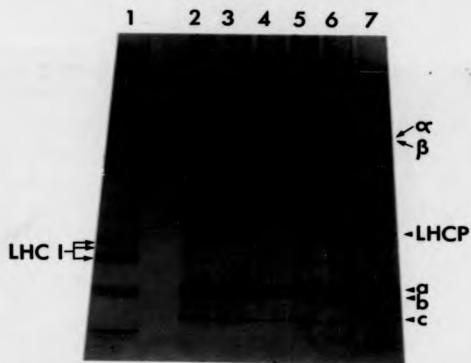


Figure 3.47

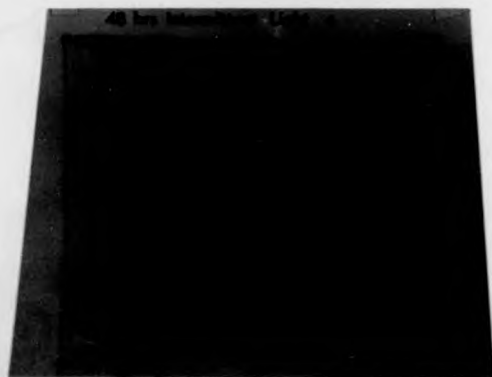


Figure 3.48

from intermittent illumination. Subsequent tracks represent thylakoids harvested after increasing lengths of time under continuous illumination. The most obvious change in the thylakoid polypeptide profiles resulting from exposure of intermittently-illuminated plants to continuous light, is the increase of stainable LHCP relative to other thylakoid polypeptides. After two days of intermittent illumination the LHCP does not appear in the thylakoid polypeptide profile, yet after 12 h continuous illumination it forms a recognisable stainable band.

Two other major stainable thylakoid polypeptides, the  $\alpha$  and  $\beta$  subunits of the ATP synthase complex, appear not to change in amount as illumination continues. This apparent stasis is a result of the fact that equal amounts of protein are loaded onto each track. Therefore, as the LHCP rapidly accumulates in the thylakoid, other thylakoid polypeptides, although increasing in absolute amount, will make an increasingly smaller contribution to the total protein in the membrane. Thus, changes in the protein profiles shown in Figure 3.47 represent changes in relative, not absolute, amounts of individual polypeptides.

The LHC I polypeptides seen in the PS I sample in track 1 are not readily discernable in tracks 2-7, and so no conclusion concerning their behaviour under these

conditions can be drawn from the stained polypeptide pattern alone. For this reason the same thylakoid samples were subjected to immunoblotting, using anti-LHCP and anti-P2 sera as the antibody probes. Figure 3.48 shows the resulting autoradiograph. In order to check the specificity of the antibodies, and to compare the relative abundance of the LHC I and LHC II polypeptides in fully-greened tissue, a sample of thylakoids isolated from the third nodes of plants grown for eleven days under a 12 h photoperiod was also blotted.

Figure 3.48 shows clearly that the LHCP is not immunologically detectable in thylakoid membranes subjected to 48 h intermittent illumination. Upon exposure to continuous light, the level of the LHCP in the membrane increases dramatically, being readily detectable by antibody after 2 h continuous illumination. Like the LHCP, the LHC I polypeptides are also undetectable in the intermittently-illuminated thylakoids. In contrast to the LHCP, however, the LHC I apoproteins do not become immunologically detectable until at least 12 h of continuous illumination have elapsed.

It is possible that this observed difference in the rate of accumulation of the two light-harvesting complexes under continuous illumination is more apparent than real. Such could be the case if the avidity of the

anti-P2 serum for its antigen were lower than that of the anti-LHCP serum for its antigen. In this case, a relatively larger concentration of the LHC I polypeptides would be required in the membrane, than would otherwise be the case, before detection by the antibody were possible.

Evidence that this argument is not sufficient to explain the observed differences between the LHC I and LHC II polypeptides in Figure 3.48 comes from examination of the fully-greened membrane track shown in this Figure. Thylakoid material in this track is derived from fully matured leaves which have ceased expansion. If differences in antibody avidity were sufficient to explain the observed differences in accumulation of the two light-harvesting complexes, then no difference in the relative intensities of the LHCP and LHC I signals would be observed between the mature membrane track and the tracks representing the greening thylakoids. Such differences in relative signal intensities can be clearly seen.

If differences in antibody avidity are insufficient to explain observed differences in accumulation rates of the LHC I and LHC II in this system, then it is necessary to argue for the differential synthesis of these two complexes. This consideration implies that in this greening system, the peripheral antenna system of

PS II is assembled earlier than that of PS I. Since the intermittent illumination system can be regarded as an atypical developmental situation unlikely to be encountered in nature, it is possible to argue that differential accumulation of the two light-harvesting systems is an artefact which does not reflect any natural situation. A similar difference in LHC I and LHC II accumulation has, however, recently been demonstrated in studies using 4-day old light-grown wheat leaves (Bredenkamp and Baker, 1986). Since the greening wheat system studied by these authors represents a natural developmental sequence, it is likely that the observed differential growth of the two light-harvesting antenna complexes represents a real phenomenon.

The clear failure of the apoproteins of the LHC I to accumulate in the thylakoid membrane under intermittent illumination, and their subsequent appearance upon continuous illumination, indicates that the successful assembly of the LHC I in the thylakoid membrane requires a 'signal' consisting of an extended period of illumination. In this respect the control of accumulation of the LHC I resembles closely that of the LHC II. The requirement for extended illumination could be attributed to a number of possible causes. Intermittent illumination may not be sufficient to initiate expression of the genes encoding the light-harvesting polypeptides (which in turn

implies that the expression of the LHC I genes is not under conventional phytochrome control). Alternatively, the intermittent light regime may in some way block successful translation of the mRNA encoding the light-harvesting proteins. Lastly, the block on accumulation of these proteins may act at the point of assembly of the complexes themselves.

In the case of the LHCP, it is known that the failure of accumulation under intermittent illumination is not due to blocks on transcription or translation, but due to the rapid turnover of the LHCP in the dark (Cuming and Bennett, 1981). In view of the similarity between the LHC II and the LHC I with respect to their behaviour under intermittent illumination, it is of interest to determine whether the post-translational control (i.e. polypeptide turnover) acting upon the LHCP is also acting upon the apoproteins of the LHC I.

In order to investigate this point, the intermittent illumination system described above was abandoned in favour of a more conventional de-etiolation system.

### [3.7b] LHC I accumulation in de-etiolating plants

As shown in Figure 3.48, 48 h of intermittent illumination yields no immunologically-detectable LHC I apoproteins in thylakoids derived from third node tissue. In order to investigate possible LHC I protein turnover



in the dark, it is necessary to start with plants in which active accumulation of the LHC I apoproteins can be demonstrated. If such plants are then subjected to darkness, failure of further LHC I accumulation, coupled with a demonstration of continued synthesis of the LHC I apoproteins, would point unequivocally to protein turnover in the dark.

(1) Loss of chlorophyll in the dark

Etiolated pea seedlings which had been grown for seven days in the dark were subjected to 48 h continuous illumination, as described in Section 2.2b. Plants so treated were then either removed to darkness for a further 16 h, or subjected to a further 16 h continuous light. After this time, third nodes were harvested and thylakoids prepared for pigment and protein content analysis.

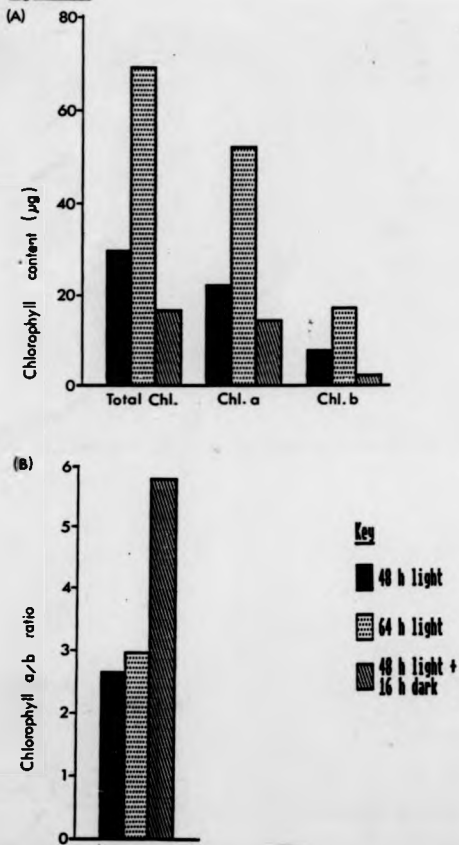
Figures 3.49A and 3.49B show an analysis of changes in the chlorophyll content of these plants during dark and light treatments. After 2 days of continuous illumination, the total chlorophyll content of the third node leaf pair has reached 30  $\mu\text{g}$ . This chlorophyll is composed of 73% chlorophyll a and 27% chlorophyll b, (a chlorophyll a/b ratio of 2.7). After a further 16 h of continuous illumination, the chlorophyll content per third node leaf pair has risen to around 68  $\mu\text{g}$ . The relative contributions of chlorophyll a and chlorophyll

**Figure 3.49** Bar charts showing changes in chlorophyll content within third node leaves upon transfer of greening plants to darkness. Third node leaves were harvested and pigments extracted in 80% (v/v) aqueous acetone. Chlorophyll was estimated using the equations given in Section 2.17. Each value shown is the mean of two replicates. Each replicate is based on the chlorophyll extracted from ten third nodes.

(A) Total chlorophyll, chlorophyll *a* and chlorophyll *b* content of plants subjected to 48 h continuous light, 64 h continuous light, or 48 h continuous light followed by 16 h darkness. The meaning of each bar is given in the key.

(B) Chlorophyll *a/b* ratios found in third node leaves illuminated as in (A).

Figure 3.49



b, however, remain approximately the same at 75% and 25% respectively, (a chlorophyll a/b ratio of 3.0).

Plants subjected to 16 h dark treatment following 48 h continuous illumination not only fail to increase their chlorophyll content (as would be expected since light is required for chlorophyll synthesis in flowering plants), but also show a substantial decrease in their chlorophyll content during the dark period. Each third node removed from these plants contains only around 16  $\mu$ g chlorophyll, indicating that the total chlorophyll content of this tissue decreases by about 50% during the 16 h of darkness. This loss of chlorophyll results in a dramatic increase in the chlorophyll a/b ratio of this dark-treated tissue to almost 6.0 (Figure 3.49B), a value very similar to that found in plants subjected to 48 h of intermittent illumination (see Figure 3.46). The chlorophyll b content of the dark-treated third node tissue declines by 69% during the dark period, while the chlorophyll a content declines by only 35%.

Measurement of the loss of the two chlorophyll species in absolute terms, however, shows that in each third node, an average of 1.3  $\mu$ g chlorophyll a is lost for every 1.0  $\mu$ g chlorophyll b. The observed increase in the chlorophyll a/b ratio is not, therefore, due to a more rapid loss of chlorophyll b than chlorophyll a, but rather to the fact that there is a much greater loss of

chlorophyll *b*, relative to its pool size in the membrane, than is the case for chlorophyll *a*.

The results shown in Figures 3.49A and 3.49B are consistent with a preferential loss of the LHC II from the thylakoid membrane during the 16 h dark period. If, however, the loss of the LHC II were alone responsible for the loss of chlorophyll in the dark, then chlorophyll *a* and chlorophyll *b* would be lost from the membrane at approximately equal rates. As shown above, there is a 30% greater loss of chlorophyll *a*. This observation suggests that one or more other chlorophyll-protein complexes are involved in this chlorophyll loss during the dark period, and that these other complexes must bind more chlorophyll *a* than chlorophyll *b*.

The LHC I binds chlorophyll *a* and chlorophyll *b* in a ratio of about 3.5:1 (Haworth *et al.*, 1983; Lee *et al.*, 1984a). In order to determine whether the LHC I is involved in the loss of chlorophyll in dark-treated plants, and to compare the behaviour of the LHC I apoproteins with that of the LHCP, third node thylakoids were isolated from light-treated and dark-treated plants and subjected to immunological analysis by immunoblotting. Subsection (ii) deals with the characterisation of this developmental system in terms of the accumulation of the LHC II, and corresponding data for the LHC I are shown in subsection (iii).

(11) Accumulation of LHC II apoproteins

Figure 3.50 shows an SDS-PAGE analysis of thylakoid membranes isolated from third node leaf material subjected to the light and dark treatments described above. For the purposes of this analysis, each gel track was loaded with membrane protein representing approximately one third of the total amount of thylakoid protein found in each third node. The procedure used to estimate the amount of membrane protein present in each thylakoid preparation in terms of whole third nodes is described in detail in Section 2.10, and is based upon a comparison of chlorophyll extracted from entire third nodes and from thylakoids isolated from the same node material.

This method of determining gel track loadings differs from that used in Figure 3.47 in one important respect. Where equal protein loadings are used to determine the amount of sample to run in each gel track, any change observed in the amount of a given protein band between tracks represents a change relative to the total protein background. On the other hand, where each track represents a given proportion of the thylakoid protein contained within a single node, a change in the amount of a given protein between tracks is an absolute change, and is independent of changes occurring in the amounts of other proteins present in the sample.

The advantage of the latter method is that the

**Figure 3.50** SDS-PAGE analysis of third node thylakoid membranes after exposure of etiolated pea seedlings to 48 h continuous light, 64 h continuous light, or 48 h continuous light followed by 16 h darkness. Pea seedlings were grown in the dark for 7 days, then exposed to 48 h continuous illumination (Section 2.2b), after which time 10 third nodes were harvested and thylakoids isolated (Section 2.12). Following this, the plants were exposed to either a further 16 h light or to 16 h darkness, after which ten third nodes were again harvested and thylakoids isolated. Harvesting of third node tissue from dark-treated plants was carried out entirely in the dark. Thylakoid membranes were treated with 80% (v/v) aqueous acetone and the precipitated proteins were recovered by centrifugation. The dried precipitates were boiled in SDS sample buffer and subjected to analysis by SDS-PAGE. Membrane material representing approximately one third of the total thylakoids contained within one harvested node was loaded onto tracks (2), (3) and (4). Loadings were determined as described in Section 2.10. PS I material was prepared by the method of Mullet *et al* (1980a), and a volume containing 10  $\mu$ g chlorophyll was boiled in SDS sample buffer and loaded onto track (1). The gel contained a 10%-16% gradient of polyacrylamide, and was stained with Coomassie brilliant blue. Track (1) PS I prepared by the method of Mullet *et al* (1980a). Tracks (2)-(4) third node thylakoids isolated from plants after 48 h light, 64 h light, and 48 h light followed by 16 h dark respectively.

RC I      The PS I reaction centre polypeptides.

LHC I      The polypeptides of the PS I peripheral light-harvesting complex.

$\alpha$   $\beta$       The  $\alpha$  and  $\beta$  subunits of the ATP synthase.

LHCP      The 26 kDa polypeptide of the LHC II

The polypeptides labelled 1,2,3 and 4 represent possible LHC I apoproteins.

(322)

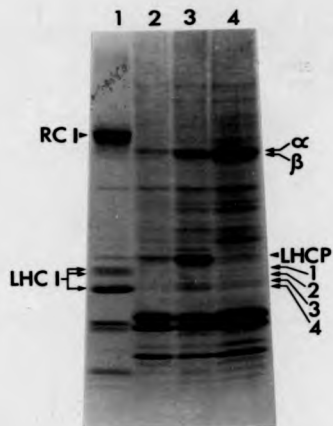


Figure 3.50



accumulation (or loss) of different polypeptides over time can be followed independently of one another. An inherent disadvantage of this method is that it is slightly less sensitive to changes in protein content than is the case for equal protein loadings. In the case of the present work, the independent monitoring of polypeptides whose accumulation in the membrane can be demonstrated to be different from that of the light-harvesting proteins provides a useful internal control.

Track 2 of Figure 3.50 shows the thylakoid polypeptide profile of plants exposed to 48 h continuous illumination. The LHCP is present in stainable quantities, and after a further 16 h continuous illumination (track 3), the LHCP has visibly increased in amount. If, however, the plants represented in track 2 are placed in darkness for 16 h, the LHCP fails to show any discernable increase (Figure 3.50, track 4). These polypeptide profiles confirm the conclusions derived from the chlorophyll data shown in Figure 3.49.

Comparison of tracks 2 and 4 suggests that there is less LHCP in the dark-treated plants than was present at the beginning of the dark period. This observation implies that not only does the LHCP fail to accumulate in the thylakoid during the dark period (accumulation occurring rapidly in the light-track 3), but that in addition, a net loss of the LHCP from the thylakoid takes

place in the dark. This observation is supported by the loss of chlorophyll in the dark shown in Figure 3.49A.

The  $\alpha$  and  $\beta$  subunits of the ATP synthase (labelled  $\alpha$  and  $\beta$  in Figure 3.50), show a very different response to dark treatment. Accumulation of these polypeptides in the light (tracks 2 and 3) parallels that of the LHCP. Unlike the LHCP, however, the  $\alpha$  and  $\beta$  subunits continue to accumulate in the thylakoid membrane when the plants are placed in the dark. Comparison of tracks 3 and 4 suggests that the rate of accumulation of these polypeptides is not altered in the absence of light. For the reasons argued above, this continued accumulation in the dark is not an apparent accumulation resulting from the loss of the LHCP from the membrane, but represents an absolute increase in the amount of these polypeptides. The loss of the LHCP in the dark is therefore a selective loss and not part of a general degradation of the thylakoid.

This conclusion is underlined in Figure 3.51 and Table 3.6. Figure 3.51 shows densitometer scans of the three thylakoid preparations shown in Figure 3.50, tracks 2, 3 and 4. The  $\alpha$  and  $\beta$  subunits of the ATP synthase are poorly resolved and form a single peak with a shoulder (peak 1). The LHCP is designated peak 2. The differences in accumulation of these polypeptides in the light and dark can clearly be seen. The densitometer scans allowed quantification of these differences in terms of a

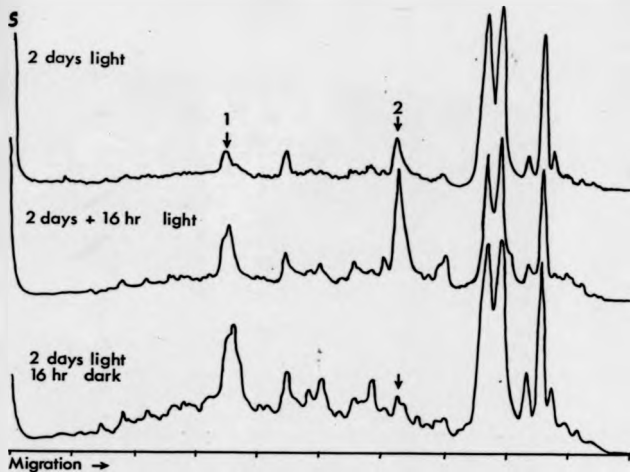


**Figure 3.51** Scanning densitometer traces of the third node thylakoid tracks shown in Figure 3.50. The Coomassie blue-stained polyacrylamide gel shown in Figure 3.50 was scanned wet using a Joyce-Loebl densitometer. Data were collected electronically using a model B BBC microcomputer and dedicated software (Warwick Control Systems, UK). The incident signal was subjected to analogue-to-digital conversion and stored on a floppy disc for subsequent printing.

Peak 1 The  $\alpha$  and  $\beta$  subunits of the ATP synthase.

Peak 2 The LHCP.

The point marked S represents the boundary between the stacking and resolving gels.

**Table 3.6** Comparison of accumulation of the  $\alpha$  and  $\beta$  subunits of the ATP synthase and the LHCP in de-etiolating seedlings during light and dark treatments.

Treatment	Ratio of peak areas ( $\alpha$ , $\beta$ /LHCP)
48 h light	1.1
64 h light	0.7
48 h light + 16 h dark	3.3

Gel tracks 2, 3 and 4 in Figure 3.50 were scanned using a Joyce-Loebl densitometer (see Figure 3.41). The analogue signals resulting from each scan were converted to digital signals using a BBC model B microcomputer. Peak areas were calculated in arbitrary units.

comparison of the areas under peak 1 and 2 for each light treatment. This quantification was done by using a computer programme to digitise the analogue signals received from the densitometer, and to calculate the area of each peak in arbitrary units. The results are expressed in Table 3.6 as peak 1/peak 2 ratios. After 48 h continuous illumination the ratio is 1.1, showing that the two peaks are present in approximately equal amounts (as judged by Coomassie blue staining). A further 16 h illumination depresses this ratio to 0.7, showing that the LHCP is accumulating in the thylakoid at a faster rate than the ATP synthase subunits. If, instead, the plants are subjected to 16 h darkness, the ratio rises to 3.3, exactly three times its starting value.

The results reported above for the loss of chlorophyll, accumulation of the ATP synthase subunits, and accumulation of the LHCP are comparable with those reported by Bennett (1981) using a similar experimental approach. Having thus characterised the experimental system, it was then possible to investigate the accumulation of the LHC I apoproteins.

(iii) Accumulation of LHC I apoproteins

The behaviour of the LHC I in this experimental system is not clear from examination of Figures 3.50 and 3.51. Track 1 of Figure 3.50 represents a PS I preparation containing the LHC I polypeptides, and

comparison of this track with the thylakoid tracks 3 and 4 suggests the existence of three or four stainable polypeptides in the thylakoids which could represent the LHC I apoproteins. These are labelled 1, 2, 3 and 4 in Figure 3.50. If these stained bands represent the LHC I apoproteins, then a careful comparison of the relative intensities of these bands with that of the LHCP in tracks 2, 3 and 4 of this Figure, shows that, unlike the LHC II, the LHC I does not fail to accumulate in the thylakoid membrane in the dark.

In order to test this conclusion, the three thylakoid samples shown in Figure 3.50 were subjected to SDS-PAGE and electrophoretically transferred to a nitrocellulose filter. The three LHC I apoproteins were then detected on the filter using the P2 antiserum together with [<sup>125</sup>I]-labelled protein A. Figure 3.52 shows the resulting autoradiograph.

Track 1 of Figure 3.52 contains PS I material prepared by the method of Mullet *et al* (1980a). This track was included both to mark the position of the three LHC I polypeptides and to demonstrate the specificity of the antibody. Tracks 2, 3 and 4 are exactly as described in Figure 3.50, using the same sample loadings. All three LHC I polypeptides are detectable after 48 h continuous illumination (track 2), and all three increase dramatically during the following 16 h illumination

**Figure 3.52** Autoradiograph of immunoblot showing the pattern of accumulation of the LHC I apoproteins in the third node thylakoids when de-etiolating pea seedlings are returned to the dark. Etiolated pea seedlings were subjected to 48 h continuous illumination followed by a further 16 h light or 16 h darkness, as described in the legend to Figure 3.50. Third nodes were harvested, thylakoids isolated and thylakoid proteins subjected to SDS-PAGE analysis exactly as described in the legend to Figure 3.50. The resolved thylakoid proteins were blotted electrophoretically onto a nitrocellulose filter, and the filter probed with the P2 antiserum. Bound antibody was detected using [ $^{125}$ I]-labelled protein A. All tracks are as shown in the Figure.

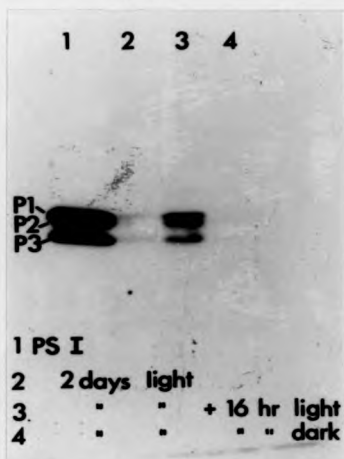


Figure 3.52



(track 3). When the plants represented by the material in track 2 are placed for 16 h in the dark, the LHC I apoproteins are no longer immunologically detectable.

It is concluded the polypeptides of the LHC I, like those of the LHC II, fail to accumulate in the developing thylakoids of de-etiolating seedlings when the seedlings are placed in the dark. In addition, a comparison of tracks 2 and 4 in Figure 3.52 strongly suggests that the LHC I polypeptides decrease in amount in the membrane during the dark period. Once again, this decrease parallels that shown by the LHCP.

The results shown in Figure 3.52 prove that the stained polypeptide bands labelled 1, 2, 3 and 4 in Figure 3.50 do not represent the LHC I apoproteins, since these stained bands do not show the failure of accumulation in the dark demonstrated by the use of the LHC I-specific P2 antiserum. This observation serves to underline the danger of using relative mobility in SDS-polyacrylamide gels as the sole criterion for polypeptide identification.

(iv) Accumulation of RC I apoproteins

Figure 3.52 demonstrates that in the young developing tissue studied, the accumulation of the peripheral light-harvesting system of PS I, like that of PS II, is light-dependent. Since the results shown in Figures 3.50 and 3.51 demonstrate that this light-dependency does not

apply to at least one non-chlorophyll binding complex (the ATP synthase), it is of interest to ask whether chlorophyll-binding complexes other than the light-harvesting complexes also show similar light-dependency in the system under study. More particularly, the question arises as to whether the accumulation of the LHC I and the PS I reaction centre (RC I) is regulated in same way, or whether these two complexes show independent controls.

In order to address this question, the RC I-specific antibody was employed to study the accumulation of the RC I polypeptides by immunoblotting, in exactly the same way as the P2 antiserum (Figure 3.52). However, it was found that the procedures used to prepare the thylakoids, and to estimate how much material to load in each gel track, abolished the ability of the RC I antiserum to recognise the 65 kDa-68 kDa RC I polypeptides on an immunoblot.

A clear example of this phenomenon is shown in Figure 3.53. This Figure represents an immunoblot identical in all respects to that shown in Figure 3.52, except that the antibody used as the probe here is the RC I-specific antibody, and the antibody is visualised using the biotin-streptavidin peroxidase system (see Section 2.15d(iii)). Track 1 of Figure 3.53 contains PS I material prepared by the method of Mullet *et al* (1980a),

**Figure 3.53** Immunoblot showing the destruction of the RC I polypeptides resulting from the acetone treatment of thylakoid membranes. Etiolated pea seedlings were subjected to 48 h continuous illumination followed by a further 16 h light or 16 h darkness, as described in the legend to Figure 3.50. Third nodes were harvested, thylakoids isolated and thylakoid proteins subjected to SDS-PAGE analysis exactly as described in the legend to Figure 3.50. The resolved thylakoid proteins were blotted electrophoretically onto a nitrocellulose filter, and the filter probed with the RC I antiserum. Bound antibody was detected using the biotin-streptavidin peroxidase system (Section 2.15d(11)). Track (1) PS I prepared by the method of Mullet *et al* (1980a). Tracks (2)-(4) third node thylakoids isolated from plants after 48 h light, 64 h light, and 48 h light followed by 16 h dark respectively. RC I The PS I reaction centre polypeptides.

**Figure 3.54** Immunoblot showing the pattern of accumulation of the RC I polypeptides in the third node thylakoids when de-etiolating pea seedlings are returned to the dark. Etiolated pea seedlings were subjected to 48 h continuous illumination followed by a further 16 h light or 16 h darkness, as described in the legend to Figure 3.50. Third nodes were harvested and thylakoids isolated. SDS sample buffer was added to the thylakoid preparations and these were boiled for two minutes prior to electrophoresis. SDS-PAGE analysis was carried out as described in the legend to Figure 3.50. The resolved thylakoid proteins were blotted electrophoretically onto a nitrocellulose filter, and the filter probed with the RC I antiserum. Bound antibody was detected using the biotin-streptavidin peroxidase system (Section 2.15d(11)).

(334)

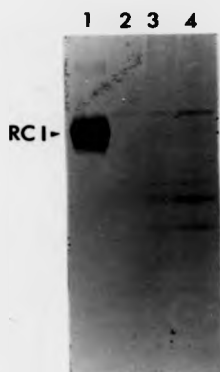


**Figure 3.53**



**Figure 3.54**

and the RC I polypeptides show up as a large smear. This track once again demonstrates the specificity of the antibody. Tracks 2, 3 and 4 are identical to tracks 2, 3 and 4 in Figure 3.50, and represent thylakoids isolated from the third nodes of plants exposed to 48 h continuous light, 64 h continuous light, and 48 h light followed by 16 h dark respectively. In these tracks the antibody recognises at least four discrete bands, one of which has an apparent molecular weight larger than that of the RC I proteins. No bands equivalent to the clear RC I band in track 1 can be seen in these thylakoid tracks.

The main difference between the material in track 1 and that in the other three tracks of Figure 3.53 is that the thylakoid material was washed in 80% (v/v) aqueous acetone prior to preparation for electrophoresis. This was done in order to extract chlorophyll which was then used to determine the appropriate track loadings. No such acetone extraction was carried out on the PS I material in track 1. The results of further experiments investigating this point show conclusively that the acetone extraction step is responsible for the disappearance of the RC I proteins, and the appearance of the four bands seen clearly in track 4 of Figure 3.53. This is the case regardless of whether the sample undergoing extraction is whole thylakoid material or purified PS I (results not shown). This observation,

together with the known specificity of the RC I antiserum, strongly suggests that the four bands observed in immunoblots after acetone extraction of the sample are derived from the RC I proteins, and are not the products of non-specific binding of the antibody.

In order to preserve the RC I polypeptides, the experimental procedure was modified to avoid acetone washing of thylakoid samples to be used for immunoblotting. Chlorophyll estimations were carried out on small aliquots of the thylakoid samples, and the remaining unextracted material was used for SDS-PAGE and blotting to nitrocellulose.

Figure 3.54 shows an immunoblot carried out using such untreated thylakoid material. The four tracks shown in this Figure are identical to those shown in Figures 3.50 and 3.52. Once again, thylakoid material representing approximately one third of a single third node was loaded onto each track. The nitrocellulose filter was probed with the RC I antiserum, and the antibody detected using the biotin-streptavidin detection system.

The first point to note about this immunoblot is that in the absence of the acetone wash, the RC I proteins are readily detectable in the thylakoid tracks. In addition, no other polypeptide bands were detectable using this antiserum. The RC I proteins are only barely detectable

in the purified PS I material contained in track 1. The reason for this poor detection is unclear but could be related to possible poor preservation of these proteins in this sample.

The second point to note about this immunoblot is that a comparison of tracks 2 and 4 shows quite clearly that there is more detectable RC I protein in the thylakoid at the end of the 16 h dark period than at the beginning. Clearly, unlike the polypeptides of the LHC I, the PS I reaction centre polypeptides continue to accumulate in the thylakoid membrane during the dark. The rate of accumulation in the dark does not seem to be quite as rapid as that in the light (track 3).

This result indicates that the PS I reaction centre and its associated peripheral light-harvesting antenna can behave independently of each other in terms of control of their assembly. This point will be more fully discussed in Section 4.3.

(v) Synthesis of LHC I apoproteins in the dark

Since the polypeptides of the LHC I, in common with those of the LHC II, fail to accumulate during the dark period, the question of the mechanism underlying this failure arises. As described above, the reason for the failure of accumulation of the LHC II has been shown to be protein instability in the dark. This, however, need not be the only means by which the observed pattern

of accumulation of the light-harvesting complexes could be achieved. There is no *a priori* reason to believe that the failure of LHC I accumulation in the dark is controlled in the same way as that of the LHC II, and not by some other mechanism such as suppression of LHC I gene transcription in the dark, or by light-dependent translation of the LHC I messages.

Any attempt to investigate the control of synthesis of the LHC I apoproteins is currently hampered by the lack of cloned nucleic acid probes with which to assay LHC I messenger RNA levels. For this reason, this study was restricted to examining LHC I protein synthesis at the post-translational stage.

Protein synthesis in light-treated and dark-treated seedlings may be conveniently followed by supplying the developing plants with a radio-labelled amino acid such as [<sup>35</sup>S]-labelled methionine. The labelled amino acid is taken up into the plant tissue via the transpiration stream, mixes with the pool of unlabelled amino acid in the plant cells, and is incorporated into protein during protein synthesis. In the case of the LHC I, a problem arises in the identification of the labelled apoproteins. As shown above, a simple separation of thylakoid proteins by SDS-PAGE is not sufficient to make an unambiguous identification of these polypeptides, and therefore a specific antibody must be used. Usually, the specific



antibody is utilised by immunoprecipitating the radio-labelled protein in question. Successful precipitation of the labelled polypeptide simultaneously confirms the identity of the protein and the fact that it is being actively synthesised.

The P2 antiserum was found to be extremely ineffective when used for immunoprecipitations from labelled thylakoid proteins, often yielding no labelled precipitate, or at best a non-specific mixture of labelled protein bands. For this reason, an alternative means of unambiguously identifying radio-labelled LHC I apoproteins among other similarly labelled thylakoid polypeptides was sought. Since definitive identification of the LHC I polypeptides requires the use of the P2 antibody, a means of identification incorporating immunoblotting was required.

The method finally developed is described in detail in Section 2.24 and Figure 2.3. The method relies upon a two-dimensional separation of the labelled thylakoid proteins, first by isoelectric focussing, then by SDS-PAGE, as described by Roscoe and Ellis (1982). This two-dimensional separation is used in order to minimise the possibility of mis-identifying any [ $^{35}$ S]-labelled LHC I polypeptides. Following this two-dimensional separation, the thylakoid proteins are blotted electrophoretically onto a nitrocellulose filter and this

filter is then autoradiographed to detect [ $^{35}$ S]-labelled polypeptides. The same filter is then probed with the P2 antiserum and the antibody detected using [ $^{125}$ I]-labelled protein A. The filter is then autoradiographed again, such that only the iodine label is detected (see Section 2.24). Comparison of the two autoradiographs will then show whether the LHC I polypeptides, detected immunologically, contain [ $^{35}$ S]methionine, and have thus been subject to active synthesis during the light treatment under study.

Etiolated pea seedlings which had been grown in the dark for seven days were subjected to either 64 h continuous illumination, or 48 h continuous illumination followed by 16 h darkness. Third nodes were then dissected from the plants and allowed to take up [ $^{35}$ S]-labelled methionine for a further 5 h in the light or the dark. Thylakoids were then isolated and subjected to two-dimensional electrophoresis, immunoblotting and double autoradiography as described in Section 2.24.

Figure 3.55 shows the results of this procedure carried out on the third nodes labelled for 5 h in the light following 64 h continuous illumination. Figure 3.55A represents the first autoradiograph showing the [ $^{35}$ S]-labelled thylakoid polypeptides synthesised during the period of exposure of the plants to the label. It can be seen that a number of the labelled proteins have

**Figure 3.55** Immunodetection of LHC I polypeptides among thylakoid proteins labelled with [ $^{35}$ S]methionine in the light. Etiolated pea seedlings were exposed to continuous light for 64 h. Ten third nodes were dissected out and left to take up [ $^{35}$ S]methionine for 5-6 h in the light. The nodes were harvested, thylakoids isolated and subjected to 2-dimensional electrophoretic analysis by IEF in the first dimension and SDS-PAGE in the second dimension. Resolved proteins were electrophoretically blotted onto a nitrocellulose filter and the dried filter autoradiographed. The filter was then incubated with P2 antiserum followed by [ $^{125}$ I]-labelled protein A. After drying, the filter was re-autoradiographed to visualise the immunologically detected LHC I apoproteins. For a full description of this method see Section 2.24 and Figure 2.3.

(A) First autoradiograph of the nitrocellulose filter showing the thylakoid polypeptides labelled with [ $^{35}$ S]methionine in the light.

LHCP The 26 kDa apoprotein of the LHC II. P1, P2 and P3 are the apoproteins of the LHC I.

Polypeptides labelled a and b are the  $\alpha$  and  $\beta$  subunits of the ATP synthase respectively.

(B) Second autoradiograph of the nitrocellulose filter showing the positions of the LHC I apoproteins detected using the P2 antiserum. To the right is a marker track containing purified PS I prepared by the method of Mullet *et al* (1980a).

**Figure 3.55****(A)****(B)**

focused to discrete spots while others appear as narrow smears of varying length. As expected for plants at this stage of development, the LHCP is very prominent among the radio-labelled proteins (see Figure 3.50, track 3), and appears as a smear spread through the upper two thirds of the first dimension IEF gel. This tendency to streak has been attributed to the poor solubility of this polypeptide resulting from its hydrophobic nature (Roscoe and Ellis, 1982).

The  $\alpha$  and  $\beta$  subunits of the ATP synthase (labelled a and b in Figure 3.55A), are also quite heavily labelled indicating that they too are being actively synthesised under the conditions defined above. These polypeptides, however, focus well in the IEF dimension, forming relatively discrete spots on the autoradiograph.

Figure 3.55B represents the second autoradiograph of the same filter, this time showing the positions of the LHC I polypeptides as revealed by the P2 antiserum. At the right can be seen the three LHC I polypeptides in a PS I marker track, thus confirming the specificity of the antibody. Unlike the LHCP, the LHC I apoproteins are resolved almost as discrete spots with a little smearing. Comparison of this Figure with Figure 3.55A clearly reveals that the LHC I polypeptides, and especially P3, are labelled with [ $^{35}$ S]methionine, indicating that they are actively synthesised in this third node tissue while

the plants are under continuous illumination. This result agrees with the pattern of accumulation of these proteins revealed in Figure 3.52.

Figure 3.56A represents the autoradiograph of the nitrocellulose filter containing the [ $^{35}$ S]-labelled thylakoid proteins derived from the plants subjected to 48 h continuous illumination followed by 16 h darkness. The radiolabel was administered to dissected third nodes in complete darkness, and all radio-labelled proteins seen in this figure are therefore the products of protein synthesis carried out in the dark.

A comparison of Figures 3.55A and 3.56A shows that proteins derived from the dark-treated thylakoids seem less able to focus in the IEF dimension than their light-treated counterparts, preferring to form streaks rather than spots in the second dimension. This phenomenon was observed in every experiment carried out using this protocol, but the reason for this behaviour is unknown.

Examination of Figure 3.56A shows that many of the thylakoid polypeptides continue to be synthesised, even after 16-21 h in the dark. The  $\alpha$  and  $\beta$  subunits of the ATP synthase continue to be heavily labelled under these conditions, a result expected from the fact that they continue to accumulate in the thylakoid in the dark (see Figures 3.50 and 3.51). Similarly, the LHCP also

**Figure 3.56**

Immunodetection of LHC I polypeptides among thylakoid proteins labelled with [ $^{35}$ S]methionine in the dark. Etiolated pea seedlings were exposed to continuous light for 48 h followed by 16 h darkness. Twenty third nodes were dissected out and left to take up [ $^{35}$ S]methionine for 5-6 h in the dark. The nodes were harvested in the dark, thylakoids isolated and subjected to 2-dimensional electrophoretic analysis by IEF in the first dimension and SDS-PAGE in the second dimension. Resolved proteins were electrophoretically blotted onto a nitrocellulose filter and the dried filter autoradiographed. The filter was then incubated with P2 antiserum followed by [ $^{125}$ I]-labelled protein A. After drying, the filter was re-autoradiographed to visualise the immunologically detected LHC I apoproteins. For a full description of this method see Section 2.24 and Figure 2.3.

(A) First autoradiograph of the nitrocellulose filter showing the thylakoid polypeptides labelled with [ $^{35}$ S]methionine in the dark.

LHCP The 26 kDa apoprotein of the LHC II. P1, P2 and P3 are the apoproteins of the LHC I.

Polypeptides labelled a and b are the  $\alpha$  and  $\beta$  subunits of the ATP synthase respectively.

(B) Second autoradiograph of the nitrocellulose filter showing the positions of the LHC I apoproteins detected using the P2 antiserum. To the left is a marker track containing purified P3 I prepared by the method of Mullet *et al* (1980a).

**Figure 3.56****(A)****(B)**



continues to be synthesised. This polypeptide, however, does not accumulate in the dark, and so must be subject to turnover.

Figure 3.56B shows the second autoradiograph of the same filter after probing with the P2 antiserum followed by iodinated protein A. On the left of the filter is the track containing the PS I material, and it can be seen that only the LHC I polypeptides are recognised by the antibody. The streaks and spots on this filter reveal the positions of the LHC I polypeptides on the two-dimensional gel. The two proteins P1 and P2 are not well resolved, and seem to form a long streak containing two quite well-defined spots. This pattern is a little different from that found with the light-treated material (see Figure 3.55B), and is probably an expression of the same lack of resolution in the IEF dimension which seems to characterise the dark-treated thylakoids.

Comparison of the autoradiographs featured in Figures 3.56A and 3.56B shows that the LHC I polypeptides are labelled with [ $^{35}$ S]methionine. Since the label was applied to the plants in the dark, and the plants had already been in darkness for 16 h prior to the application of the label, it is clear that the LHC I apoproteins continue to be synthesised in the absence of light.

This result, combined with the demonstrable failure

of the LHC I polypeptides to accumulate in the dark (Figure 3.52), points to the conclusion that these polypeptides are subject to turnover in the absence of light. In addition, the fact that the [<sup>35</sup>S]-labelled LHC I polypeptides co-purify with the thylakoid membranes indicates that in the dark, the LHC I proteins are not only synthesised, but bind to or are inserted into the thylakoid lipid bilayer, and are subsequently turned over.

The results shown in this Section demonstrate that in the developing systems under study, the polypeptides of the peripheral chlorophyll *a/b*-binding light-harvesting antennae of PS I and PS II display a remarkable similarity in the post-translational control of their assembly in the thylakoid membrane. In the actively-greening leaf tissue used in this study, this control is exercised in the form of polypeptide turnover in the absence of light. This seems to occur at the point at which the light-harvesting polypeptides are inserted into the lipid bilayer. The enzyme species responsible for this turnover have not been characterised, and neither is it yet known whether the same enzymes are responsible for the destruction of both the LHC I and LHC II polypeptides.

Intermittent illumination of pea seedlings, where the

light 'flash' in each cycle is of very limited duration compared to the intervening dark periods, induces abnormal development of the thylakoid membrane. This abnormal development is characterised by a specific inhibition of the assembly of the peripheral chlorophyll *a/b*-binding light-harvesting complexes of PS I and PS II, while the reaction centre complexes assemble normally to produce a photosynthetically-competent membrane. The failure of assembly of the LHC II under intermittent illumination is known to be due to polypeptide turnover in the dark periods between flashes (Cuming and Bennett, 1981). On the basis of the evidence presented here, it is highly likely that the same form of control applies to the assembly of the LHC I under these light conditions.

Evidence from studies involving intermittent illumination, and from the data presented in this Section for PS I (Figures 3.52 and 3.54), clearly demonstrates that assembly of the peripheral light-harvesting systems is not strictly coordinated with that of their corresponding reaction centre complexes. This apparent lack of coordination, together with the other points mentioned above, will be discussed in Part 4 of this thesis.

**PART 4**  
**GENERAL DISCUSSION**

#### [4.1] Isolation of PS I-Containing Chlorophyll-Protein Complexes

In Section 3.1 three methods for isolating sub-thylakoid fractions highly enriched for the PS I reaction centre and light-harvesting complexes were characterised. One of these methods was slightly modified from the protocol already published by Mullet *et al* (1980a). The other two methods deviated from this protocol in only relatively minor ways but resulted in major modifications in one or more of the characteristics of the sub-thylakoid fractions produced.

Both the 'high salt' and Tris-HCl methods produce PS I-containing fractions whose sedimentation behaviour is similar to that of intact membranes, in that both these preparations can be pelleted at 30,000xg, while the PS I preparation of Mullet *et al* (1980a) requires overnight sucrose density gradient centrifugation at 100,000xg. In particular, the Tris-HCl preparations show a distinct quasi-membranous morphology due mainly to the presence of crystalline arrays of LHC II.

The only difference between the standard PS I preparation method (the method of Mullet *et al*, 1980a) and the 'high salt' method is the step involving the washing of the thylakoids with buffer containing 0.8M

NaCl. The electron micrographs shown in Figures 3.16, 3.17 and 3.18 demonstrate that this salt wash results in a change in the morphology of the membrane from balloon-like vesicles to sheets, but with no obvious change in the internal structure of the membrane. This change in gross morphology is undoubtedly a result of osmotic collapse of the membrane vesicles, and is accompanied by a decrease in the size of the membrane pellet and an increase in the difficulty with which the pellet is resuspended (see Section 3.1b).

Since the subsequent washes with the Tris-glycine buffer restore the original properties of the membrane pellet, it is likely that the membranes resume their vesicular appearance prior to solubilisation. If this is the case, then the salt-induced change in the gross morphology of the membrane cannot be responsible for the altered behaviour of the PS I fraction after solubilisation.

In the absence of any plausible alternative explanation, it must be assumed that the salt wash has some direct and specific effect on the PS I particles themselves. The nature of this effect can only be guessed at, but may involve some form of interaction with charged groups on the surface of the PS I complexes.

Electron microscopy sheds more light upon the interactions resulting in the production of the Tris-HCl

material. This preparation method differs from that of Mullet *et al* (1980a) only with respect to the buffer present during the solubilisation of the thylakoid membrane with Triton X-100. Here, Tris-HCl is used instead of Tris-glycine. Like the PS I fraction produced by the 'high salt' method, the Tris-HCl preparation also sediments at 30,000g.

The electron micrographs shown in Figures 3.22 and 3.23 demonstrate that the LHC II component in the Tris-HCl preparation exists as extensive crystalline arrays of particles. These particle arrays are very similar in form to those reported by Kuhlbrandt *et al* (1983). These authors produced membrane crystals of aggregated LHC II particles from pea by precipitating the detergent-solubilised complex with monovalent and divalent cations in the presence of low concentrations of Triton X-100. Such membrane crystals are composed of regular arrays of LHC II particles organised into repeating units showing a threefold symmetry.

It has been assumed that the cation-induced formation of crystalline sheets of LHC II *in vitro* is analogous to the process of cation-induced grana formation (Kuhlbrandt *et al* (1983). Cation-induced grana formation can be inhibited by the removal of the N-terminal surface-exposed fragment of the LHC II by trypsin (see Section 1.7a). Trypsin modification of the LHC II also inhibits

the cation-induced aggregation of proteoliposomes into which the modified LHC II has been incorporated. No such inhibition is seen, however, when trypsin-modified LHC II is released from thylakoid membranes by detergent solubilisation and precipitated from the resulting solution by the addition of  $MgCl_2$ . These observations show that the N-terminal fragment of the LHCP is not required for the cation-induced formation of LHC II membrane crystals *in vitro*. This fragment only appears to be necessary when the LHC II is present in a lipid bilayer-like environment. Thus, cation-induced grana formation and cation-induced LHC II membrane crystal formation are not equivalent processes.

The production of the Tris-HCl material is also insensitive to trypsin modification of the LHC II (results not shown). Thus, the mechanism underlying the formation of the LHC II crystalline arrays shown in Figures 3.22 and 3.23 is not related to the mechanism of membrane stacking. In addition, since cations such as  $Mg^{2+}$  are absent from the solubilisation buffer, it is likely that the mechanism responsible for the formation of the Tris-HCl pellet differs from that underlying the precipitation of LHC II membrane crystals. Further work is therefore required if the agent responsible for the formation of the Tris-HCl pellet is to be identified.

Another puzzling feature of the Tris-HCl preparation



is the fact that it contains only two of the thylakoid protein complexes, the LHC II and the PS I complex. This specificity is difficult to explain. The experimental evidence described in Section 3.1c suggests that a functional association exists between these two components. It is highly unlikely, however, that the large amounts of LHC II shown in Figures 3.22 and 3.23 are associated with PS I *in vivo*, since no published electron micrographs have shown a similar distribution of particles in the thylakoid membrane. It is more likely that the massive association of these two complexes observed in the Tris-HCl pellet is an artefact of the isolation procedure. If this is the case, then the question remains as to whether the transfer of excitation energy from LHC II to PS I observed in this preparation occurs *in vivo*.

Evidence for a functional association of the LHC II with PS I reaction centres has been reported in maize (Bassi, 1985) and in barley (Bassi and Simpson, 1987). These authors report the presence of two LHC I complexes in these species. One of these, designated LHCI-730, has a 77 K fluorescence maximum at 730 nm and a chlorophyll *a/b* ratio of 3.0. A second complex, designated LHCI-680, displays a 77 K fluorescence maximum at 680 nm and a chlorophyll *a/b* ratio similar to that of LHCI-730.

Bassi and Simpson (1987) report the preparation of

PS I particles from Triton X-100-solubilised barley thylakoids which display a chlorophyll *a/b* ratio of 3.5. These preparations have approximately one third of their chlorophyll molecules associated with LHC II chlorophyll proteins, but no RC II chlorophyll proteins are present. Addition of low concentrations of octyl glucoside to these PS I preparations induces a large increase in LHC II fluorescence with a corresponding decrease in PS I fluorescence. Further reconstitution studies have led these authors to present a model for energy transfer within the PS I pigment bed where LHC II is capable of passing excitation energy to P-700 via LHCI-680 and LHCI-730. In this model, LHCI-680 acts as a connecting antenna between LHC II and PS I. Such a model is consistent with the hypothesis that phosphorylated forms of the LHC II may pass excitation energy to the PS I reaction centre, thereby bringing about a redistribution of absorbed excitation energy between the photosystems (see Section 1.7a).

Bassi (1985) has presented 77 K fluorescence emission data concerning maize bundle sheath thylakoids in which the RC I, LHC I and LHC II chlorophyll-protein complexes are present, but in which the RC II chlorophyll-proteins are absent. In this system, the 77 K fluorescence emission spectrum displays a single peak at about 730 nm due to fluorescence from the PS I pigment bed. Treatment

of these thylakoids with increasing concentrations of octylglucoside causes a decrease in the PS I fluorescence emission peak and a corresponding increase in a peak at 680 nm. This is interpreted as representing a detergent-induced detachment of LHC II from the PS I pigments.

The factors promoting the possible functional association of phosphorylated LHC II with PS I are at present unknown. According to current ideas, the lateral migration of the LHC II from appressed to unappressed membrane regions is governed by the specific interactions of charged groups residing on the external surface of the thylakoid with cations in the stroma (see Section 1.7a). This model, however, does not attempt to address the specific problem of energy transfer between different photosystem pigment beds. This transfer could come about through random contact between LHC II and PS I complexes, or by a directed coupling of the two pigment systems. At the present time it is not possible to distinguish between these two possibilities.

#### (4.2) Structural Relationships of Chlorophyll-Protein Complexes

As stated in Section 1.8, one of the aims of the present research was to investigate the structural relationships between the apoproteins of the LHC I, and also to investigate any possible similarities between the

LHC I chlorophyll-proteins and those of other chlorophyll-binding complexes, particularly those of the LHC II.

The main approach adopted in this study involved raising monoclonal and monospecific polyclonal antibodies to the LHC I apoproteins, and then testing for cross-reaction with other chlorophyll-binding polypeptides. Immunological cross-reactivity between proteins could then be taken as evidence for structural similarity.

It is important here to be clear about the meaning of structural similarity when judged immunologically. Proteins may display similarity of structure at several levels. If antibodies are raised against a non-denatured protein, the immunological determinants will generally reside on the outer surface of the protein and will depend largely upon the tertiary structure of the protein. In this case the population of antibodies raised against the protein may only recognise a limited number of sites along the polypeptide chain (Sass *et al*, 1985)

Where a protein has been denatured by treatment with SDS and reducing agents, the polypeptide chain is largely unfolded and internal immunogenic sites may now be exposed. In this case, the immunogenicity of the protein will depend upon the nature of the amino acid residues present.

In both cases it can be argued that immunological

cross-reactivity between proteins reflects structural similarity. In the former case, however, similarities in tertiary structure need not be due to similarities in amino acid sequence. Thus, immunological similarities between non-denatured polypeptides may not represent homologues in the corresponding gene nucleotide sequences. Where antibodies are raised against denatured proteins, immunological similarities are a better, although by no means complete, indicator of genetic similarities.

The LHC I antibodies prepared in this study were raised against SDS-denatured polypeptides. The polyclonal antibodies showed no cross-reaction with the polypeptides of any other chlorophyll-binding complexes except those of the LHC II. The results described in Section 3.2b indicate that the cross-reaction with the LHC II polypeptides is due to contamination of the original LHC I antigens with breakdown products of the LHCP. Lam *et al* (1984b), using antibodies raised against purified LHCP, found no cross-reaction with LHC I apoproteins in spinach. Evans and Anderson (1986), however, also working with spinach, have found that antibodies raised against three individual LHC I apoproteins cross-react not only with other LHC I polypeptides but also with the LHC II apoproteins.

In an attempt to determine whether the cross-

reactivity with the LHC II polypeptides reflects real immunological similarity in this species, Evans and Anderson (1986) affinity-purified the cross-reactive LHC I antibodies on either 'native' LHC II or on the 28 kDa apoprotein of the LHC II immobilised on a nitrocellulose filter. It was found that the affinity purified antibodies showed almost the same patterns of cross-reactivity as the crude sera. This was taken as evidence that the cross-reactivities reflected real immunological similarity between the LHC I and LHC II apoproteins.

The assay used to determine the cross-reactivities of the affinity-purified antibodies, however, took the form of an immunoblot, where the purified antibodies were each blotted against thylakoids, a PS I preparation and purified LHC II. The results obtained would be expected if proteolytic breakdown products of the LHC II were migrating closely with the LHC I apoproteins in the gel from which the proteins were blotted. Antibody affinity-purified on a possible contaminant will not distinguish between the antigen and the contaminating species where these cannot be adequately separated.

White and Green (1987) report that antibodies raised against purified CP Ia (see Section 1.7b) show cross-reaction with both the LHC II and CP29. This cross-reaction appears to be due to the antibodies raised

against the LHC I component of CP Ia. Affinity purification of the cross-reacting antibodies on highly purified CP Ia results in an antibody population which displays the same relative affinities for PS I and PS II antenna polypeptides as the unpurified antiserum. Once again, these results could be explained by contamination.

More evidence concerning the possible immunological relatedness of the PS I and PS II antenna chlorophyll proteins has been presented by Darr *et al* (1986). These authors have created a number of monoclonal hybridoma lines which secrete monoclonal antibodies raised against the polypeptides of the LHC II in pea. The specificities of these monoclonal antibodies have been examined by immunoblotting against thylakoids, PS I preparations and purified LHC II. Two classes of monoclonal antibody display some reaction with polypeptides showing similar relative mobilities to polypeptides of the LHC I on SDS-PAGE. Once again, these results could be explained by the presence of LMCP breakdown products in the 20 kDa-24 kDa molecular mass range on the blotted gels. The present author is in possession of these monoclonal antibodies, and their cross-reaction with LHC I polypeptides can now be tested using the 'clean' PS I preparation described in Section 3.2b. This work is in progress.

Although the immunological cross-reactivities

reported in this thesis are consistent with contamination, it is possible that the immunological similarities between the LHC I and LHC II apoproteins reported by the various authors cited above reflect real structural similarities. Darr et al (1986) have argued that the conflicting results of the various groups working on this problem may be due to the fact that the antigenic determinants common to the light-harvesting proteins may be only weakly immunogenic. Thus, polyclonal antibodies would contain at best, <sup>only</sup> a small proportion of immunoglobulins capable of recognising these determinants. This reasoning suggests that any structural similarities between these polypeptides are likely to be limited. The problem of the structural relationships of the various light-harvesting chlorophyll-proteins will only be resolved when full nucleotide sequences are available for the genes encoding the LHC I apoproteins.

#### [4.3] Regulation of Assembly of Photosystem I and Control of the Biogenesis of the Photosynthetic Membrane

The PS I complex, like the other protein-complexes present in the thylakoid, is a product of both nuclear and plastid genes. Current information concerning the sites of synthesis of the polypeptide constituents of both photosystems indicates that the proteins of the core complexes are plastid-encoded while those of the



peripheral antennae are encoded in the nucleus. The evolutionary significance of this arrangement, assuming that there is one, remains the subject of speculation.

It has become clear that the assembly of the core and peripheral complexes of the photosystems are not tightly coordinated. A clue to this can be found in the fact that intermittently-illuminated plants can assemble a functional non-cyclic electron transport chain in their developing thylakoids while being devoid of any peripheral light-harvesting complexes. In the case of the PS I complex, the work reported in this thesis involving the use of specific antibodies has demonstrated that in developing pea thylakoids, the PS I reaction centre can continue to accumulate in the dark independently of its associated peripheral light-harvesting system.

During the course of this study, Akoyunoglou and Akoyunoglou (1985) reported that when greening leaves of *Phaseolus vulgaris* L. are placed in the dark, a reorganisation of the PS I pigment bed occurs. This reorganisation is accompanied by a loss of thylakoid polypeptides in the molecular mass range 21 kDa-24 kDa, which these authors attribute to the LHC I, and an increase in the 69 kDa P-700-binding protein of the PS I reaction centre. These authors further demonstrate that the 21 kDa-24 kDa polypeptides are synthesised during the dark treatment, implying that these polypeptides are

subject to turnover in the dark.

Although no LHC I-specific antibodies were used to identify the LHC I apoproteins as in the present study, Akoyunoglou and Akoyunoglou (1985) demonstrated that the loss of the 21 kDa-24 kDa polypeptides in the dark is accompanied by an increase in the light intensity required for the saturation of PS I photochemical activity. This increase in saturation light intensity implies a decrease in the PS I antenna size during the dark period.

The synthesis of chlorophyll in flowering plants requires light for the photoreduction of protochlorophyllide to chlorophyllide (Castelfranco, 1983). The continued accumulation of the PS I reaction centre proteins in the thylakoids of dark-treated plants is therefore puzzling, since in the absence of chlorophyll synthesis, no assembly of the reaction centre complex should be possible.

The increase in the amount of RC I protein in the thylakoid may not, however, reflect an increase in the amount of PS I reaction centre chlorophyll-protein complex, but may simply be an accumulation of the apoprotein without associated pigment. Akoyunoglou and Akoyunoglou (1985), working with bean, have reported that an increase in the level of the 69 kDa polypeptide in the dark is accompanied by an increase in the maximum rate of

PS I-mediated electron transport. This suggests that although PS I peripheral antenna is being lost in the dark, photochemically active reaction centre complex is accumulating.

These authors observe no loss of chlorophyll *a* in the dark, but a rapid loss of chlorophyll *b*. This result is at variance with that reported in Section 3.7b(1) of this thesis and by Bennett (1981), where loss of chlorophyll *a* also takes place in the dark. Akoyunoglou and Akoyunoglou (1985) suggest that the chlorophyll *a* released by the turnover of the LHC I in the dark is utilised for the assembly of new PS I reaction centres. Chlorophyll *b* released in this way is presumably destroyed.

Since the LHC I polypeptides continue to be synthesised in the dark, then the idea that chlorophyll *a* can be recycled between antenna and core complexes implies that the 60 kDa-70 kDa PS I reaction centre apoproteins have a greater affinity for chlorophyll *a* than their corresponding light-harvesting polypeptides. It is possible that this difference in affinity is more apparent than real since the continual destruction of the LHC I apoproteins and the relative stability of the reaction centre proteins in the dark would cause the PS I reaction centre apoproteins to act as a sink for chlorophyll *a*. The same arguments may be applied to the PS II light-harvesting and reaction centre complexes (see

Argyroudi-Akoyunoglou *et al.*, 1982).

The advantage to the plant of the turnover of the peripheral light-harvesting complexes in the dark is not immediately clear. Synthesis of LHC I polypeptides on cytoplasmic ribosomes and their import into the chloroplast are energy-requiring processes. This investment of energy is wasted if these proteins are destroyed without carrying out their function. An interesting feature of this system is that it only seems to apply in developing thylakoids. Where thylakoids have achieved full development, the chlorophyll-protein complexes appear to be stable (Akoyunoglou and Akoyunoglou, 1985).

The idea that in the dark, the reaction centre complexes accumulate at the expense of the peripheral light-harvesting complexes, suggests that in developing leaves, the primary need is for the assembly of photochemically active reaction centres. The number of reaction centres and the overall organisation of the fully developed thylakoid will depend heavily upon the ability of the developing leaf cell to synthesise and assemble new reaction centre complexes in the dark. In this sense, the destruction of peripheral light-harvesting complexes in the dark may represent a means of overcoming the inherent disadvantage of the inability to synthesise chlorophyll in the dark.

There now exists a large body of literature concerning the various ways in which light can regulate the development of the photosynthetic membrane. Light may act at the level of transcription by initiating or modulating the expression of the gene encoding a given thylakoid protein component (Gallagher and Ellis, 1982; Gallagher *et al.*, 1985). In addition, there is now ample evidence that the synthesis of a number of plastid-encoded thylakoid proteins, including the P-700-binding reaction centre proteins of PS I, can be regulated at the point of translation (Kreuz *et al.*, 1986; Klein and Mullet, 1986). Here, light induces the translation of mRNA species which are already present in the etioplasts of dark-grown plants. Finally, post-translational controls of the kind already discussed enable light (or the lack of it) to exert a fine control at the point of assembly of the various thylakoid protein complexes.

All of these controls allow the plant to coordinate the synthesis of thylakoid proteins and their associated pigments. The final product of these multiple levels of coordination must be a membrane system which is capable of trapping and transducing available light energy with maximum efficiency.

It might be expected therefore that the detailed composition of the thylakoid membrane will largely be determined by the external environment. This has been

shown to be the case in a number of studies where developing plants have been grown under varying conditions of light quantity and quality (Leong and Anderson, 1983; Leong and Anderson, 1984; Leong *et al.*, 1985). Such studies have demonstrated that photosystem antenna size, the stoichiometry of the two photosystem reaction centres and the relative concentrations of the intersystem carriers, can all be regulated by the light regime in which the plants develop.

A good example of this regulation is found in the relative amounts of the PS II reaction centre and LHC II found in pea plants grown under different light intensities (Leong and Anderson, 1983). Under low light, a high proportion of the PS II-associated chlorophyll is found in the LHC II, but as light intensities approach that of full sunlight the proportion of reaction centre-associated pigment increases. These changes in the size of the photosynthetic unit no doubt reflect adaptive responses aimed at optimising the light-trapping efficiency of the thylakoid. The mechanisms by which the final concentrations of the various components of the photosynthetic electron transport chain are linked to external environmental factors is still far from being understood.

There is a great tendency in this post-Darwinian age to view molecular-biological phenomena in terms of their

adaptive value. This attitude is often taken to extremes at the expense of the wider view of the whole organism as the unit of selection. It is tempting to view the complex system of photoregulatory controls acting on the synthesis of the components of the thylakoid as having an obscure adaptive significance which will become plain as our understanding of plant molecular biology increases. It may be useful to remember that a living organism is the product of many millions of years of adaptive change, and as such represents at best a compromise between what is desirable and what is possible. An organism survives not because it is perfect but because it works.

On the basis of this argument one might expect to see the rather bewildering variety of structures and systems of regulation and control that is now emerging at the molecular level. As Sydney Brenner has said, "anything that is produced by evolution is bound to be a bit of a mess" (in Lewin, 1984).

BIBLIOGRAPHY

Akerlund, H-E. (1983) In *The Oxygen Evolving System of Photosynthesis* (eds. Inoue, Y., Crofts, A.R., Govindjee, Murata, M., Renger, G. and Satoh, K.) 201-208. Academic Press, New York.

Akoyunoglou, A. and Akoyunoglou, G. (1985) *Plant Physiol.* 79 425-431.

Allen, J.F., Bennett, J., Steinback, K.E. and Arntzen, C.J. (1981) *Nature* 291 21-25.

Allred, D.R. and Staehelin, L.A. (1985) *Plant Physiol.* 78 199-202.

Alt, J., Morris, J., Westhoff, P. and Hermann, R.G. (1984) *Curr. Genet.* 8 597-606.

Anderson, J.M. (1981) *FEBS Let.* 124 1-9.

Anderson, J.M. (1982) *Mol. Cell. Biochem.* 46 161-172.



Anderson, J.M. and Walkin, R. (1982) FEBS Lett. 148  
293-296.

Anderson, J.M., Waldron, J.C. and Thorne, S.W. (1978)  
FEBS Lett. 22 227-233.

Andersson, B. (1986) in *Encyclopedia of Plant Physiology*,  
Vol. 19. *Photosynthesis III: Photosynthetic membranes and*  
*light-harvesting systems* (eds. Staehelin, L.A. and

Arntzen, C.J.) 447-456. Springer-Verlag, Berlin/  
Heidelberg.

Andersson, B. and Anderson, J.M. (1980) Biochim. Biophys.  
Acta 523 426-439.

Andersson, B. and Anderson, J.M. (1985) in *Modern Methods*  
*of Plant Analysis New Series Vol.1, Cell Components*,  
(eds. Linskens, H.F. and Jackson, J.F.) 231-258.  
Springer-Verlag, Berlin/Heidelberg.

Andersson, B., Anderson, J.M. and Ryrie, I.J. (1982) Eur.  
J. Biochem. 123 465-472.

Apel, K. and Kloppstech, K. (1978) Eur. J. Biochem. 85  
581-588.

Argyroudi-Akoyunoglou, J.H. (1984) *FEBS Lett.* 171 47-53.

Argyroudi-Akoyunoglou, J.H., Akoyunoglou, A., Kalosakas, K. and Akoyunoglou, G. (1982) *Plant Physiol.* 70 1242-1248.

Armond, P.A., Arntzen, C.J., Briantais, J.-M. and Vernotte, C. (1976) *Arch. Biochem. Biophys.* 175 54-63.

Armond, P.A., Staehelin, L.A. and Arntzen, C.J. (1977) *J. Cell Biol.* 73 400-418.

Arnon, D.I. (1949) *Plant Physiol.* 24 1-15.

Arntzen, C.J. (1978) in *Current Topics in Bioenergetics* vol 8, (eds. Sanadi D.R. and Vernon, L.P.) 111-160. Academic Press, New York.

Arntzen, C.J. and Briantais, J.M. (1975) in *Bioenergetics of Photosynthesis* (ed. Govindjee) 52-113. Academic Press, New York.

Arntzen, C.J. and Pakrasi, H.B. (1986) in *Encyclopedia of Plant Physiology, Vol. 19. Photosynthesis III: Photosynthetic membranes and light-harvesting systems* (eds. Staehelin, L.A. and Arntzen, C.J.) 457-467. Springer-Verlag, Berlin/ Heidelberg.

Aviv, H. and Leder, P. (1972) *Proc. Natl. Acad. Sci. U.S.A.* 69 1408-1412.

Barber, J. (1976) in *The Intact Chloroplast* (ed Barber, J.) 89-134. Elsevier/North Holland, New York.

Barber, J. (1980) *FEBS Lett.* 118 1-10.

Barber, J. (1983a) *Photobiochen. Photobiophys.* 5 181-190.

Barber, J. (1983b) *Plant Cell and Environment* 6 311-322.

Barber, J. (1985) *Nature* 315 278-279.

Barber, J. (1986) in *Proceedings of the A.P.R.C. Meeting on Photosynthesis, Aberystwyth* (ed Chapman, D.), Agricultural and Food Research Council, London.

Bassi, R. (1985) *Carlsberg Res. Commun.* 50 127-143.

Bassi, R. and Simpson, D. (1987) Eur. J. Biochem. 163  
221-230.

Bengis, C. and Nelson, N. (1975) J. Biol. Chem. 250  
2783-2788.

Bengis, C. and Nelson, N. (1977) J. Biol. Chem. 252  
4564-4569.

Bennett, J. (1977) Nature 269 344-346.

Bennett, J. (1979) Eur. J. Biochem. 92 133-137.

Bennett, J. (1980) Eur. J. Biochem. 104 85-89.

Bennett, J. (1981) Eur. J. Biochem. 118 61-70.

Bennett, J. (1983) Biochem. J. 212 1-13.

Bennett, J., Jenkins, G.I. and Hartley, M.R. (1984) J.  
Cell Biochem. 25 1-13.

Bennett, J., Steinback, K.E. and Arntzen, C.J. (1980)  
Proc. Natl. Acad. Sci. U.S.A. 77 5253-5257.

Blair, G.E. and Ellis, R.J. (1973) *Biochim. Biophys. Acta* 312 223-234.

Boardman, W.K., Anderson, J.M. and Goodchild, D.J. (1978) in *Current Topics in Bioenergetics* vol 8, (eds. Sanadi D.R. and Vernon, L.P.) 35-109. Academic Press, New York.

Bonaventura, C. and Myers, J. (1969) *Biochim. Biophys. Acta* 189 366-383.

Bonnerjee, J., Ortiz, W. and Malkin, R. (1985) *Arch. Biochem. Biophys.* 240 15-20.

Boulter, D., Ellis, R.J. and Yarwood, A. (1972) *Biol. Rev.* 47 113-175.

Bramhall, S. Noack,, N. Wu, M. and Loewenberg, J.R. (1969) *Anal. Biochem.* 31 146-148.

Branton, D., Bullivant, S., Gilula, M.B., Karnovsky, M.J., Moor, H., Nishlethaler, K., Northcote, D.H., Packer, L., Satir, B., Speth, V., Staehelin, L.A., Steere, R.L. and Weinstein, R.S. (1975) *Science* 190 54-56.

Bredenkamp, G.J. and Baker, N.R. (1986) in *Proceedings of the A.F.R.C. Meeting on Photosynthesis, Aberystwyth* (ed Chapman, D.), Agricultural and Food Research Council, London.

Brogie, R., Bellemare, G., Bartlett, S.G., Chua, N-H. and Cashmore, A.R. (1981) *Proc. Natl. Acad. Sci.* 78 7304-7308.

Burke, J., Ditto, C.L. and Arntzen, C.J. (1978) *Arch. Biochem. Biophys.* 187, 252-263.

Cann, E. and Green, B.R. (1980) *Plant Physiol.* 66 428-432.

Castelfranco, P.A. (1983) *Ann. Rev. Plant Physiol.* 34 241-278.

Chang, C-H., Tiede, D., Tang, J., Smith, U., Norris, J. and Schiffer, M. (1986) *FEBS Lett.* 205 82-86.

Chow, W.S., Ford, R.C. and Barber, J. (1981) *Biochim. Biophys. Acta* 635 317-326.

Chua, N-H., Matlin, K. and Bennoun, P. (1975) *J. Cell Biol.* 67 361-377.

Chuba, P.J. and Palchaudhury, S. (1986) *Anal. Biochem.* 156 136-139.

Clark, R.D., Hawkesford, S.J., Bennett, J. and Hind, G. (1984) *FEBS Lett.* 174 137-142.

Clayton, R.K. (1980) *Photosynthesis: physical mechanisms and chemical patterns*. Cambridge University Press, Cambridge.

Cleveland, D.W., Fischer, S.G., Kirschner, M.W. and Laemmli, U.K. (1976) *J. Biol. Chem.* 252 1102-1106.

Coruzzi, G., Broglie, A., Cashmore, A. and Chua, N-H. (1983) *J. Biol. Chem.* 258 1399-1402.

Cox, R.P. and Andersson, B. (1981) *Biochem. Biophys. Res. Commun.* 103 1336-1342.

Cramer, W.A., Widger, W.R., Merymann, R.G. and Trebst, A. (1985) *Trends Biochem. Sci.* 10 125-129.

Cuming, A.C., and Bennett, J. (1981) *Eur. J. Biochem.* 118 71-80.

Cusling, A.C., Williams, R.S. and Cullimore, J.V. (1986)  
In *Society for Experimental Biology Seminar Series 29:*  
*Immunology in Plant Science* (ed. Wang, T.L.) 137-154.  
Cambridge University Press.

Darr, S.C., Somerville, S.C. and Arntzen, C.J. (1986) J.  
Cell Biol. 103 733-740.

Davis, D.J., Armond, P.A., Gross, E.L. and Arntzen, C.J.  
(1976) Arch. Biochem. Biophys. 175 64-70.

Deisenhofer, J., Epp, O., Miki, K., Huber, R. and Michel,  
H. (1984) J. Molec. Biol. 180 385-398.

Deisenhofer, J., Epp, O., Miki, K., Huber, R. and Michel,  
H. (1985) Nature 318 618-624.

Delepelaire, P. and Chua, N-H. (1981) J. Biol. Chem. 256  
9300-9397.

Douce, R. (1974) Science 183 852-853.

Douce, R. and Joyard, J. (1979) Adv. Bot. Res. 7 1-116.



Douce, R. and Joyard, J. (1982) in *Methods in Chloroplast Molecular Biology* (eds. Edelman, M., Hallik, R. and Chua, N-H.) 239-256. Elsevier/North Holland Biomedical Press, Amsterdam.

Drapeau, G.R., Bolly, Y. and Hounard, J. (1972) *J. Biol. Chem.* 247 6720-6726.

Dunauir, P., Smith, S. and Bedbrook, J. (1983) *J. Mol. Appl. Genet.* 2 285-300.

Dyer, T.A. (1985) *Oxford Survey of Plant Mol. Cell Biol.* 2 147-177.

Edelman, M. and Reifel, A. (1978) in *Chloroplast Development* (ed. Aoyunoglou, G) 641-652. Elsevier/North-Holland Biomed. Press, Amsterdam, New York.

Ellis, R.J. (1981) *Ann. Rev. Plant Physiol.* 32 111-137.

Ellis, R.J. (1984) in *Chloroplast Biogenesis Society for Experimental Biology Seminar Series*, 21, (ed. Ellis, R.J.) 1-9. Cambridge University Press, Cambridge.

Evans, P.K. and Anderson, J.M. (1986) *FEBS Lett.* 199 227-233.

Fish, L.E., Kuck, U. and Bogerad, L. (1985) J. Biol. Chem. 260 1413-1421.

Ford, R.C., Chapman, D.J., Barber, J., Pedersen, J.Z. and Cox, R.P. (1982) Biochim. Biophys. Acta 681 145-151.

Foyer, C.H. (1984) *Photosynthesis* (Wiley series on cell biology; vol. 1). John Wiley & Sons.

Fracki, R.I.R., Boardman, N.K. and Wildman, S.G. (1965) Biochemistry 4 865-876.

Gallagher, T.F. and Ellis, R.J. (1982) EMBO J. 1 1493-1498.

Gallagher, T.F., Jenkins, G.I. and Ellis, R.J. (1985) FEBS Lett. 186 241-245.

Gingras, G. and Jolchine, G. (1969) Prog. Photosynth. Res. 1 209-216.

Givan, C.V. and Harwood, J.L. (1977) Biol. Rev. 51 365-406.

Golbeck, J.H. and Warden, J.T. (1982) *Biochim. Biophys. Acta* 681 77-84.

Gollmer, I. and Apel, K. (1983) *Eur. J. Biochem.* 133 309-313.

Gounaris, K. and Barber, J. (1983) *Trends Biochem. Sci.* 8 378-381.

Gounaris, K., Barber, J. and Harwood, J.L. (1986) *Biochem. J.* 237 313-326.

Gounaris, K., Sundby, C., Andersson, B. and Barber, J. (1983) *FEBS Lett.* 156 170-174.

Gray, J.C., Phillips, A.L. and Smith, A.G. (1984) in *Chloroplast Biogenesis Society for Experimental Biology Seminar Series*, 21, (ed. Ellis, J.) 137-163. Cambridge University Press, Cambridge.

Green, B.R. and Cann, E.L. (1984) in *Advances in Photosynthesis Research*, vol. II (ed. Sybesma, C.) 95-98. Nijhoff/Junk, The Hague.

Grossman, A., Bartlett, S. and Chua, N-H. (1980) *Nature* 285 625-628.

Guevara, J., Johnston, D.A., Ramagali, L.S., Martin, B.A., Capetillo, S. and Rodriguez, L.V. (1982) *Electrophoresis* 3 197-205.

Haffner, M.H., Chin, M.B. and Lane, B.G. (1978) *Can. J. Biochem.* 56 729-733.

Haworth, P., Watson, J. and Arntzen, C.J. (1983) *Biochim. Biophys. Acta* 724 151-158.

Hayden, D.B. and Hopkins, W.G. (1976) *Can. J. Bot.* 54 1684-1689.

Heber, U. and Heldt, H.W. (1981) *Ann. Rev. Plant Physiol.* 32 139-168.

Helenius, A. and Simons, K. (1975) *Biochim. Biophys. Acta* 415 29-79.

Henderson, R. (1985) *Nature* 318 598-599.

Highfield, P.E. (1978) PhD Thesis, University of Warwick.

Hill, R. and Bendall, F. (1960) *Nature* 186 136-137.

Holloway, P.W. (1973) *Anal. Biochem.* 53 304-308.

Horton, P., Allen, J.F., Black, M.T. and Bennett, J.  
(1981) *FEBS Lett.* 125 193-196.

Horton, P. and Black, M.T. (1981) *Biochim. Biophys. Acta*  
635 53-62.

Israelachvili, J.W., Marcelja, S. and Horn, R.G. (1980) *Q. Rev. Biophys.* 13 121-200.

Jacob, J.S. and Miller, K.R. (1983) *Arch. Biochem. Biophys.* 223 282-290.

Jenkins, G.I., Hartley, M.R. and Bennett, J. (1983) *Phil. Trans. R. Soc. Lond.* 303 419-431.

Kirk, J.T.O. and Tilney-Bassett, R.A.E. (1978) *The Plastids: their Chemistry, Structure, Growth and Inheritance*, 2nd edn. Elsevier/North-Holland Biomedical Press, Amsterdam.

Klein, R.R. and Mullet, J.E. (1986) *J. Biol. Chem.* 261  
11138-11145.

Kreuz, K., Dehesh, K. and Apel, K. (1986) Eur. J. Biochem. 159 459-467.

Kuang, T.Y., Argyroudi-Akoyunoglou, J.M., Makatani, H.Y., Watson, J. and Arntzen, C.J. (1984) Arch. Biochem. Biophys. 235 618-627.

Kuhlbrandt, W., Thaler, TH. and Wehrli, E. (1983) J. Cell Biol. 96 1414-1424.

Kyle, D.J., Haworth, P. and Arntzen, C.J. (1982) Biochim. Biophys. Acta 680 336-342.

Kyle, D.J., Staehelin, L.A. and Arntzen, C.J. (1983) Arch. Biochem. Biophys. 222 527-541.

Laemmli, U.K. (1970) Nature 227 680-685.

Lagoutte, B., Setif, P. and Duranton, J. (1984) FEBS Lett. 174 24-29.

Lam, E., Ortiz, W. and Malkin, R. (1984a) FEBS Lett. 168 10-14.

Lam, E., Ortiz, W., Mayfield, S. and Malkin, R. (1984b) Plant Physiol. 74 650-655.

Leong, T-Y. and Anderson, J.M. (1983) *Biochim. Biophys. Acta* 723 391-399.

Leong, T-Y. and Anderson, J.M. (1984) *Biochim. Biophys. Acta* 766 533-541.

Leong, T-Y., Goodchild, D.J. and Anderson, J.M. (1985) *Plant Physiol.* 78 561-567.

Lewin, R. (1984) *Science* 224 1327-1329.

Malkin, R. (1982) *Ann. Rev. Plant Physiol.* 33 455-479.

Malkin, R. (1984) *Biochim. Biophys. Acta* 764 63-69.

Malkin, R. and Bearden, A.J. (1971) *Proc. Natl. Acad. Sci. U.S.A.* 68 16-19.

Markwell, J.P., Reisman, S. and Thornber, J.P. (1978) *Arch. Biochem. Biophys.* 190 136-141.

Mathis, P. (1987) in *Progress in Photosynthesis Research*, vol. 1, (ed. Biggins, J.) 151-160. Martinus Nijhoff, Dordrecht.

McCarty, R.E. and Carseli, C. (1982) in *Photosynthesis: Energy conversion by plants and bacteria*, vol. 1 (ed. Govindjee) 647-695. Academic Press, New York.

McDonnell, A. and Staehelin, L.A. (1980) *J. Cell Biol.* 84 40-56.

Michel, h. (1982) *J. Molec. Biol.* 158 567-572.

Miller, K.R. (1982) *Nature* 300 53-55.

Millner, P.A. and Barber, J. (1984) *FEBS Lett.* 162 1-6.

Morris, J. and Hermann, R.G. (1984) *Nucleic Acid Res.* 12 2837-2850.

Mullet, J.E., Baldwin, T.O. and Arntzen, C.J. (1981) in *Photosynthesis III. Structure and Molecular Organisation of the Photosynthetic Membrane* (ed. Akoyunoglou) 557-582. Balaban Intern. Sci. Services, Philadelphia.

Mullet, J.E., Burke, J.J. and Arntzen, C.J. (1980a) *Plant Physiol.* 65 814-822.

Mullet, J., Burke, J. and Arntzen, C.J. (1980b) *Plant Physiol.* 65 823-827.



Mullet, J.E., Grossman, A.R. and Chua, M-H. (1982) Cold Spring Harbor Symp. Quant. Biol. 46 979-984.

Murphy, D.J. (1982) FEBS Lett. 150 19-26.

Murphy, D.J. and Woodrow, I.E. (1983) Biochim. Biophys. Acta 725 104-112.

Nakatani, HY. Ke B., Dolan, E. and Arntzen, C.J. (1984) Biochim. Biophys. Acta 765 380-387.

Mechushtal, R. and Nelson, N. (1981) J. Cell Biol. 256 11624-11628.

Mechushtal, R., Nelson, N., Matoo, A. and Edelman, K. (1981) FEBS Lett. 125 115-119

Nicholls, D.G. (1982) *Bioenergetics: An introduction to the chemiosmotic theory*. Academic Press, London/New York.

Ogawa, T., Obata, F. and Shibata, K. (1966) Biochim. Biophys. Acta 112 223-234.

Ort, D.R. (1986) in *Encyclopedia of Plant Physiology*, Vol. 19. *Photosynthesis III: Photosynthetic membranes and light-harvesting systems* (eds. Staehelin, L.A. and Arntzen, C.J.) 143-196. Springer-Verlag, Berlin/Heidelberg.

Ortiz, W., Lam, E., Ghirardi, M. and Malkin, R. (1984) *Biochim. Biophys. Acta* 766 505-509.

Papageorgiou, G. (1975) in *Bioenergetics of Photosynthesis* (ed. Govindjee) 319-371. Academic Press, New York.

Pick, U., Gounaris, K., Adson, A. and Barber, J. (1984) *Biochim. Biophys. Acta* 765 12-20.

Quinn, P.J. and Williams, W.P. (1983) *Biochim. Biophys. Acta* 737 223-266.

Reed, D.W. and Clayton, R.K. (1968) *Biochim. Biophys. Acta* 30 471-475.

Robertson, R.M. (1983) *The Lively membranes*. Cambridge University Press, Cambridge.

Rochaix, J-D., Dron, M., Rahire, M. and Malnoe, P.

(1984) *Plant Mol. Biol.* 3 363-370.

Roscoe, T.J. and Ellis, R.J. (1982) in *Methods in Chloroplast Molecular Biology* (eds. Edelman, M., Hallik, R. and Chua, N-H.) 1015-1028. Elsevier/North Holland Biomedical Press, Amsterdam.

Rutherford, A.W. and Zimmerman, J.-L. (1984) *Biochim.*

*Biophys. Acta* 767 168-175.

Ryrie, I.J., Anderson, J.M. and Goodchild, D.J. (1980)

*Eur. J. Biochem.* 107 345-354.

Sabris, D.D., Gordon, M. and Glaston, A.W. (1970) *Plant*

*Physiol.* 45 25-32.

Sans, C.F., Hemelt, V.B., Pinkerton, F.D., Schroepfer,

G.J. and Matthews, K.S. (1985) *J. Biol. Chem.* 260

1185-1190.

Satoh, K. (1983) in *The Oxygen Evolving System of Photosynthesis* (eds. Inoue, Y., Crofts, A.R., Govindjee, Murata, M., Renger, G. and Satoh, K.) 27-38. Academic Press, New York.

Satch, K. and Butler, W.L. (1978) *Plant Physiol.* 61  
373-379.

Sauer, K. (1986) in *Encyclopedia of Plant Physiology*,  
Vol. 19. *Photosynthesis III: photosynthetic membranes and  
light-harvesting systems* (eds. Staehelin, L.A. and  
Arntzen, C.J.) 85-97. Springer-Verlag, Berlin/  
Heidelberg.

Schopf, J.W. (1978) *Sci. Am.* 239 84-102.

Sen, A., Williams, W.P., Brain, A.P.R. and Guinn, P.J.  
(1982) *Biochim. Biophys. Acta* 685 297-306.

Setif, P. and Mathis, P. (1986) in *Encyclopedia of Plant  
Physiology*, Vol. 19. *Photosynthesis III: Photosynthetic  
membranes and light-harvesting systems* (eds. Staehelin,  
L.A. and Arntzen, C.J.) 476-486. Springer-Verlag,  
Berlin/ Heidelberg.

Siefermann-Harms, D., Ross, J.W., Kaneshiro, K.H. and  
Yamanoto, H.Y. (1982) *FEBS Lett.* 149 191-196.

Slovin, J.P. and Tobin, E.M. (1982) *Planta* 154 465-472.

Sprague, S.G., Cass, E.L., Green, B.R. and Staehelin, L.A.  
(1985) J. Cell Biol. 100 552-557.

Sprey, B. and Laetsch, W.M. (1976) Z. Pflphys. 71 146-163.

Staehelin, L.A. (1976) J. Cell Biol. 71 136-158.

Staehelin, L.A., Armond, P.A. and Miller, K.R. (1977)  
Brookhaven Symp. Biol. 28 278-315.

Stayton, M.M., Black, M., Bedbrook, J. and Dunsmuir, P.  
(1986) Nucleic Acids Res. 14 9781-9796.

Steinback, K.E., McIntosh, L., Bogorad, L. and Arntzen, C.J. (1981) Proc. Natl. Acad. Sci. U.S.A. 78 7463-7467.

Steinback, K.E., Burke, J., Mullet, J.E. and Arntzen, C.J. (1978) in *Chloroplast Development* (eds. Akoyunoglou et al) 389-400. Elsevier/North-Holland Biomedical Press.

Switzer, R.C., Merrill, C.R. and Shifrin, S. (1979) Anal. Biochem. 28 231-237.

Thornber, J.P. (1975) Ann. Rev. Plant Physiol. 26  
127-158.

- Thornber, J.P. (1986) in *Encyclopedia of Plant Physiology, Vol. 19. Photosynthesis III: Photosynthetic membranes and light-harvesting systems* (eds. Staehelin, L.A. and Arntzen, C.J.) 100-142. Springer-Verlag, Berlin/ Heidelberg.
- Thornber, J.P., Cogdell, R.J., Pierson, B.K. and Seftor, R.E.B. (1983) *J. Cell. Biochem.* 23 159-169.
- Thornber, J.P., Gregory, R.F.F., Smith, C.A. and Bailey, J.L. (1967) *Biochemistry* 6 391-396.
- Thornber, J.P. and Highkin, H.R. (1974) *Eur. J. Biochem.* 41 109-116.
- Thornber, J.P., Markwell, J.P. and Reinman, S. (1979) *Photochem. Photobiol.* 22 1205-1216.
- Thornber, J.P., Olson, J.M., Williams, D.M. and Clayton, M.L. (1969) *Biochim. Biophys. Acta.* 172 351-354.
- Thornber, J.P., Smith, C.A. and Bailey, J.L. (1966) *Biochem. J.* 100 14-15.
- Tinko, M.P. and Cashmore, A.R. (1983) *Plant Mol. Biol.* 2 403-412.

Tolbert, N.E. (1980) in *The Biochemistry of Plants* Vol. 2, Metabolism and Respiration, (ed. Davies, D.D.) 488-521. Academic Press, New York.

Trebat, A. (1980) in *Methods in Enzymology* (ed. San Pietro) 63 146-165. Academic Press, New York.

Vaessen, R.T.M.J., Kreike, J. and Groot, G.S.P. (1981) FEBS Lett. 124 193-196.

Vierling, E. and Alberte, R.S. (1983) Plant Physiol. 72 625-633.

Walker, J., Auffret, A.D., Carne, A., Gurnett, A., Hanish, P., Hill, D. and Saraste, M. (1982) Eur. J. Biochem. 123 253-260.

Westhoff, P., Alt, J., Nelson, N., Bottomley, W., Bunemann, H. and Heilmann, R.G. (1983) Plant Mol. Biol. 2 95-107.

White, M.J. and Green, B. R. (1987) Eur. J. Biochem. (in press).

Whitmarsh, J. (1986) in *Encyclopedia of Plant Physiology*, Vol. 19. *Photosynthesis III: Photosynthetic membranes and light-harvesting systems* (eds. Staehelin, L.A. and Arntzen, C.J.) 508-527. Springer-Verlag, Berlin/Heidelberg.

Williams, R.S. and Bennett, J. (1983) in *Methods in Enzymology* 27 (eds. Colowick and Kaplan) 487-502. Academic Press, New York.

Witt, H.T. (1971) *Q. Rev. Biophys.* 4 365-477.

Wollman, F.A. (1986) in *Encyclopedia of Plant Physiology*, Vol. 19. *Photosynthesis III: Photosynthetic membranes and light-harvesting systems* (eds. Staehelin, L.A. and Arntzen, C.J.) 487-495. Springer-Verlag, Berlin/Heidelberg.

Wollman, F.A. and Bennoun, P. (1982) *Biochim. Biophys. Acta* 680 352-360.

Wray, W. Boulikas, T., Wray, V.P. and Hancock, R. (1981) *Anal. Biochem.* 118 197-203.

Yagamiishi, A. and Katoh, S. (1984) *Biochim. Biophys. Acta*. 765 118-124.



Yamamoto, Y. and Nishisura, M. (1983) in *The Oxygen Evolving System of Photosynthesis* (eds. Inoue, Y., Crofts, A.R., Govindjee, Murata, N., Renger, G. and Satoh, K.) 229-238. Academic Press, New York.

Yocum, C.F. (1986) in *Encyclopedia of Plant Physiology*, Vol. 19. *Photosynthesis III: Photosynthetic membranes and light-harvesting systems* (eds. Staehelin, L.A. and Arntzen, C.J.) 437-446. Springer-Verlag, Berlin/Heidelberg.

Zinth, W., Kaiser, W. and Michel, H. (1983) *Biochim. Biophys. Acta* 273 128-131.

Zuber, H. (1985) in *Antennas and Reaction Centers of Photosynthetic Bacteria* (Springer Series in Chemical Physics Vol. 42) (ed. Michel-Beyerle, M.E.) 2-14. Springer-Verlag.

Zuber, H. (1986) *Trends Biochem. Sci.* 11 414-419.